Universiteit Leiden
The Netherlands

Stem cell therapy for cardiovascular disease : answering basic questions regarding cell behavior

Bogt, K.E.A. van der

Citation

Bogt, K. E. A. van der. (2010, December 16). *Stem cell therapy for cardiovascular disease : answering basic questions regarding cell behavior*. Retrieved from https://hdl.handle.net/1887/16249

Version:	Corrected Publisher's Version
License:	Licence agreement concerning inclusion of doctoral thesis in the Institutional Repository of the University of Leiden
Downloaded from:	https://hdl.handle.net/1887/16249

Note: To cite this publication please use the final published version (if applicable).

Stem Cell Therapy for Cardiovascular Disease

Answering basic questions regarding cell behavior

PROEFSCHRIFT

ter verkrijging van

de graad van Doctor aan de Universiteit Leiden,

op gezag van de Rector Magnificus Prof. mr. P.F. van der Heijden,

volgens besluit van het College voor Promoties

te verdedigen op donderdag 16 december 2010 klokke 15.00 uur

door

Koen Elzert Adriaan van der Bogt

geboren te Nieuwveen in 1981

PROMOTIECOMMISSIE

Promotores:	Prof. Dr. J.F. Hamming
	Prof. Dr. R.C. Robbins (Stanford University, USA)
Co-promotor:	Dr. J.C. Wu (Stanford University, USA)
Overige leden:	Prof. Dr. C.L. Mummery
	Prof. Dr. P.H. Quax

The research as described in this thesis has been a collaborative effort of the Department of Cardiothoracic Surgery and the Molecular Imaging Program at Stanford University (California, USA), and the Department of Surgery, Leiden University Medical Center (The Netherlands). The printing of this thesis was financially supported by the Netherlands Heart Foundation and the J.E. Jurriaanse Foundation. The research was supported by grants from the Fulbright Foundation, the VSB fund, the Prof. Michaël-van Vloten Foundation, the American Heart Association, the Collegium Chirurgicum Neerlandicum, ADinstruments, Millar Instruments, Synthes, Triplinq Hosted Solutions, ChipSoft and Servier Nederland Farma B.V.

To my family

TABLE OF CONTENTS:

Chapter 1: General Introduction 7

PART I: **EMBRYONIC STEM CELLS**

Chapter 2: *Multimodal evaluation of in vivo magnetic resonance imaging of myocardial restoration by mouse embryonic stem cells.* 19

J Thorac Cardiovasc Surg. 2008 Oct;136(4):1028-1037.e1.

Chapter 3: *Spatial and temporal kinetics of teratoma formation from murine embryonic stem cell transplantation.* 37

Stem Cells Dev. 2007 Dec;16(6):883-91.

Chapter 4: *Molecular imaging of human embryonic stem cells: keeping an eye on differentiation, tumorigenicity and immunogenicity.* 53

Cell Cycle. 2006 Dec;5(23):2748-52.

Chapter 5: *Clinical hurdles for the transplantation of cardiomyocytes derived from human embryonic stem cells: role of molecular imaging.* 67

Curr Opin Biotechnol. 2007 Feb;18(1):38-45.

PART II: ADULT STEM CELLS

Chapter 6: *Comparison of different adult stem cell types for treatment of myocardial ischemia.* 85

Circulation. 2008 Sep 30;118(14 Suppl):S121-9.

Chapter 7: *Comparison of transplantation of adipose tissue- and bone marrow-derived mesenchymal stem cells in the infarcted heart.* 107

Transplantation. 2009 Mar 15;87(5):642-52.

Chapter 8: *Micro Computed Tomography for Characterization of Murine Cardiovascular Disease Models.* 131

JACC Cardiovasc Imaging. 2010 Jul;3(7):783-5.

Chapter 9: *Molecular Imaging of Bone Marrow Mononuclear Cell Survival and Homing in a Model of Murine Peripheral Artery Disease.* 141

Submitted

Chapter 10: Summary and Discussion 161

Chapter 11: Summary in Dutch 173

Chapter 12: List of Publications 180

Curriculum Vitae 182

Acknowledgements 184

CHAPTER 1

General introduction

STEM CELLS

Bovine non-identical twins that share the same placenta and circulation before birth, can keep producing a pool of blood cells that are a genetic mix of themselves as well as their brother's.[1, 2] Although not immediately recognized as such, it was as early as 1945 that this observation by Owen already suggested that the bone marrow hosted cells from early developmental origin that could produce more specialized progeny (blood cells) for a prolonged period throughout life. How else would it be possible that one of the twins produced cells that genetically "belonged" to his twin brother while the two had lost physical connection long ago? Despite these early suggestions, it took nearly 20 years before Mc Culloch and Till discovered a portion of bone marrow cells that could renew themselves extensively without losing their ability to produce a variety of other organ-specific cells.[3, 4] These two characteristics (self-renewal and differentiation capacity into more specialized cell types) have now been widely accepted as the requirements for calling a cell a "stem cell". As one can imagine, these characteristics automatically pose such cells as ideal candidates for both cellular and organ replacement therapies. However, before going into the therapeutic possibilities, it is important to gain some insight into different classes of stem cells. The most widely used classification of stem cells is based upon their origin and separates two groups of cells: "Embryonic stem cells (ESC)" and "adult stem cells".

Four to 5 days after fertilization, the early stage embryo consists of around 150 cells called the blastocyst. ESC from the inner mass of this blastocyst can be isolated and expanded indefinitely under strict culture circumstances and supported by a feeder layer of mouse embryonic fibroblasts.[5] The unique property of these cells lies within the capacity to develop into all three germ layers: Endo-, ecto-, and mesoderm, a phenomenon best described as pluripotency. After making the first transition to these germ layers, the cells become more restricted in their developmental potential and differentiate within germ layer boundaries to more specialized cell types, resembling the natural process of organogenesis.

On the other hand, adult or somatic stem cells are cells that have already differentiated further down the path of development. Although still capable of differentiating into multiple specialized cell types, these cells are restricted by germ layer boundaries and as such have already been programmed to become and replace cells specific to their biological environment or function. Because of this limitation, adult stem cells are referred to as being multi- but not pluripotent. Adult stem cells reside in the adult body in various places where they play a role in tissue homeostasis and repair, but are usually low in number and difficult to isolate and expand. One least imaginative example of tissue-specific stem cells is epidermal stem cells that reside in the skin where they are responsible for the fast turnover and accelerated production of progeny in case of injury.[6]

REGENERATIVE MEDICINE

Because of the above described properties of pluri- and multipotency, stem cells have contributed significantly to the field of "regenerative medicine". As the name already suggests, this discipline aims to heal disease by regeneration of damaged tissue. Adult stem cells carry this property by nature, as these cells are biologically destined to repair, for example, skin[6], gut[7], and liver[8], or to replace blood cells[9] throughout life. However, there is a range of diseases where endogenous repair fails including diabetes, Parkinson's, or coronary and peripheral artery disease. In this respect, it may prove beneficial to isolate, expand, and transplant adult stem cells to induce increased healing capacity. This approach carries great advantage because the cells are isolated from the patient and are thus not rejected through immunogenicity. It has even been reported that mesenchymal stem cells, which can be isolated from the bone marrow, may alleviate immune reaction.[10] However, most adult stem cells can prove difficult to isolate and expand, and may not be able to restore a complete spectrum of different cells needed for functional recovery. Moreover, these transplanted cells may not be able to survive in the diseased, often hostile environment after transplantation. Lastly, the cells may not integrate into the host tissue and as such cannot contribute to functional improvement.

Conversely, ESCs can be expanded in culture rapidly thus providing a possible "off-the-shelf" therapeutic. However, these cells must be directed into the desired cell type before transplantation to prevent uncontrolled differentiation and subsequent malignant potential if residual undifferentiated cells are present. In this respect, success has been achieved by driving ESCs towards brain and skin derivates as well as pancreatic cells or muscle, bone and cardiac lineages.[11] However, one major challenge remains eliminating undesired cell types as well as undifferentiated cells. A second hurdle is that, similar to organ transplants, the cells are from a different genetic background and may provoke immunorejection. Despite these problems and considerable ethical debate about the derivation of these cells, a clinical trial using ESC-derived oligodendrocyte precursor cells to treat spinal cord injury has just been initiated.[12]

STEM CELL TREATMENT FOR CARDIOVASCULAR DISEASE

Annually, more people die from cardiovascular diseases (CVDs) than from any other cause, representing 30% of all global deaths (http://www.who.int, factsheet 317). Thus, despite a wide variety of treatments ranging from medication to heart transplantation, there clearly remains a great need for new therapeutic approaches. In 2001, Orlic and colleagues reported that transplantation of bone marrow stem cells in the damaged mouse heart not only yielded an improvement in function, but also new cardiomyocytes (cardiac muscle cells) that originated directly from the transplanted cells.[13] For reasons described above, the observation that bone marrow cells were capable of differentiation into cardiomyocytes was heavily discussed and refuted

by, among others[14], our laboratory.[15] Despite these conflicting reports, it was Orlic's study that raised tremendous enthusiasm for stem cell therapy for heart disease and subsequent ultra-rapid initiation of clinical trials using bone marrow cells. Similarly, clinical trials with bone marrow cells for treatment of peripheral artery occlusive disease were initiated.[16] In the meantime, experimental studies showed promise for other adult stem cell types as well, including skeletal myoblasts[17], mesenchymal stem cells[18], and adipose-derived stromal cells.[19] While outcomes from these studies were generally promising, questions remained about the mechanism of action and the cellular behavior following cell transplantation. Unfortunately, there was few available data on the *in vivo* cellular kinetics thus leaving an unknown gap of what happened to the cells once they were transplanted into the animal.

IN VIVO MOLECULAR IMAGING OF STEM CELL KINETICS

To study the mechanism by which stem cells might or might not preserve function after transplantation, it is of great importance to gain insight into cellular behavior. Usually, this is approached by labeling cells with conventional reporter genes such as Green Fluorescent Protein (GFP, which is isolated from luminescent jelly fish).[20] However, to image GFP, extrinsic excitation light is needed, which produces significant background signal and has poor tissue penetration. This makes GFP unsuitable for reliable *in vivo* imaging of stem cells, and therefore GFP-labeled cells are typically identified histologically. Unfortunately, this requires the isolation of the target tissue and thus provides only a single time point rather than following a series of events in real time. In order to reliably investigate the behavior of transplanted stem cells, however, one must be able to track the cells longitudinally over time, whilst keeping the animal alive. To establish this goal, our group has developed novel molecular imaging techniques.[21]

Molecular imaging is defined as the *in vivo* characterization of cellular and molecular processes.[22] The backbone of reporter gene-based molecular imaging technique is the design of a suitable reporter construct. This construct carries a reporter gene linked to a promoter that can be inducible, constitutive, or tissue specific. The construct can be introduced into the target tissue by molecular biology techniques using either viral or nonviral approaches. Transcription of DNA and translation of mRNA lead to the production of reporter protein. After administration of a reporter probe, this probe reacts with the reporter protein, giving rise to signals that are detectable by a charged-coupled device (CCD) camera, positron emission tomography (PET), single photon emission computed tomography (SPECT), or magnetic resonance imaging (MRI).[23]

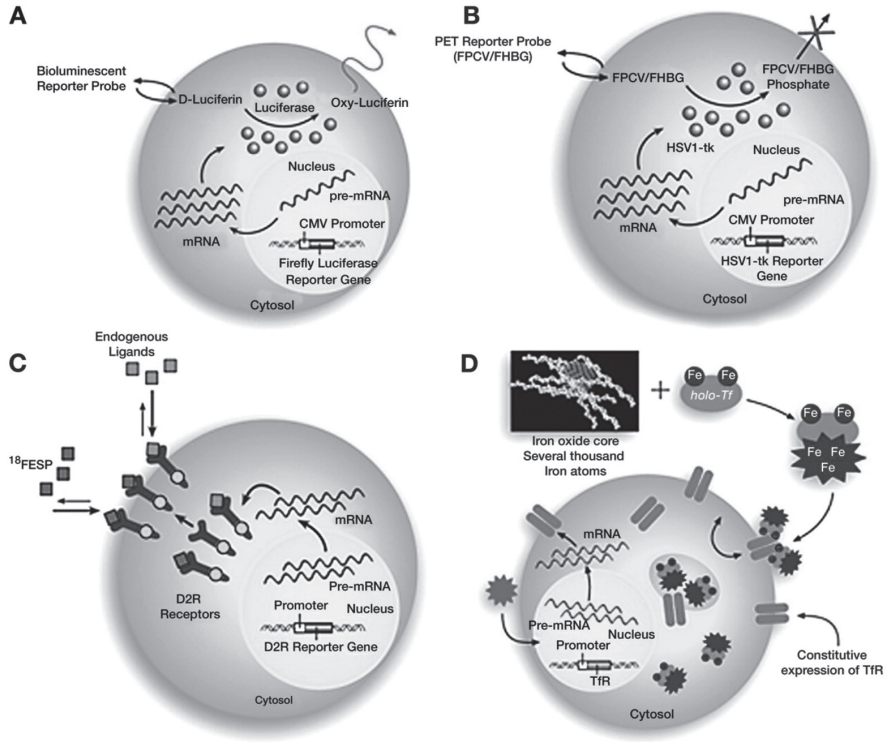

Figure 1. Examples of reporter gene and probe imaging. (a) Enzyme-based bioluminescence imaging. Expression of the firefly luciferase (Fluc) reporter gene leads to the firefly luciferase reporter enzyme, which catalyzes the reporter probe (D-luciferin) that results in a photochemical reaction. This yields low levels of photons that can be detected, collected, and quantified by a CCD camera. (b) Enzyme-based PET imaging. Expression of the herpes simplex virus type 1 thymidine kinase (HSV1-tk) reporter gene leads to the thymidine kinase reporter enzyme (HSV1-TK), which phosphorylates and traps the reporter probe (F-18 FHBG) intracellularly. Radioactive decay of F-18 isotopes can be detected via PET. (c) Receptor-based PET imaging. F-18 FESP is a reporter probe that interacts with D2R to result in probe trapping on or in cells expressing the D2R gene. (d) Receptor-based MRI imaging. Overexpression of engineered transferrin receptors (TfR) results in increased cell uptake of the transferrin–monocrystalline iron oxide nanoparticles (Tf-MION). These changes result in a detectable contrast change on MRI. Reprinted with permission from Wu et al.[24]

Recent studies from our group have shown that it is possible to monitor experimental stem cell transplantation by bioluminescence imaging (BLI).[25, 26] By introducing the Firefly Luciferase gene into the isolated cells, these donor cells can be imaged after transplantation in a naïve host. The Luciferase gene produces Luciferase protein, which will react with D-Luciferin (the

probe that is injected into the recipient animal before every imaging session) to produce a donor cell-specific signal that will be detected by the CCD camera. This approach potentially carries four major advantages: (1) It is *in vivo*, thus keeping the animal alive and permitting repeated imaging over time; (2) Luciferase protein will only be produced by donor cells that are alive, thus providing insight into cell viability; (3) D-Luciferin is systemically distributed while the CCD camera can image the whole animal, thereby monitoring signal from donor cells independent of cell location; and (4) There is no need of extrinsic excitation light, keeping background signals within acceptable limits. Following these advantages, this technique would be specifically suited to answer basic questions regarding cellular behavior after (embryonic and adult) stem cell transplantation in small animal models of cardiovascular disease.

STEM CELL THERAPY FOR CARDIOVASCULAR DISEASES: ANSWERING BASIC QUESTIONS REGARDING CELL BEHAVIOR

The scope of this thesis is to utilize molecular imaging techniques to address for the first time some basic but critical issues of both embryonic and adult stem cell therapy. Specifically, these issues involve *in vivo* cell survival, proliferation, migration, and misbehavior.

The initial part of this thesis describes the advantages and drawbacks of embryonic stem cell (ESC) transplantation. In **Chapter 2**, the effects of undifferentiated mouse ESC transplantation into the infarcted heart are described. Different *in vivo* modalities were used to assess short-term functional effects while histology tested the true regenerative capacity of these cells by means of staining for GFP and cardiomyocyte-specific markers. Moreover, non-invasive BLI and gross histology were performed to follow the fate of donor cells, and to image possible migration or misbehavior. Following this study, **Chapter 3** was designed to test some important characteristics of ESC-derived teratoma formation. Specifically, it tested the possibility that these cells can migrate through the body and form teratomas in distant locations after intramyocardial transplantation. Moreover, the potent teratogenic potential of undifferentiated mESC was visualized by testing how many undifferentiated cells are sufficient to provoke teratoma formation. The importance of these kinds of studies was acknowledged in a comment by Rao.[27]

Chapter 4 provides an overview of the potential of guided *in vitro* ESC differentiation and the wide variety of therapeutic possibilities. While giving insight into the basics of molecular imaging, it provides an introduction to the drawbacks of ESC. Getting more into detail, **Chapter 5** focuses on ESC-derived cardiomyocytes. It describes the clinical hurdles concerning differentiation efficiency, purification, integration, and immune rejection of embryonic stem cell-derived cardiomyocytes. Moreover, it outlines the role that molecular imaging can and should play in identifying these problems in both experimental and clinical settings.

After discussing the hurdles for clinical translation of ESC, the second part of this thesis focuses on the applicability of adult stem cells in cardiovascular diseases. **Chapter 6** focuses on non-invasive molecular imaging of different clinically utilized adult stem cell types. This was the first study to directly compare mononuclear cells from the bone marrow, skeletal myoblasts, mesenchymal stem cells, and fibroblasts in a mouse model of heart failure and revealed the survival of these cells in the ischemic environment of the infarcted heart. Moreover, it clarified which cell type resulted in superior functional preservation and if any of these cell types formed cardiomyocytes.

An alternative kind of mesenchymal stem cells can be isolated from the fat (adipose-derived stromal cells). These were compared to the "traditional" mesenchymal stem cell population from the bone marrow as described in **Chapter 7**. The *in vitro* morphological and growth characteristics of both cell types were analyzed. Thereafter, the cells were transplanted into the infarcted mouse myocardium and cell survival was monitored by *in vivo* BLI, while cardiac function was monitored by echocardiography. The echocardiography data was validated by pressure-volume loop measurements followed by histological analysis. Additional experiments using *in vivo* BLI examined the possibility that immunogenicity of GFP or the sex mismatch model used were of significant influence on donor cell survival in this study. This study was featured on the cover of *Transplantation*.

In **Chapter 8**, a novel small animal imaging modality to assess cardiac function is introduced. By comparison to traditional modalities such as echocardiography and catheter-based hemodynamic measurements, novel Micro-CT was tested for its ability to reliably and precisely assessing cardiac geometry and ventricular function of the infarcted mouse heart in an *in vivo*, three-dimensional fashion.

Next, **Chapter 9** makes the transition from cardiac studies to the field of stem cell therapy for peripheral artery occlusive disease. Using a mouse model of hind limb ischemia, different mononuclear cell transplantation techniques were tested while the patterns of cell survival and migration were visualized in live animals using molecular imaging. The results from this study reveal the patterns of cell survival and homing to the affected area after intramuscular and intravenous transplantation, respectively. Moreover, the effect on paw perfusion was monitored by Laser Doppler Perfusion Imaging (LDPI).

Finalizing this thesis, **Chapter 10** summarizes and discusses the most important findings and implications from the research conducted, and brings forward my opinion on the future directions of stem cell therapy for cardiovascular diseases. A synopsis in Dutch is provided in **Chapter 11**.

REFERENCES:

1. Owen RD. Immunogenetic Consequences of Vascular Anastomoses between Bovine Twins. *Science.* 1945;102(2651):400-401.
2. Weissman IL. The road ended up at stem cells. *Immunol Rev.* 2002;185:159-174.
3. Becker AJ, Mc CE, Till JE. Cytological demonstration of the clonal nature of spleen colonies derived from transplanted mouse marrow cells. *Nature.* 1963;197:452-454.
4. Siminovitch L, McCulloch EA, Till JE. The Distribution of Colony-Forming Cells among Spleen Colonies. *J Cell Physiol.* 1963;62:327-336.
5. Thomson JA, Itskovitz-Eldor J, Shapiro SS, Waknitz MA, Swiergiel JJ, Marshall VS, Jones JM. Embryonic stem cell lines derived from human blastocysts. *Science.* 1998;282(5391):1145-1147.
6. Alonso L, Fuchs E. Stem cells of the skin epithelium. *Proc Natl Acad Sci U S A.* 2003;100 Suppl 1:11830-11835.
7. van der Flier LG, Clevers H. Stem cells, self-renewal, and differentiation in the intestinal epithelium. *Annu Rev Physiol.* 2009;71:241-260.
8. Alison MR, Islam S, Lim S. Stem cells in liver regeneration, fibrosis and cancer: the good, the bad and the ugly. *J Pathol.* 2009;217(2):282-298.
9. Schulz C, von Andrian UH, Massberg S. Hematopoietic stem and progenitor cells: their mobilization and homing to bone marrow and peripheral tissue. *Immunol Res.* 2009;44(1-3):160-168.
10. Nauta AJ, Fibbe WE. Immunomodulatory properties of mesenchymal stromal cells. *Blood.* 2007;110(10):3499-3506.
11. Sakaguchi Y, Sekiya I, Yagishita K, Muneta T. Comparison of human stem cells derived from various mesenchymal tissues: superiority of synovium as a cell source. *Arthritis Rheum.* 2005;52(8):2521-2529.
12. Alper J. Geron gets green light for human trial of ES cell-derived product. *Nat Biotechnol.* 2009;27(3):213-214.
13. Orlic D, Kajstura J, Chimenti S, Jakoniuk I, Anderson SM, Li B, Pickel J, McKay R, Nadal-Ginard B, Bodine DM, Leri A, Anversa P. Bone marrow cells regenerate infarcted myocardium. *Nature.* 2001;410(6829):701-705.
14. Murry CE, Soonpaa MH, Reinecke H, Nakajima H, Nakajima HO, Rubart M, Pasumarthi KB, Virag JI, Bartelmez SH, Poppa V, Bradford G, Dowell JD, Williams DA, Field LJ. Haematopoietic stem cells do not transdifferentiate into cardiac myocytes in myocardial infarcts. *Nature.* 2004;428(6983):664-668.
15. Balsam LB, Wagers AJ, Christensen JL, Kofidis T, Weissman IL, Robbins RC. Haematopoietic stem cells adopt mature haematopoietic fates in ischaemic myocardium. *Nature.* 2004;428(6983):668-673.

16. Tateishi-Yuyama E, Matsubara H, Murohara T, Ikeda U, Shintani S, Masaki H, Amano K, Kishimoto Y, Yoshimoto K, Akashi H, Shimada K, Iwasaka T, Imaizumi T. Therapeutic angiogenesis for patients with limb ischaemia by autologous transplantation of bone-marrow cells: a pilot study and a randomised controlled trial. *Lancet*. 2002;360(9331):427-435.
17. Menasche P. Skeletal myoblast for cell therapy. *Coron Artery Dis*. 2005;16(2):105-110.
18. Wollert KC, Drexler H. Mesenchymal stem cells for myocardial infarction: promises and pitfalls. *Circulation*. 2005;112(2):151-153.
19. Zuk PA, Zhu M, Ashjian P, De Ugarte DA, Huang JI, Mizuno H, Alfonso ZC, Fraser JK, Benhaim P, Hedrick MH. Human adipose tissue is a source of multipotent stem cells. *Mol Biol Cell*. 2002;13(12):4279-4295.
20. Shimomura O, Johnson FH, Saiga Y. Extraction, purification and properties of aequorin, a bioluminescent protein from the luminous hydromedusan, Aequorea. *J Cell Comp Physiol*. 1962;59:223-239.
21. Sheikh AY, Wu JC. Molecular imaging of cardiac stem cell transplantation. *Curr Cardiol Rep*. 2006;8(2):147-154.
22. Blasberg RG, Tjuvajev JG. Molecular-genetic imaging: current and future perspectives. *J Clin Invest*. 2003;111(11):1620-1629.
23. Wu JC, Bengel FM, Gambhir SS. Cardiovascular molecular imaging. *Radiology*. 2007;244(2):337-355.
24. Wu JC, Tseng JR, Gambhir SS. Molecular imaging of cardiovascular gene products. *J Nucl Cardiol*. 2004;11(4):491-505.
25. Cao F, Lin S, Xie X, Ray P, Patel M, Zhang X, Drukker M, Dylla SJ, Connolly AJ, Chen X, Weissman IL, Gambhir SS, Wu JC. *In vivo* visualization of embryonic stem cell survival, proliferation, and migration after cardiac delivery. *Circulation*. 2006;113(7):1005-1014.
26. Wu JC, Chen IY, Sundaresan G, Min JJ, De A, Qiao JH, Fishbein MC, Gambhir SS. Molecular imaging of cardiac cell transplantation in living animals using optical bioluminescence and positron emission tomography. *Circulation*. 2003;108(11):1302-1305.
27. Rao M. Tumorigenesis and embryonic stem cell-derived therapy. *Stem Cells Dev*. 2007;16(6):903-904.

PART I

EMBRYONIC STEM CELLS

CHAPTER 2

Multimodal evaluation of *in vivo* magnetic resonance imaging of myocardial restoration by mouse embryonic stem cells

Stephen L. Hendry III*, Koen E.A. van der Bogt*, Ahmad Y. Sheikh,
Takayasu Arai, Scott J. Dylla, Micha Drukker, Michael V. McConnell,
Ingo Kutschka, Grant Hoyt, Feng Cao, Irving L. Weissman,
Andrew J. Connolly, Marc P. Pelletier, Joseph C. Wu,
Robert C. Robbins and Phillip C. Yang

Journal of Thoracic and Cardiovascular Surgery
2008 Oct;136(4):1028-1037.

*Both authors contributed equally to this study

ABSTRACT

Objective: Mouse embryonic stem cells (mESC) have demonstrated the potential to restore the infarcted myocardium following an acute myocardial infarction (AMI). Although the underlying mechanism remains controversial, MRI has provided reliable *in vivo* assessment of functional recovery following cell transplantation. Multi-modality comparison of the restorative effects of mESC and mouse embryonic fibroblasts (mEF) was performed to validate MRI data and provide mechanistic insight.

Methods: SCID beige mice (n=55) underwent coronary artery ligation followed by injection of $2.5x10^5$ mESC, $2.5x10^5$ mEF, or normal saline (NS). *In vivo* MRI of myocardial restoration by mESC was evaluated by: 1) *in vivo* pressure volume (PV) loops, 2) *in vivo* bioluminescence imaging (BLI), and 3) *ex vivo* TaqMan PCR (TM-PCR) and immunohistology.

Results: *In vivo* MRI indicated significant improvement of LVEF at 1 week in the mESC group. This finding was validated with: (1) PV loop analysis demonstrating significantly improved systolic and diastolic functions, (2) BLI and TM-PCR showing superior post-transplant survival of mESC, (3) immunohistology identifying cardiac phenotype within the engrafted mESC, and (4) TM-PCR measuring increased expression of angiogenic and anti-apoptotic genes, and decreased expression of anti-fibrotic genes.

Conclusion: This study validates *in vivo* MRI as an effective modality to evaluate the restorative potential of mESC.

INTRODUCTION

Cellular therapy is rapidly emerging as a potential therapeutic option following an acute myocardial infarction (AMI).[1] Although studies have shown that transplantation of stem cells derived from different lineages have provided significant functional recovery in the setting of AMI, the exact mechanisms of cell-mediated restoration have not been established.[2] There are several theories regarding the possible mechanisms underlying myocardial restoration following cell therapy: 1) augmentation of the infarct region's elasticity preserving regional systolic and diastolic functions; 2) contractility of engrafted cells improving systolic function; 3) angiogenesis enhancing regional myocardial perfusion; and 4) paracrine effects modulating the progression of cardiac remodeling.[3-6]

In vivo MRI has demonstrated improved cardiac function following transplantation of stem cells in both pre-clinical and clinical investigations.[1, 7-11] These findings have led to questions regarding the validity of such data, however, and more importantly, the potential mechanisms underlying myocardial restoration. This investigation addresses these issues by validating *in vivo* MRI evaluation of myocardial restoration through a systematic comparison of the restorative potential of "non-specific" mouse embryonic fibroblasts (mEF) to the more biologically active, self-renewing, pluripotent mouse embryonic stem cells (mESC) in a murine model of AMI. This is the first study to validate *in vivo* MRI at a functional level, and to conduct a multimodality evaluation of physiologic, cellular, and molecular mechanisms of mESC-mediated myocardial restoration.

METHODS

Cell culture. Undifferentiated D3-derived mESC (ATCC, Manassas, VA) were cultured in DMEM (Invitrogen, Carlsbad, CA) with 15% fetal calf serum (FCS, Hyclone, Logan, UT), 100 mg/mL penicillin-streptomycin, 1mM sodium pyruvate, 2mM L-glutamine, NEAA, 0.1mM b mercaptoethanol (Invitrogen, Carlsbad, CA) and 106 u/mL leukemia inhibitory factor (Chemicon International, Temecula, CA). Fresh mouse embryonic fibroblasts (mEF) were prepared from 13-day embryos, whose carcasses were minced and passed 10 times through a 21-gauge needle. Cells were seeded in 10 cm culture dishes and were propagated for two passages in DMEM with 10% FCS and 100 mg/mL penicillin-streptomycin solution. Both mESC and mEF were transfected with a lentiviral vector carrying a cytomegalovirus promoter driving both a firefly luciferase (fluc) reporter gene and green fluorescent protein (GFP). Cells underwent FACS sorting for GFP and single clone selection; the clone was adapted to feeder-free conditions. Prior to injection, the cells were trypsinized (0.25% trypsin/0.02% EDTA) washed with DMEM containing 10% serum. Following centrifugation, the cells were washed with PBS, centrifuged and resuspended in PBS for injection one hour after trypsinization.

Experimental animals. Animal care and interventions were provided in accordance with the Laboratory Animal Welfare Act, the *Guide for the Care and Use of Laboratory Animals* (National Institutes of Health, publication 78-23, revised 1978). Immunotolerant SCID-beige female mice (8-12 weeks, Charles River, Wilmington, MA) were anesthetized in an isoflorane inhalational chamber and endotracheally intubated with a 20 gauge angiocath (Ethicon Endo-Surgery, Inc. Cincinnati, OH). Ventilation was maintained with a Harvard rodent ventilator. Myocardial infarction was created by ligation of the mid-left anterior descending (LAD) artery through a left thoracotomy. The mice were randomized into three groups: 1) LAD ligation with normal saline (NS) injection (n=10), 2) LAD ligation with mESC injection (n=25), or 3) LAD ligation with mEF injection (n=20). The infarct region was injected with 25mL using a Hamilton syringe containing 250,000 mESC, mEF, or NS. Cell suspensions contained rhodamine beads (6×10^5) to ensure injection accuracy. Following chest tube placement, the chest was closed in 2 layers with 5-0 vicryl.

***In vivo* MRI.** One week after transplantation, cardiac MRI was obtained using a Unity Inova console (Varian, Inc., Palo Alto, CA) controlling a 4.7T, 15cm horizontal bore magnet (Oxford Instruments, Ltd., Oxford, UK) with GE Techron Gradients (12G/cm) and a volume coil with a diameter of 3.5cm (Varian, Inc., Palo Alto, CA). The ECG gating was optimized using 2 subcutaneous precordial leads with respiratory motion and body temperature monitors (SA Instruments, Inc., Stony Brook, NY). LV function was evaluated using ECG-triggered cine sequence (TE 2.8-ms, TR 160-ms, FA 60°, FOV 3.0cm2, matrix 128×128, slice gap 0-mm, slice thickness 1.0-mm, 8 NEX, and 12 cardiac phases). The imaging plane was localized using double-oblique acquisition. The data were analyzed using MR Vision software (Winchester, MA). LV ejection fraction (LVEF), end-diastolic (LVED), and end-systolic (LVES) volumes were calculated by tracing the endocardial borders in end-systole and -diastole.

Pressure-volume (PV) loop analysis. One week after transplantation, ventricular performance was assessed by PV loop analysis using a 1.4 F conductance catheter (Millar Instruments, Houston, TX) prior to euthanasia. The closed chest technique was utilized which consisted of a midline neck incision to access the left external jugular vein with PE10 tubing (Intramedic-Becton Dickinson). The right carotid was cannulated with the Millar catheter and advanced through the aortic valve into the LV. The PV relations were measured at baseline and during inferior vena cava occlusion. The measurements of segmental conductance were recorded which allowed extrapolation of the left ventricular volume. When coupled with pressure, the generation of ventricular PV relationships allowed precise hemodynamic characterization of ventricular systolic and diastolic function and loading conditions.[12] These data were analyzed using PVAN 3.4 Software (Millar Instruments, Inc.) and Chart/Scope Software (AD Instruments, Inc.).

***In vitro* firefly luciferase (fluc) assay.** On the day of operation, parallel sets of cells from the same plates as the injected cells were trypsinized, resuspended in PBS and divided into a 6-well plate in different concentrations. After administration of D-luciferin (Xenogen, California, USA, 4.5ug/mL), peak signal expressed as photons per second per centimeter square per steridian (p/s/cm^2/sr) was measured using a charged coupled device (CCD) camera (Xenogen, California, USA).

***In vivo* optical bioluminescence imaging (BLI).** Optical BLI was performed using 8 x 5 minute acquisition scans on a CCD camera (IVIS 50, Xenogen, California, USA). Recipient mice were anesthetized and placed in the imaging chamber. After acquisition of a baseline image, mice were intraperitoneally injected with D-luciferin (Xenogen, USA, 400 mg/kg body weight). Peak signal (p/s/cm^2/sr) from a fixed region of interest (ROI) was evaluated using the Living Image 2.50 software (Xenogen, USA).

***Ex vivo* TaqMan PCR (TM-PCR) for cell survival and expression of genes of interest.** Since the transplanted cells were derived from male mice and were transplanted into female recipients, the surviving mESC in the explanted hearts could be quantified using TM- PCR to track the SRY locus found on the Y chromosome. Whole explanted hearts were minced and homogenized in DNAzol (Invitrogen, Carlsbad, CA). RNA was extracted from the mice myocardium after treatment with TRIzol reagent (Invitrogen, Carlsbad, CA). Taqman PCR was performed using SuperScript II RT-PCR kit (Invitrogen, Carlsbad, CA). To assess the expression of several genes of interest, relative quantitation of mouse primers was performed for: matrix metalloproteinase (MMP)-1β, -2, -9, -14, tumor necrosis factor (TNF)-α, vascular endothelial growth factor (VEGF)-A, procollagen-2α1, transforming growth factor (TGF)-β, angiotensin converting enzyme (ACE), insulin-like growth factor (IGF) 1, Flk-1, and NFkβ-1 (Applied Biosystems, Foster City, CA). The fluorogenic probes contained a 5'-FAM report dye and 3'-BHQ1 quencher dye. TaqMan 18S Ribosomal RNA (Applied Biosystems, Foster City, CA) was used as control gene. RT-PCR reactions were conducted in iCylcer IQ Real-Time Detection Systems (Bio-Rad, Hercules, CA).

Histological analysis. Hearts were flushed with NS and subsequently placed in 2% paraformaldehyde for 2 hours at room temperature followed by 12-24 hours in 30% sucrose at 4°C. The tissue was embedded in Optical Cutting Temperature (OCT) Compound (Tissue-Tek. Sakura Finetek USA Inc., Torrance, CA) and snap frozen on dry ice. Five-micron sections were cut in both the proximal and apical regions of the infarct zone. Slides were stained for H&E, GFP (anti-green fluorescent protein, rabbit IgG fraction, anti-GFP Alexa Fluor 488 conjugate, 1:200, Molecular Probes, Inc.), Troponin I (H-170 rabbit polyclonal IgG for cardiac muscle, 1:100, Santa

Cruz Biotech, Santa Cruz, CA), and Connexin 43 (rabbit polyclonal, 1:100, Sigma). Stained tissue was examined by Leica DMRB fluorescent microscope and a Zeiss LSM 510 two-photon confocal laser scanning microscope. Cell engraftment was confirmed by identification of GFP expression under fluorescent microscopy. Colocalization of troponin, alpha sarcomeric actin, and connexin 43 with GFP was visualized with streptavidin-conjugated to Alexa Fluor Red 555 (Invitrogen Molecular Probes, Carlsbad, CA).

Statistical analysis. Descriptive statistics included mean and standard error. Comparison between groups was performed using students' t-test for independent and normally distributed data variables using SPSS 11.0. For comparison between multiple groups, ANOVA with Bonferroni correction was utilized. Significance was assumed when $p<0.05$.

RESULTS

Quantitation of left ventricular ejection fraction (LVEF) by *in vivo* MRI. As seen in **figure 1a and b**, MRI indicated that AMI led to significant reduction in LVEF at 1 week in all groups compared to sham operated, normal hearts [60.9±1.4% (n=5)] ($p<0.01$), illustrating the effectiveness of this murine AMI model. A significant improvement of LVEF in the mESC-treated [40.2 ±2.0% (n=23)] group was seen versus mEF- [29.4 ± 1.5% (n=17)] and NS-treated [26.4 ± 1.8% (n=6)] ($p<0.05$) groups. No significant improvement was observed in the mEF- versus NS-treated group. Measurements of LV end-diastolic and –systolic volumes are included in **Table 1**.

Measurement of maximal elastance (EMax) and end systolic elastance (Ees) by pressure-volume (PV) loop analysis. As seen in **figure 1c**, PV loop analysis demonstrated significantly compromised Emax (mmHg/mL) in the mEF- [9.95 ± 1.4 (n=4)] and NS-treated [5.8 ± 1.2 (n=4)] groups compared to normal hearts [22.6 ± 2.5 (n=5)] ($p<0.05$) at 1 week. However, a preserved Emax (mmHg/mL) was noticeable in the mESC-treated group [18.4 ± 3.5 (n=4)], which was significantly higher than the mEF- and NS-treated groups ($p<0.05$). No significant improvement was observed in Emax in the mEF- versus the NS-treated group. The Ees data paralleled these findings with a significant decrease in the NS-treated [4.1 ± 0.7 (n=4)] group versus normal hearts [12.5 ± 1.2 (n=5)] ($p<0.05$) and a significant preservation of Ees in the mESC-treated [8.8 ± 1.5 (n=4)] versus the mEF- and NS-treated groups ($p<0.05$). No significant improvement was observed in Ees in the mEF- versus NS-treated group. As shown in **figure 1d**, the left ventricular volumes measured by PV-loop in the mEF and NS groups demonstrate negative remodeling, while mESC treated hearts showed the least dilatation. The improved systolic and diastolic functions measured by the PV loops provide physiologic confirmation of *in vivo* MRI data, as left ventricular volumes measured by MRI and PV loop correlate (**figure 1e**). For further results of invasive hemodynamic measurements, please refer to **Table 1**.

	Normal	mESC	mEF	NS
MRI				
LVEF (%)	60.9 ± 1.4	40.2 ±2.0	29.4 ± 1.5	26.4 ± 1.8
LVED volume (mL)	4.23 ± 0.5	4.53 ± 0.6	5.74 ± 0.6	8.32 ± 0.7
LVES volume (mL)	1.63 ± 0.2	2.67 ± 0.2	4.09 ± 0.3	6.14 ± 0.5
PV-Loop				
Heart rate (bpm)	277.25 ± 10.60	302.75 ± 26.93	319.25 ± 16.45	260.00 ± 22.51
End-systolic Volume (uL)	26.72 ± 0.49	21.65 ± 4.82	40.56 ± 8.67	45.82 ± 8.89
End-diastolic Volume (uL)	29.29 ± 0.47	24.00 ± 5.56	43.15 ± 9.21	49.40 ± 9.67
End-systolic Pressure (mmHg)	83.86 ± 9.17 †	85.92 ± 5.91 †	71.40 ± 6.55	49.84 ± 5.35
End-diastolic Pressure (mmHg)	5.15 ± 1.21	19.14 ± 7.01	6.50 ± 0.54	8.21 ± 1.64
Arterial Elastance (Ea) (mmHg/uL)	29.34 ± 9.50	37.50 ± 11.56	22.04 ± 3.88	10.62 ± 3.35
dPdt max (mmHg/sec)	4100.50 ± 412.10	3867.50 ± 751.61	3108.75 ± 293.20	2157.00 ± 358.83
dPdt min (mmHg/sec)	-2993.25 ± 138.66 †	-2779.75 ± 144.06 †	-2397.75 ± 107.80	-1578.50 ± 304.29
Tau_w (msec)	15.01 ± 1.32	21.38 ± 4.32	15.13 ± 1.16	12.75 ± 3.89
Maximal Power (mWatts)	0.79 ± 0.10	0.78 ± 0.07	1.15 ± 0.45	0.84 ± 0.27
Preload adjusted maximal power (mWatts/µL^2)	9.21 ± 1.19	18.88 ± 6.13 †	5.87 ± 0.76	3.69 ± 1.25

Table 1. Steady-state hemodynamic measurements by MRI and PV-loop. † indicates p<0.05 vs. NS (†), no symbols indicate p=NS (ANOVA).

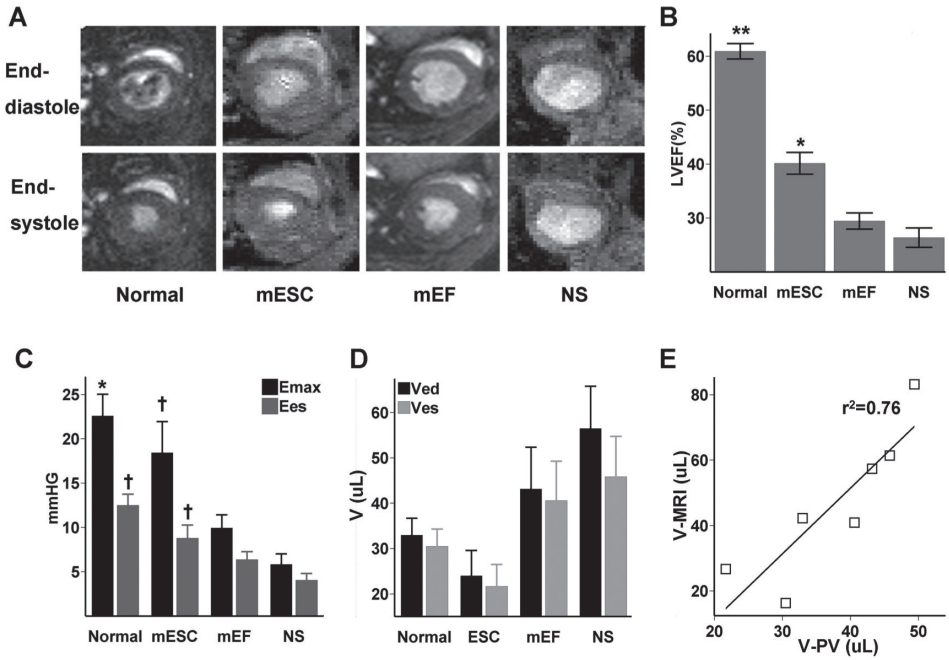

Figure 1. Functional outcomes after mESC and mEF transplantation. (a) Representative MR images of each group (normal, mESC, mEF, and NS) shown in end-diastole and end-systole at one week after LAD ligation and cell transplantation. The mESC-treated group demonstrated increased LVEF with visual confirmation from the MR images. (b) One week after LAD ligation and cell transplantation, MRI indicated significant improvement in the left ventricular ejection fraction (LVEF) in the mESC versus mEF and NS groups. ** Indicate $p<0.01$ vs. all groups, * represents $p<0.05$ vs. MEF and NS (ANOVA). (c) One week after LAD ligation and cell transplantation, PV loop analysis demonstrated compromised Emax (mmHg/µL) in the mEF and NS groups compared to normal hearts. A preserved Emax (mmHg/µL) was noticeable in the mESC group, which was significantly higher than the NS group. No significant improvement was observed in Emax in the mEF group versus the NS group. The Ees data show significant decrease in the NS group versus normal hearts and a significant preservation of Ees in the mESC group versus the NS group. No significant improvement was observed in the mEF group versus NS. * Indicates $p<0.05$ vs. mEF and NS, † indicates $p<0.05$ vs. NS ($n>4$/ group, ANOVA). (d) PV loop measurements of left ventricular volumes in end-systole (Ves) and end-diastole (Ved) show a decreased ventricular dilatation in the mESC group (p=NS). (e) Scatter plot of average left ventricular volumes in each group measured by PV loop (V-PV) and MRI (V-MRI), with $r^2=0.76$.

Determination of transplanted cell survival by *in vivo* BLI and *ex vivo* TaqMan PCR. Stable mESC and mEF transfection with GFP and firefly luciferase (fluc) generated mESC-GFP$^+$-fluc$^+$ and mEF-GFP$^+$-fluc$^+$ cell lines. The cells were selected and tested for fluc signal by bioluminescence imaging (BLI). Expression of fluc signal correlated robustly with cell number (r^2=0.99 and r^2=0.95, respectively, **figure 2a-c**). Thus, BLI was validated as a tool to monitor cell viability quantitatively as the signal intensity reflected the number of viable cells *in vitro*. Following transplantation of the transfected cells, BLI signal from the mESC-treated group decreased until post operative day (POD) 2. At POD 8 and 14, there was a significant ($p<0.01$) increase in signal due to the rapid division of the undifferentiated mESC (**figure 3a-b**); probably commencing teratoma formation as already shown in our earlier work.[13] However, in the mEF-treated group, signal increased until POD 2 but decreased thereafter, suggesting cell death (**figure 3a-b**). *Ex vivo* TaqMan PCR (TM-PCR) results indicated significantly lower cycle numbers over time in the mESC-treated group compared to the increasing cycle numbers in the mEF-treated group (**figure 3c**), which is representative of higher number of viable male donor cells in the mESC group.[14] Thus, *ex vivo* TM-PCR correlated well with the BLI results (**figure 3d**). This finding supports *in vivo* MRI data in which cell survival, a major biological property, is significantly enhanced in order for the transplanted mESC to remain biologically active to restore the injured myocardium.

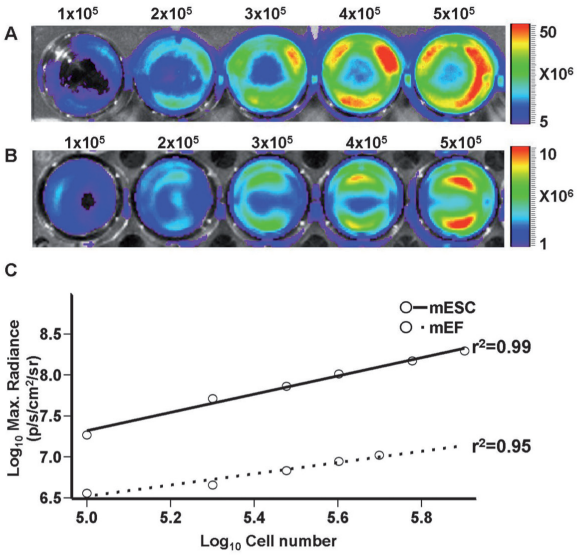

Figure 2. *In Vitro* Firefly Luciferase (fluc) signal correlates with cell number. (a, b) Bioluminescence (BLI) image showing increasing fluc signal with increasing cell number in mouse embryonic stem cells (mESC, a) and embryonic fibroblasts (mEF, b). Bars represent maximum radiance (p/s/cm^2/sr). (c) Correlation plot showing robust correlation of fluc signal and cell number for mESC and mEF (r^2=0.99 and r^2=0.95, respectively).

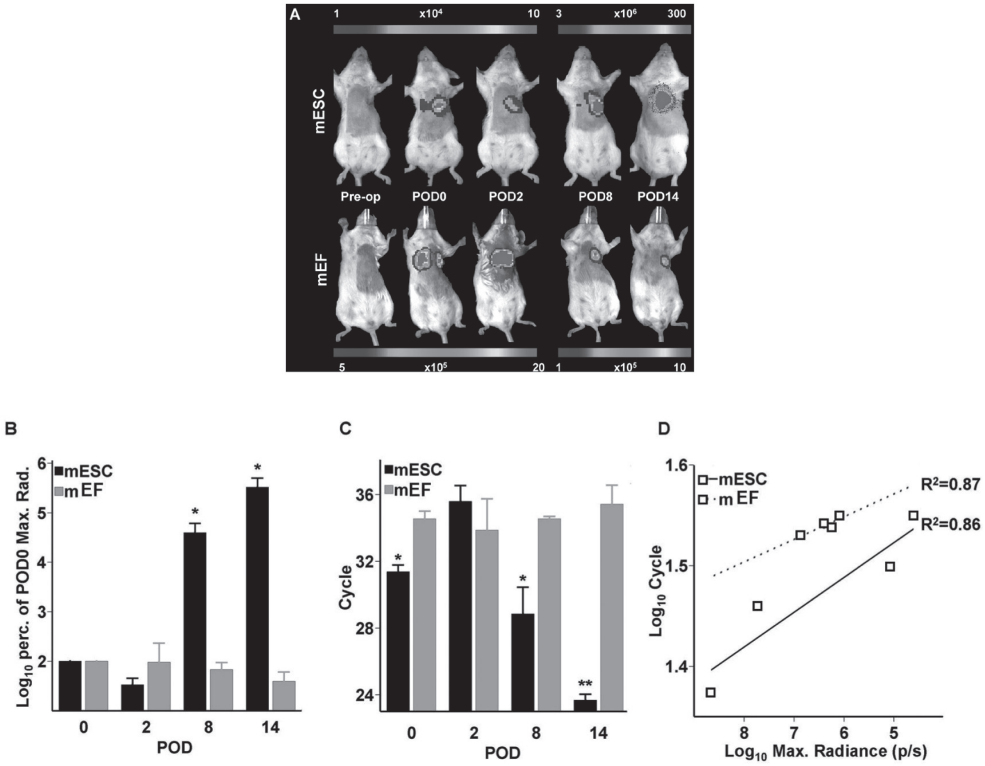

Figure 3. Transplanted Cell Survival by *in vivo* Bioluminescence and ex vivo TaqMan PCR. (a) Representative BLI images of mESC survival, tracked longitudinally at post-operative day (POD) 0, 2, 8, and 14. The survival decreases from POD 0 to POD 2 after which there is a notable increase at POD 8 and 14 due to rapid division. Color bars represent maximum radiance (p/s/cm^2/sr). (b) Normalized plot indicating significant ($p<0.01$) mESC proliferation starting on POD 2 and gradual cell death in the mEF group starting on POD 2 ($n>4$/group). Y-axis shows the $\log_{10}$ percentage of the average BLI signal on POD 0. * Indicates $p<0.01$ vs. mESC on POD 0, 2, and all mEF time points (ANOVA). (c) Ex vivo TaqMan PCR for SRY gene representing the male mESC survival at POD 0, 2, 8, and 14 which demonstrates a similar trend as seen in the *in vivo* BLI ($n>4$/group). * Indicates $p<0.05$ vs. mEF, ** indicate $p<0.01$ vs. mEF (ANOVA). (d) Correlation plot showing correlation ($r^2=0.86$ and $r^2=0.87$ for mESC and mEF, respectively) between *in vivo* BLI and ex vivo TaqMan PCR.

Gene expression profiling by TM-PCR for matrix metalloproteinase (MMP)-1β, -2, -9, -14, tumor necrosis factor (TNF)-a, vascular endothelial growth factor (VEGF)-A, procollagen-2a1, insulin-like growth factor (IGF) 1, transforming growth factor (TGF) -b, angiotensin converting enzyme (ACE), Flk-1, and NFkβ-1. Relative quantitation of mRNA expression of 12 genes (4 mice/group) using RT-PCR demonstrated significant increase of TNF-a in the mESC-treated group when compared to mEF- and NS-treated groups (501% vs. 77% and 219%, respec-

tively, p<0.01). Significant up-regulation of VEGF-A was also observed in mESC-treated group compared to the mEF and NS-treated groups (104% vs. 13% and 42%, respectively, p<0.01). On the other hand, mESC-treated mice demonstrated a trend towards down-regulation of MMP-1β and procollagen-2α1 expression when compared to NS-treated groups (p>0.05). The mRNA expressions of the remainder of genes; IGF1, NFkβ-1, MMP-2, -9, -14, TGFb, ACE, and Flk-1 did not demonstrate significant difference among mESC- mEF- and NS-treated groups. The gene expression profiles of TNF-α, which may have had an enhanced anti-apoptotic effects, and VEGF-A, consistent with proangiogenic effects, were demonstrated in the mESC-treated group (**figure 4**).

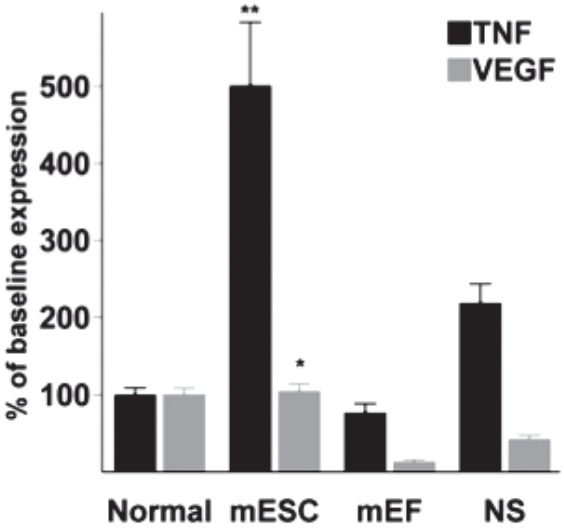

Figure 4. Relative quantitation of TNF-α and VEGF-A expression. Relative quantitation of mRNA expression on POD 7, normalized to the percentage of expression in normal, sham-operated hearts. A significant upregulation is noticeable in the mESC group. ** indicate p<0.01 vs. all groups, * indicates p<0.01 vs. mEF and NS (ANOVA).

Immunohistology of mESC cardiomyocyte differentiation. As seen in **figure 5** (**a-d**), cross-sectional images of H&E stained hearts demonstrate thinning of myocardial tissue and dilatation of LV chamber after LAD ligation. However, in the mESC treated mice, restoration of the LV wall mass and reduction of LV dilatation are seen. Co-localization of GFP with troponin and α-sarcomeric actin in isolated cells demonstrated potential differentiation of the mESC into cardiomyocytes as shown in **figure 5** (**e-h**). Colocalization of GFP with Connexin 43 suggest the formation of gap junctions as represented in **figure 5i**.

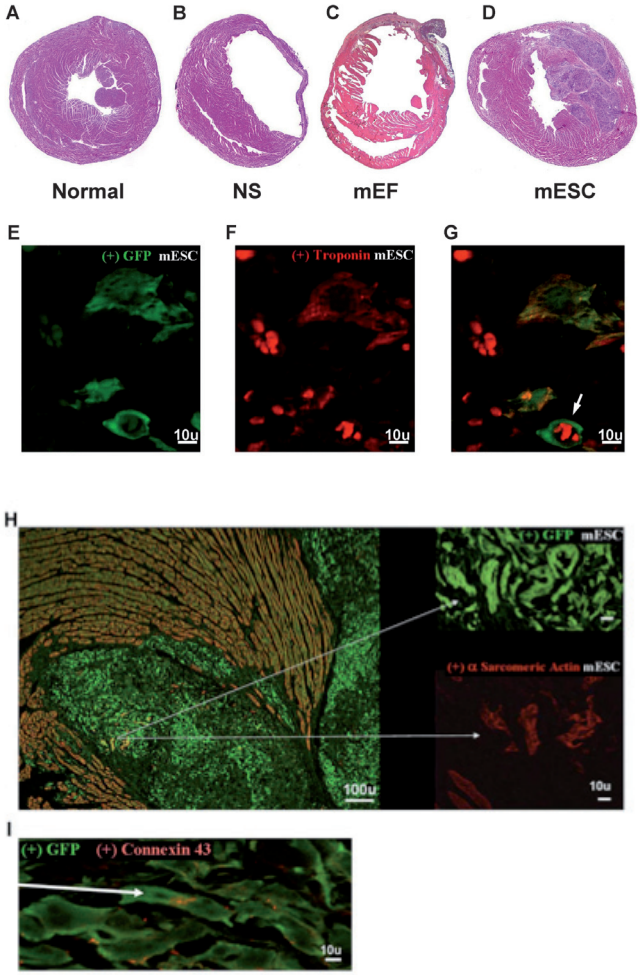

Figure 5. Histopathology of Anti-remodeling Effect and Cardiomyocyte Differentiation after mESC transplantation on POD 7. (a-d) Cross-sectional representative images of H&E stained (a) normal heart, (b) LAD ligation control, demonstrating thinning and dilatation of the ventricular wall, (c) mEF treated heart and (d) mESC treated heart demonstrating the restoration of the LV wall mass. (e) Confocal microscopy picture showing GFP positive stained mESC. (f) Confocal microscopy picture showing same cells as 5D expressing troponin. The 7-micron clustered round structures probably represent non-specifically stained red blood cells. (g) Overlay of 5D-E, showing co-localization of GFP with troponin, suggestive for a mESC-derived cardiomyocyte. Note that the non-specifically colored blood cells locate inside a GFP-stained blood vessel (white arrow), suggesting mESC- derived neovasculogenesis. (h) Image showing co-localization of GFP-positive mESC with alpha sarcomeric actin. (i) Image showing co-localization of GFP with connexin 43 (white arrow).

DISCUSSION

Cardiomyocyte death or dysfunction following an acute myocardial infarction (AMI) results in pathological remodeling of the left ventricle with eventual sequela of heart failure. Despite recent reports of the regenerative potential of cell-based therapies in the injured myocardium, a definitive mechanism of the enhanced myocardial function has not been elucidated. In the present study, we have provided independent support for *in vivo* MRI data by PV-loop and established the fundamental biological importance of cell survival, cell differentiation, and paracrine effects as potential mechanisms of mESC underlying myocardial restoration. The investigation focused on the immediate effects of cell transplantation post-AMI because teratoma formation would have likely interfered with reliable measurements during longer follow-up[15], as greatly increased mESC BLI signal on POD 14 confirmed. Our data demonstrated significantly improved LVEF measured by *in vivo* MRI, the most commonly utilized clinical end-point. This finding has been confirmed by end-systolic and maximal elastance values as measured by PV loop indicating improved systolic and diastolic functions as early as one week following mESC treatment. The improvement of diastolic function can be attributed to the augmentation of the infarct region's elasticity and recovery in the overall maximal elastance in the mESC-treated group. Moreover, we found a correlation between left ventricular volumes as measured by MRI and PV-loop.

These findings challenge the current notion that myocardial function is improved irrespective of cell type.[16, 17] The preservation of cardiac performance following cell transplantation cannot be attributed merely to the physical scaffolding effect but also must arise from the biological properties of the transplanted cells. During myocardial ischemia, the ischemic region develops diastolic and subsequent systolic abnormality.[18] Studies have confirmed the Frank-Starling relationship in which contractile function is preserved with reduction in ventricular volume.[19] In fact, our PV-loop results indicate a reduction in ventricular volume in the mESC group. This reduction involves complex yet fundamental biological processes. First, the prolonged survival kinetics of mESC can offer a longer lasting scaffolding effect, which may help to explain both the reduction in pathological remodeling and sustained restoration. More importantly, however, the persistence of viable mESC generates biologically active stimuli to salvage the injured myocytes. Thus, this enhanced survival of mESC enables a second potential mechanistic explanation for *in vivo* MRI findings of myocardial restoration: paracrine effect. The results from *ex vivo* TM-PCR demonstrate that the potential anti-apoptotic cytokine, TNF-a, was significantly upregulated in the mESC-treated group. TNF-α has been shown to have negative inotropic effects, to induce resistance to hypoxic stress in cardiomyocytes, and to play a role in the recruitment of stem cells.[20-23] It must be stated, however, that the increased TNF-a expression could also be attributable to a greater mass effect of mESC, with a subsequent greater endoge-

nous inflammatory reaction, a greater mESC-induced monocyte influx, or teratoma formation leading to endogenous TNF-a production. In addition, the observed up-regulation of VEGF-A in this study may promote angiogenesis to attenuate the ischemic insult to recover the injured cardiomyocytes. Finally, non-significant trends towards down-regulation of matrix metalloproteinase-1 (MMP-1) and procollagen 2α-1 have also been detected, which may contribute to decreased cardiac matrix remodeling in failing hearts.[24] Surprisingly, we did not observe upregulation of MMP-2 and -9. This may have been because the absence of T-cells in the SCID mice, on which MMP-2 and -9 expressions have been shown to depend.[25] Taken together, these TM-PCR results suggest that multiple mechanisms underlie the restoration by mESC.

The pluripotency of mESC may lead to regeneration of cardiac tissue after cardiomyogenic differentiation.26 In order to contract synchronously with host cardiomyocytes, newly formed mESC-derived cardiomyocytes must undergo electromechanical coupling through the formation of gap junctions *in vivo* with the host myocardium.26, 27 This study provides possible evidence that donor mESC are capable of engrafting within the host myocardium and differentiating into cardiomyocytes. While these findings are encouraging, it must be noted that this was a low-frequency event, making it less likely that the observed functional improvement can be attributed to robust cardiac regeneration by mESC-derived cardiomyocytes.

There are several limitations of this study. First of all, in order to investigate the acute effect of cell survival, we chose to compare fast-growing, undifferentiated mESC and less active mEF. This gave us the opportunity to study the relationship between cardiac function and cell survival in a relatively short period of one week. However, it must be stated that eventual teratoma formation, as suggested by our BLI findings on POD 14 and consistent with the literature[13, 15, 28], would likely hamper long term restoration of cardiac function. Secondly, this study does not provide insight in acute post-operative infarct size, which may have been dependent upon cell type. All operations, however, were conducted by the same experienced micro-surgeon that was blinded to the study. Moreover, after one week, all operated groups had a significant compromised LVEF on MRI, which lead to the assumption that infarct size had been comparable in all study groups. Third, we focused on validating the most important MRI data, namely LVED and LVES. Wall thickness, which could have correlated with cell survival, was not measured since we did not anticipate regenerative changes in the immediate period after AMI. Other studies are currently underway to address the regenerative changes by measuring wall thickness.

In conclusion, this is the first study to provide a fundamental functional and biological evaluation of *in vivo* MRI in mESC therapy. This study has shown that mESC are superior to mEF in restoring cardiac function in the immediate post-AMI period. A very fundamental notion that

the cells must at the very least survive to restore the myocardium is confirmed as the enhanced survival of mESC is attributed as one of the key factors in myocardial restoration. Improved survival of transplanted cells may not only offer a physical scaffolding mechanism but, more importantly, biological support by generating sustained paracrine effects after injury. We have also observed that mESC retain the ability to differentiate into cardiomyocytes, albeit at low frequency. Unfortunately, although the pluripotency and robust proliferation are among the major advantages of embryonic stem cells, these characteristics also contribute to teratoma formation[13, 15], which, for the present, prevents clinical translation. Further research regarding directed differentiation of mESC into cardiomyocytes may lead to a safe regenerative therapy for myocardial disease in the future.

ACKNOWLEDGEMENTS

We greatly appreciate the assistance in immunohistology from Ms. Pauline Chu and the help from Ms. Sally Zhang and Mr. Anant Patel with PCR. This work was supported by the NRSA Fellowship HL082447-01 (SLH), Donald W. Reynolds Foundation (PCY), Falk Cardiovascular Research Fund (RCR), NIH F32 and NIH K23 HL04338-01 (PCY).

REFERENCES:

1. Schachinger V, Erbs S, Elsasser A, Haberbosch W, Hambrecht R, Holschermann H, Yu J, Corti R, Mathey DG, Hamm CW, Suselbeck T, Assmus B, Tonn T, Dimmeler S, Zeiher AM. Intracoronary bone marrow-derived progenitor cells in acute myocardial infarction. *N Engl J Med.* 2006;355(12):1210-1221.
2. Chien KR. Stem cells: lost in translation. *Nature.* 2004;428(6983):607-608.
3. Kato S, Spinale FG, Tanaka R, Johnson W, Cooper Gt, Zile MR. Inhibition of collagen cross-linking: effects on fibrillar collagen and ventricular diastolic function. *Am J Physiol.* 1995;269(3 Pt 2):H863-868.
4. Kofidis T, de Bruin JL, Yamane T, Tanaka M, Lebl DR, Swijnenburg RJ, Weissman IL, Robbins RC. Stimulation of paracrine pathways with growth factors enhances embryonic stem cell engraftment and host-specific differentiation in the heart after ischemic myocardial injury. *Circulation.* 2005;111(19):2486-2493.
5. Li RK, Weisel RD, Mickle DA, Jia ZQ, Kim EJ, Sakai T, Tomita S, Schwartz L, Iwanochko M, Husain M, Cusimano RJ, Burns RJ, Yau TM. Autologous porcine heart cell transplantation improved heart function after a myocardial infarction. *J Thorac Cardiovasc Surg.* 2000;119(1):62-68.
6. Tomita S, Li RK, Weisel RD, Mickle DA, Kim EJ, Sakai T, Jia ZQ. Autologous transplantation of bone marrow cells improves damaged heart function. *Circulation.* 1999;100(19 Suppl):II247-256.
7. Arai T, Kofidis T, Bulte JW, de Bruin J, Venook RD, Berry GJ, McConnell MV, Quertermous T, Robbins RC, Yang PC. Dual *in vivo* magnetic resonance evaluation of magnetically labeled mouse embryonic stem cells and cardiac function at 1.5 t. *Magn Reson Med.* 2006;55(1):203-209.
8. Meyer GP, Wollert KC, Lotz J, Steffens J, Lippolt P, Fichtner S, Hecker H, Schaefer A, Arseniev L, Hertenstein B, Ganser A, Drexler H. Intracoronary bone marrow cell transfer after myocardial infarction: eighteen months' follow-up data from the randomized, controlled BOOST (BOne marrOw transfer to enhance ST-elevation infarct regeneration) trial. *Circulation.* 2006;113(10):1287-1294.
9. Orlic D, Kajstura J, Chimenti S, Jakoniuk I, Anderson SM, Li B, Pickel J, McKay R, Nadal-Ginard B, Bodine DM, Leri A, Anversa P. Bone marrow cells regenerate infarcted myocardium. *Nature.* 2001;410(6829):701-705.
10. Lunde K, Solheim S, Aakhus S, Arnesen H, Abdelnoor M, Egeland T, Endresen K, Ilebekk A, Mangschau A, Fjeld JG, Smith HJ, Taraldsrud E, Grogaard HK, Bjornerheim R, Brekke M, Muller C, Hopp E, Ragnarsson A, Brinchmann JE, Forfang K. Intracoronary injection of

mononuclear bone marrow cells in acute myocardial infarction. *N Engl J Med.* 2006;355(12):1199-1209.

11. Assmus B, Honold J, Schachinger V, Britten MB, Fischer-Rasokat U, Lehmann R, Teupe C, Pistorius K, Martin H, Abolmaali ND, Tonn T, Dimmeler S, Zeiher AM. Transcoronary transplantation of progenitor cells after myocardial infarction. *N Engl J Med.* 2006;355(12):1222-1232.
12. Kass DA, Midei M, Graves W, Brinker JA, Maughan WL. Use of a conductance (volume) catheter and transient inferior vena caval occlusion for rapid determination of pressure-volume relationships in man. *Cathet Cardiovasc Diagn.* 1988;15(3):192-202.
13. Swijnenburg RJ, Tanaka M, Vogel H, Baker J, Kofidis T, Gunawan F, Lebl DR, Caffarelli AD, de Bruin JL, Fedoseyeva EV, Robbins RC. Embryonic stem cell immunogenicity increases upon differentiation after transplantation into ischemic myocardium. *Circulation.* 2005;112(9 Suppl):I166-172.
14. Muller-Ehmsen J, Whittaker P, Kloner RA, Dow JS, Sakoda T, Long TI, Laird PW, Kedes L. Survival and development of neonatal rat cardiomyocytes transplanted into adult myocardium. *J Mol Cell Cardiol.* 2002;34(2):107-116.
15. Nussbaum J, Minami E, Laflamme MA, Virag JA, Ware CB, Masino A, Muskheli V, Pabon L, Reinecke H, Murry CE. Transplantation of undifferentiated murine embryonic stem cells in the heart: teratoma formation and immune response. *Faseb J.* 2007;21(7):1345-1357.
16. Jain M, DerSimonian H, Brenner DA, Ngoy S, Teller P, Edge AS, Zawadzka A, Wetzel K, Sawyer DB, Colucci WS, Apstein CS, Liao R. Cell therapy attenuates deleterious ventricular remodeling and improves cardiac performance after myocardial infarction. *Circulation.* 2001;103(14):1920-1927.
17. Weisel RD, Li RK, Mickle DA, Yau TM. Cell transplantation comes of age. *J Thorac Cardiovasc Surg.* 2001;121(5):835-836.
18. Bhatnagar SK, al-Yusuf AR. Left ventricular blood flow analysis in patients with and without a thrombus after first Q wave acute anterior myocardial infarction: two-dimensional Doppler echocardiographic study. *Angiology.* 1992;43(3 Pt 1):188-194.
19. Li RK, Mickle DA, Weisel RD, Zhang J, Mohabeer MK. *In vivo* survival and function of transplanted rat cardiomyocytes. *Circ Res.* 1996;78(2):283-288.
20. Chen Y, Ke Q, Yang Y, Rana JS, Tang J, Morgan JP, Xiao YF. Cardiomyocytes overexpressing TNF-alpha attract migration of embryonic stem cells via activation of p38 and c-Jun amino-terminal kinase. *Faseb J.* 2003;17(15):2231-2239.
21. Kurrelmeyer KM, Michael LH, Baumgarten G, Taffet GE, Peschon JJ, Sivasubramanian N, Entman ML, Mann DL. Endogenous tumor necrosis factor protects the adult cardiac myocyte against ischemic-induced apoptosis in a murine model of acute myocardial infarction. *Proc Natl Acad Sci U S A.* 2000;97(10):5456-5461.

22. Nakano M, Knowlton AA, Dibbs Z, Mann DL. Tumor necrosis factor-alpha confers resistance to hypoxic injury in the adult mammalian cardiac myocyte. *Circulation*. 1998;97(14):1392-1400.
23. Sivasubramanian N, Coker ML, Kurrelmeyer KM, MacLellan WR, DeMayo FJ, Spinale FG, Mann DL. Left ventricular remodeling in transgenic mice with cardiac restricted overexpression of tumor necrosis factor. *Circulation*. 2001;104(7):826-831.
24. Gunja-Smith Z, Morales AR, Romanelli R, Woessner JF, Jr. Remodeling of human myocardial collagen in idiopathic dilated cardiomyopathy. Role of metalloproteinases and pyridinoline cross-links. *Am J Pathol*. 1996;148(5):1639-1648.
25. Yu Q, Horak K, Larson DF. Role of T lymphocytes in hypertension-induced cardiac extracellular matrix remodeling. *Hypertension*. 2006;48(1):98-104.
26. Klug MG, Soonpaa MH, Koh GY, Field LJ. Genetically selected cardiomyocytes from differentiating embronic stem cells form stable intracardiac grafts. *J Clin Invest*. 1996;98(1):216-224.
27. Soonpaa MH, Koh GY, Klug MG, Field LJ. Formation of nascent intercalated disks between grafted fetal cardiomyocytes and host myocardium. *Science*. 1994;264(5155):98-101.
28. Cao F, Lin S, Xie X, Ray P, Patel M, Zhang X, Drukker M, Dylla SJ, Connolly AJ, Chen X, Weissman IL, Gambhir SS, Wu JC. *In vivo* visualization of embryonic stem cell survival, proliferation, and migration after cardiac delivery. *Circulation*. 2006;113(7):1005-1014.

CHAPTER 3

Spatial and Temporal Kinetics of Teratoma Formation from Murine Embryonic Stem Cell Transplantation

Feng Cao, Koen E.A. van der Bogt, Amir Sadrzadeh, Xiaoyan Xie,

Ahmad Y. Sheikh, Haichang Wang, Andrew J. Connolly,

Robert C. Robbins and Joseph C. Wu

Stem Cells and Development 2007 Dec;16(6):883-91.

ABSTRACT

Pluripotent embryonic stem cells (ESCs) have the potential to form teratomas composed of derivatives from all three germ layers in animal models. This tumorigenic potential prevents clinical translation of ESC research. In order to understand the biology and physiology of teratoma formation, we investigated the influence of undifferentiated ESC number, migration, and long-term follow up after transplantation. Murine ESCs were stably transduced with a self-inactivating (SIN) lentiviral vector with a constitutive ubiquitin promoter driving a double fusion (DF) reporter gene that consists of firefly luciferase and enhanced green fluorescent protein (Fluc-eGFP). To assess effects of cell numbers, varying numbers of ES-DF cells (1, 10, 100, 1000, and 10000) were injected subcutaneously into the dorsal regions of adult nude mice. To assess cell migration, $1x10^6$ ES-DF cells were injected intramyocardially into adult Sv129 mice and leakage to other extra-cardiac sites was monitored. To assess effects of long-term engraftment, $1x10^4$ ES-DF cells were injected intramyocardially into adult nude rats and cell survival response was monitored for 10 months. Our results show that ES-DF cells caused extra-cardiac teratoma in both immunocompetent and immunodeficient hosts; the lowest number of undifferentiated ESCs capable of causing teratoma was 500 to 1000; and long-term engraftment could be visualized for >300 days. Collectively, these results illustrate the potent tumorigenic potential of ESCs that present an enormous obstacle for future clinical studies.

INTRODUCTION

Embryonic stem cells (ESCs) can divide for unlimited generations without losing their ability to differentiate into cells of all three germ layers: ectoderm, mesoderm, and endoderm.[1] This pluripotency has given ESCs a major advantage over adult stem cells, which are generally tissue-specific and whose plasticity is more limited. Therefore, ESCs have great potential as future treatments for a wide variety of diseases, including cardiovascular[2], neurodegenerative[3], and endocrine[4] disorders. Ironically, the pluripotency and fast growth kinetics of ESCs also underlie their major disadvantage, as these characteristics can easily turn into undefined growth *in vivo*, giving rise to teratoma. Teratoma is a complex tumor consisting of cell lines from different germ layers which are known to develop after ESC transplantation in animal models.[5, 6] Therefore, prior to future clinical translation of ESC-based therapy, basic characteristics of teratoma formation must be elucidated.

Previous studies have shown that the tumorigenic potential of ESCs seems to decrease with increasing purity of pre-differentiated target cell populations, such as cardiomyocytes[7] or oligodendrocyte progenitor cells.[3] However, the maximum number of contaminant undifferentiated ESCs in these pre-differentiated populations for safe non-tumorigenic application remains unknown. Secondly, it has been shown recently that the tumorigenic potential of ESCs is dependent upon the site of transplantation.[8] Whether it is also possible that transplanted ESCs can form teratoma in distant graft sites need to be examined. Lastly, as teratoma formation usually presents around two to four weeks after transplantation[2, 8], the long-term fate of transplanted, undifferentiated cells has never been investigated. By studying these issues, this study aims to evaluate the *in vivo* tumorigenic characteristics of ESCs.

METHODS

Culture of undifferentiated ESCs. The murine ES-D3 cell line was derived originally from Sv129 mice and obtained commercially from ATCC (Manassas, VA). Undifferentiated cells were maintained with 1000 IU/mL leukemia inhibitory factor (Chemicon, ESGRO, ESG1107) and murine embryonic fibroblasts (MEFs) feeder layer inactivated by 10 ug/mL mitomycin C (Sigma). Murine ESCs were cultured on 0.1% gelatin-coated plastic dishes in ES medium containing Dulbecco Modified Eagle Medium (DMEM) supplemented with 15% fetal calf serum, 0.1 mmol/L β-mercaptoethanol, 2 mmol/L glutamine, and 0.1 mmol/L nonessential amino acids (Gibco) as described previously.[9] Culture medium was changed every day. Murine ESCs were passaged every 1 or 2 days. Images were obtained using a ZEISS Axiovert microscropy (Sutter Instrument).

Lentiviral transduction of ESCs with a double fusion (DF) reporter gene. The self-inactivating (SIN) lentiviral vector was constructed by deleting 133 bp in the U3 region of the 3' LTR,

including the TATA box and binding sites for transcription factors Sp1 and NF-kappaB as first described by Miyoshi *et al.*.[10] The deletion is transferred to the 5' LTR after reverse transcription and integration in infected cells, resulting in the transcriptional inactivation of the LTR in the proviruses. For the DF construct, pFUG-DF containing Fluc-eGFP was co-transfected into 293T cells with HIV-1 packaging vector (δ8.9) and vesicular stomatitis virus G glycoprotein-pseudotyped envelop vector (pVSVG) as described.[11] Lentivirus supernatant was concentrated by sediment centrifugation using a SW29 rotor at 50,000g for two hours. The concentrated virus was titered on 293T cells. ESCs were transduced at a multiplicity of infection (MOI) of 10. The infectivity was determined by eGFP expression as analyzed on FACScan (Becton Dickinson, San Jose, CA). These ESCs underwent a total of 3 rounds of FACS to increase the percentage of GFP+ to >95%. Note the sorter cannot guarantee 100% positive cells because of the setting, compensation, autofluorescence, and false positives. These stably transduced ESCs (termed ES-DF cells) are then used for subsequent *in vitro* studies and *in vivo* imaging as described next.

Effect of reporter genes on ESC proliferation. The control non-transduced ESCs and stably transduced ESCs (ES-DF cells) were plated uniformly in 96-well plates at a density of 5,000 cells per well. The CyQuant cell proliferation assay (Molecular Probes, Eugene, OR) was measured using a microplate spectrofluorometer (Gemini EM, Sunnyvale, CA) at 24, 48, and 72 hour time points. Eight samples were assayed and averaged.

Intramyocardial transplantation of ESCs into mice and rats. All animal study protocols were approved by the Stanford Animal Research Committee. Adult immunocompetent Sv129 mice (20-25g) and nude athymic rats (200-250g) underwent aseptic lateral thoracotomy. Briefly, animals received isoflurane (2% for mice, 3% for rats) for general anesthesia, banamine (2.5 mg/kg) for pain relief, and normal saline (0.2-2 ml) for volume replacement. Harvested ES-DF cells (after 3 rounds of FACS to increase eGFP+ cells to ~95-98%) were kept on ice for <30 minutes for optimal viability prior to injection into the mouse or rat myocardium. Sv129 mice (n=10) were injected intramyocardially with $1x10^6$ ES-DF cells in 50 µl PBS. Nude athymic rats (n=5) were injected intramyocardially with lower numbers of cells ($1x10^4$ ES-DF cells in 50 µl PBS) purposely to allow long-term study. Control animals (n=5 in each group) received non-transduced ESCs in equal numbers. All animals recovered uneventfully and underwent subsequent BLI.

Subcutaneous transplantation of varying numbers of ES-DF cells into mice. Adult nude mice (20-25g) received isoflurane (2%) for general anesthesia. Harvested ES-DF cells were kept on ice for <30 minutes for optimal viability. Mice (n=10) were injected subcutaneously within dorsal regions with 1, 10, 100, 1000 or 10,000 of ES-DF cells accompanied by 99999, 99990, 99900, 99000, and 90000 of irradiated MEFs, respectively, in 20 µl of Matrigel (BD Biosciences,

San Jose, CA). The final total cell number was 100,000 in each site. Afterwards, animals underwent longitudinal BLI as described below.

Optical bioluminescence imaging (BLI) of mESC transplantation. BLI was performed using the Xenogen *In Vivo* Imaging System (IVIS, Xenogen, Alameda, CA), which is an ultra-sensitive charged coupled device (CCD) camera.[12] Animals received isoflurane (2% for mice, 3% for rats) for general anesthesia. After intraperitoneal injection of the reporter probe D-Luciferin (250 mg/kg body weight), animals were imaged for 30 min using 1-min acquisition intervals repetitively for the study period. The gray-scale photographic images and BLI color images were analyzed using the Igor image analysis software (Wavemetrics, Lake Oswego, OR) and overlaid using the LivingImage software (Xenogen, Alameda, CA). Region of interest (ROI) were drawn over the signals and BLI was quantified in units of maximum photons per second per centimeter square per steridian (p/s/cm^2/sr) as described.[2]

Postmortem immunohistochemical staining. After completion of study periods, animals were sacrificed according to protocols approved by the Stanford Animal Research Committee. Explanted subcutaneous teratomas were routinely processed for hematoxylin and eosin (H&E). Slides were interpreted by an expert pathologist (A.J.C) blinded to the study.

Data analysis. Data are given as mean ± SD. For statistical analysis, the two-tailed Student's t–test was used. Differences were considered significant at $P<0.05$.

RESULTS

Lentiviral transduction and characterization of murine ES-DF cells. The DF construct consists of Fluc and eGFP reporter genes linked by a 14-amino acid long linker (LENSHASAGYQAST) as shown in **figure 1a**. After 48 hours of transduction, there was no change in morphology of ESCs (**figure 1b**) and the percentage of eGFP was quantified as 21±4 based on the average of three FACS scans (**figure 1c**). In order to obtain more purified GFP$^{(+)}$ cells, the cells were passaged 4 to 5 times and sorted three time during a 2 week period. After the third sort, the percentage of ESCs expressing eGFP was typically 95±3. These stably transduced ESCs (ES-DF) were used for further *in vitro* and *in vivo* analysis. To ensure that the construct and the lentiviral transduction did not favorably influence tumorigenic potential, we examined the growth kinetics of control non-transduced ESCs and ES-DF *in vitro*. Both control ESCs and ES-DF cells showed no significant differences in proliferation rate (P=NS) (**figure 1d**). Taken together, these data suggest that lentiviral transduction is a robust method to introduce reporter genes into ESCs without significantly affecting their self-renewal and pluripotency characteristics.

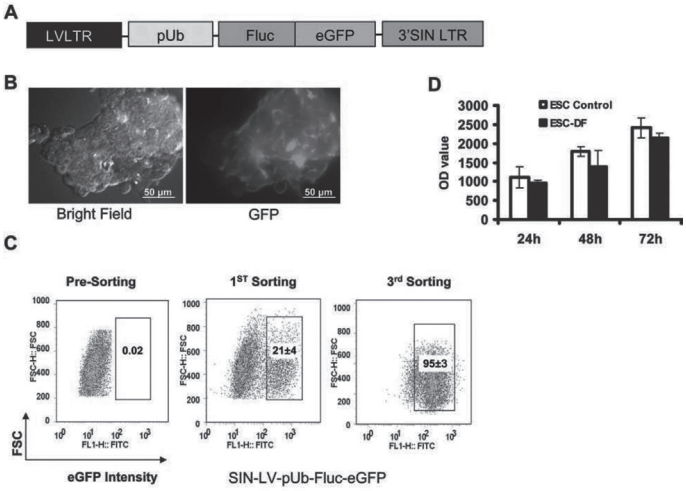

Figure 1. Stable lentiviral transduction of murine embryonic stem cells (ESCs) with a double fusion (DF) reporter gene. (a) Schematic overview of the lentiviral DF reporter construct with firefly luciferase (Fluc) and enhanced green fluorescent protein (eGFP). These reporter genes were cloned into a self-inactivating (SIN) lentiviral vector (LV) driven by an ubiquitin promoter (pUB). (b) Morphology of the transduced ES-DF cells, which clearly showed green fluorescence (left: brightfield, right: fluorescence). (c) Flow cytometry plots showing non-transduced control ESCs do not express GFP (left). After lentiviral transduction, the transduction efficiency is ~21±4% after the first round (middle) and ~95±3% after the third round of sorting (right). (d) CyQuant cell proliferation assay showing that lentiviral transduction and DF reporter gene expression did not significantly affect growth of ES-DF cells compared to control non-transduced ESCs.

Minimal number of undifferentiated murine ESCs causing teratoma formation. At present, it is not feasible to select or grow 100% pure ESC-derived progenitor cells.[13, 14] Thus, it is likely that at the time of therapeutic transplantation, mixed cell populations may still contain some undifferentiated ESCs. Therefore, we set out to determine the lowest threshold of undifferentiated ESC contaminant that can still cause teratoma formation. In order to do so, we first investigated the minimal reproducible cell number that can be imaged *in vitro*. The results from *in vitro* BLI indicated that 10,000 ES-DF cells were easily noticeable (**figure 2a**). Marginal signal from 1000 ES-DF cells led us to hypothesize that it is possible to image as low as 500 to 1000 cells *in vivo* if they are located within a compact region. Indeed, 7 days after subcutaneous transplantation of 500 to 1000 ES-DF cells, which were kept localized to the same region by Matrigel, faint signals were noticeable on BLI *in vivo* (**figure 2b**). Moreover, these 500 to 1000 ES-DF cells induced tumor growth over a time period of 3 months, which was confirmed by histology (**figure 2c**). By contrast, no such tumorigenic transformation was observed after transplantation of 1, 10, or 100 ES-DF cells.

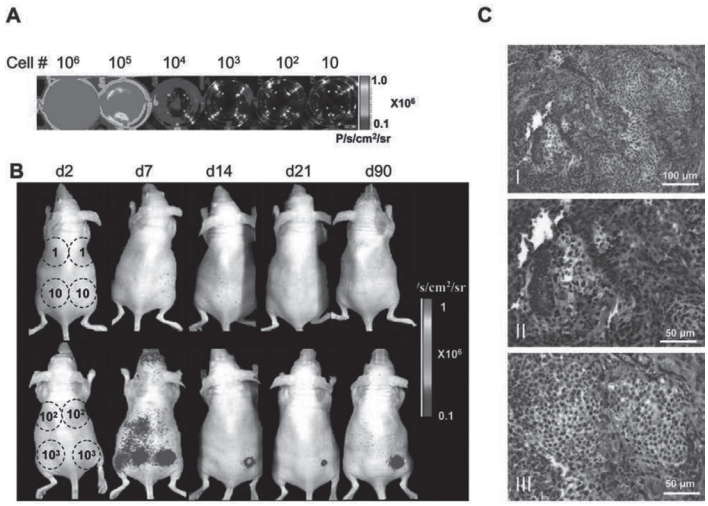

Figure 2. Potential for different numbers of undifferentiated ESCs to form teratomas *in vivo*. (a) *In vitro* BLI shows the ability to image different numbers of ESCs, with a lower threshold of around 1000 ESCs. (b) Different numbers of undifferentiated ESCs, as marked on the picture, were then subcutaneously transplanted into nude mice and accompanied by irradiated non-proliferating mouse embryonic fibroblasts to achieve a total cell number of 100,000 in 20 µl Matrigel. BLI imaging for 3 months revealed teratoma formation with only 500 to 1000 ESCs. (c) Postmortem H&E staining confirmed teratoma formation in the 500 to 1000 ESCs group: (I) lower power field of mesenchymal and gland cell differentiation; (II) gland cells; and (III) cartilage formation (arrow).

ESC survival and migration after intramyocardial injection. Previous studies have shown that transplantation of undifferentiated murine ESCs into immunodeficient mice leads to teratoma formation using conventional histological techniques.[15] However, these histological techniques do not allow for *in vivo* longitudinal tracking of tumorigenicity. To demonstrate the importance of following cell fate in a whole-body living animal system, we injected $1x10^6$ ES-DF cells intramyocardially into immunocompetent syngeneic Sv129 mice. Cell survival was monitored longitudinally for about 35 days. **Figure 3a** shows a representative Sv129 mouse whereby BLI revealed teratoma formation. Quantitative analysis showed cardiac bioluminescence signals increased from $1.3x10^6 \pm 1.0x10^5$ at day 2 to $1.9x10^7 \pm 1.3x10^6$ at day 7 to $5.4x10^7 \pm 4.7x10^6$ at day 14 and to $4.2x10^8 \pm 3.7x10^7$ p/s/cm²/sr at day 35. As early as 4 days after intramyocardial delivery, a strong BLI signal was present within the chest region. Moreover, a separate focal signal within the long femur bone marrow was noticeable, which is likely due to leakage from the intramyocardial injection and seeding peripherally. At day 35, all mice were too weak for further follow-up and had to be euthanized. During necropsy, the organs were explanted and imaged immediately. *Ex vivo* bioluminescence signals were found in the heart, spine, humerus, femur, submandible (**figure 3b**).

Animals injected with control non-transduced ESCs showed no bioluminescence signals as expected (data not shown). Finally, histological examination with H&E staining also confirmed presence of teratoma formation in the heart, femur, and submandible (**figure 4**). Interestingly, only a small amount of intramyocardially transplanted ES-DF cells expressed the cardiac-specific marker troponin T, suggesting that the *in vivo* differentiation of ESCs into cardiomyocytes also occurred at a low frequency (**figure 4a**).

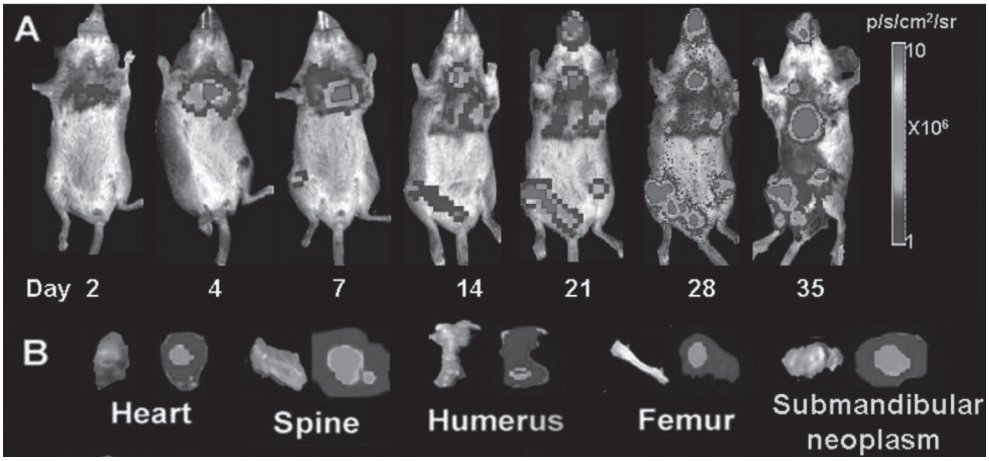

Figure 3. Noninvasive bioluminescence imaging of ESC survival, proliferation, and teratoma formation in Sv129 mice. (a) One million ES-DF cells were injected intramyocardially into immunocompetent syngeneic Sv129 mice hearts. Imaging of the same representative animal over 5 weeks showed a progressive increase in intra-cardiac and extra-cardiac signals. (b) Ex vivo imaging of explanted organs from the same sacrificed animal at week 5. Robust signals were seen in the heart, spine, humerus, femur, and submandible.

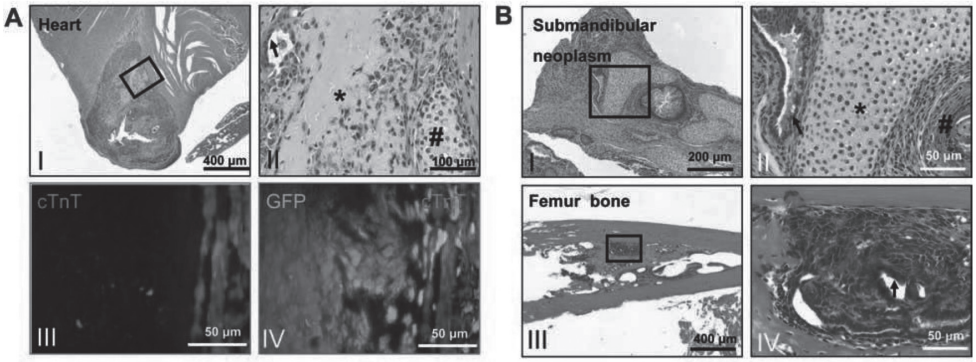

Figure 4. Postmortem histology confirms teratoma formation. (a) Representative H&E staining of a section of heart showing (I) teratoma (lower power field) with (II) epithelium (arrow), cartilage (#), and osteoid (*) formation inside (higher power field). Few numbers of the transplanted ES-DF cell population were found to differentiate into cardiomyocytes as assessed by double-staining of GFP and cardiac troponin T (cTNT) (III, IV). (b) Teratoma formation was also observed in extra-cardiac organs: (I) H&E staining showing submandibular teratoma formation (lower power field) and (II) typical gland (arrow), cartilage (*), and epidermis (#) development (high power field of I). Concordantly, teratoma formation was observed (III) in the femur bone with multiple cell lineages including (IV) gland cells (arrow).

Long-term tracking of ESC fate by BLI. In order to investigate whether lower cell number would have a different outcome, we decided to inject a smaller number (~10,000) of ES-DF cells and follow the animals for a longer period. Since the smaller size of mice was only able to bear teratoma formation for up to 5 weeks, we switched to the larger size rats. This also allowed us to test the influence of different animal species. After intramyocardial injection of 10,000 ES-DF cells, nude rats were followed by BLI longitudinally (**figure 5a**, **5b**). After 10 months, animals were sacrificed and hearts were explanted for visual inspection of gross morphology. Histological sectioning of all hearts confirmed differentiation into all three germ layers (**figure 5c**). These results indicate that, even after deliberate local delivery into the left ventricular mass, the process is still associated with extra-cardiac leakage and seeding to other organs.

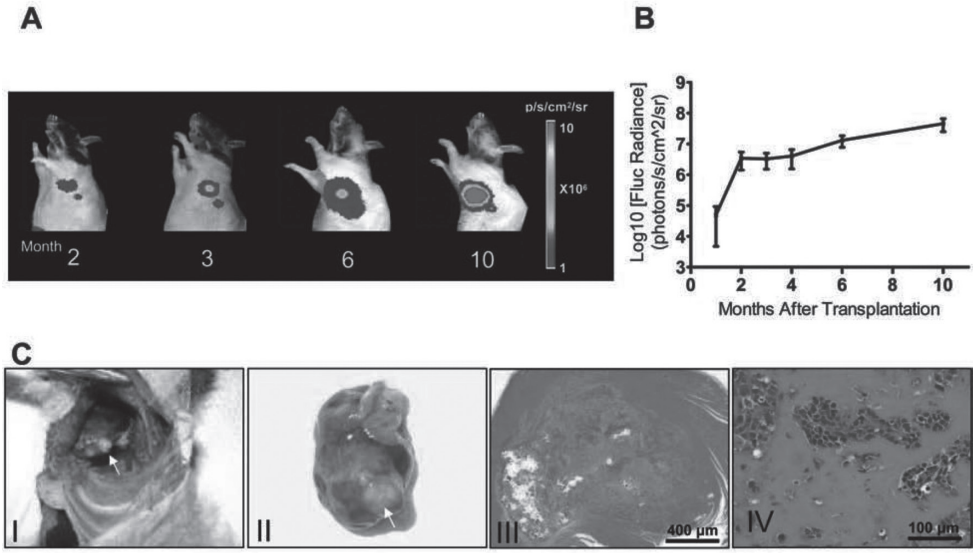

Figure 5. Long term noninvasive tracking of ESC survival kinetics in nude rats. (a) *In vivo* visualization of ESC growth and migration until 10 months after transplantation into the hearts of nude rats. (b) Growth curve of transplanted ES-DF cells *in vivo*. Y-axis shows BLI signal from a fixed region of interest (p/s/cm2/sr) over the heart, while the X-axis represents time after transplantation (months). (c) Gross (I) in situ and (II) ex vivo picture of the heart from figure 5a containing a visible teratoma. H&E staining of slides from the explanted heart confirms (III) clear-edged teratoma formation within the cardiac tissue (lower magnification), including (IV) bone formation.

DISCUSSION

ESCs hold great promise in regenerative medicine. However, several critical obstacles need to be resolved before ESCs can play a role in clinical medicine. Among these are the immunogenicity of ESCs, and perhaps more importantly from the safety standpoint, the tumorigenic ability of ESCs.[6, 16] This study has shown that molecular imaging is a reliable tool for long-term *in vivo* imaging of ESCs. Our major findings are as follows: (a) reporter genes do not affect ES cell viability and proliferation; (b) as low as 500-1000 undifferentiated ESCs are capable of inducing teratoma formation; and (c) ESCs are capable of causing teratomas in both intra-cardiac and extra-cardiac sites after local intramyocardial delivery.

Although the risk of teratoma formation may be reduced by prolonged cell differentiation before its engraftment, in reality pre-differentiated ESCs or ESC-derived precursor cells might still form teratoma after transplantation into animals.[17] Recently, Harkany *et al.* observed teratoma formation after transplantation of 400 murine ESCs in the brain of naive mice.[18] Here we pre-

sent further evidence that even 500 to 1000 murine ESCs were sufficient to induce teratoma formation, while less than 100 ESCs were not. In contrast, Nussbaum *et al*. have shown that 50,000 intramyocardially injected murine ESCs were not noticeable in the heart and spleen and did not form teratoma after 3 weeks.[16] Several factors might underlie the discrepancy between the findings. First of all, to mimic cell contamination, we have transplanted different numbers of ESCs accompanied by MEFs to achieve a total cell number of 100,000 cells. The MEFs might have contributed to better ESC engraftment, survival, and subsequent teratoma formation. Secondly, using conventional histological staining, Nussbaum *et al*. investigated teratoma formation at the site of transplantation (myocardium) and at one distant location (spleen), with both locations free of ESCs.[16] This was in concordance with a recent report, whereby teratomas were induced in the kidney capsule of immunodeficient mice but without any human ESC activity in the spleen after 8 weeks as well.[19] By contrast, using more sensitive *in vivo* whole body molecular imaging, which was validated by immediate *ex vivo* imaging of explanted organs, we did observe profound activity at other distant locations, such as the submandible and femur, suggesting ESC leakage during transplantation and subsequent engraftment and proliferation into teratoma. Taken together, these findings suggest longitudinal noninvasive imaging may give more valuable insight into teratoma formation and migration compared to conventional histology.

Previously, we had demonstrated the feasibility of using triple fusion reporter gene to track the fate of transplanted murine ESCs in living subjects by fluorescence, bioluminescence and positron emission tomography (PET) modalities.[2] This was followed by another study showing that not only does the herpes simplex virus thymidine kinase (HSV-tk) PET reporter gene can be used to monitor ESC engraftment, it also serves useful purpose as a suicide gene to ablate ESC misbehavior.[20] In the current study, we further expanded on these initial observations by using a SIN lentiviral vector with ubiquitin promoter driving the bioluminescence (Fluc) and fluorescence (eGFP) to address the influence of undifferentiated ESC number, migration, and long-term follow up after transplantation. The human immunodeficiency virus type 1 (HIV-1)-based lentiviral vector has been shown to be an excellent tool for stable and efficient gene transfer to mouse[21] and human ESCs.[22] The enhanced safety of the self-inactivating (SIN) lentivirus is achieved by (a) using a three-plasmid expression system which consists of packaging, envelop, and vector constructs[23], (b) by eliminating accessory genes (*vif, vpr, vpu,* and *nef*) from the packaging construct without losing the ability to transducer nondividing cells[24], and (c) by deleting the viral enhancer and promoter sequences from the long terminal repeat (LTR) sequence[10]. The double fusion construct we employed consists of two optical reporter genes (Fluc-eGFP) separated by a 14-amino acid linker. The Fluc enzyme catalyzes the oxidation of the D-luciferin (ATP and oxygen dependent) reporter probe into oxyluciferin, which emits low energy photons (2-3 eV) at 560 nm wavelength that can

be detected by an ultra-sensitive CCD camera[12]. By contrast, GFP does not require a substrate (or reporter probe) such as D-luciferin but rather relies on excitation wavelength in the visible light range of 395-600 nm. Wild-type GFP emits green (509 nm) light when excited by violet (395 nm) light. The variant eGFP has a shifted excitation spectrum to longer wavelength (488 nm) and has increased brightness (35-fold).[25] Thus, by using the double fusion reporter gene construct, we were able to perform FACS to isolate stably transduced ESCs (via eGFP) and track their fate in living animals (via Fluc) at a rapid and high-throughput fashion.[26]

In this study, we were able to reliably monitor the fate of 10,000 transplanted ESCs in the heart for a period as long as 10 months in living animals. The clinical relevance of these findings is profound. As an example, current clinical trials involving bone marrow stem cells for the infarcted heart report injecting a mean cell number of 6.8×10^7 to 2.36×10^8.[27-29] Assuming that the same cell numbers of human ESC-derived cardiac cells are used as treatment in the future, then ~500 undifferentiated ESCs (enough to give rise to teratomas in this study) as contaminant would represent a total population of less than 0.001%. Yet current selection methods for pre-differentiated ESC-derived cardiomyocytes typically yield a maximum purity of 70% for human ESCs[30] and 90% for murine ESCs.[14] This scenario highlights the tedious and careful clinical protocols that need to be devised to avoid contaminants.

Several limitations of the study need to be raised. First, we have focused on murine rather than human ESCs. While murine and human ESCs have been compared for their gene expression pattern[31], there is a lack of comparison studies on teratoma formation. In the future, the same issue of minimal human ESCs that can cause teratoma formation will need to be addressed. Second, ESCs tend to differentiate at an earlier stage when implanted subcutaneously (compared to intra-hepatic transplantation) as described by Cooke and colleagues[8]. In this respect, the well vascularized, growth factor-rich, and perhaps immune-privileged porous structure in the liver may help to maintain ESCs in undifferentiated state.[8] Thus, it is plausible that when transplanted in the liver, the minimal cell number needed for teratoma formation might be even lower than the 500 to 1,000 cells found on subcutaneous study in the present study. Third, we used nude mice while others have relied on severe combined immunodeficient (SCID) mice. Nude mice (lacking furs) are easier to image but have more natural killer (NK) cell activity as compared to SCID mice[32], which could also contribute to transplanted cell death by NK cell-mediated cytotoxicity.[33] Moreover, decreased tumor engraftment and higher regression rates of several tumor cell lines have been observed in nude mice as compared to increased tumor growth and larger tumor mass in SCID mice.[34, 35] These observations suggest that the actual cell number needed for teratoma formation could be even lower in the case of SCID mice.

In summary, we have provided important insight into the influence of ESC number, cell migration, and engraftment period on teratoma formation. These findings are an additional stimulus for further research on this topic. Therefore, our ongoing work is focusing on optimizing *in vitro* differentiating systems to acquire purer populations for transplantation, *in vivo* imaging of stem cell behavior, and how to control teratoma formation after transplantation. All these issues need thorough understanding in order for ESCs to play the prominent role they are expected to play in clinical treatments.

REFERENCES

1. Thomson JA, Itskovitz-Eldor J, Shapiro SS, Waknitz MA, Swiergiel JJ, Marshall VS, Jones JM. Embryonic stem cell lines derived from human blastocysts. *Science.* 1998;282(5391):1145-1147.
2. Cao F, Lin S, Xie X, Ray P, Patel M, Zhang X, Drukker M, Dylla SJ, Connolly AJ, Chen X, Weissman IL, Gambhir SS, Wu JC. *In vivo* visualization of embryonic stem cell survival, proliferation, and migration after cardiac delivery. *Circulation.* 2006;113(7):1005-1014.
3. Keirstead HS, Nistor G, Bernal G, Totoiu M, Cloutier F, Sharp K, Steward O. Human embryonic stem cell-derived oligodendrocyte progenitor cell transplants remyelinate and restore locomotion after spinal cord injury. *J Neurosci.* 2005;25(19):4694-4705.
4. Fujikawa T, Oh SH, Pi L, Hatch HM, Shupe T, Petersen BE. Teratoma formation leads to failure of treatment for type I diabetes using embryonic stem cell-derived insulin-producing cells. *Am J Pathol.* 2005;166(6):1781-1791.
5. Asano T, Sasaki K, Kitano Y, Terao K, Hanazono Y. *In vivo* tumor formation from primate embryonic stem cells. *Methods Mol Biol.* 2006;329:459-467.
6. Swijnenburg RJ, Tanaka M, Vogel H, Baker J, Kofidis T, Gunawan F, Lebl DR, Caffarelli AD, de Bruin JL, Fedoseyeva EV, Robbins RC. Embryonic stem cell immunogenicity increases upon differentiation after transplantation into ischemic myocardium. *Circulation.* 2005;112(9 Suppl):I166-172.
7. Kehat I, Khimovich L, Caspi O, Gepstein A, Shofti R, Arbel G, Huber I, Satin J, Itskovitz-Eldor J, Gepstein L. Electromechanical integration of cardiomyocytes derived from human embryonic stem cells. *Nat Biotechnol.* 2004;22(10):1282-1289.
8. Cooke MJ, Stojkovic M, Przyborski SA. Growth of teratomas derived from human pluripotent stem cells is influenced by the graft site. *Stem Cells Dev.* 2006;15(2):254-259.
9. Boheler KR, Czyz J, Tweedie D, Yang HT, Anisimov SV, Wobus AM. Differentiation of pluripotent embryonic stem cells into cardiomyocytes. *Circ Res.* 2002;91(3):189-201.
10. Miyoshi H, Blomer U, Takahashi M, Gage FH, Verma IM. Development of a self-inactivating lentivirus vector. *J Virol.* 1998;72(10):8150-8157.
11. De A, Lewis XZ, Gambhir SS. Noninvasive imaging of lentiviral-mediated reporter gene expression in living mice. *Mol Ther.* 2003;7(5 Pt 1):681-691.
12. Zhao H, Doyle TC, Coquoz O, Kalish F, Rice BW, Contag CH. Emission spectra of bioluminescent reporters and interaction with mammalian tissue determine the sensitivity of detection *in vivo*. *J Biomed Opt.* 2005;10(4):41210.
13. Chung Y, Klimanskaya I, Becker S, Marh J, Lu SJ, Johnson J, Meisner L, Lanza R. Embryonic and extraembryonic stem cell lines derived from single mouse blastomeres. *Nature.* 2006;439(7073):216-219.
14. Fukuda H, Takahashi J, Watanabe K, Hayashi H, Morizane A, Koyanagi M, Sasai Y, Hashimoto

N. Fluorescence-activated cell sorting-based purification of embryonic stem cell-derived neural precursors averts tumor formation after transplantation. *Stem Cells.* 2006;24(3):763-771.

15. Andrews PW. From teratocarcinomas to embryonic stem cells. *Philos Trans R Soc Lond B Biol Sci.* 2002;357(1420):405-417.
16. Nussbaum J, Minami E, Laflamme MA, Virag JA, Ware CB, Masino A, Muskheli V, Pabon L, Reinecke H, Murry CE. Transplantation of undifferentiated murine embryonic stem cells in the heart: teratoma formation and immune response. *Faseb J.* 2007;21(7):1345-1357.
17. Brederlau A, Correia AS, Anisimov SV, Elmi M, Paul G, Roybon L, Morizane A, Bergquist F, Riebe I, Nannmark U, Carta M, Hanse E, Takahashi J, Sasai Y, Funa K, Brundin P, Eriksson PS, Li JY. Transplantation of human embryonic stem cell-derived cells to a rat model of Parkinson's disease: effect of *in vitro* differentiation on graft survival and teratoma formation. *Stem Cells.* 2006;24(6):1433-1440.
18. Harkany T, Andang M, Kingma HJ, Gorcs TJ, Holmgren CD, Zilberter Y, Ernfors P. Region-specific generation of functional neurons from naive embryonic stem cells in adult brain. *J Neurochem.* 2004;88(5):1229-1239.
19. Blum B, Benvenisty N. Clonal analysis of human embryonic stem cell differentiation into teratomas. *Stem Cells.* 2007;25(8):1924-1930.
20. Cao F, Drukker M, Lin S, Sheikh AY, Xie X, Li Z, Connolly AJ, Weissman IL, Wu JC. Molecular imaging of embryonic stem cell misbehavior and suicide gene ablation. *Cloning Stem Cells.* 2007;9(1):107-117.
21. Oka M, Chang LJ, Costantini F, Terada N. Lentiviral vector-mediated gene transfer in embryonic stem cells. *Methods Mol Biol.* 2006;329:273-281.
22. Gropp M, Itsykson P, Singer O, Ben-Hur T, Reinhartz E, Galun E, Reubinoff BE. Stable genetic modification of human embryonic stem cells by lentiviral vectors. *Mol Ther.* 2003;7(2):281-287.
23. Naldini L, Blomer U, Gage FH, Trono D, Verma IM. Efficient transfer, integration, and sustained long-term expression of the transgene in adult rat brains injected with a lentiviral vector. *Proc Natl Acad Sci U S A.* 1996;93(21):11382-11388.
24. Kafri T, Blomer U, Peterson DA, Gage FH, Verma IM. Sustained expression of genes delivered directly into liver and muscle by lentiviral vectors. *Nat Genet.* 1997;17(3):314-317.
25. Massoud TF, Gambhir SS. Molecular imaging in living subjects: seeing fundamental biological processes in a new light. *Genes Dev.* 2003;17(5):545-580.
26. Wu JC, Tseng JR, Gambhir SS. Molecular imaging of cardiovascular gene products. *J Nucl Cardiol.* 2004;11(4):491-505.
27. Assmus B, Honold J, Schachinger V, Britten MB, Fischer-Rasokat U, Lehmann R, Teupe C, Pistorius K, Martin H, Abolmaali ND, Tonn T, Dimmeler S, Zeiher AM. Transcoronary transplanta-

tion of progenitor cells after myocardial infarction. *N Engl J Med.* 2006;355(12):1222-1232.

28. Lunde K, Solheim S, Aakhus S, Arnesen H, Abdelnoor M, Egeland T, Endresen K, Ilebekk A, Mangschau A, Fjeld JG, Smith HJ, Taraldsrud E, Grogaard HK, Bjornerheim R, Brekke M, Muller C, Hopp E, Ragnarsson A, Brinchmann JE, Forfang K. Intracoronary injection of mononuclear bone marrow cells in acute myocardial infarction. *N Engl J Med.* 2006;355(12):1199-1209.
29. Schachinger V, Erbs S, Elsasser A, Haberbosch W, Hambrecht R, Holschermann H, Yu J, Corti R, Mathey DG, Hamm CW, Suselbeck T, Assmus B, Tonn T, Dimmeler S, Zeiher AM. Intracoronary bone marrow-derived progenitor cells in acute myocardial infarction. *N Engl J Med.* 2006;355(12):1210-1221.
30. Xu C, Police S, Rao N, Carpenter MK. Characterization and enrichment of cardiomyocytes derived from human embryonic stem cells. *Circ Res.* 2002;91(6):501-508.
31. Sato N, Sanjuan IM, Heke M, Uchida M, Naef F, Brivanlou AH. Molecular signature of human embryonic stem cells and its comparison with the mouse. *Dev Biol.* 2003;260(2):404-413.
32. Shouval D, Rager-Zisman B, Quan P, Shafritz DA, Bloom BR, Reid LM. Role in nude mice of interferon and natural killer cells in inhibiting the tumorigenicity of human hepatocellular carcinoma cells infected with hepatitis B virus. *J Clin Invest.* 1983;72(2):707-717.
33. Rideout WM, 3rd, Hochedlinger K, Kyba M, Daley GQ, Jaenisch R. Correction of a genetic defect by nuclear transplantation and combined cell and gene therapy. *Cell.* 2002;109(1):17-27.
34. Hudson WA, Li Q, Le C, Kersey JH. Xenotransplantation of human lymphoid malignancies is optimized in mice with multiple immunologic defects. *Leukemia.* 1998;12(12):2029-2033.
35. Taghian A, Budach W, Zietman A, Freeman J, Gioioso D, Suit HD. Quantitative comparison between the transplantability of human and murine tumors into the brain of NCr/Sed-nu/nu nude and severe combined immunodeficient mice. *Cancer Res.* 1993;53(20):5018-5021.

CHAPTER 4

Molecular Imaging of Human Embryonic Stem Cells: Keeping an Eye on Differentiation, Tumorigenicity, and Immunogenicity

Koen E.A. van der Bogt, Rutger-Jan Swijnenburg,

Feng Cao and Joseph C. Wu

Cell Cycle 2006 Dec;5(23):2748-52

ABSTRACT

Human embryonic stem cells (hESCs) are capable of differentiation into every cell type of the human being. They are under extensive investigation for their regenerative potential in a variety of debilitating diseases. However, the field of hESC research is still in its infancy, as there are several critical issues that need to be resolved before clinical translation. Two major concerns are the ability of undifferentiated hESCs to form teratomas and the possibility of a provoked immune reaction after transplantation of hESCs into a new host. Therefore, it is imperative to develop non-invasive imaging modalities that allow for longitudinal, repetitive, and quantitative assessment of transplanted cell survival, proliferation, and migration *in vivo*. Reporter gene-based molecular imaging offers these characteristics and has great potential in the field of stem cell therapy. Moreover, it has recently been shown that reporter gene imaging can be combined with therapeutic strategies. Here, we provide an outline of the current status of hESC research and discuss the concerns of tumorigenicity and immunogenicity. Furthermore, we describe how molecular imaging can be utilized to follow and resolve these issues.

INTRODUCTION

Adult stem cells have great promise as potential treatments for a variety of intractable diseases. However, these cells are generally limited in their plasticity. Therefore, it would be ideal to obtain or create a cell line that is truly able to differentiate into every cell of the body. The first such cell line was derived in the 1960's and originated from teratomas that developed spontaneously in male mice of the 129 strain. These "embryonal carcinoma" (EC) cells were capable of teratoma formation after transplantation of single cells into a new host,[1] confirming their ability to differentiate into progeny of all three germ layers (ectoderm, mesoderm and endoderm)--a phenomenon known as 'pluripotency'.[2] Further research led to the first isolation of murine embryonic stem cells (mESCs) in 1981 from the epiblast of blastocyst-stage mouse embryos,[3, 4] followed by the establishment of the first human embryonic stem cell (hESC)-line in 1998.2 To date, there are more than 300 hESC lines, but only 22 hESC lines are commercially available and registered in the "NIH Human Embryonic Stem Cell Registry".[5]

Although most studies using hESCs in disease models show auspicious results, there are several concerns about hESC transplantation. First, the pluripotent character of hESCs is somewhat a double-edged sword. They are an attractive candidate for cell based therapies, but their pluripotency can also lead to risk of teratoma formation after transplantation. Second, since it is presently impossible to transplant hESCs syngeneically, the possibility that hESCs might provoke an immune reaction following allogeneic transplantation must be considered. This review will discuss these issues and how molecular imaging can help resolve them.

DERIVATION, MAINTENANCE, AND DIFFERENTIATION

Traditionally, hESCs are isolated from the inner cell mass of the human blastocyst, or as recently shown, can be derived from single blastomeres.[6] The isolated cells can be expanded *in vitro*, with an average doubling time of 30-35 h.[7] However, strict homeostatic culture conditions and the addition of inhibiting compounds are necessary to keep the hESCs in an undifferentiated state, a condition required for maintaining a normal karyotype and an unlimited capacity for self-renewal. This is possible by growing hESCs on a cellular feeder layer. Inactivated murine embryonic fibroblasts prove to be an effective feeder layer for the undifferentiated growth of hESCs because they secrete differentiation-inhibiting factors.[8] Due to the risk of cross-species retroviral infection, however, this is an unattractive option in the long term. Recently, several reports have described the culture of hESCs in animal-free conditions, using human feeder cells consisting of foreskin,[9] pure human fibroblast populations,[10] or uterine endometrial cells and serum-free medium.[11] Generally, these undifferentiated hESCs express transcription factors OCT-3/4, Sox-2, and NANOG; surface markers CD9, CD133, and SSEA-3/4; proteoglycans TRA-1-60/81 and TRA-2-54; and enzyme alkaline phosphatases and telomerase.[12, 13]

Following withdrawal of inhibitory factors, hESCs will aggregate into three-dimensional clusters of cells in an early stage of differentiation, thereby losing pluripotency. These clusters, named Embryoid Bodies (EBs),[14] form the first step of further differentiation into any type of progeny. Within the EBs, a microenvironment exists in which various signals will promote differentiation into all three germ layers. Although differentiation generally occurs spontaneously, much effort currently focuses on stimulating directed differentiation to achieve sufficiently large populations for clinical use. The generation of pure, differentiated cultures is indispensable for developing cell based therapies, and will help us better understand cellular developmental processes and test pharmacological strategies.

Differentiation into Mesoderm Lineages

While reports have been published of hESCs differentiating into various mesodermal lineages, including kidney, muscle, bone and blood cells,[15] it is cardiomyogenesis that has received the most attention. Cardiomyogenesis typically manifests as a beating area within the EBs around 5 days after EB-formation, the surface of which increases gradually with time.[16] Kehat and colleagues were the first to show that hESC-derived cardiomyocytes within these beating EBs actually resemble the structural and functional properties of early stage human cardiomyocytes.[16] Since then, several other methods have been tested to improve the efficiency of *in vitro* differentiation of hESCs into cardiomyocytes with moderate success.[17-19]

Differentiation into Ectoderm Lineages

Using different growth factors and stimulating environments, hESCs can also be driven to differentiate into brain, skin, and adrenal derivates.[15] The potential of hESC-derived cultures for the treatment of neurodegenerative disorders is under intensive investigation. While many groups have described neuronal differentiation within the EB,[20-22] factor-induced neuronal differentiation seems to be limited to the addition of retinoic acid (RA) and nerve growth factor (betaNGF),[21] or the use of serum-free, conditioned medium.[23] The coculture of hESCs with murine skull bone marrow-derived stromal cells also seems to induce neuronal differentiation.[24]

Differentiation into Endoderm Lineages

From the beginning, hESCs were shown to be capable of differentiating *in vitro* into liver and pancreatic cells when exposed to a variety of growth factors.[15] The creation of insulin-secreting pancreatic cell populations has generated much interest, as this might ultimately provide a cell-based therapy for patients with type I diabetes.[25] However, the identification of insulin-producing cells has proven to be difficult and susceptible to artifacts.[26] Thus, the *in vitro* pancreatic differentiation from hESCs remains a challenging multi-step culturing procedure at present.[27]

In summary, although much is being done to improve the efficacy of *in vitro* differentiation systems, little is known about the cellular interactions that occur during natural differentiation. Most of the *in vitro* differentiation methods are to some extent dependent on EB formation. The process of *in vitro* EB formation mimics the natural transcriptional pathways occurring in the developing embryo, leading not only to the differentiation into the desired cell type, but also to the production of undesired cells. The most dangerous example of the latter is undifferentiated hESCs that retain the ability to form teratomas. Until we understand the precise pathways of pluripotent differentiation, the acquisition of desired, transplantable cell types can only rely on stimulating known pathways and the pre-transplantation selection of the desired cell type.

TERATOMA FORMATION

At present no selection method exists that can yield a 100% pure population, which is a major obstacle for clinical translation. When transplanted in immunodeficient mice, hESCs form teratomas consisting of human tissues from all germ layers.[2, 28] The formation and composition of teratomas seem to be influenced by several factors, including graft site,[29] transplanted cell number, and developmental phase of the host,[24] as described next.

One factor influencing hESC-based teratoma formation is the site of transplantation, which affects both growth and composition of the tumor. As recently shown by Cooke and colleagues, teratomas rising from hESCs will grow faster and contain more undifferentiated cells when transplanted in the *liver* of nude mice, as compared to *subcutaneous* transplantation.[29] It is of major interest why hESCs differentiate at the subcutaneous site but remain undifferentiated in the liver. The authors hypothesize that this was due to the well vascularized, growth factor-rich, immune-privileged porous structure in the liver.[29] These findings are not only a stimulant for further research on graft site and teratoma formation, but also indicate the importance of *in vivo* experiments, as there may be factors present in the liver that could help maintain hESCs in an undifferentiated state *in vitro*.

Another factor influencing teratoma formation is the number of undifferentiated hESCs that are viable after transplantation. As discussed earlier, transplantation of pure undifferentiated hESC inevitably leads to teratoma formation.[2, 28] Interestingly, transplantation of selected hESC-derived cells in a more developed phase will not automatically lead to teratomas, even when this population is not 100% pure.[30] However, there are no extant studies that assess the minimal cell number needed for teratoma formation, or stated otherwise, the maximum percentage of contamination with undifferentiated hESC. Our laboratory is actively investigating these issues.

Recently, Muotri and colleagues have studied undifferentiated hESC after *in utero* transplantation into the lateral brain ventricle of day-14 mouse embryos.[24] The results showed that hESCs integrated into the brain, giving rise to neuronal and glial lineages, but not to teratomas. These findings suggest that hESCs are susceptible to environmental cues that can modulate its differentiation and tumorigenic potential, as was suggested in earlier studies with hESCs in chick embryos.[31]

Taken together, these observations and questions are not only a stimulant for further research on teratoma biology, but also indicate the importance of developing novel imaging techniques to track their growth *in vivo* longitudinally, repetitively, and quantitatively.

IMMUNOGENICITY

Another hurdle facing clinical transplantation of hESCs is the potential immunologic barrier. The immune response generated after transplantation is directed towards alloantigens, which are antigens presented on the cell surface that are considered non-self by the recipient immune system.[32] The major system of alloantigens responsible for cell incompatibility is the major histocompatibility complex (MHC). In humans, MHC-I molecules are expressed on the surface of virtually all nucleated cells and present antigens to CD8+ cytotoxic T cells, while MHC-II molecules are normally more restricted to antigen presenting cells such as dendritic cells and macrophages, and are selectively recognized by CD4+ helper T cells.[33]

It has been shown that hESCs express low levels of MHC-I in their undifferentiated state.[34, 35] In one study, the MHC-I expression increased two to four-fold when the cells were induced to spontaneously differentiate to EB, and an eight to ten-fold when induced to differentiate into teratomas.[34] In contrast, a different group observed MHC-I downregulation after differentiation induced with retinoic acid or on Matrigel or in extended cultures.[35] In both studies, MHC-I expression was strongly upregulated after treatment of the cells with interferon-γ, a potent MHC expression-inducing cytokine known to be released during the course of an immune response. MHC-II antigens were not expressed on hESCs or hESC derivatives.[34] The latter finding confirms that, in contrast to tissue allografts, hESC transplants are devoid of highly immunogenic mature dendritic cells, or any other type of specialized antigen presenting cells. Thus, the transplanted cells may not express MHC-II molecules required for effective priming of alloreactive CD4+ T cells through direct recognition.

Previously, our group tested allogeneic undifferentiated mESCs for their ability to trigger alloimmune response in a murine model of myocardial infarction.[36] We found progressive intragraft infiltration of inflammatory cells mediating both adaptive (T cells, B cells, and dendritic

cells) and innate (macrophages and granulocytes) immunity. Cellular infiltration progressed from mild infiltration at two weeks to vigorous infiltration at four weeks, leading to rejection of the mESC allograft. Moreover, we found an accelerated immune response against mESCs that had differentiated *in vivo* for 2 weeks, suggesting that mESC immunogenicity increases upon their differentiation.[36]

Although it was previously reported that hESCs failed to elicit immune responses during the first 48 hours after intramuscular injection of immunocompetent mice,[37] a recent report using a similar model found hESCs to be completely eliminated at 1 month post-transplantation.[38] Thus, questions regarding the exact character and intensity of immune responses towards allogeneic hESCs and their derivatives remain. Solutions that reduce or eliminate the potential immunological response to transplanted allogeneic hESCs are urgently needed. Possible strategies to minimize rejection of hESC transplants have been extensively reviewed elsewhere.[39, 40] Examples of these strategies include: (1) forming HLA isotyped hESC-line banks; (2) creating a universal donor cell by genetic modification; (3) inducing tolerance by hematopoietic chimerism; or (4) generating isogeneic hESC lines by somatic nuclear transfer. To optimize these techniques in the future, it is crucial to develop sensitive and reliable imaging methods for monitoring the viability of transplanted cells *in vivo*.

MOLECULAR IMAGING

To date, most studies on stem cell therapy have relied on conventional reporter genes such as GFP[41] and β-galactosidase (lacZ) to monitor cell survival and differentiation. However, these reporter genes cannot be used to reliably track *in vivo* characteristics of transplanted cells due to poor tissue penetration and the need for extrinsic excitation light, which produces an unacceptable amount of background signal. Instead, GFP-labeled cells are typically identified histologically, which provides only a single snapshot representation rather than a complete picture of cell survival over time. To solve these shortcomings, our group has been developing reporter gene-based molecular imaging techniques.[42]

Molecular imaging can be broadly defined as the *in vivo* characterization of cellular and molecular processes.[43] The backbone of reporter gene-based molecular imaging technique is the design of a suitable reporter construct. This construct carries a reporter gene linked to a promoter/enhancer, which can be inducible, constitutive, or tissue specific. The construct can be introduced into the target tissue by molecular biology techniques using either viral or non-viral techniques. Transcription of DNA and translation of mRNA lead to the production of reporter protein. After administration of a reporter probe, the reporter protein reacts with the reporter probe, giving rise to signals that are detectable by a charged-coupled device (CCD)

camera, positron emission tomography (PET), single photon emission computed tomography (SPECT), or magnetic resonance imaging (MRI) (**figure 1**). For thorough review, please refer to other relevant articles.[43, 44]

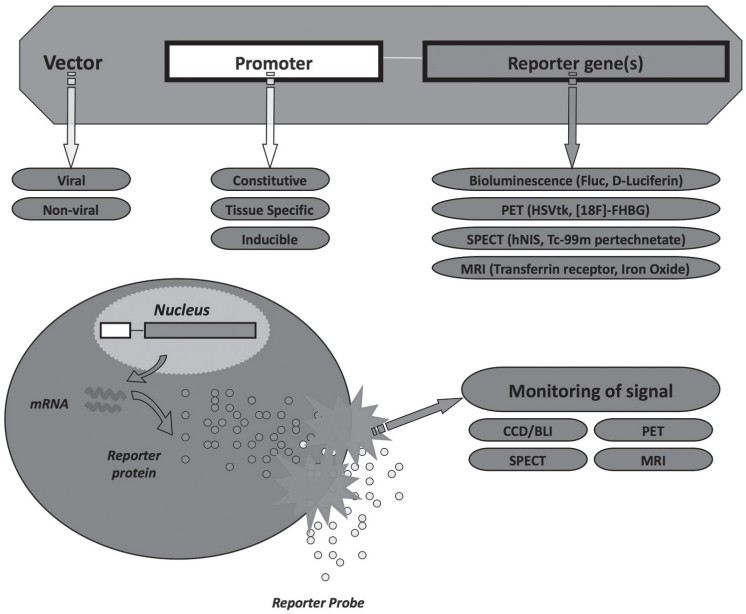

Figure 1. Schematic overview of molecular imaging. Outline of a vector containing a DNA reporter construct with the reporter gene(s) driven by a promoter of choice. Transcription and translation lead to production of mRNA and reporter protein, respectively. After administration of a reporter probe systemically, the reporter probe will be catalyzed by specific cells that have the reporter proteins. This amplification process can be detected by a sensitive imaging device. Examples of reporter genes and their specific reporter probes are listed per imaging modality. Abbreviations: Fluc, Firefly luciferase; PET, positron emission tomography; HSV-ttk, herpes simplex virus truncated thymidine kinase; [^{18}F]-FHBG, 9-(4-[^{18}F]-fluoro-3hydroxymethylbutyl) guanine; SPECT, single photon emission computed tomography; hNIS, human sodium/iodide symporter; MRI, magnetic resonance imaging; CCD, charged coupled device; BLI, bioluminescence imaging.

Imaging ESC Transplantation, Tumorigenicity, and Immunogenicity

A major advantage of reporter gene imaging is the incorporation of the reporter construct into the cellular DNA. This ensures that the reporter gene will only be expressed by living cells and will be passed on equally to the cell's progeny. Thus, this imaging modality can provide significant insight into cell viability and proliferation. As discussed earlier, monitoring cell viability is a critical requirement to assess immunogenicity, as a provoked immune reaction can kill transplanted cells. Monitoring cell proliferation is another important feature, considering the tumorigenic po-

tential of undifferentiated hESCs. Moreover, the ability to image the whole-body will allow us to track cell migration in other organs. This is a major advantage when compared to tissue biopsies using GFP-labeled cells.

In addition, multiple reporter genes can also be introduced into the same cell for multimodality imaging. Recently, our group has tested the efficacy of mESC with a self-inactivating lentiviral vector carrying triple-fusion (TF) construct containing firefly luciferase (Fluc), monomeric red fluorescent protein (mRFP), and herpes simplex virus truncated thymidine kinase (HSV-ttk).[45] The mRFP in the construct facilitates the imaging of single cells by fluorescence microscopy and allows for the isolation of a stable clone population by fluorescence activated cell sorter (FACS). The Fluc can be used to perform high throughput bioluminescence imaging (BLI) for assessment of cell survival, proliferation and migration at relatively low costs. Finally, the HSV-ttk allows for deep-tissue PET imaging of gene expression in small animals[45, 46] as well as in patients.[47, 48] After transplantation into the hearts of athymic nude rats, mESCs could be successfully followed for 4 weeks using BLI and PET imaging. Between week 2 and 4, both BLI and PET reporter gene signals increased rapidly, indicating teratoma formation. This was confirmed by histological analysis.[45]

Because of the risk of teratoma formation, it would be ideal to have an *in vivo* imaging modality in combination with a fail-safe suicide-gene mechanism. Using the antiviral drug ganciclovir, which is toxic against cells expressing HSV-ttk, Cao and colleagues were able to ablate teratoma formation and follow this progress non-invasively.[49] This study reveals the excellent potential of reporter gene imaging for future use with hESC transplantation. In fact, preliminary studies in our lab suggest that as low as 100 undifferentiated hESCs (H9 line) can cause teratoma formation after subcutaneous injection (**figure 2**). Whether lower cell numbers (e.g. 1, 10, 50), other graft sites (e.g. intramuscular, intravenous), or different cell lines (e.g., federally and non-federally approved) have similar kinetics of teratoma formation will need to be determined carefully in the future.

Finally, a very critical question with regard to reporter genes is whether they will affect ESC differentiation and hamper efforts for clinical applications. A previous study from our lab has shown that the TF reporter genes affect <2% of total genes of mESC using transcriptional profiling analysis.[50] A more recent follow up study using proteomic analysis show that there were no significant differences between control mESCs versus mESCs with reporter genes.[51] Importantly, reporter probes such as D-Luciferin (for Fluc) and [^{18}F]-FHBG (for HSV-ttk) had no adverse effects on mESC viability and proliferation as well.[45] Ongoing studies are evaluating the effects of reporter gene expression and reporter probes on various hESC cell lines.

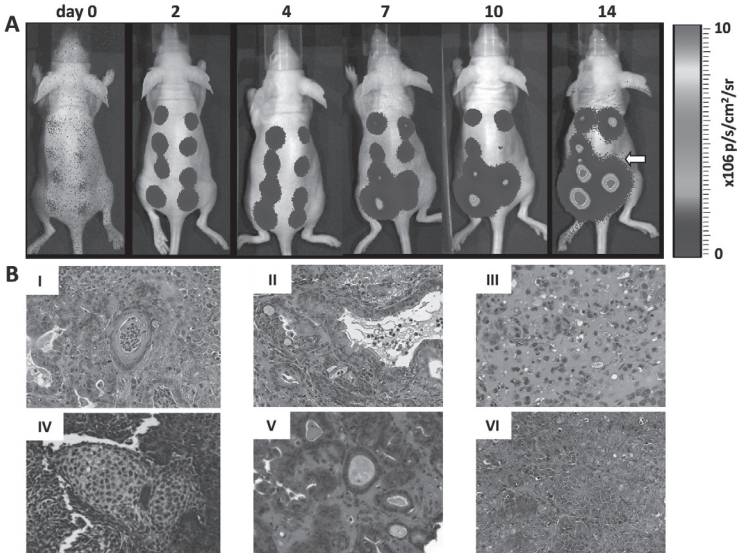

Figure 2. *In vivo* bioluminescence imaging of teratoma formation after transplantation of 100 hESCs. (a) Bioluminescence image showing longitudinal follow up after transplantation of 100 hESCs stably expressing a double fusion reporter gene (Fluc-GFP). Faint imaging signals were seen as early as 2 hrs after transplant, which became progressively stronger over 2 weeks. Histology at 8 weeks confirmed teratoma formation. Note one of the hESC transplanted sites did not successfully engraft (arrow) as there were no detectable signals by 2 weeks. (b) Histology from a representative explanted teratoma showing hESCs that have differentiated into Histology from a representative explanted teratoma showing hESCs that have differentiated into derivates from different germ layers. (I) squamous cell differentiation with keratin pearl; (II) respiratory epithelium with ciliated columnar and mucin producing goblet cells; (III) osteoid (non-mineralized bone) formation; (IV) cartilage formation; (V) gland cells; and (VI) rosette consistent with neuroectodermal differentiation (400x magnification).

CONCLUSION

Clearly, the capacity of hESCs to differentiate into almost all human cell types highlights their promising role in regenerative therapies for the treatment of heart disease, Parkinson's disease, leukemia, diabetes, and other degenerative disorders. But the pluripotency of hESCs may also pose major risks such as teratoma formation. Likewise, hESCs might not be immunoprivileged and could trigger host immune responses, leading to decreased cell survival or acute rejection. These are issues that can become significant barriers to future clinical application of hESC-based therapies. To meet these challenges, researchers must gain a better understanding of the *in vivo* behavior of transplanted hESCs. This review outlines the burgeoning application of molecular imaging to track transplanted hESCs *in vivo*. Continuing research merging molecular imaging and hESC biology will likely lead to significant advances in the future, both scientifically and medically.

REFERENCES

1. Kleinsmith LJ, Pierce GB, Jr. Multipotentiality Of Single Embryonal Carcinoma Cells. *Cancer Res.* 1964;24:1544-1551.
2. Thomson JA, Itskovitz-Eldor J, Shapiro SS, Waknitz MA, Swiergiel JJ, Marshall VS, Jones JM. Embryonic stem cell lines derived from human blastocysts. *Science.* 1998;282(5391):1145-1147.
3. Evans MJ, Kaufman MH. Establishment in culture of pluripotential cells from mouse embryos. *Nature.* 1981;292(5819):154-156.
4. Martin GR. Isolation of a pluripotent cell line from early mouse embryos cultured in medium conditioned by teratocarcinoma stem cells. *Proc Natl Acad Sci U S A.* 1981;78(12):7634-7638.
5. NIH. National Institutes of Health - Human Embryonic Stem Cell Registry.
6. Klimanskaya I, Chung Y, Becker S, Lu SJ, Lanza R. Human embryonic stem cell lines derived from single blastomeres. *Nature.* 2006.
7. Amit M, Carpenter MK, Inokuma MS, Chiu CP, Harris CP, Waknitz MA, Itskovitz-Eldor J, Thomson JA. Clonally derived human embryonic stem cell lines maintain pluripotency and proliferative potential for prolonged periods of culture. *Dev Biol.* 2000;227(2):271-278.
8. Xu C, Inokuma MS, Denham J, Golds K, Kundu P, Gold JD, Carpenter MK. Feeder-free growth of undifferentiated human embryonic stem cells. *Nat Biotechnol.* 2001;19(10):971-974.
9. Amit M, Margulets V, Segev H, Shariki K, Laevsky I, Coleman R, Itskovitz-Eldor J. Human feeder layers for human embryonic stem cells. *Biol Reprod.* 2003;68(6):2150-2156.
10. Richards M, Fong CY, Chan WK, Wong PC, Bongso A. Human feeders support prolonged undifferentiated growth of human inner cell masses and embryonic stem cells. *Nat Biotechnol.* 2002;20(9):933-936.
11. Lee JB, Lee JE, Park JH, Kim SJ, Kim MK, Roh SI, Yoon HS. Establishment and maintenance of human embryonic stem cell lines on human feeder cells derived from uterine endometrium under serum-free condition. *Biol Reprod.* 2005;72(1):42-49.
12. Hoffman LM, Carpenter MK. Characterization and culture of human embryonic stem cells. *Nat Biotechnol.* 2005;23(6):699-708.
13. Wei H, Juhasz O, Li J, Tarasova YS, Boheler KR. Embryonic stem cells and cardiomyocyte differentiation: phenotypic and molecular analyses. *J Cell Mol Med.* 2005;9(4):804-817.
14. Doetschman TC, Eistetter H, Katz M, Schmidt W, Kemler R. The *in vitro* development of blastocyst-derived embryonic stem cell lines: formation of visceral yolk sac, blood islands and myocardium. *J Embryol Exp Morphol.* 1985;87:27-45.
15. Schuldiner M, Yanuka O, Itskovitz-Eldor J, Melton DA, Benvenisty N. Effects of eight growth factors on the differentiation of cells derived from human embryonic stem cells. *Proc Natl Acad Sci U S A.* 2000;97(21):11307-11312.

16. Kehat I, Kenyagin-Karsenti D, Snir M, Segev H, Amit M, Gepstein A, Livne E, Binah O, Itskovitz-Eldor J, Gepstein L. Human embryonic stem cells can differentiate into myocytes with structural and functional properties of cardiomyocytes. *J Clin Invest*. 2001;108(3):407-414.
17. Passier R, Oostwaard DW, Snapper J, Kloots J, Hassink RJ, Kuijk E, Roelen B, de la Riviere AB, Mummery C. Increased cardiomyocyte differentiation from human embryonic stem cells in serum-free cultures. *Stem Cells*. 2005;23(6):772-780.
18. Xu C, Police S, Rao N, Carpenter MK. Characterization and enrichment of cardiomyocytes derived from human embryonic stem cells. *Circ Res.* 2002;91(6):501-508.
19. Yao S, Chen S, Clark J, Hao E, Beattie GM, Hayek A, Ding S. Long-term self-renewal and directed differentiation of human embryonic stem cells in chemically defined conditions. *Proc Natl Acad Sci U S A*. 2006;103(18):6907-6912.
20. Reubinoff BE, Itsykson P, Turetsky T, Pera MF, Reinhartz E, Itzik A, Ben-Hur T. Neural progenitors from human embryonic stem cells. *Nat Biotechnol.* 2001;19(12):1134-1140.
21. Schuldiner M, Eiges R, Eden A, Yanuka O, Itskovitz-Eldor J, Goldstein RS, Benvenisty N. Induced neuronal differentiation of human embryonic stem cells. *Brain Res.* 2001;913(2): 201-205.
22. Zhang SC, Wernig M, Duncan ID, Brustle O, Thomson JA. *In vitro* differentiation of transplantable neural precursors from human embryonic stem cells. *Nat Biotechnol.* 2001;19(12): 1129-1133.
23. Schulz TC, Palmarini GM, Noggle SA, Weiler DA, Mitalipova MM, Condie BG. Directed neuronal differentiation of human embryonic stem cells. *BMC Neurosci.* 2003;4:27.
24. Muotri AR, Nakashima K, Toni N, Sandler VM, Gage FH. Development of functional human embryonic stem cell-derived neurons in mouse brain. *Proc Natl Acad Sci U S A.* 2005;102(51):18644-18648.
25. Assady S, Maor G, Amit M, Itskovitz-Eldor J, Skorecki KL, Tzukerman M. Insulin production by human embryonic stem cells. *Diabetes.* 2001;50(8):1691-1697.
26. Rajagopal J, Anderson WJ, Kume S, Martinez OI, Melton DA. Insulin staining of ES cell progeny from insulin uptake. *Science.* 2003;299(5605):363.
27. Segev H, Fishman B, Ziskind A, Shulman M, Itskovitz-Eldor J. Differentiation of human embryonic stem cells into insulin-producing clusters. *Stem Cells.* 2004;22(3):265-274.
28. Reubinoff BE, Pera MF, Fong CY, Trounson A, Bongso A. Embryonic stem cell lines from human blastocysts: somatic differentiation *in vitro*. *Nat Biotechnol.* 2000;18(4):399-404.
29. Cooke MJ, Stojkovic M, Przyborski SA. Growth of teratomas derived from human pluripotent stem cells is influenced by the graft site. *Stem Cells Dev.* 2006;15(2):254-259.
30. Kehat I, Khimovich L, Caspi O, Gepstein A, Shofti R, Arbel G, Huber I, Satin J, Itskovitz-Eldor J, Gepstein L. Electromechanical integration of cardiomyocytes derived from human embryonic stem cells. *Nat Biotechnol.* 2004;22(10):1282-1289.

31. Goldstein RS, Drukker M, Reubinoff BE, Benvenisty N. Integration and differentiation of human embryonic stem cells transplanted to the chick embryo. *Dev Dyn.* 2002;225(1):80-86.
32. Janeway CA, Jr. The role of self-recognition in receptor repertoire development. Members of the Janeway Laboratory. *Immunol Res.* 1999;19(2-3):107-118.
33. Lechler RI, Lombardi G, Batchelor JR, Reinsmoen N, Bach FH. The molecular basis of allore-activity. *Immunol Today.* 1990;11(3):83-88.
34. Drukker M, Katz G, Urbach A, Schuldiner M, Markel G, Itskovitz-Eldor J, Reubinoff B, Mandelboim O, Benvenisty N. Characterization of the expression of MHC proteins in human embryonic stem cells. *Proc Natl Acad Sci U S A.* 2002;99(15):9864-9869.
35. Draper JS, Pigott C, Thomson JA, Andrews PW. Surface antigens of human embryonic stem cells: changes upon differentiation in culture. *J Anat.* 2002;200(Pt 3):249-258.
36. Swijnenburg RJ, Tanaka M, Vogel H, Baker J, Kofidis T, Gunawan F, Lebl DR, Caffarelli AD, de Bruin JL, Fedoseyeva EV, Robbins RC. Embryonic stem cell immunogenicity increases upon differentiation after transplantation into ischemic myocardium. *Circulation.* 2005;112(9 Suppl):I166-172.
37. Li L, Baroja ML, Majumdar A, Chadwick K, Rouleau A, Gallacher L, Ferber I, Lebkowski J, Martin T, Madrenas J, Bhatia M. Human embryonic stem cells possess immune-privileged properties. *Stem Cells.* 2004;22(4):448-456.
38. Drukker M, Katchman H, Katz G, Even-Tov Friedman S, Shezen E, Hornstein E, Mandelboim O, Reisner Y, Benvenisty N. Human embryonic stem cells and their differentiated derivatives are less susceptible to immune rejection than adult cells. *Stem Cells.* 2006;24(2):221-229.
39. Boyd AS, Higashi Y, Wood KJ. Transplanting stem cells: potential targets for immune attack. Modulating the immune response against embryonic stem cell transplantation. *Adv Drug Deliv Rev.* 2005;57(13):1944-1969.
40. Drukker M. Immunogenicity of human embryonic stem cells: can we achieve tolerance? *Springer Semin Immunopathol.* 2004;26(1-2):201-213.
41. Ro S. Magnifying stem cell lineages: the stop-EGFP mouse. *Cell Cycle.* 2004;3(10): 1246-1249.
42. 4Sheikh AY, Wu JC. Molecular imaging of cardiac stem cell transplantation. *Curr Cardiol Rep.* 2006;8(2):147-154.
43. Blasberg RG, Tjuvajev JG. Molecular-genetic imaging: current and future perspectives. *J Clin Invest.* 2003;111(11):1620-1629.
44. Wu JC, Tseng JR, Gambhir SS. Molecular imaging of cardiovascular gene products. *J Nucl Cardiol.* 2004;11(4):491-505.
45. Cao F, Lin S, Xie X, Ray P, Patel M, Zhang X, Drukker M, Dylla SJ, Connolly AJ, Chen X, Weiss-

man IL, Gambhir SS, Wu JC. *In vivo* visualization of embryonic stem cell survival, proliferation, and migration after cardiac delivery. *Circulation.* 2006;113(7):1005-1014.

46. Wu JC, Chen IY, Sundaresan G, Min JJ, De A, Qiao JH, Fishbein MC, Gambhir SS. Molecular imaging of cardiac cell transplantation in living animals using optical bioluminescence and positron emission tomography. *Circulation.* 2003;108(11):1302-1305.
47. Jacobs A, Voges J, Reszka R, Lercher M, Gossmann A, Kracht L, Kaestle C, Wagner R, Wienhard K, Heiss WD. Positron-emission tomography of vector-mediated gene expression in gene therapy for gliomas. *Lancet.* 2001;358(9283):727-729.
48. Penuelas I, Mazzolini G, Boan JF, Sangro B, Marti-Climent J, Ruiz M, Ruiz J, Satyamurthy N, Qian C, Barrio JR, Phelps ME, Richter JA, Gambhir SS, Prieto J. Positron emission tomography imaging of adenoviral-mediated transgene expression in liver cancer patients. *Gastroenterology.* 2005;128(7):1787-1795.
49. Cao F, Drukker M, Lin S, Sheikh A, Xie X, Li Z, Weissman I, Wu J. Molecular Imaging of Embryonic Stem Cell Misbehavior and Suicide Gene Ablation. *Cloning and Stem Cells - in press.*
50. Wu JC, Spin JM, Cao F, Lin S, Xie X, Gheysens O, Chen IY, Sheikh AY, Robbins RC, Tsalenko A, Gambhir SS, Quertermous T. Transcriptional profiling of reporter genes used for molecular imaging of embryonic stem cell transplantation. *Physiol Genomics.* 2006;25(1):29-38.
51. Wu JC, Cao F, Dutta S, Xie X, Kim E, Chungfat N, Gambhir SS, Mathewson S, Connolly AJ, Brown M, Wang EW. Proteomic analysis of reporter genes for molecular imaging of transplanted embryonic stem cells (in press). *Proteomics.* 2006; ( ).

CHAPTER 5

Clinical Hurdles for the Transplantation of Cardiomyocytes derived from Human Embryonic Stem Cells: Role of Molecular Imaging

Rutger-Jan Swijnenburg, Koen E.A. van der Bogt, Ahmad Y. Sheikh,

Feng Cao and Joseph C. Wu

Current Opinion in Biotechnology 2007 Feb;18(1):38-45

ABSTRACT

Over the past few years, human embryonic stem cells (hESCs) have gained popularity as a potentially ideal cell candidate for tissue regeneration. In particular, hESCs are capable of cardiac lineage-specific differentiation and confer improvement of cardiac function following transplantation into animal models. Although such data are encouraging, there remain significant hurdles before safe and successful translation of hESC-based treatment into clinical therapy, including the inability to assess cells following transplant. To this end, *molecular imaging* has proven a reliable methodology for tracking the long-term fate of transplanted cells. Imaging reporter genes introduced into the cells prior to transplantation enable non-invasive and longitudinal studies of cell viability, location, and behavior *in vivo*. Therefore, molecular imaging is expected to play an increasing role in characterizing the biology and physiology of hESC-derived cardiac cells in living subjects.

INTRODUCTION

Coronary artery disease remains the leading cause of death in the Western world.[1] As the human heart is not capable of regenerating the great numbers of cardiac cells that are lost after myocardial infarction, impaired cardiac function is the inevitable result of ischemic disease. Recently, three randomized clinical trails reported either clinically marginal[2, 3] or no[4] significant benefit following adult bone marrow cell transplantation for patients suffering from acute and/or chronic ischemic heart disease. These reports add to a growing body of evidence that adult-derived stem cells have limited capacity to aid renewal and regeneration of damaged organs and structures. By contrast, hESCs show greater promise, as they are capable of self-renewal and differentiation. hESCs were first isolated by Thompson and colleagues in 1998.[5] They are derived from the inner cell mass of the human blastocyst and can be kept in an undifferentiated, self-renewing state when cultured in the presence of inhibitory compounds, such as mouse embryonic fibroblast feeder layer cells. Compared to adult stem cells harvested from the bone marrow, hESCs have the advantage of being pluripotent, which provides them with the ability to differentiate into virtually all cells of the human body. For cardiac applications, hESCs have the ability to differentiate into cardiac cell lineages.[6, 7] These hESC-derived cardiac cells have structural and functional properties of human cardiomyocytes and can integrate with host myocardium after transplantation into rats[8] and pigs.[9] However, in order to critically evaluate and optimize hESC-based therapy for the heart, new methodologies for assessing the viability, location, and behavior of transplanted cells are needed. This article aims to provide a concise overview of the major hurdles that need to be addressed before hESC-derived cardiac cell transplantation can become a clinical reality. This is followed by an outline of potential of molecular imaging tools that may help to overcome these challenges in the future.

HURDLES FOR CLINICAL TRANSLATION

Although substantial progress has been made in recent years towards improving culture conditions, differentiation strategies, and potential hESC-based cardiac regeneration, several unresolved issues exist between the laboratory and bedside that still need to be bridged **(figure 1)**. This article will cover some of the major areas of concern regarding hESC-derived cardiac cell transplantation, including: (1) optimization of *in vitro* differentiation into cardiac cells; (2) purification of cardiac cells to minimize post-transplant cellular misbehavior such as teratoma formation; (3) *in vivo* integration and function with host myocardium; and (4) evaluation of post-transplant immune rejection and cell death.

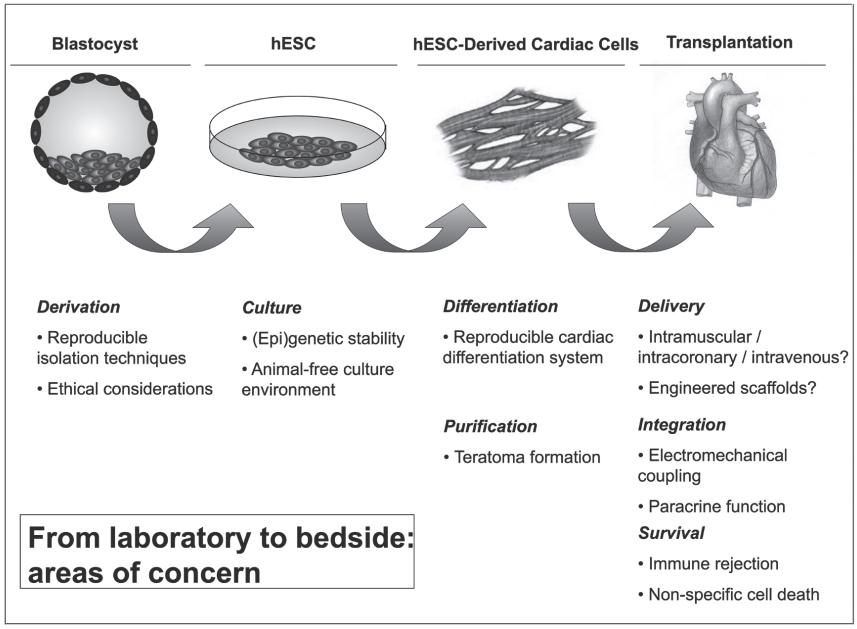

Figure 1. Human embryonic stem cells: from laboratory to bedside. Areas of concern in derivation, culture, differentiation, purification, delivery, integration, and survival are outlined.

In vitro differentiation to cardiomyocytes

Following removal of the inhibitory feeder layer cells, hESCs can aggregate into clusters of cells known as embryoid bodies (EBs). Within these EBs, various signals are activated to promote differentiation of cells into all three germ layers, including mesoderm-derived cardiac cells **(figure 2)**. Formation of cardiomyocytes usually starts 5 days after EB-formation, presenting as a beating area within the EB. Moreover, the hESC-derived cardiac cells within these beating areas actually resemble the structural and functional properties of early stage human cardiomyocytes.[6] Unfortunately, the rate of spontaneous differentiation of hESCs into cardiac cells is low. Typically ~8% of the EBs grown in suspension undergo differentiation into beating clusters, and ~30% of the cells contained in these clusters are actual cardiomyocytes.[6]

Mouse ESCs (mESCs) were originally isolated in 1981[10], and subsequent studies have focused on different strategies to induce cardiac-specific differentiation of mESCs *in vitro*. Retinoic acid was one of the first agents described that significantly increase the percentage of cardiomyocytes arising from ESCs.[11] Similar effects have been described for oxytocin[12], dynorphin B[13], nitric oxide[14], and ascorbic acid.[15] However, the efficacy of these compounds can be dose-dependent and bound to a specific time period in embryonic development.[11] Other groups have focused on the role of growth factors in mESC-derived cardiac cell differentiation, inclu-

ding transforming growth factor-β2[16], basic fibroblast growth factor, and bone-morphogenetic protein-2.[17] Interestingly, findings from mESC studies *do not* appear to translate to hESC research. Thus far, only 5-aza-2'-deoxycytidine[7], combination of activin A and BMP-4[18], and co-culture with murine END-2 visceral endoderm-like cells[19] have been shown to enhance cardiomyogenesis in hESC cultures.

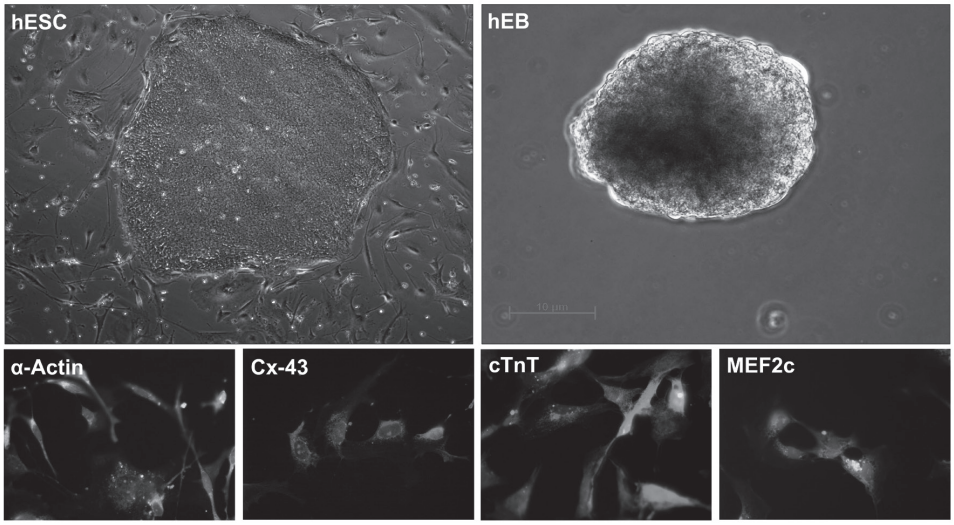

Figure 2. Undifferentiated hESCs (H9 cell line) grow indefinitely in culture on mouse embryonic fibroblast feeder layer cells (upper left panel). Following withdrawal of inhibitory feeder cells, hESCs can aggregate into EBs (upper right panel). Formation of cardiac cells usually starts 5 days after differentiation, initially presenting as a beating cluster within the EB. After isolation of EBs and further enrichment by Percoll gradient separation, these hESC-derived cardiac cells (lower panels) express cardiac lineage specific makers as shown by immunofluorescent staining of GFP-labeled cells with skeletal muscle alpha actin (α-Actin), connexin-43 (Cx-43), cardiac troponin T (cTnT), and Myosin Enhancer Factor 2c (MEF2c) (all in red; counterstaining with DAPI, blue).

Purification of hESC-derived cardiac cells

Once ESCs are successfully induced to adopt cardiac fate, it becomes yet another challenge to isolate and further purify such subpopulations while avoiding contamination by undifferentiated, pluripotent ESCs. Following transplantation, undifferentiated ESCs could cause teratoma formation, which are complex tumors comprised of cellular or oganoid components reminiscent of normal derivatives from the three germ layers.[20] This indicates the need to achieve a highly, if not completely, pure population of cardiomyocytes prior to transplantation. Currently, selection methods for ESC-derived cardiac cells include Percoll density gradient-based isolation, which can enrich up to ~70% pure cardiac cell population for hESC[7] and ~90% for mESC.[21] An alternative strategy for cardiac cell purification combines genetic engineering and

molecular biology techniques. Klug *et al.* utilized a fusion gene consisting of an alpha-cardiac myosin heavy chain (α-MHC) promoter that drives expression of aminoglycoside phosphotransferase, which is an enzyme that confers resistance to the antibiotic geneticin (G418). Once the transgenic mESCs differentiate into cardiac cells, activation of the cardiac specific α-MHC promoter leads to expression of aminoglycoside phosphotransferase and allows these cells to survive against treatment with G418. The resultant surviving cells represent 99% pure cardiomyocyte population[22]. Similarly, Muller *et al.* reported transfection of mESCs with a fusion gene of of myosin light chain-2v (MLC-2v) linked to enhanced green fluorescent protein (eGFP). In this case, mESC-derived cardiac cells expressed eGFP that enabled fluorescent-activated cell sorting (FACS) and collection of cardiomyocyte population (97% pure).[23]

In vivo integration and function of ESC-derived cardiac cells

Data from rodent models evaluating the fate of mESC transplantation into the heart have demonstrated mixed results. Early reports by Min *et al.* evaluating transplantation of mESC-derived beating cells into immunocompetent rat myocardium showed long-term (up to 32 weeks) cell survival, improvement of cardiac function, and improved angiogenesis in the infarct zone[24, 25]. Most notably, no adverse sequelae such as graft rejection, arrythmogenesis, or teratoma formation were observed. By contrast, two more recent studies demonstrated that mESCs transplanted into hearts of both immunocompetent mice[20] and athymic nude rats[26] formed teratomas by as early as 3 to 4 weeks following transplantation. At present, there are few published studies testing the efficacy of hESC-derived cardiac cell transplantation for cardiac repair. Kehat *et al.* showed promising results by injecting hESC-derived cardiac cells into swine heart with complete atrioventricular block.[9] They demonstrated electromechanical and structural coupling of the transplanted cells with the host myocardium. Xue *et al.* also showed functional integration and active pacing of hESC-derived cardiac cells following transfer into healthy myocardium of guinea pigs.[27] Furthermore, Laflamme *et al*. demonstrated that hESC-derived cardiac cells transplanted into athymic rat hearts successfully engrafted, proliferated, and expressed several cardiomyocyte markers.[8] Notably, none of these studies reported cellular misbehavior or teratoma formation. It is also not clear what percentage of these transplanted cells actually survived after transplantation

Immune rejection of allogeneic hESC transplantation

Several factors threaten hESC-derived cardiac cell survival following delivery into a new host, which, if properly modulated, might prevent the drastic post-transplant death of donor cells presently observed. One such major factor is cellular rejection based on immunological incompatibility. Theoretically, hESCs represent an immune-privileged cell population, since embryos consisting of 50% foreign material derived from the father are not rejected by the ma-

ternal host.[28] However, the understanding the immunogenicity of hESCs and their derivatives remains a challenge.

It has been shown that mESCs do not express major histocompatibility complex (MHC) antigens, the major system of alloantigens responsible for cell incompatibility.[29] Furthermore, mESCs can inhibit T-lymphocyte proliferation *in vitro* and establish multi-lineage mixed chimerism *in vivo*.[30] However, when allogeneic undifferentiated mESCs were transplanted into a murine model of myocardial infarction, our group found progressive intra-graft infiltration of inflammatory cells mediating both adaptive (T cells, B cells, and dendritic cells) and innate (macrophages and granulocytes) immunity, leading to rejection of the mESC allograft[20]. In contrast to mESCs, hESCs express low levels of MHC-I antigens.[31, 32] Drukker *et al.* observed that MHC-I expression increased two to four-fold when cells were induced to spontaneously differentiate to EBs[31], and eight to ten-fold when cells differentiated into teratomas. In contrast, Draper *et al.* reported MHC-I downregulation upon hESC differentiation towards EB.[32] Thus, questions regarding the character and intensity of immune responses towards allogeneic hESC-derived cardiac cells still remain. Solutions that reduce or eliminate the potential immunological response are needed, including: (1) forming MHC isotyped hESC-line banks; (2) creating a universal donor cell by genetic modification; (3) inducing tolerance by hematopoietic chimerism; (4) generating isogeneic hESC lines by somatic nuclear transfer; (5) and/or using immunosuppressive medication. Details of these strategies to minimize rejection of hESC-derived transplants have been extensively reviewed by others.[33, 34]

IMAGING HESC-DERIVED CARDIAC CELLS

Non-invasive cell tracking

As outlined earlier, hESC-derived cardiac cell transplantation is potentially feasible, but there are several aspects that require improvement. For clinical translation to occur, it is essential that tools be developed for longitudinal tracking and evaluation of transplanted cell viability and behavior. Traditionally, cell therapy studies have relied upon conventional reporter genes such as GFP and β-galactosidase (LacZ) to monitor cell survival and differentiation. However, visualizing GFP and LacZ cells requires postmortem tissue analysis, which provides only a single snapshot representation of cell fate, not a complete picture over time. Moreover, sampling error inherent in *ex vivo* analysis requires large numbers of animals be sacrificed to develop a realistic picture of longitudinal survival kinetics.

Another technique for measuring the efficacy of cell therapy is to assess secondary endpoints. Cardiac contractility can be monitored by conventional methodologies such as echocardiography or magnetic resonance imaging (MRI). Cardiac perfusion can be assessed using posi-

tron emission tomography (PET) or single-photon emission computed tomography (SPECT). However, these data cannot be correlated to the biological state of the cells, as the cells themselves can neither be visualized nor assayed in the living subject. Aiming to provide insight into the location and survival of transplanted cells, recent studies have reported labeling mESCs with magnetic iron particles and following them by MRI.[35] Although these iron particles are robust and facilitate repeated imaging over time, they do not reliably provide insight into cell *proliferation* and *viability*, due to the disparate passing of the particles from parent to daughter cells and the ability of non-specific immune cells (e.g., macrophages) to engulf particles, respectively.

Molecular imaging: direct vs. indirect approach

Ideally, a non-invasive method for *in vivo* tracking of hESC-derived cardiac cells should be capable of providing insight into the following processes: (1) localization and migration of the cells, (2) cell survival and proliferation kinetics, and (3) cell differentiation or de-differentiation patterns. Molecular imaging of reporter genes offers potential promise in meeting these goals. Molecular imaging can be broadly defined as the visualization of molecular and cellular processes in the living subject. For *in vivo* molecular imaging to work, two basic elements are required: a molecular probe that detects a quantifiable signal based on the presence of gene, RNA, or protein, and a method to monitor these probes *in vivo*.[36] In general, molecular imaging can be divided into two categories: (a) *direct* imaging of probe-target interaction or (b) *indirect* imaging based on reporter gene and reporter probe.

The most commonly used *direct* cardiac imaging modality utilizes ^{18}F-fluorodeoxyglucose ([^{18}F]-FDG), a glucose analog which can cross intact membranes into living cells and is phosphorylated by the endogenous enzyme, hexokinase, trapping the probe inside the cell. The phosphorylated [^{18}F] will undergo positron annihilation to give off two 511 keV photon signals that can be detected by PET, providing a measurement of cell or tissue viability[37] This approach has recently been shown feasible for imaging clinical cardiac cell therapy. Hofmann *et al.* labeled autologous bone marrow cells with [^{18}F]-FDG from nine patients suffering from acute myocardial infarction.[38] The [^{18}F]-FDG labeled cells were injected into either the infarct-related coronary artery or the antecubital vein five to ten days following coronary stenting. PET imaging was performed 50 to 75 minutes after the procedure and successfully detected the transplanted cell population in all patients, with higher signals in the intra-coronary group. Although PET is a valuable tool to monitor the location of cells shortly after transplant, the short half-life of the [^{18}F]-FDG radiotracer (~110 minutes) does not permit long-term follow-up of cell survival and/or migration. Furthermore, [^{18}F]-FDG is not passed on to daughter cells during cell division and therefore does not provide insight into cell proliferation.

The concept behind *indirect* molecular imaging is an expansion upon basic reporter gene technology whereby a promoter or enhancer region of interest is linked to the imaging reporter gene. The nature of the promoter can be inducible, constitutive, or tissue specific. The construct can be introduced into the target cell using either viral or non-viral techniques. Once incorporated, the reporter gene produces the reporter protein which then interacts with the introduced reporter probe, producing an analytic signal that can be detected by the detector system. Depending on the reporter gene used, available imaging modalities include PET, SPECT, MRI or a charged-coupled device (CCD) camera.[39] The two most widely used reporter gene imaging systems are firefly luciferase (Fluc)-based optical bioluminescence imaging and herpes simplex virus thymidine kinase (HSV-tk)-based PET imaging. For bioluminescence imaging, the Fluc reporter protein catalyzes the D-Luciferin reporter probe to produce low-energy photons (2-3 eV) that can be captured by an ultra-sensitive CCD camera. The reporter probe can be administered before every imaging session, allowing for multiple imaging acquisitions over time. For PET imaging, the HSV-tk reporter protein phosphorylates radiolabeled thymidine analogue 9-(4-[18F]fluoro-3-(hydroxymethylbutyl)guanine ([^{18}F]-FHBG) reporter probe, which emits high-energy photons (511 keV) that can be detected by PET. The reporter gene technique has been used to assay survival and localization of transplanted rat embryonic cardiomyoblasts[40] and more recently of mESCs.[26]

Reporter gene imaging of ESCs and ESC-derived cardiac cells

Regarding transplantation of hESC-derived cardiac cell transplantation, reporter gene imaging can be used to monitor critical events. First, since the reporter gene can be integrated into the DNA of transplanted cells, its expression is limited to only living cells, and thus facilitates assessment of cell survival. Second, the reporter gene can be passed onto daughter cells, thus providing insight into cell proliferation. This is an important feature given the tumorigenic potential of undifferentiated ESCs discussed earlier. Third, it is possible to introduce several reporter genes into the same cell, facilitating a multi-modality imaging approach. Recently, Cao *et al*. tested the efficacy of mESC with a self-inactivating lentiviral vector carrying the triple-fusion (TF) construct that consists of firefly luciferase (Fluc), red fluorescence protein (mRFP), and herpes simplex virus truncated thymidine kinase (HSV-ttk).[26] The mRFP facilitates imaging of single cells by fluorescence microscopy and allows for the isolation of a stable clone population by FACS. The Fluc allows for bioluminescence imaging for assessment of cell survival, proliferation, and migration in small animals. Finally, the HSV-ttk affords the ability to use PET imaging in small and large animals, as well as humans. Following transplantation into the hearts of athymic nude rats, mESC survival, migration, and proliferation was monitored for 4 weeks by bioluminescence and PET imaging. PET imaging, both with [^{18}F]-FHBG to image cells and [^{18}F]-FDG to image myocardial viability, proved to be a very sensitive tool to assess the tomographic

location of mESC engraftment **(figure 3)**. However, reporter gene signals increased rapidly within 4 weeks due to teratoma formation. Histologic samples obtained from both intra- and extra-cardiac sites revealed spontaneous differentiation of the mESC into all three germ layers. In a subsequent study, our group also demonstrated the ability of an anti-viral drug to selectively target teratomas expressing the HSV-ttk reporter gene.[41] Thus, in addition to its use for monitoring cell fate, the reporter gene also serves as an inducible suicide gene that facilitates selective cellular ablation. This could be an important tool in controlling cellular misbehavior and/or teratoma formation of transplanted hESC-derived cells.

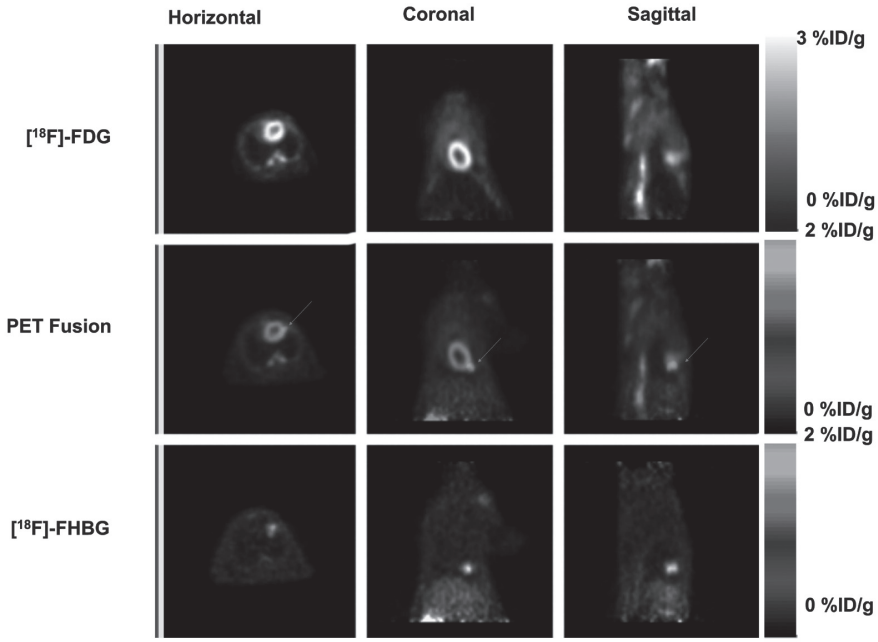

Figure 3. Positron emission tomography imaging of transplanted mESCs in the myocardium. Two weeks after mESC transplantation, nude rats underwent [18F]-FHBG reporter probe imaging (top row) followed by [18F]-FDG myocardial viability imaging (middle row). Fusion of [18F]-FHBG and [18F]-FDG images (bottom row) shows the exact anatomic location of transplanted mESC (arrow) at the anterolateral wall in horizontal, coronal, and sagittal views. (Reproduced with permission from Cao et al.[26])

Recently, our group has successfully transduced hESCs (H9 line) with a lentiviral vector containing a double fusion (DF) reporter gene that consists of Fluc and eGFP. Cardiac cells derived from hESCs using EB formation and Percoll gradient enrichment constitutively express Fluc and eGFP. Following transplantation into ischemic myocardium of severe combined immuno-

deficient (SCID) mice, these cells can be monitored by bioluminescence imaging for >3 months (Cao *et al.,* unpublished data). By contrast, injection of undifferentiated hESCs caused teratoma formation during the same period (**figure 4**). Taken together, these results highlight the valuable role of molecular imaging for following the developmental fate of transplanted hESCs and their derivates.

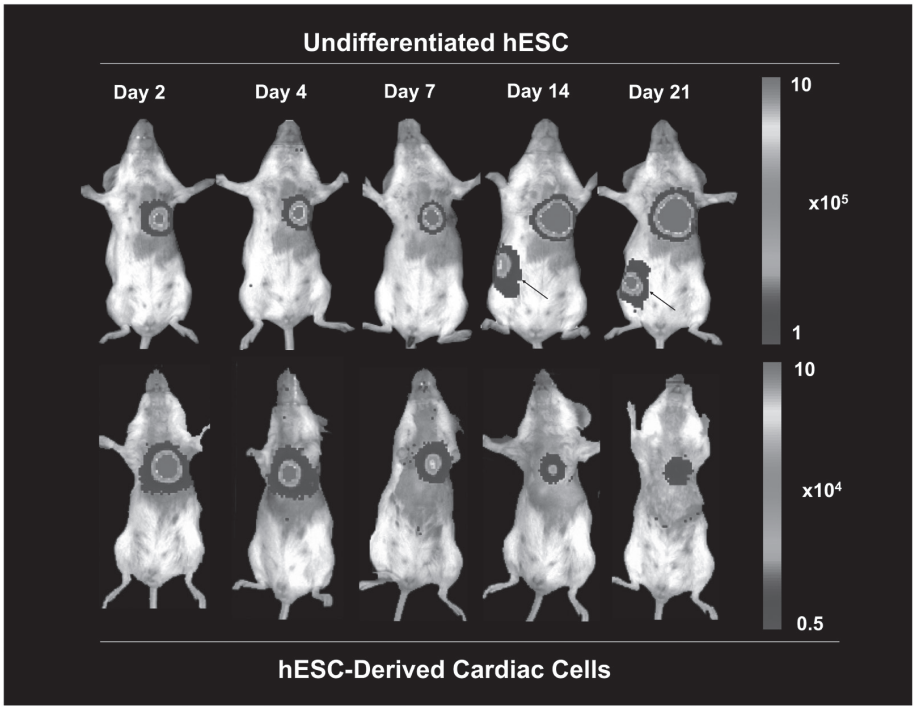

Figure 4. Comparison of undifferentiated hESCs versus hESC-derived cardiac cell survival and behavior *in vivo*. Both hESC (top row) and hESC-derived cardiac cells (bottom row) were transplantated into ischemic myocardium of SCID mice. Bioluminescence imaging during the first three weeks following transplantation reveals acute donor cell death followed by stable survival of hESC-derived cardiac cells. In contrast, undifferentiated hESCs proliferate uncontrollably in the heart as well as other seeded organs (arrows) to cause teratoma formation.

Finally, a critical question with regard to reporter genes is whether the might influence the biology and physiology of the stem cells. In the study by Cao *et al.,* the TF construct had no influence on mESC morphology, viability, proliferation, and differentiation capacity *in vitro.*[26] Likewise, both the bioluminescence (D-luciferin) and PET ([^{18}F]-FHBG) reporter probes had no adverse effects on mESC behavior. In two recent studies, the TF reporter genes affected <2% of the total mESC genome using transcriptional profiling analysis[42] and caused no significant differences in protein expression quantified by proteomic analysis.[43] Ongoing studies are also evaluating the effects of reporter gene and reporter probe on hESCs as well.

CONCLUSION

The last several years have produced revolutionary advancemences in exploring the capabilities of stem cells for treatment of cardiovascular disease. In particular, initial animal results involving hESC-derived cardiac cells appear promising for improving cardiac function after ischemic injury. Nonetheless, we are still years away from safely translating these initial observations into therapy for humans. There are several issues within the field that require improvement, especially those related to *in vitro* differentiation and purification, as well as *in vivo* integration and survival of the transplanted cells. As the field of hESC-derived cell transplantation emerges, there will be an urgent need for reliable methodologies to track and assess behavior of the cells following transfer into the injured heart. Molecular imaging serves these needs and will likely play a prominent role in future hESC research.

ACKNOWLEDGEMENTS

This work is supported by the National Heart, Lung, and Blood Institute (JCW) and the European Society for Organ Transplantation-Astellas Study and Research Grant 2006 (RJS).

REFERENCES

1. Thom T, Haase N, Rosamond W, Howard VJ, Rumsfeld J, Manolio T, Zheng ZJ, Flegal K, O'Donnell C, Kittner S, Lloyd-Jones D, Goff DC, Jr., Hong Y, Adams R, Friday G, Furie K, Gorelick P, Kissela B, Marler J, Meigs J, Roger V, Sidney S, Sorlie P, Steinberger J, Wasserthiel-Smoller S, Wilson M, Wolf P. Heart disease and stroke statistics--2006 update: a report from the American Heart Association Statistics Committee and Stroke Statistics Subcommittee. *Circulation*. Feb 14 2006;113(6):e85-151.
2. Assmus B, Honold J, Schachinger V, Britten MB, Fischer-Rasokat U, Lehmann R, Teupe C, Pistorius K, Martin H, Abolmaali ND, Tonn T, Dimmeler S, Zeiher AM. Transcoronary transplantation of progenitor cells after myocardial infarction. *The New England journal of medicine*. Sep 21 2006;355(12):1222-1232.
3. Schachinger V, Erbs S, Elsasser A, Haberbosch W, Hambrecht R, Holschermann H, Yu J, Corti R, Mathey DG, Hamm CW, Suselbeck T, Assmus B, Tonn T, Dimmeler S, Zeiher AM. Intracoronary bone marrow-derived progenitor cells in acute myocardial infarction. *The New England journal of medicine*. Sep 21 2006;355(12):1210-1221.
4. Lunde K, Solheim S, Aakhus S, Arnesen H, Abdelnoor M, Egeland T, Endresen K, Ilebekk A, Mangschau A, Fjeld JG, Smith HJ, Taraldsrud E, Grogaard HK, Bjornerheim R, Brekke M, Muller C, Hopp E, Ragnarsson A, Brinchmann JE, Forfang K. Intracoronary injection of mononuclear bone marrow cells in acute myocardial infarction. *The New England journal of medicine*. Sep 21 2006;355(12):1199-1209.
5. Thomson JA, Itskovitz-Eldor J, Shapiro SS, Waknitz MA, Swiergiel JJ, Marshall VS, Jones JM. Embryonic stem cell lines derived from human blastocysts. *Science*. Nov 6 1998;282(5391):1145-1147.
6. Kehat I, Kenyagin-Karsenti D, Snir M, Segev H, Amit M, Gepstein A, Livne E, Binah O, Itskovitz-Eldor J, Gepstein L. Human embryonic stem cells can differentiate into myocytes with structural and functional properties of cardiomyocytes. *J Clin Invest*. Aug 2001;108(3):407-414.
7. Xu C, Police S, Rao N, Carpenter MK. Characterization and enrichment of cardiomyocytes derived from human embryonic stem cells. *Circ Res*. Sep 20 2002;91(6):501-508.
8. Laflamme MA, Gold J, Xu C, Hassanipour M, Rosler E, Police S, Muskheli V, Murry CE. Formation of human myocardium in the rat heart from human embryonic stem cells. *Am J Pathol*. Sep 2005;167(3):663-671.
9. Kehat I, Khimovich L, Caspi O, Gepstein A, Shofti R, Arbel G, Huber I, Satin J, Itskovitz-Eldor J, Gepstein L. Electromechanical integration of cardiomyocytes derived from human embryonic stem cells. *Nat Biotechnol*. Oct 2004;22(10):1282-1289.
10. Evans MJ, Kaufman MH. Establishment in culture of pluripotential cells from mouse embryos. *Nature*. Jul 9 1981;292(5819):154-156.

11. Wobus AM, Kaomei G, Shan J, Wellner MC, Rohwedel J, Ji G, Fleischmann B, Katus HA, Hescheler J, Franz WM. Retinoic acid accelerates embryonic stem cell-derived cardiac differentiation and enhances development of ventricular cardiomyocytes. *J Mol Cell Cardiol.* Jun 1997;29(6):1525-1539.
12. Paquin J, Danalache BA, Jankowski M, McCann SM, Gutkowska J. Oxytocin induces differentiation of P19 embryonic stem cells to cardiomyocytes. *Proc Natl Acad Sci U S A.* Jul 9 2002;99(14):9550-9555.
13. Ventura C, Zinellu E, Maninchedda E, Maioli M. Dynorphin B is an agonist of nuclear opioid receptors coupling nuclear protein kinase C activation to the transcription of cardiogenic genes in GTR1 embryonic stem cells. *Circ Res.* Apr 4 2003;92(6):623-629.
14. Kanno S, Kim PK, Sallam K, Lei J, Billiar TR, Shears LL, 2nd. Nitric oxide facilitates cardiomyogenesis in mouse embryonic stem cells. *Proc Natl Acad Sci U S A.* Aug 17 2004;101(33):12277-12281.
15. Takahashi T, Lord B, Schulze PC, Fryer RM, Sarang SS, Gullans SR, Lee RT. Ascorbic acid enhances differentiation of embryonic stem cells into cardiac myocytes. *Circulation.* Apr 15 2003;107(14):1912-1916.
16. Behfar A, Zingman LV, Hodgson DM, Rauzier JM, Kane GC, Terzic A, Puceat M. Stem cell differentiation requires a paracrine pathway in the heart. *Faseb J.* Oct 2002;16(12):1558-1566.
17. Kawai T, Takahashi T, Esaki M, Ushikoshi H, Nagano S, Fujiwara H, Kosai K. Efficient cardiomyogenic differentiation of embryonic stem cell by fibroblast growth factor 2 and bone morphogenetic protein 2. *Circ J.* Jul 2004;68(7):691-702.
18. Yao S, Chen S, Clark J, Hao E, Beattie GM, Hayek A, Ding S. Long-term self-renewal and directed differentiation of human embryonic stem cells in chemically defined conditions. *Proc Natl Acad Sci U S A.* May 2 2006;103(18):6907-6912.
19. Mummery C, Ward-van Oostwaard D, Doevendans P, Spijker R, van den Brink S, Hassink R, van der Heyden M, Opthof T, Pera M, de la Riviere AB, Passier R, Tertoolen L. Differentiation of human embryonic stem cells to cardiomyocytes: role of coculture with visceral endoderm-like cells. *Circulation.* Jun 3 2003;107(21):2733-2740.
20. Cao YA, Bachmann MH, Beilhack A, Yang Y, Tanaka M, Swijnenburg RJ, Reeves R, Taylor-Edwards C, Schulz S, Doyle TC, Fathman CG, Robbins RC, Herzenberg LA, Negrin RS, Contag CH. Molecular imaging using labeled donor tissues reveals patterns of engraftment, rejection, and survival in transplantation. *Transplantation.* Jul 15 2005;80(1):134-139.
21. E LL, Zhao YS, Guo XM, Wang CY, Jiang H, Li J, Duan CM, Song Y. Enrichment of cardiomyocytes derived from mouse embryonic stem cells. *J Heart Lung Transplant.* Jun 2006;25(6):664-674.
22. Klug MG, Soonpaa MH, Koh GY, Field LJ. Genetically selected cardiomyocytes from diffe-

rentiating embronic stem cells form stable intracardiac grafts. *J Clin Invest*. Jul 1 1996;98(1):216-224.

23. Muller M, Fleischmann BK, Selbert S, Ji GJ, Endl E, Middeler G, Muller OJ, Schlenke P, Frese S, Wobus AM, Hescheler J, Katus HA, Franz WM. Selection of ventricular-like cardiomyocytes from ES cells *in vitro*. *Faseb J*. Dec 2000;14(15):2540-2548.
24. Min JY, Yang Y, Converso KL, Liu L, Huang Q, Morgan JP, Xiao YF. Transplantation of embryonic stem cells improves cardiac function in postinfarcted rats. *J Appl Physiol.* Jan 2002;92(1):288-296.
25. Min JY, Yang Y, Sullivan MF, Ke Q, Converso KL, Chen Y, Morgan JP, Xiao YF. Long-term improvement of cardiac function in rats after infarction by transplantation of embryonic stem cells. *The Journal of thoracic and cardiovascular surgery*. Feb 2003;125(2):361-369.
26. Cao F, Lin S, Xie X, Ray P, Patel M, Zhang X, Drukker M, Dylla SJ, Connolly AJ, Chen X, Weissman IL, Gambhir SS, Wu JC. *In vivo* visualization of embryonic stem cell survival, proliferation, and migration after cardiac delivery. *Circulation*. Feb 21 2006;113(7):1005-1014.
27. Xue T, Cho HC, Akar FG, Tsang SY, Jones SP, Marban E, Tomaselli GF, Li RA. Functional integration of electrically active cardiac derivatives from genetically engineered human embryonic stem cells with quiescent recipient ventricular cardiomyocytes: insights into the development of cell-based pacemakers. *Circulation*. Jan 4 2005;111(1):11-20.
28. Li L, Baroja ML, Majumdar A, Chadwick K, Rouleau A, Gallacher L, Ferber I, Lebkowski J, Martin T, Madrenas J, Bhatia M. Human embryonic stem cells possess immune-privileged properties. *Stem Cells*. 2004;22(4):448-456.
29. Tian L, Catt JW, O'Neill C, King NJ. Expression of immunoglobulin superfamily cell adhesion molecules on murine embryonic stem cells. *Biology of reproduction*. Sep 1997;57(3):561-568.
30. Bonde S, Zavazava N. Immunogenicity and engraftment of mouse embryonic stem cells in allogeneic recipients. *Stem Cells*. Oct 2006;24(10):2192-2201.
31. Drukker M, Katz G, Urbach A, Schuldiner M, Markel G, Itskovitz-Eldor J, Reubinoff B, Mandelboim O, Benvenisty N. Characterization of the expression of MHC proteins in human embryonic stem cells. *Proc Natl Acad Sci U S A*. Jul 23 2002;99(15):9864-9869.
32. Draper JS, Pigott C, Thomson JA, Andrews PW. Surface antigens of human embryonic stem cells: changes upon differentiation in culture. *Journal of anatomy*. Mar 2002;200(Pt 3):249-258.
33. Drukker M. Immunogenicity of human embryonic stem cells: can we achieve tolerance? *Springer Semin Immunopathol*. Nov 2004;26(1-2):201-213.
34. Boyd AS, Higashi Y, Wood KJ. Transplanting stem cells: potential targets for immune attack. Modulating the immune response against embryonic stem cell transplantation. *Adv Drug Deliv Rev*. Dec 12 2005;57(13):1944-1969.

35. Arai T, Kofidis T, Bulte JW, de Bruin J, Venook RD, Berry GJ, McConnell MV, Quertermous T, Robbins RC, Yang PC. Dual *in vivo* magnetic resonance evaluation of magnetically labeled mouse embryonic stem cells and cardiac function at 1.5 t. *Magn Reson Med*. Jan 2006;55(1):203-209.
36. Blasberg RG, Tjuvajev JG. Molecular-genetic imaging: current and future perspectives. *J Clin Invest*. Jun 2003;111(11):1620-1629.
37. Schelbert HR. 18F-deoxyglucose and the assessment of myocardial viability. *Semin Nucl Med*. Jan 2002;32(1):60-69.
38. Hofmann M, Wollert KC, Meyer GP, Menke A, Arseniev L, Hertenstein B, Ganser A, Knapp WH, Drexler H. Monitoring of bone marrow cell homing into the infarcted human myocardium. *Circulation*. May 3 2005;111(17):2198-2202.
39. Wu JC, Tseng JR, Gambhir SS. Molecular imaging of cardiovascular gene products. *J Nucl Cardiol*. Jul-Aug 2004;11(4):491-505.
40. Wu JC, Chen IY, Sundaresan G, Min JJ, De A, Qiao JH, Fishbein MC, Gambhir SS. Molecular imaging of cardiac cell transplantation in living animals using optical bioluminescence and positron emission tomography. *Circulation*. Sep 16 2003;108(11):1302-1305.
41. Cao F, Drukker M, Lin S, Sheikh A, Xie X, Li Z, Weissman I, Wu J. Molecular imaging of embryonic stem cell misbehavior and suicide gene ablation. *Cloning and Stem Cells*. 2007 (in press).
42. Wu JC, Spin JM, Cao F, Lin S, Xie X, Gheysens O, Chen IY, Sheikh AY, Robbins RC, Tsalenko A, Gambhir SS, Quertermous T. Transcriptional profiling of reporter genes used for molecular imaging of embryonic stem cell transplantation. *Physiological genomics*. Mar 13 2006;25(1):29-38.
43. Wu JC, Cao F, Dutta S, Xie X, Kim E, Chungfat N, Gambhir S, Mathewson S, Connolly AJ, Brown M, Wang EW. Proteomic analysis of reporter genes for molecular imaging of transplanted embryonic stem cells. *Proteomics*. Nov 2 2006.

PART II

ADULT STEM CELLS

CHAPTER 6

Comparison of Different Adult Stem Cell Types for Treatment of Myocardial Ischemia

Koen E.A. van der Bogt, Ahmad Y. Sheikh, Sonja Schrepfer, Grant Hoyt, Feng Cao, Katie Ransohoff, Rutger-Jan Swijnenburg, Jeremy Pearl, Michael Fischbein, Christopher H. Contag, Robert C. Robbins and Joseph C. Wu

Circulation 2008 Sep 30;118(14 Suppl):S121-9.

ABSTRACT

Introduction: A comparative analysis of the efficacy of different cell candidates for the treatment of heart disease remains to be described. This study is designed to evaluate the therapeutic efficacy of 4 cell types in a murine model of myocardial infarction.

Methods: Bone marrow mononuclear cells (MN), mesenchymal stem cells (MSC), skeletal myoblasts (SkMb) and fibroblasts (Fibro) were isolated from male L2G transgenic mice (FVB background) that constitutively express firefly luciferase (Fluc) and green fluorescence protein (GFP). Cells were characterized by flow cytometry, bioluminescence imaging (BLI), and luminometry. Female FVB mice (n=60) underwent LAD ligation and were randomized into 5 groups to intramyocardially receive one cell type (5×10^5) or PBS as control. Cell survival was measured *in vivo* by BLI and *ex vivo* by TaqMan PCR at week 6. Cardiac function was assessed by echocardiography and invasive hemodynamic measurements were made at week 6.

Results: Fluc expression correlated with the cell number in all groups ($r^2>0.93$). *In vivo* BLI revealed acute donor cell death of MSC, SkMb, and Fibro within 3 weeks after transplantation. By contrast, cardiac signals were still present after 6 weeks in the MN group, as confirmed by TaqMan PCR ($P<0.01$). Echocardiography showed significant preservation of fractional shortening in the MN group compared to controls ($P<0.05$). Measurements of left ventricular end-systolic/diastolic volumes revealed that the least amount of ventricular dilatation occurred in the MN group ($P<0.05$). Histology confirmed the presence of MN, although there was no evidence of transdifferentiation by donor MN into cardiomyocytes.

Conclusion: This is the first study to directly compare a variety of cell candidates for myocardial therapy. Compared to MSC, SkMB, and Fibro, our results suggest that MN cells exhibit a more favorable survival pattern, which translates into a more robust preservation of cardiac function.

INTRODUCTION

Coronary artery disease is the number one cause of morbidity and mortality in the US. Despite a wide range of therapeutic approaches, heart failure remains the leading cause of death in the Western world.[1] Recently, cell therapy has generated much enthusiasm as a novel potential treatment for ischemic heart disease. Numerous animal studies, each evaluating a particular class of cells for its regenerative potential in the infarcted heart, have been conducted.[2] Furthermore, the administration of skeletal myoblasts (SkMb)[3], bone marrow-derived mononuclear cells (MN)[4-6] and mesenchymal stem cells (MSC)[7] as a therapy for end-stage heart disease has already been translated from bench top to bedside. Although the majority of experimental studies have shown encouraging results, clinical outcomes are divergent, which highlights the present imperfect understanding of the *in vivo* behavior and the mechanism(s) of action of the cells.[8] Moreover, differences in cell type and dose, study design, patient population, and timing of cell transplant hamper inter-study comparisons.

Recently, molecular imaging has proven to be a valuable tool to track cells on an *in vivo* and quantitative bases in mice.[9] As opposed to post-mortem histology, molecular imaging is non-invasive and facilitates repetitive imaging, thereby providing unprecedented insight into cell position and count. These characteristics make molecular imaging an extremely useful method to monitor cell survival, proliferation, migration, and even misbehavior.[10] In order to understand which cell type will generate optimal therapeutic responses, we evaluated the efficacy of various therapeutic stem cell candidates in a uniform, controlled murine model of ischemic heart failure. Results gathered from this head-to-head comparison study should yield valuable information regarding the optimal cell type for cardiac regenerative therapy.

METHODS

Transgenic L2G animals expressing Fluc-GFP. All animal study protocols were approved by the Stanford Animal Research Committee. The donor group consisted of 8-week old male L2G mice (n=10), which were bred on FVB background and ubiquitously express green fluorescent protein (GFP) and firefly luciferase (Fluc) reporter genes driven by a β-actin promoter as previously described.[11] Recipient animals (n=70) consisted of syngeneic, female FVB mice (8 weeks old, Jackson Laboratories, Bar Harbor, ME, USA). To compare the efficacy of different adult stem cell types, animals were randomized into 5 recipient groups (n=12/group): (1) bone marrow derived mononuclear cells (MN), (2) skeletal myoblasts (SkMb), (3) bone marrow derived mesenchymal cells (MSC), (4) fibroblasts (Fibro), and (5) saline (PBS). To compare the effects of myocardial milieus on MN survival, animals were randomized into 2 recipient groups (n=5/group): (1) injection at the infarct site and (2) injection at the peri-infarct site.

Preparation of fibroblasts (Fibro). Donor mice were euthanized by cervical dislocation after anesthesia with 5% isoflurane, and were placed in 70% ethanol for 5 minutes. For the isolation of Fibro, skin biopsies were taken from the tail and ears, minced, and incubated overnight in collagenase type II (400 U/mL, Gibco-Invitrogen, Carlsbad, CA, USA,), dissolved in DMEM (Gibco, NY, USA) supplemented with 20% heat-inactivated fetal bovine serum (FBS, Hyclone, Logan, UT, USA), 1% antibiotics/antimycotic solution (penicillin/streptomycin, Gibco-Invitrogen, Carlsbad, CA, USA) at 37°C and 5% CO_2 in air.[12] The next day, cells were dislodged from digested tissue by repeated pipetting and were passed through 70 µm sterile netting into sterile 14-ml centrifuge tubes. The samples were centrifuged for 5 minutes at 1200 rpm, and the cell pellet was resuspended in DMEM, 20% FBS, 1% penicillin/streptomycin to be plated in a 25 cm^2 tissue flask at 37°C/5%CO_2.

Preparation of skeletal myoblasts (SkMb). After the skin was isolated, the muscles were dissected from the legs, minced, and placed in a Dispase solution (grade II, 2.4U/mL, Gibco-Invitrogen, Carlsbad, CA, USA) for 45 minutes under regular pipetting. The suspension was filtered through a 70 µm nylon mesh and was centrifuged at 1200 rpm for 5 minutes. The cell pellet was resuspended into 45% DMEM/45% Ham's F10 medium (Gibco-Invitrogen, Carlsbad, CA, USA), supplemented with 10% FBS and 1% penicillin/streptomycin and plated in 25 cm^2 collagen-coated tissue flasks. When confluent, cells were dislodged and passaged using PBS. Cells were grown for 5 passages, after which they were transferred into DMEM, 10% FBS, and 1% penicillin/streptomycin medium supplemented with 2.5 ng/mL Basic Fibroblast Growth Factor (Gibco-Invitrogen, Carlsbad, CA, USA) to achieve confluent SkMb cultures.[13]

Preparation of bone marrow mononuclear cells (MN) and mesenchymal stem cells (MSC). Finally, the long bones were explanted, washed, and flushed with PBS using a 25-gauge needle to collect bone marrow. After passing through a 70 µm strainer, the isolate was centrifuged at 1200 rpm for 5 minutes, washed, and resuspended into DMEM, 20% FBS, and 1% penicillin/streptomycin medium to grow MSC. All plated cells were allowed to grow for 6 passages before transplantation to avoid contamination with other cell types. To acquire the MN fraction, the bone marrow isolate was centrifuged for 40 minutes at 1600 rpm using a 14 mL tube with 3 mL Ficoll-Paque Premium (GE Healthcare, Piscataway, NJ, USA) gradient and 4 mL cell/saline suspension. MN were prepared freshly before application.

Characterization of stem cells by flow cytometry. Cells were incubated in 2% FBS/PBS at 4°C for 30 min with 1 µL monoclonal FITC-conjugated antibodies against CD34, CD45, C-kit, CD11b, and CD90 (BD, San Jose, CA, USA), and processed through a FACSCalibur system (BD, San Jose, CA, USA) according to the manufacturer's protocol.

***In vitro* firefly luciferase (Fluc) assays.** Cells were dislodged from culture flasks (SkMb, MSC and Fibro) or processed directly after isolation (MN) to be resuspended in PBS. Cell suspensions were divided into a 6-well plate in known concentrations. After administration of D-Luciferin (Xenogen, Alameda, CA, USA, 4.5ug/mL), peak signal expressed as photons per second per centimeter square per steridian (photons/s/cm^2/sr) was measured using a charged coupled device (CCD) camera (IVS200, Xenogen, Alameda, CA, USA) as described.[14] Same amounts of dislodged cells were lysed using 200 µL of 10X Passive Lysis Buffer (Promega, Madison, WI, USA) and centrifuged at maximum speed for 2 minutes at 4°C. For every sample, 20 µL supernatant was added to 100 µL Luciferase Assay Reagent (LAR-II, Promega, Madison, WI, USA) and luminosity in relative light units (RLU) was measured on a TD-20/20n luminometer (Turner Biosystems, Sunnyvale, CA, USA). All samples were conducted in triplets.

Surgical model for myocardial infarction. Female FVB mice (8 weeks old) were intubated with a 20-gauge angiocath (Ethicon Endo-Surgery, Inc. Cincinnati, OH) and placed under general anesthesia with isoflurane (2%). Myocardial infarction (MI) was created by ligation of the mid-left anterior descending (LAD) artery with 8-0 ethilon suture through a left anterolateral thoracotomy as described.[15] Ten minutes afterwards, the infarct region was confirmed by myocardial blanching. Injections were made at 2 sites near the peri-infarct zone (medial and lateral zones) with a total volume of 50 µL containing 5x10^5 cells or PBS respective of group randomization using a Hamilton syringe with a 29-gauge needle. All surgical procedures were performed in a blinded fashion by one micro-surgeon (G.H.) with several years of experience on this model.

***In vivo* optical bioluminescence imaging (BLI).** BLI was performed using the IVIS 200 (Xenogen, Alameda, CA, USA) system. Recipient mice were anesthetized with isoflurane, shaved, and placed in the imaging chamber. After acquisition of a baseline image, mice were intraperitoneally injected with D-Luciferin (400 mg/kg body weight). Mice were imaged on day 2, 4, 7, and weekly until sacrifice at week 6. Peak signals (photons/s/cm^2/sr) from a fixed region of interest (ROI) were evaluated as described.[11]

Echocardiography to assess left ventricular fractional shortening (LVFS). Echocardiography studies were performed 4 and 6 weeks post-operation. Three independent two-dimensional transversal-targeted M-mode traces were obtained at the level of the papillary muscles using a 14.7-MHz transducer on a Sequoia C512 Echocardiography system (Siemens, Malvern, PA, USA). Using the enclosed software, left ventricular end-diastolic and end-systolic posterior and anterior dimensions were measured by a blinded investigator (A.Y.S.) and processed to calculate left ventricular fractional shortening (LVFS).

Measurement of hemodynamics with pressure-volume loops. Invasive, steady-state hemodynamic measurements were conducted by closed-chest pressure-volume (PV) loop analysis prior to sacrifice at week 6. The animal was placed under general anesthesia as described above. After midline neck incision, a 1.4-F conductance catheter (Millar Instruments, Houston, TX, USA) was retrogradally advanced through the right carotid artery into the left ventricle. The measurements of segmental conductance were recorded which allowed extrapolation of the left ventricular volume, which was coupled with pressure. These data were analyzed in a blinded fashion using PVAN 3.4 Software (Millar Instruments, Houston, TX, USA) and Chart/Scope Software (AD Instruments, Colorado Springs, CO, USA).

***Ex vivo* TaqMan PCR.** In our protocol, the transplanted cells were derived from male mice and were transplanted into female recipients, which facilitate quantification of male cells in the explanted female hearts by tracking the Sry locus found on the Y chromosome. After the invasive hemodynamic measurements at week 6, animals were sacrificed and hearts were randomly selected for explantation, followed by mincing and homogenization in 2 mL DNAzol (Invitrogen, Carlsbad, CA, USA). DNA was isolated according to the manufacturer's protocol. The DNA was quantified on a ND-1000 spectrophotometer (NanoDrop Technologies, Wilmington, DE, USA) and 500 ng DNA was processed for TaqMan PCR using primers specific for the Sry locus. RT-PCR reactions were conducted in iCylcer IQ Real-Time Detection Systems (Bio-Rad, Hercules, CA, USA). Detection levels were compared to a standard curve to assess the number of viable cells per sample. All samples were conducted in triplets.

Postmortem histology. Hearts (n=3/group at week 2) were flushed with saline and placed in 2% paraformaldehyde for 2 hours at room temperature followed by 12-24 hours in 30% sucrose at 4°C. The tissue was embedded in Optical Cutting Temperature (OCT) Compound (Tissue-Tek. Sakura Finetek USA Inc., Torrance, CA) and snap frozen on dry ice. Five-micron sections were cut in both the proximal and apical regions of the infarct zone. Slides were stained for GFP (anti-green fluorescent protein, rabbit IgG fraction, anti-GFP Alexa Fluor 488 conjugate, 1:200, Molecular Probes, Inc.), troponin I (H-170 rabbit polyclonal IgG for cardiac muscle, 1:100, Santa Cruz Biotech, Santa Cruz, CA), and connexin 43 (rabbit polyclonal, 1:100, Sigma). Sections were counterstained with 4,6-diamidino-2-phenylindole (DAPI). Stained tissue was examined by Leica DMRB fluorescent microscope and a Zeiss LSM 510 two-photon confocal laser scanning microscope. Cell engraftment was confirmed by identification of GFP expression under fluorescent microscopy. Colocalization of troponin, alpha sarcomeric actin, and connexin 43 with GFP was visualized with streptavidin-conjugated to Alexa Fluor Red 555 (Invitrogen Molecular Probes, Carlsbad, CA).

Statistical analysis. Statistics were calculated using SPSS 14.0 (SPSS Inc., Chicago, IL, USA). Descriptive statistics included mean and standard error. Comparison between groups was performed using a one-way between groups ANOVA, or one-way repeated measures ANOVA when compared over time, and significance was assumed according to the Bonferroni-Holm's procedure.

Statement of Responsibility: The authors had full access to and take full responsibility for the integrity of the data. All authors have read and accept the manuscript as written.

Conflict of Interest Disclosures: None.

RESULTS

Cell characterization. The MN population consisted of CD34$^+$, CD45$^+$ and CD11b$^+$, representing portions of hematopoietic cells as well as macrophages, granulocytes, and natural killer cells (**figure 1a**).[16] After 6 passages of MSC, flow cytometry results showed absence of CD34, CD45 and C-kit markers (**figure 1b**), indicating depletion of hematopoeitic cells within the MSC. Moreover, these cells expressed the MSC markers CD90 and CD106, with negative expression of CD105 (data not shown). Myoblast cultures steadily differentiated into myotubes under high confluence or after prolonged culture without replating (**figure 2c-d**), which confirmed their fate.[13]

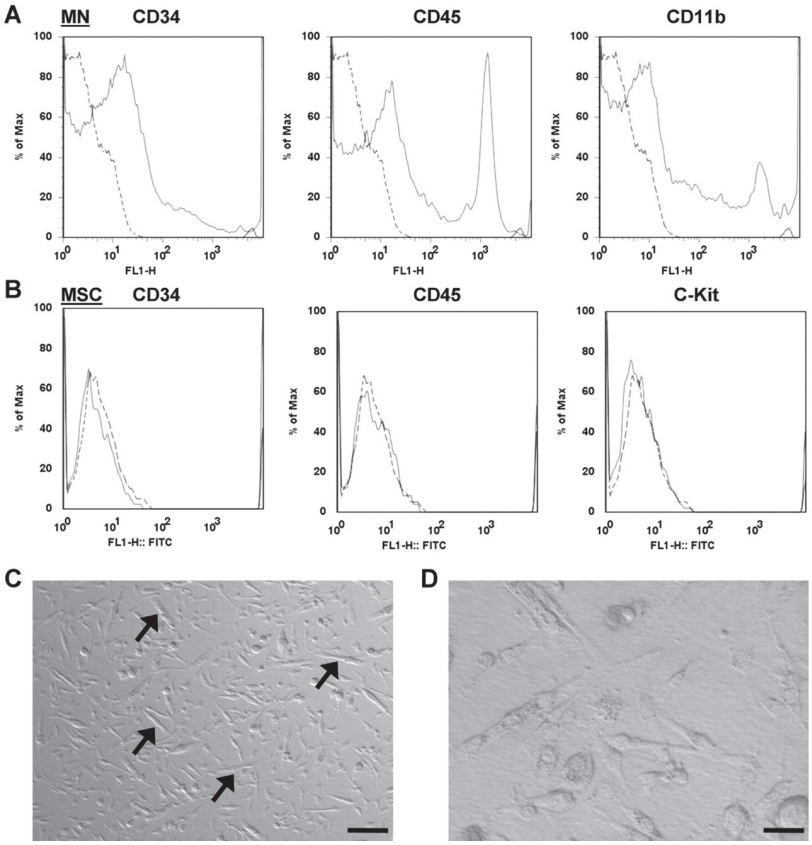

Figure 1. Characterization of cell types based on cell surface expression and cell morphology. (a) Flow cytometry results from bone marrow-derived mononuclear cells (MN) and (b) bone marrow-derived mesenchymal cells (MSC). Green lines represent isotype controls. (c) After prolonged non-passaged culture, skeletal myoblasts (SkMb) change morphologically (100x Bright-field Hoffman modulated contrast image, bar represents 40µm). (d) SkMb form longitudinal myotubes, confirming myoblast phenotype (400x Bright-field Hoffman modulated contrast image, bar represents 10 µm).

Firefly luciferase (Fluc) expression. After culturing for 6 passages, cells were processed for *ex vivo* BLI. Cell number correlated well with BLI signal in all groups (MN: r^2=0.98, SkMb: r^2=0.94, MSC: r^2=0.94, Fibro: r^2=0.93), indicating that BLI is a valid tool to assess cell viability. However, Fluc expression level differed per cell type, as MN showed poor *ex vivo* signal compared to other cell groups (**figure 2a-b**). We hypothesized this was a consequence of the Ficoll selection in the MN group, which may have accounted for hibernation of the cells due to the hostile environment, thereby preventing proper D-Luciferin uptake. In order to test this hypothesis, we lysed the cells and measured intracellular Fluc enzyme. Our *in vitro* luminometry results indeed showed that the Fluc enzyme was present in all cell types and correlated well with cell number (MN: r^2=0.99, SkMb: r^2=0.95, MSC: r^2=1.00, Fibro: r^2=0.93) (**figure 2c**). It also correlated well with the *ex vivo* BLI findings (MN: r^2=0.99, SkMb: r^2=0.98, MSC: r^2=0.90, Fibro: r^2=0.95; **figure 2d**). Thus, BLI is a reliable tool to measure viable cell numbers *ex vivo* and can be used instead of *in vitro* luminometry.

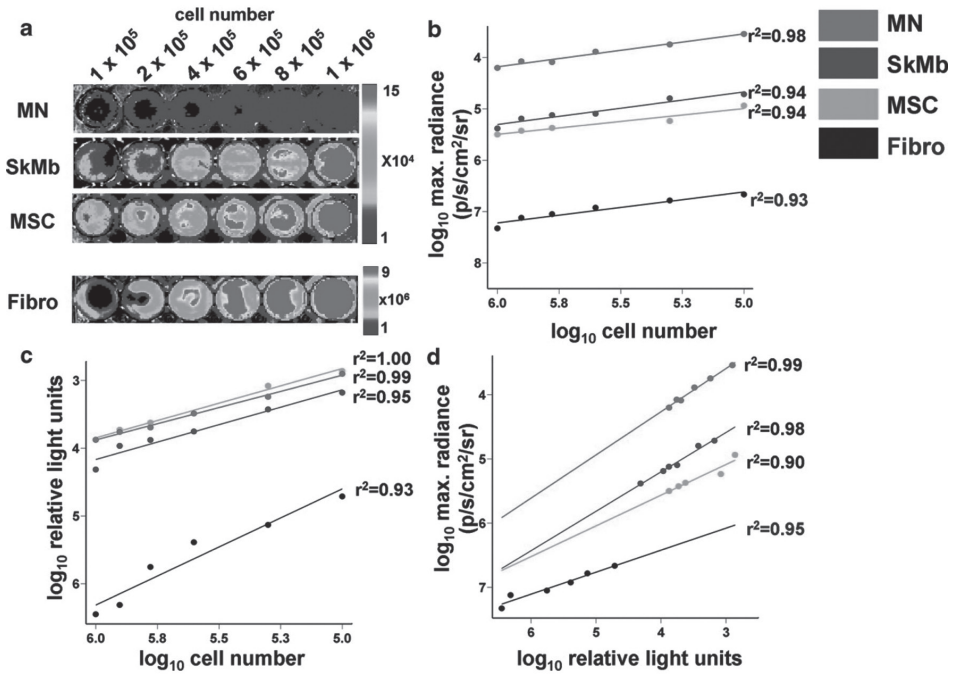

Figure 2. Optical bioluminescence imaging (BLI) signal from firefly luciferase (Fluc) expression reflects viable cell number. (a) BLI of varying numbers of cells in 24-well plates with increasing signals. Scale bars represent peak signal in photons/s/cm²/sr. Cell numbers from all cell types showed robust correlation with (b) Fluc signal on ex vivo BLI and (c) *in vitro* Fluc enzyme on luminometry. (d) Both assays (BLI and luminometry) also correlated well with each other.

***In vivo* kinetics and biodistribution of transplanted cells.** In our study, increasing BLI signals in the MN group suggested a growing number of cells from day 2 to week 2 post-transplant. Moreover, presence of extra-cardiac signals was consistent with migration to other organs such as the femur, spleen, and liver (**figure 3a**). In contrast, for SkMB, MSC, and Fibro, BLI signals decreased acutely from day 2 to week 2. By week 4, the BLI signals equaled background level (**figure 3b-e**). Interestingly, robust signals were seen at day 2 to day 4 in the lungs, suggesting leakage of SkMb, MSC, and Fibro with subsequent intracappillary retention. This might have accounted for the higher rates of acute-phase mortality in these groups (data not shown). In order to assess the effects of myocardial milieu on MN survival, we also compared infarct versus peri-infarct targeted injection. Similarly, we observed significant donor cell death after an initial increase in BLI signal and no major differences in the cell survival pattern between the two modes of injection after 4 weeks (**figure 4**).

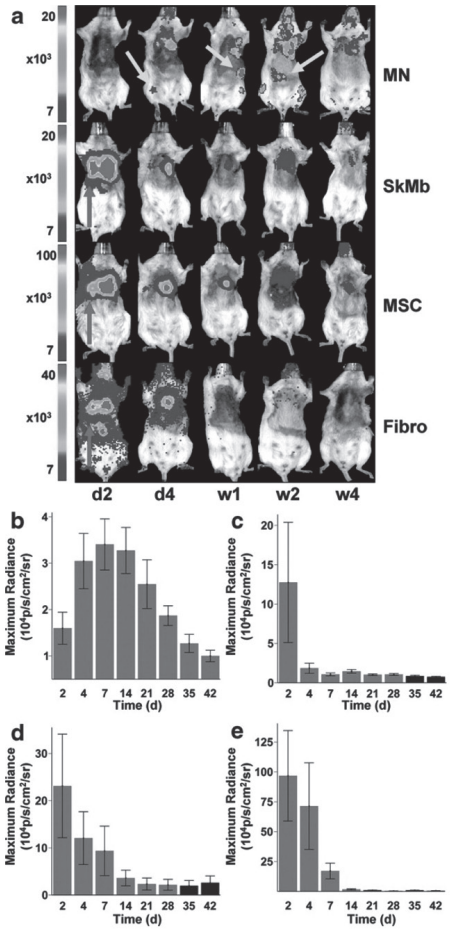

Figure 3. Longitudinal in vivo optical bioluminescence imaging (BLI) of transplanted cell survival. (a) Images from the same representative animal from each group reveal cell proliferation, death, and migration. MN show retention in the heart, and furthermore can home in on the femur, spleen, and liver (yellow arrows). BLI images from animals 2 days after injection of SkMb, MSC, and Fibro show retention not only in the heart, but also in the lungs (red arrows). Decreasing signal intensity over time is indicative of acute donor cell death in these groups. Scale bars represent BLI signal in photons/s/cm^2/sr. (b) Quantification of BLI signals on fixed regions of interest (ROI) over the heart reveal an early increase in signal from day 2 until day 7 in the MN group, while signal intensity in the SkMb (c), MSC (d), and Fibro (e) groups clearly decreases until background signal (black bars) at week 3 to 4. Bars represent mean ± SEM.

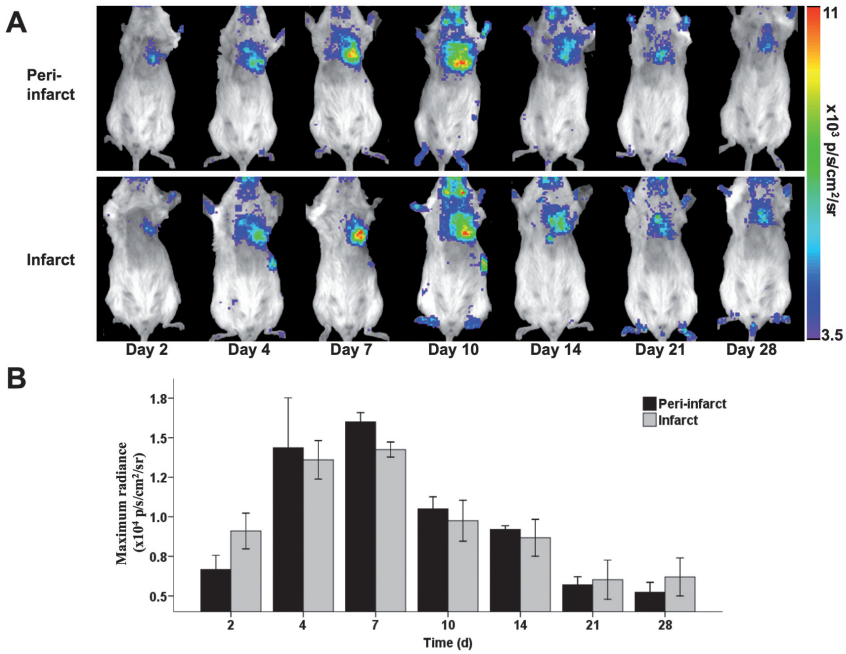

Figure 4. Cardiac injection site does not affect MN survival. (a) Pictures of representative animals injected with MN at the infarct versus peri-infarct zone. Note the acute proliferation phase from day 2 to day 7 followed by cell death from day 7 to day 28. Scale bars represent BLI signal in photons/s/cm²/sr. (b) Graphic representation of quantified BLI signals on fixed regions of interest (ROI) over the heart showing similar cell survival patterns in both groups.

***Ex vivo* quantitative analysis of transplanted cells.** Previously, Muller-Ehmsen and colleagues have shown that post-mortem TaqMan PCR, which is based on the quantification of the Sry locus on the donor Y chromosome in the female recipient tissue, can be used to quantify cell survival in the heart.[17] To confirm increasing MN number during the first week, we explanted representative hearts on day 4 and 7, on which we performed *ex vivo* quantitative TaqMan PCR. Using a standard curve of cell number versus TaqMan cycle (data not shown), we were able to estimate the number of surviving cells. Indeed, this assay confirmed an increase in MN (2167±113 vs. 4408±544 cells, P<0.01) as shown in **figure 5a**. Next we performed TaqMan PCR on hearts injected with MN, SkMB, MSC, and Fibro at week 6 (n=6 per group). Similar to BLI data, the Taqman data confirmed the superior cell survival of MN (1853±568), which was significantly better than SkMb (97±62, *P*=0.001), MSC (341±192, *P*=0.005) and Fibro (no detectable cells, *P*<0.001, ANOVA) (**figure 5b**). Taken together, these *ex vivo* quantitative assays validate the *in vivo* BLI technique, suggesting that the latter can be used to follow cell fate in living subjects and may provide valuable insights into cell migration, proliferation, and death.

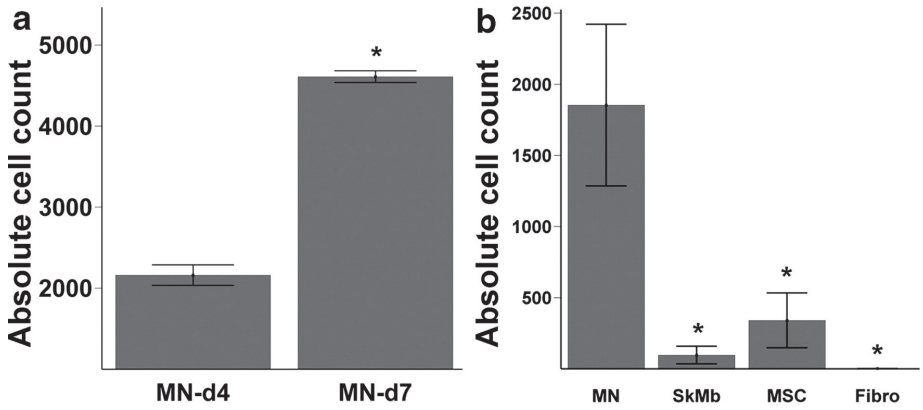

Figure 5. Ex vivo quantitative TaqMan PCR confirms BLI findings. (a) To confirm that the increase of MN signals actually represented increased MN in the hearts, ex vivo TaqMan PCR on extracted DNA from explanted hearts was conducted on day 4 and 7 (n=2 on both time points). TaqMan PCR cycle number was recalculated to absolute cell number using a simultaneously ran standard curve. Bars represent mean ± SEM. * represents P<0.05. (b) At week 6, significantly more MN cells were present in the recipient hearts compared to SkMB, MSC, and Fibro (n=6 per group). Bars represent mean ± SEM. * indicates MN vs. other groups: P<0.05.

Functional effects of cell transplantation. Echocardiographic measurements of cardiac performance were conducted 4 and 6 weeks after cell transplantation (**figure 6a**). At 6 weeks, LVFS for MN (37.1±2.5%) was significantly higher than PBS (30.2±1.9%, *P*<0.001) and Fibro (30.1±2.8%, *P*=0.004) groups. LVFS in the SkMb (35.2±1.8%) group was also significantly better than the PBS group (*P*=0.001), while MSC (32.4±2.1%) had no significant preservative effects compared to Fibro and PBS groups (repeated measurements ANOVA) (**figure 6b**). The LVFS in the PBS group was comparable with the literature.[18] Previously, it has been reported that cell transplantation accounted only for short-term preservation of cardiac function after MI.[19] In the present study, all cell groups showed decreased LVFS on week 6 compared to week 4. These findings suggest that the beneficial effects of cell transplantation may last only for the acute post MI period.

Validation of non-invasive measurements of left ventricular dimensions. Echocardiography readings from week 6 indicated that MN preserved both left-ventricular end-systolic (LVsd) and end-diastolic (LVdd) diameters (data not shown). To validate these findings, we performed invasive hemodynamic measurements. As expected, the left-ventricular end-systolic volume (Ves) 6 weeks after MN injection (42.6±2.0 µL) was significantly less than MSC (58.9±3.4 µL, *P*=0.002) and Fibro (65.1±2.7 µL, *P*<0.001), while the Ves after SkMb injection (49.7±2.7µL) was significantly decreased compared to Fibro (*P*=0.002). Moreover, the left-ventricular end-

diastolic volume (Ved) in the MN group (49.7±3.1 µL) was lower than all other groups and significantly decreased compared to Fibro (70.7±2.5 µL, $P<0.001$). No significant changes were observed in the SkMb (61.5±3.8 µL) and MSC (63.3±3.9 µL) groups (ANOVA). Importantly, these findings match the echocardiography results as mean values of LVsd vs. Ves and LVdd vs. Ved correlated robustly ($r^2=0.99$ and $r^2=0.88$, respectively, **figures 6c-d**).

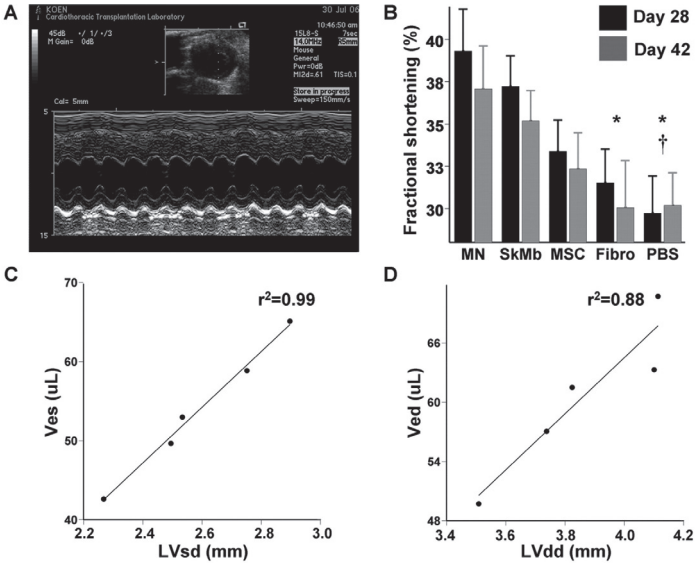

Figure 6. Measurements of functional consequences of cell transplantation into the infarcted mouse heart. (a) Representative M-mode traced picture taken at the level of the papillary muscle whereby left ventricular diameters can be measured. Scale bar is included on the left side. (b) Quantification of LVFS at 4 weeks (black) and 6 weeks (grey) after myocardial infarction and cell transplantation. MN appear to have the greatest functional protective effect compared to other groups. However, there is a general trend toward decreasing cardiac performance at 6 weeks instead. Immediately after echocardiography at week 6, invasive three-dimensional steady-state measurements of ventricular volumes at end-systole (Ves) and end-diastole (Ved) were conducted. Non-invasive echocardiography and invasive hemodynamic measurements correlate robustly between (c) Ves vs. LVsd ($r^2=0.99$) and (d) Ved vs. LVdd ($r^2=0.88$). Bars represent mean±SEM. MN (*) or SkMb (†) vs. indicated groups: $P<0.05$.

Transdifferentiation does not account for better cardiac performance. In our study, GFP-expressing MN could easily be found, confirming engraftment and BLI results (**figure 7**). However, histological samples showed no overlay of donor-specific GFP, nucleus-specific DAPI, and cardiac specific troponin I and connexin 43 markers two weeks after transplantation. Thus, concordant with earlier findings[15, 20], we have not observed MN-derived cardiomyocyte formation. Furthermore, we had difficulty identifying GFP-expressing SkMb, MSC, or Fibro, indicating that only very low counts of these cells were present in the heart (data not shown).

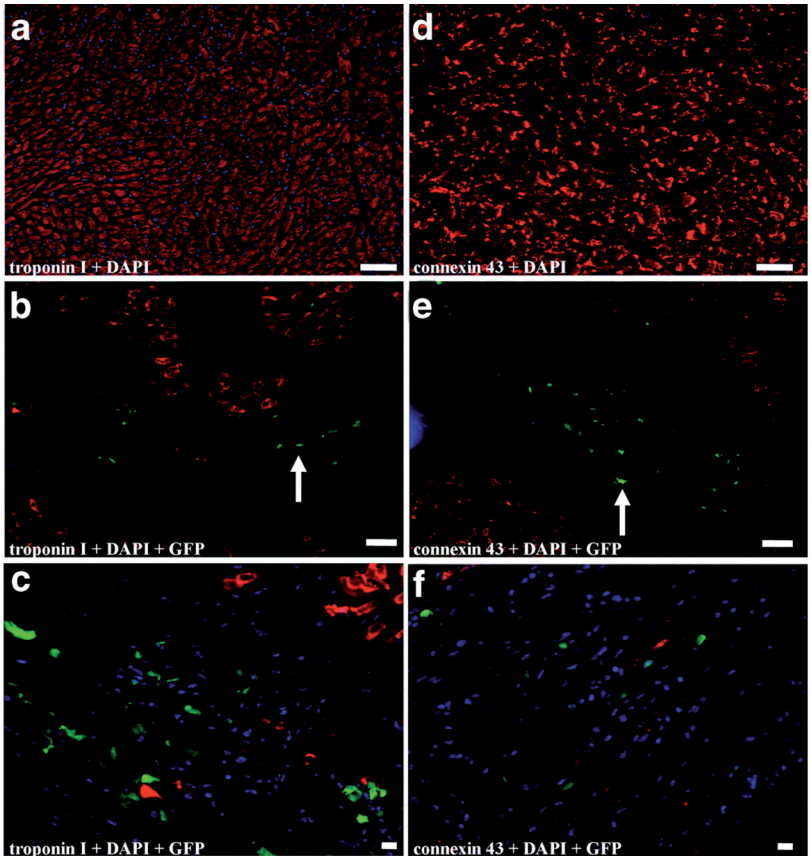

Figure 7. Immunohistochemical staining reveals no evidence of MN transdifferentiation into cardiomyocytes. (a) Representative figure with staining for (b-c) troponin I and DAPI. Although GFP-expressing MN can be found in the myocardium (arrow), there is no cell population with overlay of GFP, DAPI and troponin I to suggest transdifferentiation of MN to cardiomyocytes. (d) Representative figure with staining for (e-f) connexin 43 and DAPI. Although GFP-expressing MN can be found in the myocardium (arrow), there is no cell population with overlay of GFP, DAPI and connexin 43 to suggest transdifferentiation of MN to cardiomyocytes. Bars represent 50 µm.

DISCUSSION

This study is the first to evaluate the efficacy of three different clinical cell candidates for the treatment of myocardial infarction, as compared to a cellular control (Fibro) and non-cellular control (PBS). Our major findings are as follow: (1) molecular imaging using the Fluc reporter gene is a reliable tool for monitoring donor cell survival, proliferation and migration *in vivo*; (2) compared to SkMb, MSC and Fibro, MN show the most favorable survival pattern after injection into the infarcted heart; (3) MN injection leads to a better, but transient, preservation of cardiac function; and (4) this preservation is probably not due to substantial repopulation of the infarcted myocardium (as most cells die by imaging and TaqMan analysis) nor transdifferentiation into MN-derived cardiomyocytes.

Most animal studies assessing the therapeutic potential of cell therapy have used conventional, post-mortem histological or RT-PCR techniques to gain insight in donor cell location and count.[2] However, these techniques cannot monitor the kinetics of cell migration or cell survival in the same subject *in vivo*. In this respect, studies have shown the possibility of labeling donor cells with iron particles or radioactive probes to image cell location *in vivo*. Unfortunately, iron particles are non-specific, as they can be ingested by macrophages following transplanted cell death[21], and the relatively short half-lives of radioactive probes hamper long-term imaging of the cells.[9] By contrast, the current study demonstrates that molecular imaging of the Fluc reporter gene can provide longitudinal *in vivo* imaging of donor cell survival, proliferation, and migration and is in those aspects superior to the aforementioned imaging techniques. These advantages are a result of the stable genetic integration of the reporter gene (Fluc) in the donor cells, which are also equally transferred to progeny cells. As long as the donor/progeny cells are viable, transcription will lead to reporter gene mRNA followed by translation into reporter protein. Following systemic introduction, the reporter probe (D-Luciferin) will be catalyzed by all cells that have the reporter protein, leading to a signal which can be detected by a sensitive CCD camera.[22] However, due to the use of low-energy photons (2-3 eV), BLI is limited by photon attenuation and photon scattering within deep tissues. At present, this technique is not suitable for large animal or human studies.[23] Current studies in our laboratory are therefore aiming to combine multi-fusion reporter gene constructs (thereby enabling PET and BLI imaging) and iron labeling (for MRI).

Using *in vivo* BLI, *ex vivo* TaqMan PCR, and *ex vivo* histology, we have shown superior engraftment of MN compared to SkMB, MSC, and Fibro. Until now, little data exist on survival of transplanted cells in the infarcted heart. Müller-Ehmsen and colleagues used conventional PCR techniques to show that MN and MSC gradually died off until 6 weeks after transplantation of $1x10^5$ cells, with the percentage of engrafted MN being as low as ~2%. Moreover, the authors

found evidence of MN migration to spleen and liver.[24] Splenic and hepatic homing of MN, as also observed in this study, is most likely due to leakage from the initial injection. This has been shown earlier using RT-PCR in mice[24], SPECT imaging in large animal models[25], and PET imaging in humans.[26] In fact, the BLI findings of MN homing resemble leukocyte scans, showing white blood cells are effectively attracted by the liver and spleen.[27] The mechanism by which these organs retain circulating MN may be attributed to chemoattractant properties of the tissue or the biological role that these organs have. For example, the liver expresses high levels of stromal derived factor-1 (SDF-1), which is a developmental and postnatal chemoattractant for stem cells.[28] This has been extrapolated to cardiac stem cell therapy by exogenous myocardial SDF-1 over-expression, which improved the rate of c-kit$^+$ cell homing and improved LV function in hearts with post-infarction LV remodeling.[29]

In addition, increasing *in vivo* BLI signal during the first 2 weeks showed that MN were capable of either proliferation or homing in on the ischemic myocardium after an initial washout during this period of time, which was independent of injection site (infarct or peri-infarct). Although the survival pattern of MN was superior compared to other cell types, it must be stated that the cell number by TaqMan PCR at week 6 equaled ~1,800 cells, representing only ~0.4% of the initially injected cell number. For MSC, we found the *in vivo* imaging signals to decrease dramatically within one week. This pattern concurs with the findings from others who found drastic MSC death between day 3 and 7 after myocardial delivery.[30]

To date, there is intense investigative effort to uncover the mechanism by which stem cells may preserve the function of damaged hearts. Based on our current findings, the preservation of cardiac function by MN transplantation is not attributable to repopulation or transdifferentiation. Rather, the functional benefits of MN transplantation might be due to an augmentation of the natural process of myocardial healing by paracrine signaling and promoting neovascularization, among other factors. It has recently been shown that mice over-expressing MCP-1, which leads to an increased influx of MN into the damaged myocardium after infarction, had decreased infarcted areas and scar formation, and yielded better left ventricular function compared to wild-type mice.[31] Moreover, in the infarcted myocardium, CD11b$^+$ macrophages are an important source of cytokines and growth factors[32] and potential regulators of the extracellular matrix synthesis.[33] Specifically, transplantation of activated macrophages into the infarcted rat heart has been shown to accelerate vascularization and tissue repair and to improve cardiac remodeling and function.[34] Regarding paracrine signaling, bone marrow stem cells can secrete vascular endothelial growth factor (VEGF), basic fibroblast growth factor (bFGF), angiopoetin-1 (Ang-1), and monocyte chemoattractant protein-1 (MCP-1), leading to an increase in collateral perfusion and cardiac function in pigs with myocardial infarction.[35, 36] Concordantly,

results from the Doppler substudy of the REPAIR-AMI trial have recently shown clinical proof of restored microvascular function associated with an improved maximal vascular conductance capacity.[37]

The clinical relevance of this study is significant. Different clinical trials have been conducted with divergent results that raise questions about which optimal cell type to use.[8] Although each cell type has its own advantages and limitations, our study is the first to detect a clear survival and modest functional benefit of MN compared to other clinical cellular candidates. However, questions remain regarding which portion of MN is responsible for the benefit, whether this benefit is transient, and whether a significant difference in cardiac function could translate into a clinical difference. These issues need to be addressed in future studies. Nevertheless, by using multi-modality evaluation, this study has demonstrated that MN confer a survival pattern in the infarcted mouse heart superior to those of SkMb and MSC. Moreover, MN exhibited a modest but transient preservation of cardiac function compared to cellular and non-cellular controls. Finally, our findings highlight the importance of being able to track stem cells *in vivo* and should be an impetus for further research on the development of clinically applicable molecular imaging techniques to closely follow stem cell fate in humans.

ACKNOWLEDGEMENTS

The authors thank V. Mariano for animal care, P. Chu for assistance with histology, and R. Wolterbeek for statistical advice. This work was supported in part by grants from the NIH HL089027, NIH HL074883, and Burroughs Wellcome Foundation Career Award for Medical Scientist (JCW). K.E.A. van der Bogt was supported by the American Heart Association (Medical Student Research Award), Fulbright committee, VSB fund, Michael van Vloten fund, and Jo Keur Grant.

REFERENCES

1. Rosamond W, Flegal K, Friday G, Furie K, Go A, Greenlund K, Haase N, Ho M, Howard V, Kissela B, Kittner S, Lloyd-Jones D, McDermott M, Meigs J, Moy C, Nichol G, O'Donnell C J, Roger V, Rumsfeld J, Sorlie P, Steinberger J, Thom T, Wasserthiel-Smoller S, Hong Y. Heart Disease and Stroke Statistics--2007 Update. A Report From the American Heart Association Statistics Committee and Stroke Statistics Subcommittee. *Circulation*. 2006.
2. Laflamme MA, Murry CE. Regenerating the heart. *Nat Biotechnol*. 2005;23(7):845-856.
3. Hagege AA, Marolleau JP, Vilquin JT, Alheritiere A, Peyrard S, Duboc D, Abergel E, Messas E, Mousseaux E, Schwartz K, Desnos M, Menasche P. Skeletal myoblast transplantation in ischemic heart failure: long-term follow-up of the first phase I cohort of patients. *Circulation*. 2006;114(1 Suppl):I108-113.
4. Lunde K, Solheim S, Aakhus S, Arnesen H, Abdelnoor M, Egeland T, Endresen K, Ilebekk A, Mangschau A, Fjeld JG, Smith HJ, Taraldsrud E, Grogaard HK, Bjornerheim R, Brekke M, Muller C, Hopp E, Ragnarsson A, Brinchmann JE, Forfang K. Intracoronary injection of mononuclear bone marrow cells in acute myocardial infarction. *N Engl J Med*. 2006;355(12):1199-1209.
5. Assmus B, Honold J, Schachinger V, Britten MB, Fischer-Rasokat U, Lehmann R, Teupe C, Pistorius K, Martin H, Abolmaali ND, Tonn T, Dimmeler S, Zeiher AM. Transcoronary transplantation of progenitor cells after myocardial infarction. *N Engl J Med*. 2006;355(12):1222-1232.
6. Schachinger V, Erbs S, Elsasser A, Haberbosch W, Hambrecht R, Holschermann H, Yu J, Corti R, Mathey DG, Hamm CW, Suselbeck T, Assmus B, Tonn T, Dimmeler S, Zeiher AM. Intracoronary bone marrow-derived progenitor cells in acute myocardial infarction. *N Engl J Med*. 2006;355(12):1210-1221.
7. Chen SL, Fang WW, Ye F, Liu YH, Qian J, Shan SJ, Zhang JJ, Chunhua RZ, Liao LM, Lin S, Sun JP. Effect on left ventricular function of intracoronary transplantation of autologous bone marrow mesenchymal stem cell in patients with acute myocardial infarction. *Am J Cardiol*. 2004;94(1):92-95.
8. Rosenzweig A. Cardiac cell therapy--mixed results from mixed cells. *N Engl J Med*. 2006;355(12):1274-1277.
9. Chang GY, Xie X, Wu JC. Overview of stem cells and imaging modalities for cardiovascular diseases. *J Nucl Cardiol*. 2006;13(4):554-569.
10. Cao F, Van Der Bogt KE, Sadrzadeh A, Xie X, Sheikh AY, Wang H, Connolly AJ, Robbins RC, Wu JC. Spatial and temporal kinetics of teratoma formation from murine embryonic stem cell transplantation. *Stem Cells Dev*. 2007.
11. Cao YA, Wagers AJ, Beilhack A, Dusich J, Bachmann MH, Negrin RS, Weissman IL, Contag CH. Shifting foci of hematopoiesis during reconstitution from single stem cells. *Proc Natl*

Acad Sci U S A. 2004;101(1):221-226.

12. Salmon AB, Murakami S, Bartke A, Kopchick J, Yasumura K, Miller RA. Fibroblast cell lines from young adult mice of long-lived mutant strains are resistant to multiple forms of stress. *Am J Physiol Endocrinol Metab.* 2005;289(1):E23-29.
13. Rando TA, Blau HM. Primary mouse myoblast purification, characterization, and transplantation for cell-mediated gene therapy. *J Cell Biol.* 1994;125(6):1275-1287.
14. Cao F, Lin S, Xie X, Ray P, Patel M, Zhang X, Drukker M, Dylla SJ, Connolly AJ, Chen X, Weissman IL, Gambhir SS, Wu JC. In vivo visualization of embryonic stem cell survival, proliferation, and migration after cardiac delivery. *Circulation.* 2006;113(7):1005-1014.
15. Balsam LB, Wagers AJ, Christensen JL, Kofidis T, Weissman IL, Robbins RC. Haematopoietic stem cells adopt mature haematopoietic fates in ischaemic myocardium. *Nature.* 2004;428(6983):668-673.
16. Dziennis S, Van Etten RA, Pahl HL, Morris DL, Rothstein TL, Blosch CM, Perlmutter RM, Tenen DG. The CD11b promoter directs high-level expression of reporter genes in macrophages in transgenic mice. *Blood.* 1995;85(2):319-329.
17. Muller-Ehmsen J, Whittaker P, Kloner RA, Dow JS, Sakoda T, Long TI, Laird PW, Kedes L. Survival and development of neonatal rat cardiomyocytes transplanted into adult myocardium. *J Mol Cell Cardiol.* 2002;34(2):107-116.
18. Rohde LE, Ducharme A, Arroyo LH, Aikawa M, Sukhova GH, Lopez-Anaya A, McClure KF, Mitchell PG, Libby P, Lee RT. Matrix metalloproteinase inhibition attenuates early left ventricular enlargement after experimental myocardial infarction in mice. *Circulation.* 1999;99(23):3063-3070.
19. Dai W, Hale SL, Martin BJ, Kuang JQ, Dow JS, Wold LE, Kloner RA. Allogeneic mesenchymal stem cell transplantation in postinfarcted rat myocardium: short- and long-term effects. *Circulation.* 2005;112(2):214-223.
20. Murry CE, Soonpaa MH, Reinecke H, Nakajima H, Nakajima HO, Rubart M, Pasumarthi KB, Virag JI, Bartelmez SH, Poppa V, Bradford G, Dowell JD, Williams DA, Field LJ. Haematopoietic stem cells do not transdifferentiate into cardiac myocytes in myocardial infarcts. *Nature.* 2004;428(6983):664-668.
21. Terrovitis J, Stuber M, Youssef A, Preece S, Leppo M, Kizana E, Schar M, Gerstenblith G, Weiss RG, Marban E, Abraham MR. Magnetic Resonance Imaging Overestimates Ferumoxide-Labeled Stem Cell Survival After Transplantation in the Heart. *Circulation.* 2008.
22. van der Bogt KE, Swijnenburg RJ, Cao F, Wu JC. Molecular imaging of human embryonic stem cells: keeping an eye on differentiation, tumorigenicity and immunogenicity. *Cell Cycle.* 2006;5(23):2748-2752.
23. Li Z, Suzuki Y, Huang M, Cao F, Xie X, Connolly AJ, Yang PC, Wu JC. Comparison of Reporter Gene and Iron Particle Labeling for Tracking Fate of Human Embryonic Stem

Cells and Differentiated Endothelial Cells in Living Subjects. Stem Cells. 2008.

24. Muller-Ehmsen J, Krausgrill B, Burst V, Schenk K, Neisen UC, Fries JW, Fleischmann BK, Hescheler J, Schwinger RH. Effective engraftment but poor mid-term persistence of mononuclear and mesenchymal bone marrow cells in acute and chronic rat myocardial infarction. *J Mol Cell Cardiol.* 2006;41(5):876-884.
25. Hou D, Youssef EA, Brinton TJ, Zhang P, Rogers P, Price ET, Yeung AC, Johnstone BH, Yock PG, March KL. Radiolabeled cell distribution after intramyocardial, intracoronary, and interstitial retrograde coronary venous delivery: implications for current clinical trials. *Circulation.* 2005;112(9 Suppl):I150-156.
26. Hofmann M, Wollert KC, Meyer GP, Menke A, Arseniev L, Hertenstein B, Ganser A, Knapp WH, Drexler H. Monitoring of bone marrow cell homing into the infarcted human myocardium. *Circulation.* 2005;111(17):2198-2202.
27. Datz FL, Luers P, Baker WJ, Christian PE. Improved detection of upper abdominal abscesses by combination of 99mTc sulfur colloid and 111In leukocyte scanning. *AJR Am J Roentgenol.* 1985;144(2):319-323.
28. Kucia M, Reca R, Miekus K, Wanzeck J, Wojakowski W, Janowska-Wieczorek A, Ratajczak J, Ratajczak MZ. Trafficking of normal stem cells and metastasis of cancer stem cells involve similar mechanisms: pivotal role of the SDF-1-CXCR4 axis. *Stem Cells.* 2005;23(7):879-894.
29. Zhang G, Nakamura Y, Wang X, Hu Q, Suggs LJ, Zhang J. Controlled release of stromal cell-derived factor-1 alpha in situ increases c-kit+ cell homing to the infarcted heart. *Tissue Eng.* 2007;13(8):2063-2071.
30. Mangi AA, Noiseux N, Kong D, He H, Rezvani M, Ingwall JS, Dzau VJ. Mesenchymal stem cells modified with Akt prevent remodeling and restore performance of infarcted hearts. *Nat Med.* 2003;9(9):1195-1201.
31. Morimoto H, Takahashi M, Izawa A, Ise H, Hongo M, Kolattukudy PE, Ikeda U. Cardiac overexpression of monocyte chemoattractant protein-1 in transgenic mice prevents cardiac dysfunction and remodeling after myocardial infarction. *Circ Res.* 2006;99(8):891-899.
32. Frangogiannis NG, Smith CW, Entman ML. The inflammatory response in myocardial infarction. *Cardiovasc Res.* 2002;53(1):31-47.
33. Frangogiannis NG, Mendoza LH, Lindsey ML, Ballantyne CM, Michael LH, Smith CW, Entman ML. IL-10 is induced in the reperfused myocardium and may modulate the reaction to injury. *J Immunol.* 2000;165(5):2798-2808.
34. Leor J, Rozen L, Zuloff-Shani A, Feinberg MS, Amsalem Y, Barbash IM, Kachel E, Holbova R, Mardor Y, Daniels D, Ocherashvilli A, Orenstein A, Danon D. Ex vivo activated human macrophages improve healing, remodeling, and function of the infarcted heart. *Circulation.* 2006;114(1 Suppl):I94-100.

35. Fuchs S, Baffour R, Zhou YF, Shou M, Pierre A, Tio FO, Weissman NJ, Leon MB, Epstein SE, Kornowski R. Transendocardial delivery of autologous bone marrow enhances collateral perfusion and regional function in pigs with chronic experimental myocardial ischemia. *J Am Coll Cardiol.* 2001;37(6):1726-1732.
36. Kamihata H, Matsubara H, Nishiue T, Fujiyama S, Tsutsumi Y, Ozono R, Masaki H, Mori Y, Iba O, Tateishi E, Kosaki A, Shintani S, Murohara T, Imaizumi T, Iwasaka T. Implantation of bone marrow mononuclear cells into ischemic myocardium enhances collateral perfusion and regional function via side supply of angioblasts, angiogenic ligands, and cytokines. *Circulation.* 2001;104(9):1046-1052.
37. Erbs S, Linke A, Schachinger V, Assmus B, Thiele H, Diederich KW, Hoffmann C, Dimmeler S, Tonn T, Hambrecht R, Zeiher AM, Schuler G. Restoration of microvascular function in the infarct-related artery by intracoronary transplantation of bone marrow progenitor cells in patients with acute myocardial infarction: the Doppler Substudy of the Reinfusion of Enriched Progenitor Cells and Infarct Remodeling in Acute Myocardial Infarction (REPAIR-AMI) trial. *Circulation.* 2007;116(4):366-374.

CHAPTER 7

Comparison of Transplantation of Adipose Tissue- and Bone Marrow- Derived Mesenchymal Stem Cells in the Infarcted Heart

Koen E.A. van der Bogt, Sonja Schrepfer, Jin Yu, Ahmad Y. Sheikh,

Grant Hoyt, Johannes A. Govaert, Jeffrey B. Velotta,

Christopher H. Contag, Robert C. Robbins and Joseph C. Wu

Transplantation 2009 Mar 15;87(5):642-52.

ABSTRACT

Background: Mesenchymal stem cells hold promise for cardiovascular regenerative therapy. Derivation of these cells from the adipose tissue might be easier compared to bone marrow. However, the *in vivo* fate and function of adipose stromal cells (ASC) in the infarcted heart has never been compared directly to bone marrow derived mesenchymal cells (MSC).

Methods: ASC and MSC were isolated from transgenic FVB mice with β-actin promoter driving firefly luciferase and green fluorescent protein (Fluc-GFP) double fusion reporter gene, and were characterized using flow cytometry, microscopy, bioluminescence imaging (BLI) and luminometry. FVB mice (n=8/group) underwent myocardial infarction followed by intramyocardial injection of $5x10^5$ ASC, MSC, fibroblasts (Fibro, positive control), or saline (negative control). Cell survival was measured using BLI for 6 weeks and cardiac function was monitored by echocardiography and pressure-volume (PV) analysis. Ventricular morphology was assessed using histology.

Results: ASC and MSC were $CD34^-$, $CD45^-$, c-Kit^-, $CD90^+$, Sca-1^+, shared similar morphology, and had a population doubling time of ~2 days. Cells expressed Fluc reporter genes in a number-dependent fashion, as confirmed by luminometry. After cardiac transplantation, both cell types showed drastic donor cell death within 4-5 weeks. Furthermore, transplantation of either cell type was not capable of preserving ventricular function and dimensions, as confirmed by PV-loops and histology.

Conclusion: This is the first study comparing the *in vivo* behavior of both cell types in the infarcted heart. ASC and MSC do not tolerate well in the cardiac environment, resulting in acute donor cell death and a subsequent loss of cardiac function similar to control groups.

INTRODUCTION

Almost 80 million Americans suffer from cardiovascular disease (CVD), and with an average of one death every 36 seconds, CVD is the number one killer of Americans. Despite a wide range of therapeutic options to prevent progression of heart failure, end-stage disease can only be treated by heart transplantation which is, in turn, hampered by a lack of suitable donor organs.[1] Bone marrow mononuclear stem cells (BMSC) have raised hope as a new therapeutic modality as they were believed to differentiate into cardiomyocytes when transplanted into the infarcted murine myocardium.[2] Although this observation is subject to controversy[3], BMSC-mediated cardiac repair has recently been introduced into clinical medicine[4]. A small stromal subset of BMSC, called mesenchymal stem cells (MSC), is capable of proliferation *in vitro*[5] and therefore gains popularity as a candidate to replace the infarcted myocardium. MSC have been proposed to improve cardiac function after myocardial infarction in both animals[6] and humans[7], and might even have an immunomodulating effect.[8] However, the process of bone marrow harvesting can be painful and is limited in the quantity of aspirate.

Recently, stromal cells have been isolated from the adipose tissue[9], which would be an ideal source regarding procurement procedure (e.g., elective abdominoplasty) and yield. These adipose stromal cells (ASC) largely express the same surface markers as MSC[10] and have shown to preserve cardiac function after infarction.[11] Although the *in vitro* properties of ASC and MSC have been compared before[12-14], there are no reports evaluating the cellular behavior and functional effects of either cell type when transplanted into the ischemic myocardium. Here, we present the first report using a molecular imaging technique to unveil and compare the *in vivo* behaviors and functional effects of ASC and MSC following transplantation into the infarcted heart.

METHODS

Animals. All animal study protocols were approved by the Stanford Animal Research Committee. The donor group consisted of male L2G mice (n=4, 8 weeks old), which were bred on FVB background and ubiquitously express green fluorescent protein (GFP) and firefly luciferase (Fluc) reporter genes driven by a β-actin promoter as previously described [15]. Recipient animals (n=37) consisted of syngeneic, female FVB mice (8 weeks old, Jackson Laboratories, Bar Harbor, ME). Animals were randomized into 4 recipient groups (n=8/ group): (1) adipose tissue-derived stromal cells (ASC), (2) bone-marrow-derived mesenchymal cells (MSC), (3) fibroblasts (Fibro) as cellular control group, and (4) phosphate buffered saline (PBS) as non-cellular control group.

Cell culture of Fibro, ASC, and MSC. Donor mice were sacrificed by cervical dislocation after ample anesthesia with isoflurane, and were placed in 70% ethanol for 5 minutes. **(A)** For the

isolation of Fibro, skin biopsies were taken from the tail and ears, minced and incubated overnight in collagenase type II (400 U/mL, Gibco-Invitrogen, Carlsbad, CA), dissolved in DMEM (Gibco, NY) supplemented with 20% heat-inactivated fetal bovine serum (FBS, Hyclone, Logan, UT), 1% antibiotics/antimycotic solution (Penicillin/Streptomycin, Gibco-Invitrogen, Carlsbad, CA) at 37°C and 5% CO_2 in air as described [16]. The next day, cells were dislodged from digested tissue by repeated pipetting and were passed through 70 µm sterile netting into sterile 15-ml centrifuge tubes. The samples were centrifuged for 5 minutes at 1200 rounds per minute (rpm), and the cell pellet was resuspended in DMEM/20% FBS/1%Penicillin-Streptomycin to be plated in a 25 cm^2 tissue flask at 37°C/5%CO_2. **(B)** For the isolation of ASC, the adipose tissue was isolated from the inguinal and abdominal region as described before.[17] In brief, the adipose tissue was washed in PBS and digested using 5 mL 0.075% collagenase (type I, Gibco-Invitrogen, Carlsbad, CA) in PBS for 30 minutes, followed by deactivation by DMEM/20% FBS/1%Penicillin-Streptomycin. After centrifuging for 5 minutes at 1200 rpm, the cell pellet was resuspended and incubated for 10 minutes in ACK lysing buffer to eliminate red blood cells. The suspension was centrifuged, resuspended in DMEM/ 20% FBS/1%Penicillin-Streptomycin, filtered through a 70 µm mesh, and plated in a 25 cm^2 tissue flask at 37°C/ 5%CO_2 to grow ASC. **(C)** For the isolation of MSC, the long bones were explanted, washed and flushed with PBS using a 25-Gauge needle to collect bone marrow. After passing through a 70 µm strainer, the isolate was centrifuged at 1200 rpm for 5 minutes, washed and resuspended into DMEM/20%FBS/1%Penicillin/Streptomycin medium to grow MSC as described.[5]

Flow cytometry. At passage 8-10, the cells were labeled using specific FITC-conjugated antibodies against CD34, CD45, C-kit, Sca-1, CD90, and CD106 and processed through a FACSCalibur system (BD, San Jose, CA) according to the manufacturer's protocol. Results were compared to appropriate isotype controls.

***In vitro* firefly luciferase (Fluc) assays.** Cells were dislodged from culture flasks to be resuspended in PBS. Cell suspensions were divided into a 6-well plate in known concentrations. After administration of D-Luciferin (Xenogen, Alameda, CA, 4.5ug/mL), peak signal (photons/second/square centimeter/steridian or p/s/cm^2/sr) was measured using a charged coupled device (CCD) camera (IVS200, Xenogen, Alameda, CA). Same amounts of dislodged cells were lysed using 200 µL of 10X Passive Lysis Buffer (Promega, Madison, WI) and centrifuged at maximum speed for 2 minutes at 4°C. For every sample, 20 µL of supernatant was added to 100 µL of Luciferase Assay Reagent (LAR-II, Promega, Madison, WI) and luminosity in relative light units (RLU) was measured on a 20/20n luminometer (Turner Biosystems, Sunnyvale, CA). All samples were conducted in triplets.

Surgical model. Female FVB mice (8 weeks old) were intubated with a 20-gauge angiocath (Ethicon Endo-Surgery, Inc. Cincinnati, OH) and were placed under general anesthesia with isoflurane (2%). Myocardial infarction (MI) was created by ligation of the mid-left anterior descending (LAD) artery with 8-0 Ethilon suture through a left anterolateral thoracotomy. After approximately 10 minutes, the infarct region was injected with $5x10^5$ cells or PBS respective of group randomization using a Hamilton syringe with a 29-gauge needle. The chest was closed in 4 layers with 5-0 vicryl suture. All surgical procedures were performed in a blinded fashion by one micro-surgeon (G.H.) with several years of experience with this model.

Echocardiography. Echocardiography studies were performed 2, 4 and 6 weeks postoperatively. Three independent two-dimensional transversal-targeted M-mode traces were obtained at the level of the papillary muscles using a 14.7-MHz transducer on a Sequoia C512 Echocardiography system (Siemens, Malvern, PA). Using the enclosed software, left ventricular end-diastolic and end-systolic posterior and anterior dimensions were measured by a blinded member of our group (A.Y.S.) and processed to calculate left ventricular fractional shortening (LVFS).

***In vivo* optical bioluminescence imaging (BLI).** BLI was performed using the IVIS200 (Xenogen, Alameda, CA) system. Recipient mice were anesthetized with isoflurane, shaved and placed in the imaging chamber. After acquisition of a baseline image, mice were intraperitoneally injected with D-Luciferin (400 mg/kg body weight; Xenogen, CA). Mice were imaged on postoperative day 2, 4, 7, 10, and at week 2, 4, 5, and 6. Peak signal ($p/s/cm^2/sr$) from a fixed region of interest (ROI) was evaluated using Living Image 2.50.1 software (Xenogen, CA).

Invasive hemodynamics. Invasive hemodynamic measurements were conducted by closed-chest pressure-volume (PV) loop analysis prior to sacrifice at week 6. The animal was placed under general anesthesia as described above. After midline neck incision, a 1.4 F conductance catheter (Millar Instruments, Houston, TX) was retrogradely advanced through the right carotid artery into the left ventricle. The measurements of segmental conductance were recorded which allowed extrapolation of the left ventricular volume, which was coupled with pressure. These data were analyzed in a blinded fashion using PVAN 3.4 Software (Millar Instruments, Houston, TX) and Chart/Scope Software (AD Instruments, Colorado Springs, CO).

Postmortem histology. Hearts (n=3/group at week 6) were flushed with saline and placed in 2% paraformaldehyde for 2 hours at room temperature followed by 12-24 hours in 30% sucrose at 4°C. The tissue was embedded in Optical Cutting Temperature (OCT) Compound (Tissue-Tek. Sakura Finetek USA Inc., Torrance, CA) and snap frozen on dry ice. Five-micron sec-

tions were cut in both the proximal and apical regions of the infarct zone. Slides were stained for H&E. Stained tissue was examined by Leica DMRB fluorescent microscope.

***Ex vivo* TaqMan PCR.** Animals were sacrificed and hearts were explanted, followed by mincing and homogenization in 2 mL DNAzol (Invitrogen, Carlsbad, CA, USA). DNA was isolated according to the manufacturer's protocol. The DNA was quantified on a ND-1000 spectrophotometer (NanoDrop Technologies, Wilmington, DE, USA) and 500 ng DNA was processed for TaqMan PCR using primers specific for the *Sry* locus selectively found on the Y chromosome in the male donor cells. RT-PCR reactions were conducted in iCylcer IQ Real-Time Detection Systems (Bio-Rad, Hercules, CA, USA). Lower cycle numbers represent higher donor cell counts.[18] Samples were conducted in triplets.

Effects of gender mismatch, myocardial ischemia, and green fluorescent protein (GFP) on cell survival. To investigate the effect of our gender mismatch model, we injected $5x10^5$ male and female cells into the hindlimbs of male FVB mice (n=5). To assess the effects of myocardial milieus (ischemia vs. non-ischemia) on cell survival, 5x105 MSC were injected into non-infarcted hearts from female FVB recipients (n=3). To evaluate whether GFP could have an effect on transplanted cell survival, $5x10^5$ GFP^+-$Fluc^+$ cells were injected into the hindlimbs of female FVB mice that previously received intramyocardial GFP-Fluc plasmid injection 3 months prior (n=3). As control, $5x10^5$ GFP^+-$Fluc^+$ were similarly injected in non-manipulated FVB mice (n=3). In these experiments, cell survival was measured using *in vivo* optical bioluminescence imaging as described above.

Statistics. Statistics were calculated using SPSS 15.0 (SPSS Inc., Chicago, IL). Descriptive statistics included mean and standard error. Comparison between groups was performed using a one-way between groups ANOVA, or, when compared over time, one-way repeated measures ANOVA, both with Bonferroni correction. A logarithmic transformation of values was performed when needed to ensure normal distribution within each group and significance was assumed when $P<0.05$.

RESULTS

Characterization of ASC, MSC, and Fibro. After culturing for approximately 8 passages, hematopoietic cells were eliminated from both ASC and MSC cultures. This was confirmed by flow cytometry showing absent CD34, CD45, and C-kit markers. Moreover, both populations were Sca-1^+, $CD90^+$, and $CD106^+$ (MSC) or $CD106^-$ (ASC) (**figure 1)**, consistent with prior literature comparing expression patterns of ASC and MSC.[13]

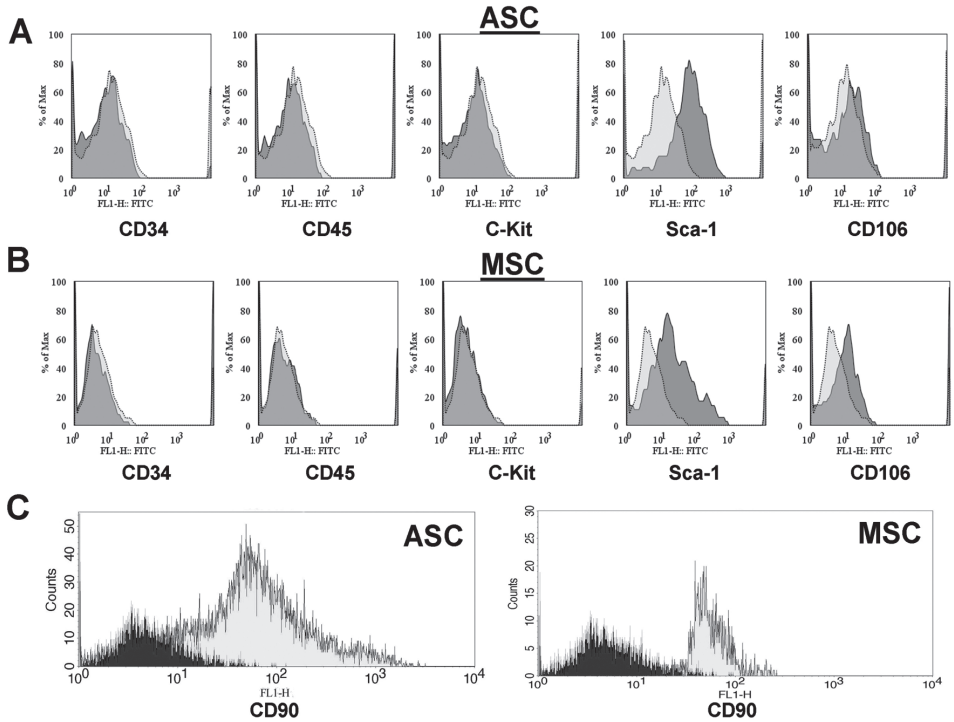

Figure 1. ***In vitro*** **assessment of cell surface marker expression.** (a) After 8-10 passages, flow cytometry showed that the ASC population was depleted from hematopoietic cells. Moreover, these cells tested negative for CD106, but positive for the stem cell antigen (Sca-1). (b) MSC also showed negative hematopoietic expression, but differed from their adipose tissue-derived counterparts regarding a positive expression for CD106. Dotted, light grey areas represent isotype controls. (c) Both ASC and MSC expressed the mesenchymal-specific marker CD90 (Black areas represent isotype controls).

On microscopy, both cell types showed spindle-shaped morphology (**figure 2a**). Following isolation, MSC have slower population doubling time compared to ASC and Fibro before eventually growing like ASC and Fibro with an average population doubling time of approximately 2 days at passage 7 (**figure 2b**). All populations were furthermore tested for the expression of the reporter gene firefly luciferase (Fluc) (**figure 2c**). In all groups, cell number and Fluc signal correlated robustly with r^2 values of 0.95 (ASC), 0.80 (MSC), and 0.97 (Fibro). Moreover, the assay of Fluc enzyme activity by luminometry also showed good correlation with cell number (ASC: r^2=0.95, MSC: r^2=0.85, Fibro: r^2=0.98, **figure 2d**).

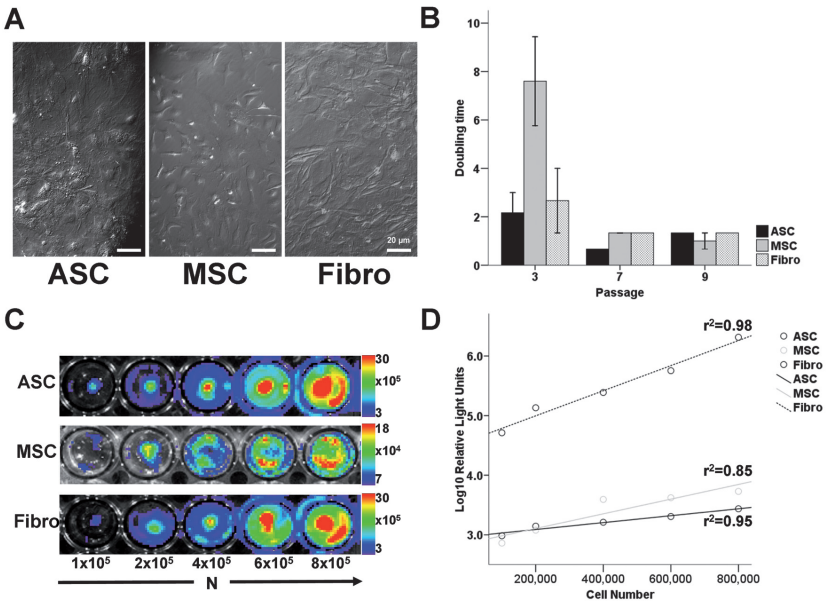

Figure 2. *In vitro* characterization of morphology, expansion time, and reporter gene expression. (a) When kept into culture, all cell types shared a spindle-shaped morphology (Bright-field Hoffman modulated contrast image, bar represents 20µm). (b) After an initial period of relatively slower *in vitro* growth of MSC, all cell types had mutual doubling times of approximately 2 days at passage 9. Bars represent mean ± SEM. (c) *In vitro* optical bioluminescence imaging (BLI) signal from firefly luciferase (Fluc) expression of increasing numbers of cells in 24-well plates show a correlative increase in signal intensity. Scale bars represent peak signal in photons/s/cm^2/sr. (d) Lysates from the cell populations shown in figure 2c also showed robust correlation of cell number with Fluc enzyme on conventional luminometry.

Importantly, Fluc enzyme activity correlated well with the previous BLI findings (ASC: r^2=0.86, MSC: r^2=0.75, Fibro: r^2=0.95). Taken together, these data suggest that BLI is a reliable tool for measuring viable cell numbers and can be used instead of luminometry. Moreover, we found a robust correlation between *in vivo* BLI signals and *ex vivo* TaqMan PCR cycle counts of *Sry* expression, indicating that cardiac BLI signal is representative of the presence of male donor cells in the female hearts **(figure 3)**.

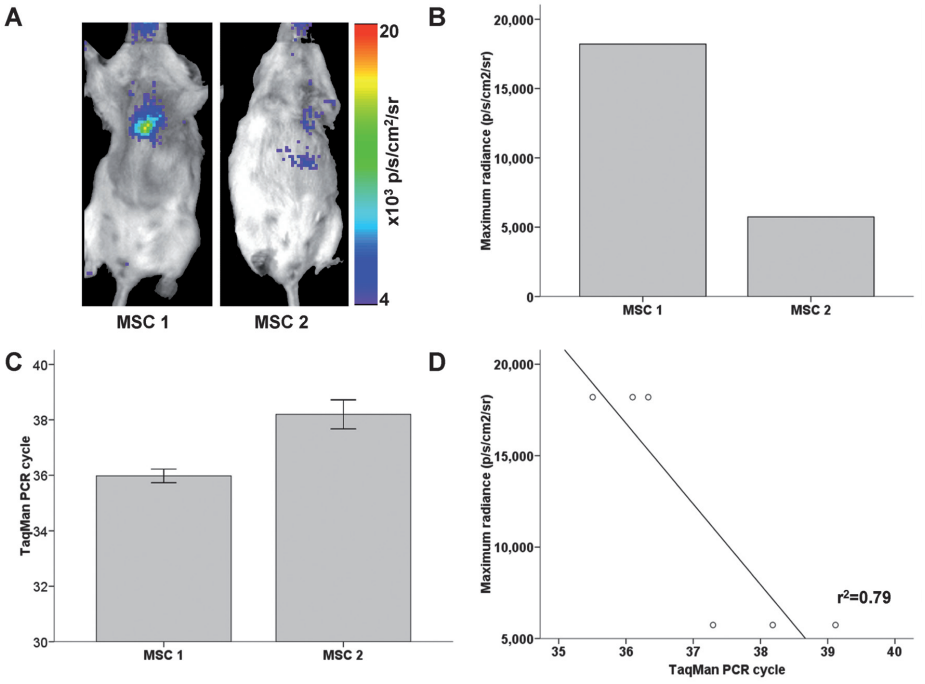

Figure 3. *In vivo* optical bioluminescence signals parallel ex vivo male donor cell Sry expression on TaqMan PCR. Facilitated by the male-to-female transplant model, *in vivo* BLI signals were controlled by TaqMan PCR-assessment of Sry expression of the male donor cells in the female hearts. (a,b) The hearts of 2 mice (MSC 1,2) with different BLI signals were explanted, the DNA was extracted, and TaqMan PCR was performed on 3 samples from each heart. (c) Higher BLI signal in MSC 1 correspond to lower PCR cycle counts, indicating higher Sry expression caused by increased donor cell count. (d) Correlation plot of BLI signals vs. TaqMan PCR cycle (r^2=0.79).

Kinetics of cell survival by longitudinal bioluminescence imaging. Previously, several groups have used RT-PCR or histological techniques and observed radical cell death after MSC transplantation into the ischemic myocardium.[18, 19] However, these techniques do not allow for longitudinal imaging of cellular kinetics. Our BLI data showed that 2 days after intramyocardial transplantation, all cell types exhibited robust signals from the cardiac region, thereby confirming successful transplantation.[20] However, in the following days, all three cell types experienced significant donor cell death (**figure 4a**). Quantitative analysis shows decreased signals at day 7-10 as compared to day 2, which reached background levels by week 4-5 (**figure 4b-d**). When normalized to the signal of day 2, there were no significant differences between ASC, MSC, and the Fibro control group (**figure 4e**, *P*=NS, repeated measurements ANOVA).

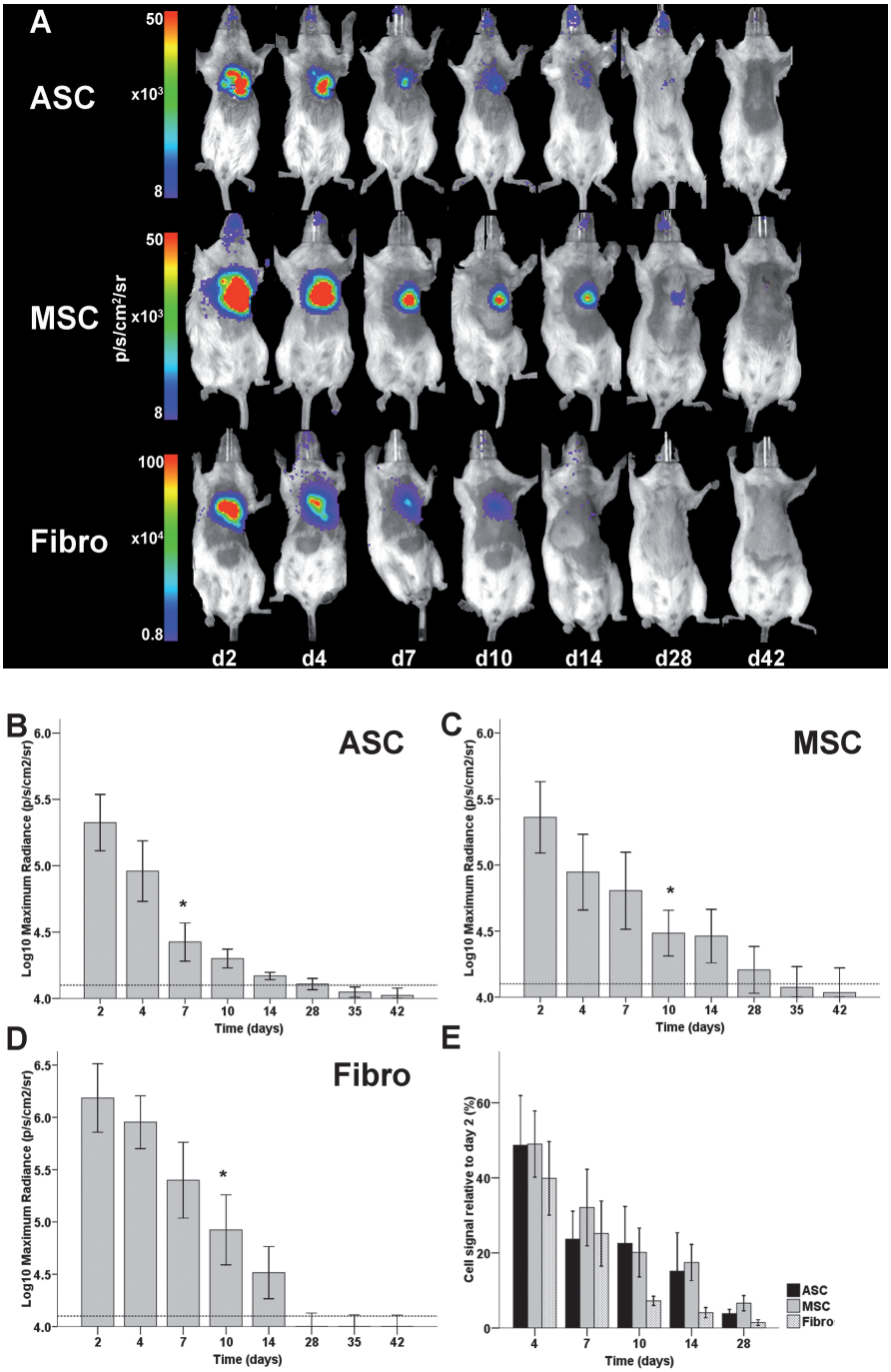

Figure 4. Longitudinal *in vivo* optical bioluminescence imaging (BLI) of intramyocardially transplanted cells in living mice. (a) Representative figures of animals within each group show that, after an initial strong cardiac signal 2 days after transplantation, robust cell death resulted in a remarkable decrease in signal over 4

weeks. Scale bars represent BLI signal in photons/s/cm²/sr. (b-d) Graphic representation of decreasing signals in the (b) ASC, (c) MSC, and (d) Fibro groups which are indicative of cell death. Background signals (dotted line) were reached between week 3 (Fibro) to week 5 (MSC) (n>7 in all groups, * indicates P<0.05 compared to the signal on day 2, ANOVA). (e) Normalized graph of reporter gene signals from transplanted cells showing that, when compared over time and controlled for initial differences in signal between cell types, there were no significant differences between ASC, MSC, and cellular control groups (Bars represent mean ± SEM, p=NS, repeated measurements ANOVA).

Influence of gender mismatch, myocardial milieus, and GFP expression on *in vivo* transplanted cell survival. To enable *ex vivo* validation of our *in vivo* BLI study, we performed a gender mismatch model with male donors and female recipients followed by TaqMan PCR of male *Sry* gene. From studies with organ transplant patients, it has been noticed that male patients receiving female grafts have decreased graft survival and require more immunosuppressant drugs [21]. Although this effect was generally less apparent in male-female transplants [21], we set out to investigate the role of gender mismatch by transplanting equal numbers of male and female ASC into hindlimbs of male mice. As shown in **figure 5**, there were no significant differences in cell survival between the cell types from both genders. After two weeks, BLI signals were $6.3 \times 10^4 \pm 0.8 \times 10^4$ p/s/cm²/sr for male ASC and $5.7 \times 10^4 \pm 1.3 \times 10^4$ p/s/cm²/sr for female ASC (*P*=NS).

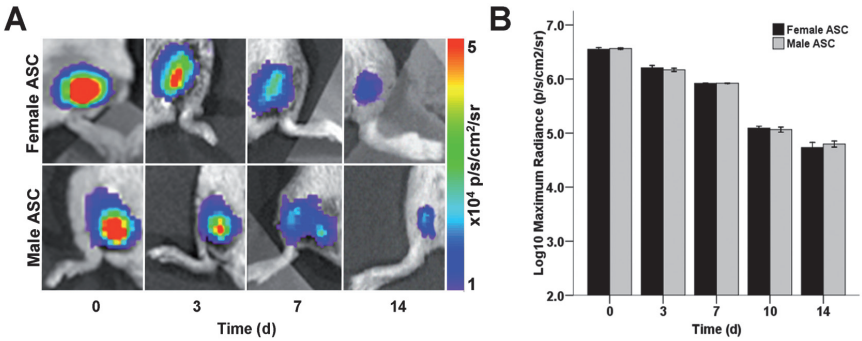

Figure 5. Effect of donor-recipient gender mismatch on *in vivo* cell survival. To assess whether gender mismatch had influenced cell survival, both 5×10^5 male and female ASC were transplanted into male mice. (a, b) Imaging signals from either cell type were comparable without any significant differences. Scale bars represent BLI signal in photons/s/cm²/sr (Bars represent means ± SEM, n=5, p=NS, ANOVA).

In our study, it is also possible that GFP can elicit an immune response [22], which may have led to a decreased survival in our cardiac experiments. In order to differentiate between the effects of ischemic versus normal cardiac tissue on stem cell survival, MSC were also transplanted into non-infarcted hearts. While acute survival was observed in the non-ischemia group, the cells were still not capable of surviving for a prolonged period (**figure 6**).

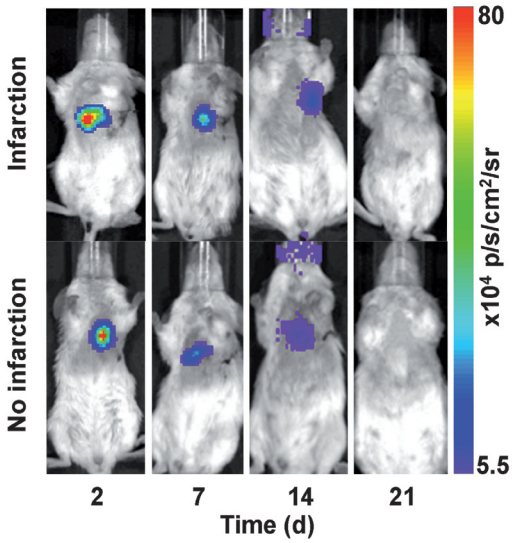

Figure 6. Effect of ischemia on *in vivo* cell survival. In order to differentiate between the effects of ischemic versus normal cardiac tissue on stem cell survival, $5x10^5$ MSC were transplanted into both infarcted and non-infarcted hearts. No significant differences in cell survival were observed in a 3-week period. Scale bar represents BLI signal in photons/s/cm^2/sr (n=3/group, p=NS, ANOVA).

In order to explore the influence of GFP-expression on cell survival, we transplanted GFP^+-$Fluc^+$ into the hindlimbs of naïve FVB mice or FVB mice that were pre-sensitized by means of previous Fluc-GFP plasmid injection. By comparison of cell survival pattern, again there were no significant differences between BLI signals from both animals (**figure 7**). In summary, while both gene mismatch and GFP immunogenicity could have affected cell survival, our direct comparison studies suggest that they were not the main contributing factors for the loss of imaging signal, and thus cell survival, in our experiments.

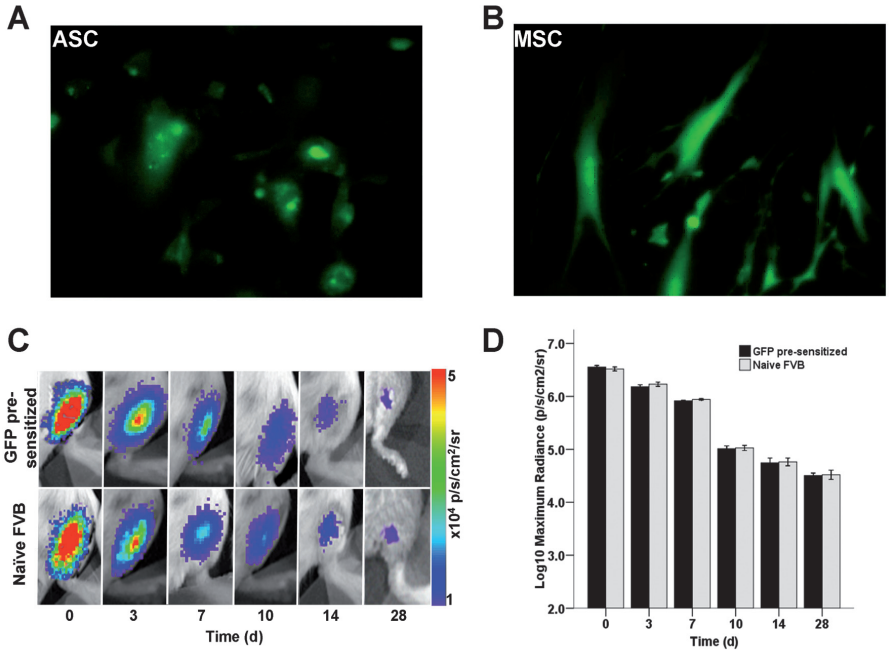

Figure 7. Effect of donor GFP-expression on *in vivo* cell survival. Both (a) ASC (b) and MSC expressed GFP (*in vitro* fluorescence microscopy pictures), which might have influenced cell survival by possible immunogenicity. However, after transplantation of $5x10^5$ GFP^+-$Fluc^+$ MSC into pre-sensitized and naïve FVB mice, (c) longitudinal BLI and (d) quantification of signal intensity revealed no significant differences between imaging signals from day 0 to day 28. Scale bars represent BLI signal in photons/s/cm^2/sr (Bars represent means ± SEM, n=3/group, p=NS, ANOVA).

Assessment of cardiac contractility by echocardiography. Previously, it has been observed that ASC[11] and MSC[23] preserved left ventricular dimensions and fractional shortening after infarction. However, there is no comparative functional data available between both cell types, after prolonged time in culture. In the current study, measurements of left ventricular dimensions revealed a gradual increase in diameters in both diastole and systole, suggesting negative remodeling in all groups without any significant benefits of cell transplantation when evaluated at weeks 2, 4, and 6 (**figure 8a-c**). For the cell groups (ASC, MSC, Fibro), after an initial non-significant increase in left ventricular fractional shortening (LVFS) compared to the PBS group at week 2, the increasing ventricular dilatation resulted in a declining LVFS over time (**figure 8d**). By week 6 after cell transplantation, there was a trend toward improved LVFS in the ASC (33.1±1.0%) and MSC (33.0±3.5%) groups compared to the Fibro (31.3±2.2%) and PBS (32.0±1.8%) control groups, of which the latter (**figure 8d**, *P* =NS, repeated measurements ANOVA) had similar values compared to the literature [24]. For complete echocardiography results, please refer to **table 1**.

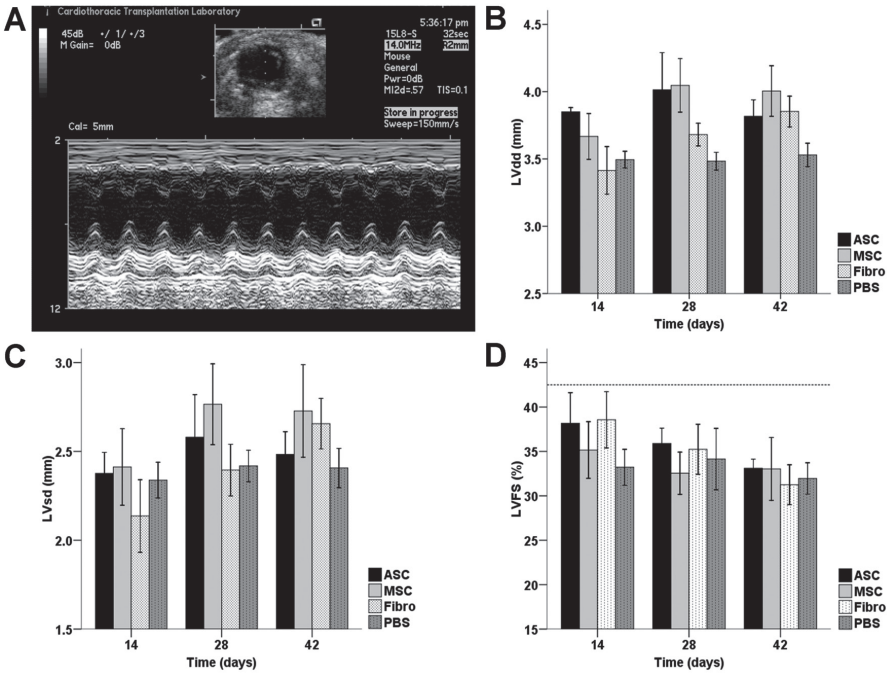

Figure 8. *In vivo* measurements of cardiac function over time. (a) Representative M-mode traced two-dimensional picture taken at the level of the papillary muscle whereby left ventricular diastolic and systolic diameters can be measured. (b,c) Cell transplantation after myocardial infarction was not capable of preventing an increase in left ventricular diastolic (LVdd, b) or systolic diameters (LVsd, c). (d) Left ventricular performance, as measured by left ventricular fractional shortening (LVFS), was preserved only in the short term after cell transplantation. The dotted line represents the mean pre-operative fractional shortening of all operated animals. Six weeks after transplantation, there was a comparable LVFS in the ASC and MSC groups. Although cardiac function was slightly better than control groups, there was no significant difference when controlled for the trend over time (Bars represent means ± SEM, n>7 in all groups, p=NS, repeated measurements ANOVA).

	Time (days)	ASC	MSC	Fibro	PBS
LVFS (%)	14	38.2 ± 3.5	35.2 ± 3.2	38.6 ± 3.2	33.2 ± 2.0
LVFS (%)	28	35.9 ± 1.7	32.5 ± 2.4	35.2 ± 2.8	34.2 ± 3.4
LVFS (%)	42	33.1 ± 1.0	33.0 ± 3.5	31.3 ± 2.2	32.0 ± 1.8
LVdd (mm)	14	3.9 ± 0.3	3.7 ± 0.2	3.4 ± 0.2	3.5 ± 0.6
LVdd (mm)	28	4.0 ± 0.3	4.0 ± 0.2	3.7 ± 0.1	3.4 ± 0.1
LVdd (mm)	42	3.8 ± 0.1	4.0 ± 0.2	3.9 ± 0.1	3.5 ± 0.1
LVsd (mm)	14	2.4 ± 0.1	2.4 ± 0.2	2.1 ± 0.2	2.3 ± 0.1
LVsd (mm)	28	2.6 ± 0.2	2.8 ± 0.2	2.4 ± 0.1	2.4 ± 0.1
LVsd (mm)	42	2.5 ± 0.1	2.7 ± 0.3	2.7 ± 0.1	2.4 ± 0.1

Table 1. Non-invasive echocardiography measurements. Values are reported in mean ± SEM. No symbols indicate P=NS (Repeated measurements ANOVA).

Hemodynamic measurements using pressure-volume (PV) loops. Recently, it has been shown that MSC were capable of preserving myocardial compliance, as measured by invasive hemodynamic measurements.[25] Thus, to validate the echocardiography measurements of ventricular dimensions, invasive steady-state hemodynamic measurements of left ventricular diastolic and systolic volumes were conducted immediately after echocardiography at week 6. When plotted versus each other, mean diastolic and systolic volumes and diameters from each group correlated with r^2 values of 0.88 and 0.70, respectively (**figure 9a-c**). Stroke work and cardiac output, important parameters of ventricular performance[26], did not differ among cellular groups but was slightly better than the PBS control group (**figure 9d,e**, *P*=NS, ANOVA). Ventricular contraction was not different between groups, but there was a trend towards an improved ventricular relaxation, as measured by the minimum $\Delta P/\Delta t$, in the ASC and MSC groups (**figure 9f, g**, *P*=NS, ANOVA). Furthermore, an increase in arterial elastance, suggestive of higher afterload caused either by arterial stiffening or increased peripheral resistance[27], was seen in the PBS group but this was not significantly different from the ASC and MSC group and the Fibro controls (**figure 9d**, *P*=NS, ANOVA).

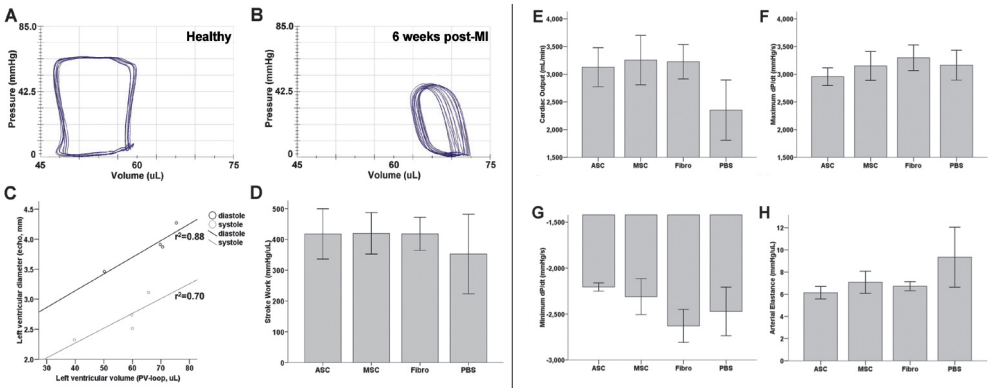

Figure 9. Invasive steady-state pressure-volume measurements of cardiac performance. (a,b) Pressure-volume recordings of (a) a normal, non-operated animal, and (b) PBS control animal 6 weeks after infarction with typical right shift. (c) Mean values of left ventricular volumes, as measured by pressure-volume loops, were correlative with the earlier acquired left ventricular diameters, as measured by echocardiography (dots represent mean measured values from each group). (d, e) Although transplantation of ASC and MSC resulted in a similar trend of preservation of (d) stroke work and (e) cardiac output compared to the PBS group, there was no significant difference compared to the cellular control. (f) Although maximum dP/dt was not different among groups, there was a (g) trend towards better minimum dP/dt, which is indicative of better ventricular relaxation. (h) Similarly, there was a trend towards lower afterload, as shown by lower arterial elastance, in all cellular groups compared to the PBS group (Bars represent means ± SEM, n>6 in every group, p=NS, ANOVA).

Post-mortem histology. Immediately after PV-analysis, the animals were euthanized after which the hearts were explanted. Gross morphology showed that ventricular dilatation and fibrous scar formation had not been prevented by cell transplantation (**figure 10**). As suggested by the BLI, echocardiography, and PV findings, transplantation of both ASC and MSC did not result in either repopulation (data not shown), or endogenous preservation of myocardial tissue.

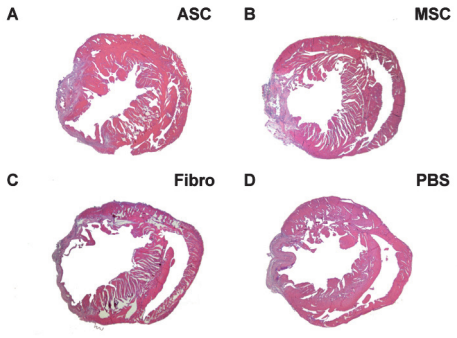

Figure 10. Macroscopic pictures of representative explanted hearts show no prevention of cardiac remodeling after cell transplantation. 6 weeks after transplantation of (a) ASC, (b) MSC, and (c) Fibro there are no gross signs of tissue preservation compared to (d) PBS (H&E stained slides of representative hearts).

DISCUSSION

This study has evaluated for the first time the *in vivo* behavior and functional effects of both adipose tissue-derived stromal cells (ASC) and bone marrow-derived mesenchymal stem cells (MSC) after injection into the ischemic myocardium, as compared to a cellular (Fibro), and non-cellular (PBS) control group. The major findings are as follows: (1) molecular imaging using the Fluc reporter gene is a reliable tool for repetitively monitoring donor cell survival *in vivo*; (2) similar to the Fibro control group, ASC and MSC rapidly die off after injection into the infarcted heart; and (3) ASC and MSC were not capable of significantly preventing left ventricular remodeling and subsequent loss of cardiac function.

Until now, ASC and MSC studies have been largely based on *in vitro* studies[10] or investigations that monitored cell location and quantity by post-mortem histological analysis[28] or PCR techniques.[18] To study the true *in vivo* behavior of stem cells, one needs to be able to repetitively image cell location and count in a non-invasive fashion. One such approach would be the labeling of stem cells with iron particles which would enable imaging by MRI.[29] However, this technique does not provide insight into cell number since the same amount of iron particles are divided among daughter cells during cell proliferation or ingested by macrophages in case of cell death.[30] By contrast, the current study demonstrates that molecular imaging of the Fluc reporter gene with the D-Luciferin reporter probe can provide repetitive, longitudinal *in vivo* imaging of donor cell survival in the infarcted heart of the same animal, thereby preventing sampling biases that can occur with the use of multiple animals that need to be sacrificed on different time points to perform conventional histological staining.[31]

The clinical relevance of this study is significant. MSC have been suggested as potential treatments for a wide variety of diseases including graft versus host disease, osteogenesis imperfecta, rheumatoid arthritis, multiple sclerosis, and myocardial infarction[32]. Since the ASC and MSC appear to be comparable cells with also similar *in vivo* behavior, it would be possible to yield stromal cells from fat instead of bone marrow. Not only would this provide a less restricting source regarding yield, it would also be a more patient friendly isolation procedure. In fact, it has even been proposed that human ASC are superior to MSC with regard to their paracrine and angiogenic potential in response to ischemia.[33] Despite these reported advantages, an important finding from our study is that both MSC and ASC do not survive for longer term following transplantation into the infarcted heart. Based on our quantitative measurements of BLI signals, all cells have died by week 6. This is in concordance with earlier PCR findings from Muller-Ehmsen *et al.,* who noticed robust cell death after transplantation with less than 2% of the initially transplanted MSC being present at 6 weeks after cardiac transplantation.[18] Similarly, Nakamura and colleagues were only able to find 4.4% engraftment of MSC[19] 1 week after intramyocardial transplantation, while Amsalem *et al.* were unable to find any MSC 4 weeks after transplantation.[23] Moreover, Mangi and colleagues observed robust cell death early after transplantation, which was mitigated by transfecting the MSC with the pro-survival gene Akt-1.[34] Thus, although prolonged survival of MSC and ASC has been proven possible in different models[35, 36], the environment in the heart proves hostile to these cells, resulting in decreased cell survival.

There have been several studies reporting preservation of cardiac function after myocardial infarction and subsequent ASC[11] and MSC[37] transplantation. On the contrary, in this study we did not observe any functional benefit from ASC or MSC after transplantation into the infarcted heart. In fact, after an initial preservation, we have observed decreasing fractional shortening in both ASC and MSC groups from week 2 to week 6. Although these differences could be a consequence of differences in the experimental animal and surgical models, the observed short-term effect of cell transplantation is in concordance with findings from a growing body of experimental studies. Ultra-sensitive small animal MRI has recently been used to show that MSC fail to repair the ischemic heart and do not have any beneficial effect on cardiac function after infarction.[38] This non-beneficial effect corresponds to other studies, which show that non-transduced MSC do not ameliorate functional heart failure after transplantation.[39] In addition, Dai and colleagues observed no long-term functional effect after an initial significant benefit 1 month after transplantation of MSC in infarcted rat hearts.[28] In combination with the BLI data of the current study and as suggested in a recent review[40], the dismal cell survival of ASC and MSC might underlie this short term effect. This poor survival pattern makes robust repopulation impossible and furthermore limits the protective paracrine action of the cells. This paracrine ef-

fect has been shown to be of crucial importance in MSC function.[34, 41] By transfecting MSC with Akt-1, researchers have observed not only a better cell survival under hypoxic conditions, but also a robust increase in paracrine factors which resulted in a preservation of morphology and function of the infarcted heart[34, 41], effects that were also shown using MSC transfected with the pro-survival gene Bcl-2.[39] Thus, further research is needed to identify the factors responsible for the acute donor cell death in the heart (both infarcted and non-infarcted). Improving stem cell survival may offer a sustained paracrine effect which could lead to protective effects on resident cardiomyocytes from apoptosis and a subsequent preservation of cardiac function.

Several limitations of this study can be raised. First, we used Fluc- and GFP-expressing cells in order to be able to investigate cellular fate in case of robust cell survival after 6 weeks. It has been suggested that GFP could impair actin-myosin interactions in muscle cells[42] which might have influenced cardiac function. However, the lack of functional benefit of transplantation of either cell type in this study is also in concordance with other studies using non-GFP-labeled MSC.[28, 38] Second, we chose to use longer-term cultured cells because this generally increases purity and also because the ability to culture these cells underlies a crucial advantage which is important for its off-the-shelf clinical potential. However, it has been shown that higher passage MSC had decreased growth factor release under hypoxic conditions and that passage number of MSC was inversely correlated to the protective effect on infarcted hearts.[43] Thus, it is possible that the lack of functional benefit is a consequence of dismal cell survival, diminished paracrine signaling, and high passage of the cells.

In conclusion, we have reported that the stromal population from the adipose tissue has close *in vitro* resemblance with its counterpart from the bone marrow. Importantly, using non-invasive molecular imaging techniques, this study has shown for the first time that these cells also have similar *in vivo* behavior in the infarcted heart. Finally, we did not observe a clear functional benefit after transplantation of both cell types. These results should be a stimulus for further research regarding improvement of cellular behavior to ultimately be able to restore cardiac function after myocardial infarction by transplanting long-term cultured, off-the-shelf adipose tissue-derived stromal cells.

ACKNOWLEDGEMENTS

This study was supported in part by grants from the NIH HL074883 and Burroughs Wellcome Award (JCW). K.E.A. van der Bogt was supported by the American Heart Association (Medical Student Research Award), Fulbright committee, VSB fund, and the Michael van Vloten fund.

The authors thank V. Mariano for animal care and ms. P. Chu for assistance with histology.

REFERENCES

1. Rosamond W, Flegal K, Friday G, Furie K, Go A, Greenlund K, Haase N, Ho M, Howard V, Kissela B, Kittner S, Lloyd-Jones D, McDermott M, Meigs J, Moy C, Nichol G, O'Donnell C J, Roger V, Rumsfeld J, Sorlie P, Steinberger J, Thom T, Wasserthiel-Smoller S, Hong Y. Heart Disease and Stroke Statistics--2007 Update. A Report From the American Heart Association Statistics Committee and Stroke Statistics Subcommittee. *Circulation*. 2006.
2. Orlic D, Kajstura J, Chimenti S, Jakoniuk I, Anderson SM, Li B, Pickel J, McKay R, Nadal-Ginard B, Bodine DM, Leri A, Anversa P. Bone marrow cells regenerate infarcted myocardium. *Nature*. 2001;410(6829):701-705.
3. Balsam LB, Wagers AJ, Christensen JL, Kofidis T, Weissman IL, Robbins RC. Haematopoietic stem cells adopt mature haematopoietic fates in ischaemic myocardium. *Nature*. 2004;428(6983):668-673.
4. Lunde K, Solheim S, Aakhus S, Arnesen H, Abdelnoor M, Egeland T, Endresen K, Ilebekk A, Mangschau A, Fjeld JG, Smith HJ, Taraldsrud E, Grogaard HK, Bjornerheim R, Brekke M, Muller C, Hopp E, Ragnarsson A, Brinchmann JE, Forfang K. Intracoronary injection of mononuclear bone marrow cells in acute myocardial infarction. *N Engl J Med*. 2006;355(12):1199-1209.
5. Schrepfer S, Deuse T, Lange C, Katzenberg R, Reichenspurner H, Robbins RC, Pelletier MP. Simplified protocol to isolate, purify, and culture expand mesenchymal stem cells. *Stem Cells Dev*. 2007;16(1):105-107.
6. Silva GV, Litovsky S, Assad JA, Sousa AL, Martin BJ, Vela D, Coulter SC, Lin J, Ober J, Vaughn WK, Branco RV, Oliveira EM, He R, Geng YJ, Willerson JT, Perin EC. Mesenchymal stem cells differentiate into an endothelial phenotype, enhance vascular density, and improve heart function in a canine chronic ischemia model. *Circulation*. 2005;111(2):150-156.
7. Chen SL, Fang WW, Ye F, Liu YH, Qian J, Shan SJ, Zhang JJ, Chunhua RZ, Liao LM, Lin S, Sun JP. Effect on left ventricular function of intracoronary transplantation of autologous bone marrow mesenchymal stem cell in patients with acute myocardial infarction. *Am J Cardiol*. 2004;94(1):92-95.
8. Aggarwal S, Pittenger MF. Human mesenchymal stem cells modulate allogeneic immune cell responses. *Blood*. 2005;105(4):1815-1822.
9. Zuk PA, Zhu M, Mizuno H, Huang J, Futrell JW, Katz AJ, Benhaim P, Lorenz HP, Hedrick MH. Multilineage cells from human adipose tissue: implications for cell-based therapies. *Tissue Eng*. 2001;7(2):211-228.
10. Lee RH, Kim B, Choi I, Kim H, Choi HS, Suh K, Bae YC, Jung JS. Characterization and expression analysis of mesenchymal stem cells from human bone marrow and adipose tissue. *Cell Physiol Biochem*. 2004;14(4-6):311-324.

11. Li B, Zeng Q, Wang H, Shao S, Mao X, Zhang F, Li S, Guo Z. Adipose tissue stromal cells transplantation in rats of acute myocardial infarction. *Coron Artery Dis.* 2007;18(3):221-227.
12. Sakaguchi Y, Sekiya I, Yagishita K, Muneta T. Comparison of human stem cells derived from various mesenchymal tissues: superiority of synovium as a cell source. *Arthritis Rheum*. 2005;52(8):2521-2529.
13. Wagner W, Wein F, Seckinger A, Frankhauser M, Wirkner U, Krause U, Blake J, Schwager C, Eckstein V, Ansorge W, Ho AD. Comparative characteristics of mesenchymal stem cells from human bone marrow, adipose tissue, and umbilical cord blood. *Exp Hematol.* 2005;33(11):1402-1416.
14. Wang M, Crisostomo PR, Herring C, Meldrum KK, Meldrum DR. Human progenitor cells from bone marrow or adipose tissue produce VEGF, HGF, and IGF-I in response to TNF by a p38 MAPK-dependent mechanism. *Am J Physiol Regul Integr Comp Physiol.* 2006;291(4):R880-884.
15. Cao YA, Wagers AJ, Beilhack A, Dusich J, Bachmann MH, Negrin RS, Weissman IL, Contag CH. Shifting foci of hematopoiesis during reconstitution from single stem cells. *Proc Natl Acad Sci U S A.* 2004;101(1):221-226.
16. Salmon AB, Murakami S, Bartke A, Kopchick J, Yasumura K, Miller RA. Fibroblast cell lines from young adult mice of long-lived mutant strains are resistant to multiple forms of stress. *Am J Physiol Endocrinol Metab.* 2005;289(1):E23-29.
17. Zuk PA, Zhu M, Ashjian P, De Ugarte DA, Huang JI, Mizuno H, Alfonso ZC, Fraser JK, Benhaim P, Hedrick MH. Human adipose tissue is a source of multipotent stem cells. *Mol Biol Cell.* 2002;13(12):4279-4295.
18. Muller-Ehmsen J, Krausgrill B, Burst V, Schenk K, Neisen UC, Fries JW, Fleischmann BK, Hescheler J, Schwinger RH. Effective engraftment but poor mid-term persistence of mononuclear and mesenchymal bone marrow cells in acute and chronic rat myocardial infarction. *J Mol Cell Cardiol.* 2006;41(5):876-884.
19. Nakamura Y, Wang X, Xu C, Asakura A, Yoshiyama M, From AH, Zhang J. Xenotransplantation of long-term-cultured swine bone marrow-derived mesenchymal stem cells. *Stem Cells.* 2007;25(3):612-620.
20. Sheikh AY, Lin SA, Cao F, Cao YA, van der Bogt KE, Chu P, Chang CP, Contag CH, Robbins RC, Wu JC. Molecular Imaging of Bone Marrow Mononuclear Cell Homing and Engraftment in Ischemic Myocardium. *Stem Cells.* 2007.
21. Zeier M, Dohler B, Opelz G, Ritz E. The effect of donor gender on graft survival. *J Am Soc Nephrol.* 2002;13(10):2570-2576.
22. Bubnic SJ, Nagy A, Keating A. Donor hematopoietic cells from transgenic mice that express GFP are immunogenic in immunocompetent recipients. *Hematology.* 2005;10(4):289-295.

23. Amsalem Y, Mardor Y, Feinberg MS, Landa N, Miller L, Daniels D, Ocherashvilli A, Holbova R, Yosef O, Barbash IM, Leor J. Iron-oxide labeling and outcome of transplanted mesenchymal stem cells in the infarcted myocardium. *Circulation.* 2007;116(11 Suppl):I38-45.
24. Rohde LE, Aikawa M, Cheng GC, Sukhova G, Solomon SD, Libby P, Pfeffer J, Pfeffer MA, Lee RT. Echocardiography-derived left ventricular end-systolic regional wall stress and matrix remodeling after experimental myocardial infarction. *J Am Coll Cardiol.* 1999;33(3):835-842.
25. Berry MF, Engler AJ, Woo YJ, Pirolli TJ, Bish LT, Jayasankar V, Morine KJ, Gardner TJ, Discher DE, Sweeney HL. Mesenchymal stem cell injection after myocardial infarction improves myocardial compliance. *Am J Physiol Heart Circ Physiol.* 2006;290(6):H2196-2203.
26. Lips DJ, van der Nagel T, Steendijk P, Palmen M, Janssen BJ, van Dantzig JM, de Windt LJ, Doevendans PA. Left ventricular pressure-volume measurements in mice: comparison of closed-chest versus open-chest approach. *Basic Res Cardiol.* 2004;99(5):351-359.
27. Shioura KM, Geenen DL, Goldspink PH. Assessment of cardiac function with the pressure-volume conductance system following myocardial infarction in mice. *Am J Physiol Heart Circ Physiol.* 2007;293(5):H2870-2877.
28. Dai W, Hale SL, Martin BJ, Kuang JQ, Dow JS, Wold LE, Kloner RA. Allogeneic mesenchymal stem cell transplantation in postinfarcted rat myocardium: short- and long-term effects. *Circulation.* 2005;112(2):214-223.
29. Kraitchman DL, Heldman AW, Atalar E, Amado LC, Martin BJ, Pittenger MF, Hare JM, Bulte JW. *In vivo* magnetic resonance imaging of mesenchymal stem cells in myocardial infarction. *Circulation.* 2003;107(18):2290-2293.
30. Li Z, Suzuki Y, Huang M, Cao F, Xie X, Connolly AJ, Yang PC, Wu JC. Comparison of Reporter Gene and Iron Particle Labeling for Tracking Fate of Human Embryonic Stem Cells and Differentiated Endothelial Cells in Living Subjects. *Stem Cells.* 2008.
31. Chang GY, Xie X, Wu JC. Overview of stem cells and imaging modalities for cardiovascular diseases. *J Nucl Cardiol.* 2006;13(4):554-569.
32. Dazzi F, Horwood NJ. Potential of mesenchymal stem cell therapy. *Curr Opin Oncol.* 2007;19(6):650-655.
33. Kim Y, Kim H, Cho H, Bae Y, Suh K, Jung J. Direct comparison of human mesenchymal stem cells derived from adipose tissues and bone marrow in mediating neovascularization in response to vascular ischemia. *Cell Physiol Biochem.* 2007;20(6):867-876.
34. Mangi AA, Noiseux N, Kong D, He H, Rezvani M, Ingwall JS, Dzau VJ. Mesenchymal stem cells modified with Akt prevent remodeling and restore performance of infarcted hearts. *Nat Med.* 2003;9(9):1195-1201.
35. Degano IR, Vilalta M, Bago JR, Matthies AM, Hubbell JA, Dimitriou H, Bianco P, Rubio N, Blanco J. Bioluminescence imaging of calvarial bone repair using bone marrow and

adipose tissue-derived mesenchymal stem cells. *Biomaterials.* 2008;29(4):427-437.

36. Shen LH, Li Y, Chen J, Zacharek A, Gao Q, Kapke A, Lu M, Raginski K, Vanguri P, Smith A, Chopp M. Therapeutic benefit of bone marrow stromal cells administered 1 month after stroke. *J Cereb Blood Flow Metab.* 2007;27(1):6-13.
37. Tang YL, Zhao Q, Qin X, Shen L, Cheng L, Ge J, Phillips MI. Paracrine action enhances the effects of autologous mesenchymal stem cell transplantation on vascular regeneration in rat model of myocardial infarction. *Ann Thorac Surg.* 2005;80(1):229-236; discussion 236-227.
38. Carr CA, Stuckey DJ, Tatton L, Tyler DJ, Hale SJ, Sweeney D, Schneider JE, Martin-Rendon E, Radda GK, Harding SE, Watt SM, Clarke K. Bone marrow-derived stromal cells home to and remain in the infarcted rat heart but fail to improve function: an *in vivo* cine-MRI study. *Am J Physiol Heart Circ Physiol.* 2008;295(2):H533-542.
39. Li W, Ma N, Ong LL, Nesselmann C, Klopsch C, Ladilov Y, Furlani D, Piechaczek C, Moebius JM, Lutzow K, Lendlein A, Stamm C, Li RK, Steinhoff G. Bcl-2 engineered MSCs inhibited apoptosis and improved heart function. *Stem Cells.* 2007;25(8):2118-2127.
40. Wollert KC, Drexler H. Mesenchymal stem cells for myocardial infarction: promises and pitfalls. *Circulation.* 2005;112(2):151-153.
41. Gnecchi M, He H, Noiseux N, Liang OD, Zhang L, Morello F, Mu H, Melo LG, Pratt RE, Ingwall JS, Dzau VJ. Evidence supporting paracrine hypothesis for Akt-modified mesenchymal stem cell-mediated cardiac protection and functional improvement. *Faseb J.* 2006;20(6):661-669.
42. Agbulut O, Coirault C, Niederlander N, Huet A, Vicart P, Hagege A, Puceat M, Menasche P. GFP expression in muscle cells impairs actin-myosin interactions: implications for cell therapy. *Nat Methods.* 2006;3(5):331.
43. Crisostomo PR, Wang M, Wairiuko GM, Morrell ED, Terrell AM, Seshadri P, Nam UH, Meldrum DR. High passage number of stem cells adversely affects stem cell activation and myocardial protection. *Shock.* 2006;26(6):575-580.

CHAPTER 8

Micro Computed Tomography for Characterization of Murine Cardiovascular Disease Models

Ahmad Y. Sheikh*, Koen E.A. van der Bogt*, Timothy C. Doyle,
Maryam K. Sheikh, Katherine J. Ransohoff, Ziad A. Ali, Owen P. Palmer,
Robert C. Robbins, Michael P. Fischbein and Joseph C. Wu

Journal of the American College of Cardiology:
Cardiovascular Imaging 2010 Jul;3(7):783-5

*Both authors contributed equally to this study

LETTER TO THE EDITOR

It can hardly be argued that cardiac imaging methodologies targeting small animal models have been crucial for rapidly transitioning therapies from the bench to bedside. The adaptation of ultrasound for imaging murine hearts, for example, has allowed characterization of the developing and adult rodent heart, making it an essential tool for the study of developmental biology and cardiovascular disease. Nevertheless, additional imaging tools may prove useful adjuncts and/or alternatives to such established traditional modalities.

Ideally, a cardiovascular imaging modality should provide structural-functional quantitation, and be non-invasive, fast, cost-effective, precise, and accurate. While the combination of echocardiography and small animal cardiac MRI has proven to meet several of these criteria, there is certainly room for other modalities to be employed as well. At our institution, experimentation with a Micro-CT scanner eventually produced contrast-enhanced, high-resolution 3-dimensional imaging of the murine heart and associated structures. Indeed, early success with CT imaging of murine hearts has also been described in limited detail by other investigators [1,2] but to our knowledge, a validation of this technique by direct comparison to multiple established methodologies has not been described. Hence, we present the first study aimed to directly compare this novel imaging modality with both conventional echocardiography and conductance catheter (CC) measurement techniques using an established murine model of ischemic heart disease. Specifically, we have tested the hypothesis that Micro-CT can provide reliable information about ventricular structure and function following surgical LAD-ligation induced myocardial infarction (MI) in mice.

We randomized adult (8-10 weeks old) female FVB mice (n=19) to surgical LAD ligation or sham procedure. Dual cardiac and respiratory gated, IV contrast enhanced (20 µL/g Fenestra VC; ART Inc., Montreal, Canada) CT scans were performed pre-operatively and at 4, 8, and 12 weeks post-procedure using the eXplore Locus RS150 MicroCT (GE Healthcare, Fairfield, CT). Scans were performed with a 70 kVp, 40 mAmp x-ray source, acquiring 286 views over 200°, averaging two frames per view, 4x4 binning on the CCD detector. The heart was centered in a 46.25 mm axial field of view (84.7 mm trans-axial FOV), and sub-regions of the scanned data were reconstructed at an isotropic resolution of 97.3 µm. End-diastolic and end-systolic images were prospectively acquired with a temporal resolution of 15 milliseconds (ms) by gating on ECG P- and S'-waves, respectively (see **figure 1a-b** for animal set-up and gating reference). Continual imaging of the cardiac cycle (at 10-15 ms intervals) was also conducted of a representative animal at each time point (**figure 2** demonstrates continuous imaging of control animal). Post-acquisition analysis was performed using GE image analysis software (**figure 1c-d**).

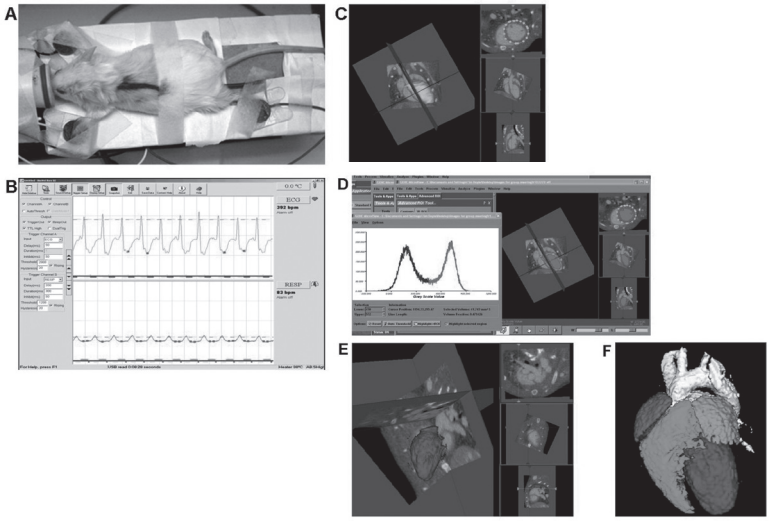

Figure 1. Outline of image acquisition and processing by Micro-CT. (a) Mouse positioned on CT scanner bed with 3 lead ECG. (b) Screen shot of ECG (top) and respiratory (bottom) tracings. Red squares occurring at the same time in both ECG and respiratory tracings indicate image acquisition points during maximum LV contraction (S') and inspiration. (c) Region of interest (orange dots) created around heart chamber (LV shown). (d) Histogram used to isolate voxels representing chamber volume. (e) Rendered surface of blood within chamber (LV). (f) Representative composite image of cardiac chambers and great vessels.

All operators obtaining and analyzing the CT scans were able to obtain measurements with minimal variability (±0.5-4.0%, data not shown). Echocardiography was performed by obtaining three independent two-dimensional transversal-targeted M-mode traces at the level of the papillary muscles using a 14.7-MHz transducer on a Sequoia C512 Echocardiography system (Siemens, Malvern, PA, USA). Using the Siemens proprietary software, left ventricular end-diastolic and end-systolic posterior and anterior dimensions were measured and processed to calculate left ventricular fractional shortening (LVFS). Invasive, steady-state hemodynamic measurements were conducted by closed-chest pressure-volume (PV) loop analysis using a 1.4-F conductance catheter (Millar Instruments, Houston, TX, USA) at week 12. These data were analyzed using PVAN 3.4 Software (Millar Instruments, Houston, TX, USA) and Chart/Scope Software (AD Instruments, Colorado Springs, CO, USA).

Mean left ventricular diastolic (LVDV) and systolic (LVSV) volumes were not significantly different between the sham and MI groups at baseline (37.2±2.0 µL vs. 39.7±1.8 µL in diastole and 11.2±0.6 µL vs. 11.4±0.8 µL in systole, respectively, *P*=NS). However, these volumes gradually increased in the MI group, finally reaching a mean diastolic value of 133.2±21.2 µL, compared to 55.4±1.0 µL in the sham operated group at 12 weeks post-operation (*P*=0.002, **figure 3a-c)**. Similarly, LVSV increased to 100.1±19.6 µL as compared to 19.9±1.2 µL in the sham group (*P*=0.002, **figure 3d**). This MI-induced increase in volumes mirrored functional failure, with deteriorating LVEF from an initial 70.6±2.5% to 26.2±2.8% after 12 weeks. By contrast, LVEF in the sham group remained around baseline (68.6±2.6%, *P*<0.0005, **Figure 3e**).

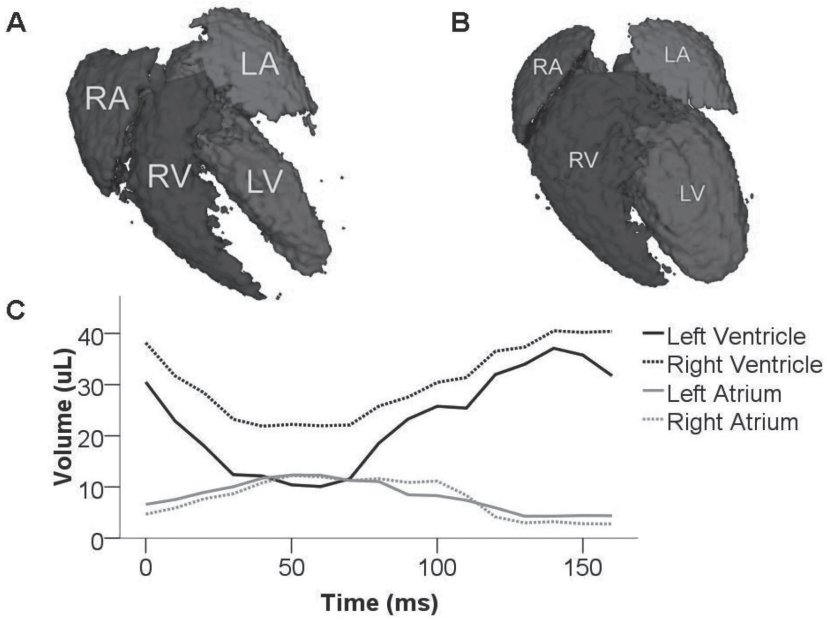

Figure 2. Quantification of cardiac chamber volumes by Micro-CT. Representative reconstruction of cardiac chamber volumes in (a) end-systole and (b) end-diastole allowed for extrapolation of chamber volumes and loading conditions during (c) the entire cardiac cycle.

As shown in **figure 4**, volumes measured by Micro-CT correlated well with dimensions acquired from echocardiography in both diastole (r^2=0.73) and systole (r^2=0.82). Similarly, volumes derived from the conductance catheter (CC)-based approach showed a correlative trend with those from the Micro-CT (r^2=0.83 in systole and r^2=0.81 in diastole). When volumes and dimensions were processed to calculate functional measurements of ventricular contraction, Micro-CT proved to correlate well with echocardiography (r^2=0.72, **figures 4d)**. These observations suggest that Micro-CT imaging can provide reliable volumetric assessment of cardiac chambers and ventricular function. For detailed echocardiography, CC, histological results, and representative images, please refer to **figures 5-7**.

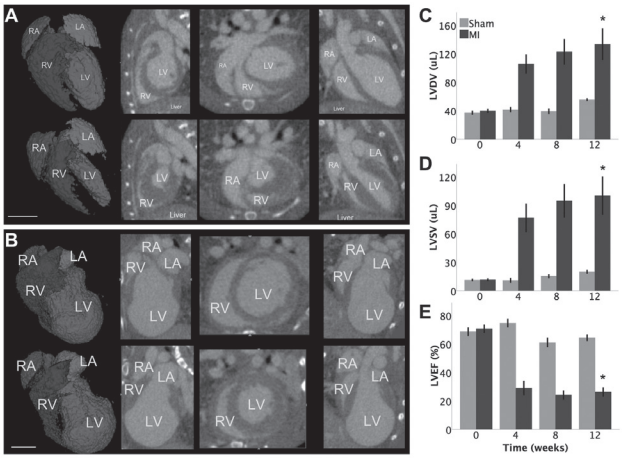

Figure 3: Gated Micro-CT provides insight into myocardial infarction-induced cardiac remodeling. (a) End diastolic (top row) and end systolic (bottom row) images of a normal mouse heart with chambers labeled in yellow. From left to right: rendered surface of blood volume, sagittal, axial, and coronal views. (b) Similar series of images from the same animal 12 weeks following LAD ligation (scale bar=5mm in both panels), showing clear signs of negative remodeling. (c) Graphic representation of increasing left ventricular diastolic volume (LVDV) over time following myocardial infarction as compared to relatively stable volumes in the sham-operated group. (d) Similarly, left ventricular systolic volume (LVSV) increased due to loss of cardiac muscle after infarction. (e) Myocardial infarction led to dilated cardiomyopathy with a significant loss of left ventricular ejection fraction (LVEF) as early as one month following LAD ligation (Bars represent mean±SE. *P<0.05 compared to sham group by repeated measurements ANOVA).

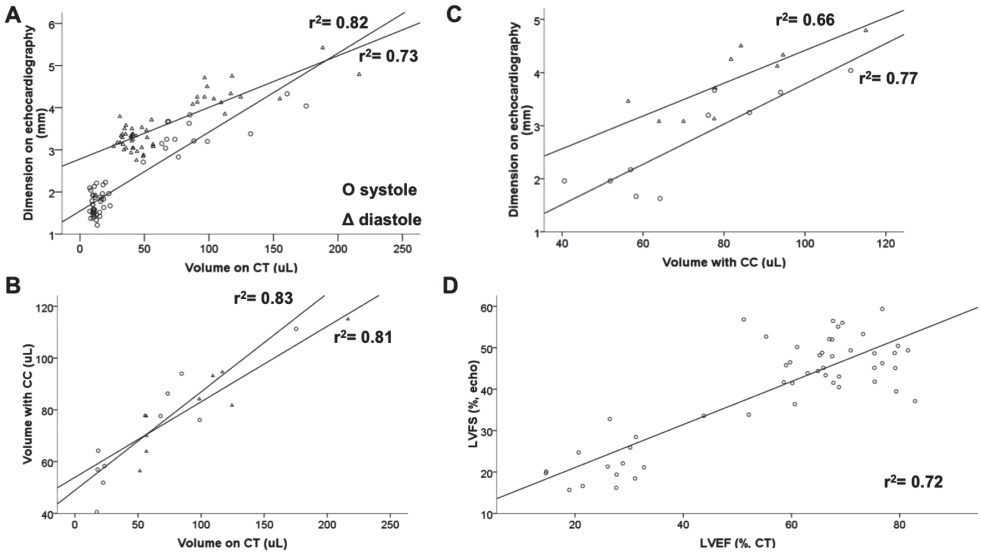

Figure 4. Micro-CT findings correlate robustly with established methods of measuring murine cardiac function. (a,b) Volumes derived from Micro-CT image analysis correlate well with dimensions measured using echocardiography and volumes assessed with the conductance catheter (CC) in both systole and diastole. (c) Echocardiography measurements of chamber length correlated well with volumes derived from CC measurements. (d) *In vivo* functional measurements from Micro-CT and echocardiography correlated well with a r^2 value of 0.72.

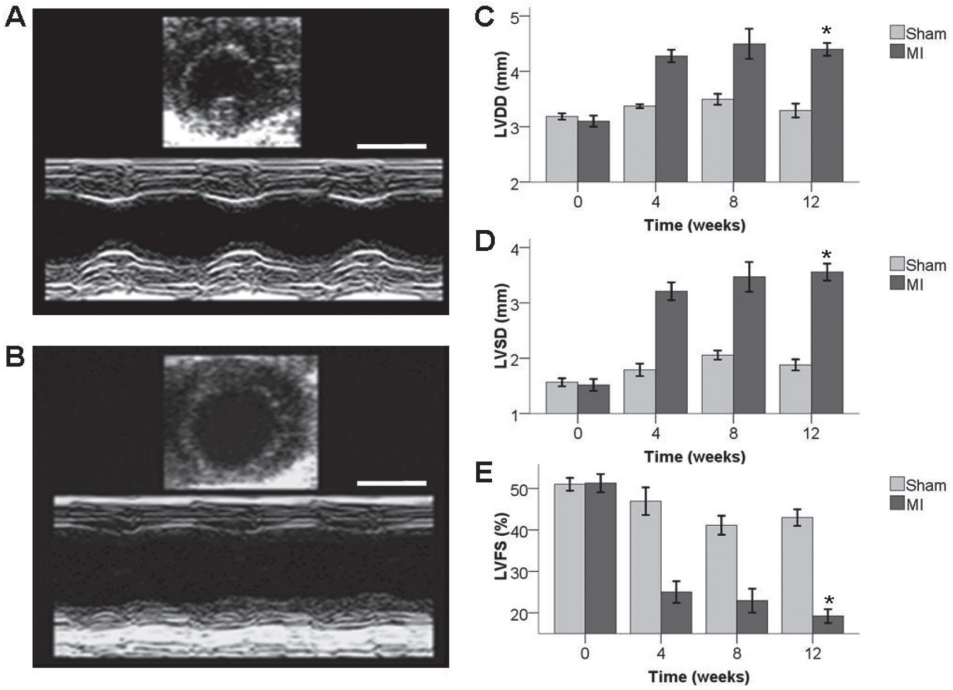

Figure 5. Echocardiographic M-mode traced measurements of ventricular diameters and calculated left ventricular fractional shortening (LVFS). (a) Representative M-mode traced picture taken at the level of the papillary muscle of a pre-operative heart whereby left ventricular diameters can be measured. Scale bar represents 5 mm. (b) The same heart as in (a) shows extensive dilatation at 12 weeks post-MI. (c-e) A gradual MI-induced increase in ventricular diameters in diastole (LVDD, c), and systole (LVSD, d) translated in a significantly compromised LVFS over a period of 12 weeks as compared to the sham group (Bars represent mean±SE. * represents P<0.05 compared to sham group by repeated measurements ANOVA).

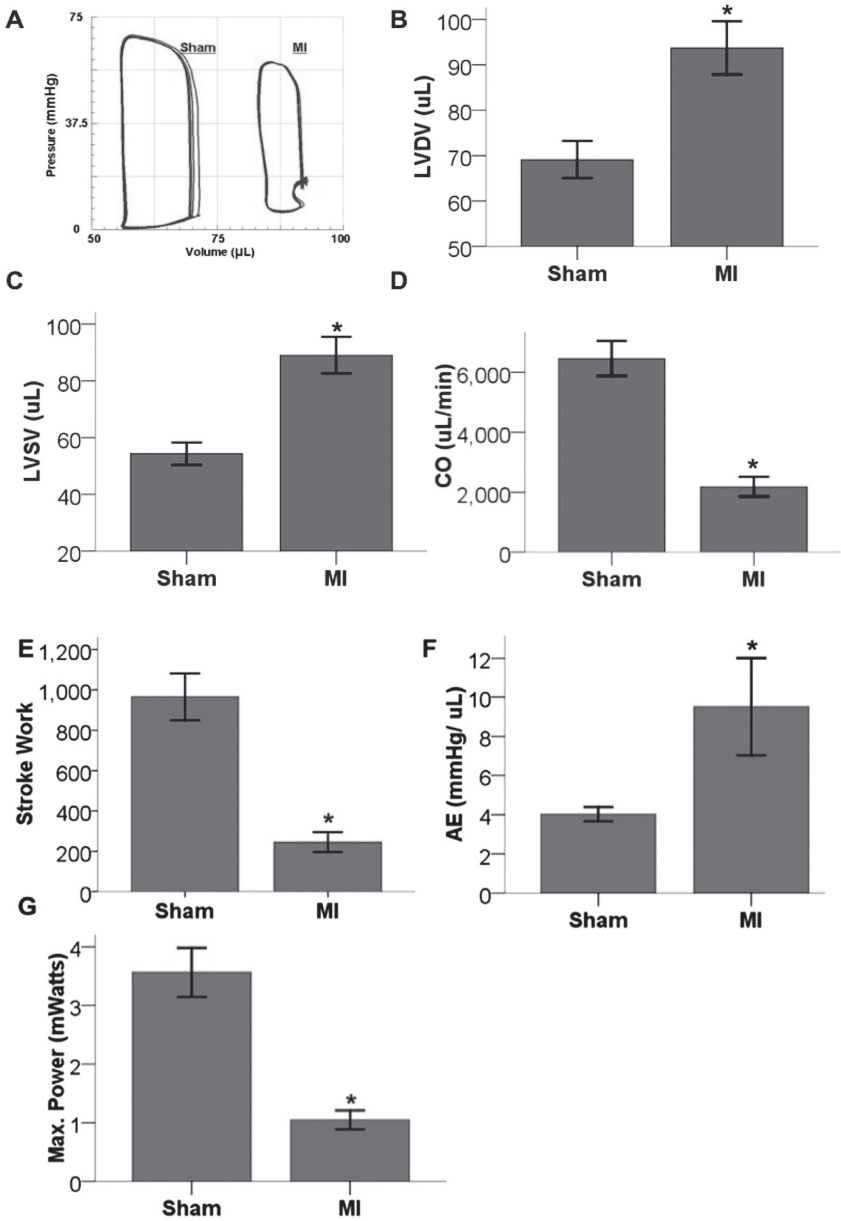

Figure 6. Conductance catheter (CC) based assessment of cardiovascular function. (a) Representative pressure-volume loops of sham (left) and MI (right) animals at 12 weeks post-MI, showing typical right shift indicating increased ventricular dilatation and volumes compared to pre-operative assessment. (b,c) Confirming findings by Micro-CT and echocardiography, extrapolation of pressure-volume loops showed significantly increased ventricular volumes in end-diastole (LVDV, B) and end-systole (LVSV, C) post-MI. (d,e) Cardiac output (CO)

as well as stroke work (SW) were both significantly diminished as well. (f) As a confirmatory measure of CHF, the arterial elastance (AE) was also significantly increased at the 12-week post-MI time point. (g) Finally, significantly decompensated MI-induced heart failure was illustrated by a markedly decreased maximum power generated by the left ventricle (Bars represent mean±SE. * represents P<0.05 compared to sham group by Student's t-test).

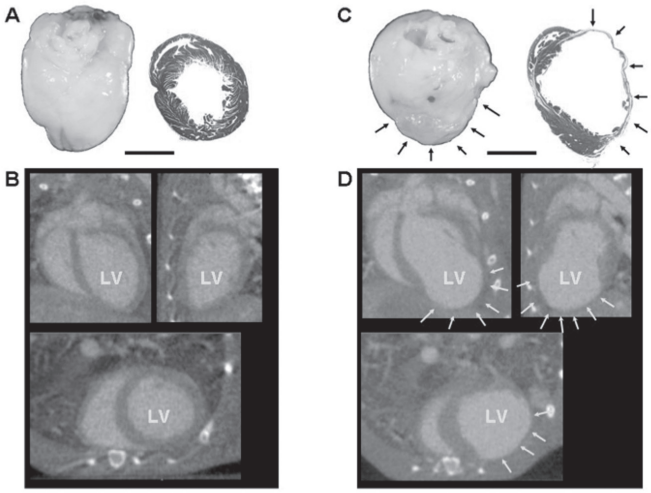

Figure 7. Post-mortem histological analysis confirms *in vivo* Micro-CT images. (a,b) Representative heart 12 weeks following sham procedure appears both grossly and histologically normal, corresponding to the *in vivo* images acquired by Micro-CT immediately prior to CC-measurements and sacrifice. (c) By contrast, a representative fixed heart 12 weeks post-infarction shows an aneurysmal, infarcted region and fibrosis on Masson-Trichrome staining (black arrows). (d) Corresponding *in vivo* Micro-CT images from the same heart with the infarcted area marked by yellow arrows clearly resembles the post-mortem images from (c). Scale bars represent 5 mm.

Over the past decade, cardiac CT has become an important clinical imaging modality for the characterization of cardiac structure and function, as well as coronary artery pathology [3, 4]. However, cardiac CT imaging has long been inapplicable to pre-clinical, small animal models due to the high spatial and temporal resolution required to visualize mouse hearts with rates of over 400 beats a minute. Recent advances in technology have allowed adaptation of CT imaging to the small animal laboratory, adding a valuable asset to the pre-clinical research tool chest. As shown in the present study, Micro-CT can provide accurate and precise measurements of the murine heart, and can serve as a useful adjunct to established measurements of cardiac function. Further refinements of this emerging technology are ongoing, and we predict that Micro-CT scanning will continue to be used in the small animal laboratory with increasing frequency.

REFERENCES:

1. Nahrendorf M, Badea C, Hedlund LW, Figueiredo JL, Sosnovik DE, Johnson GA, Weissleder R. High-resolution imaging of murine myocardial infarction with delayed-enhancement cine micro-CT. *Am J Physiol Heart Circ Physiol.* 2007;292(6):H3172-3178.
2. Detombe SA, Ford NL, Xiang F, Lu X, Feng Q, Drangova M. Longitudinal follow-up of cardiac structure and functional changes in an infarct mouse model using retrospectively gated micro-computed tomography. *Invest Radiol.* 2008;43(7):520-529.
3. Pouleur AC, le Polain de Waroux JB, Kefer J, Pasquet A, Vanoverschelde JL, Gerber BL. Direct comparison of whole-heart navigator-gated magnetic resonance coronary angiography and 40- and 64-slice multidetector row computed tomography to detect the coronary artery stenosis in patients scheduled for conventional coronary angiography. *Circ Cardiovasc Imaging.* 2008;1(2):114-121.
4. Ruzsics B, Lee H, Powers ER, Flohr TG, Costello P, Schoepf UJ. Images in cardiovascular medicine. Myocardial ischemia diagnosed by dual-energy computed tomography: correlation with single-photon emission computed tomography. *Circulation.* 2008;117(9):1244-1245.

CHAPTER 9

Molecular Imaging of Bone Marrow Mononuclear Cell Survival and Homing in a Murine Model of Peripheral Artery Disease

Koen E.A. van der Bogt[1,2]*, Alwine A. Hellingman[2]*,
Maarten A. Lijkwan[1,2], Ernst Jan Bos[1,2], Margreet R. de Vries[3],
Michael P. Fischbein[1], Paul H. Quax[2,3], Robert C. Robbins[1],
Jaap F. Hamming[2] and Joseph C. Wu[4]

Submitted

* Both authors contributed equally to this study.

ABSTRACT

Introduction: Bone marrow mononuclear stem cell (MNC) therapy is a promising treatment for peripheral artery disease (PAD). This study aims to provide insight into cellular kinetics using molecular imaging following different transplantation methods.

Methods and Results: MNCs were isolated from F6 transgenic mice (FVB background) that express firefly luciferase (Fluc) and green fluorescence protein (GFP). Male FVB mice (n=38) underwent femoral artery ligation and were randomized into 3 groups receiving: (1) single intramuscular (i.m.) injection of $2x10^6$ MNC; (2) weekly i.m. injection of $5x10^5$ MNC; and (3) i.m. injection of PBS. To assess the biodistribution following system delivery, we also injected (1) $5x10^6$ MNCs intravenously (i.v.) and (2) PBS i.v. as control (n=10/group). Cellular kinetics, measured by *in vivo* bioluminescence imaging (BLI), revealed near-complete donor cell death 4 weeks after i.m. transplantation. Following i.v. transplantation, BLI monitored cells homed on the injured area in the limb, to liver, spleen, and bone marrow. *Ex vivo* BLI showed presence of MNCs in the scar tissue as well the adductor muscle. However, no significant effects on neovascularization were observed, as monitored by Laser-Doppler-Perfusion-Imaging and histology**.**

Conclusion: This is the first detailed study to assess the kinetics of transplanted MNCs in PAD using *in vivo* molecular imaging. MNC survival after i.m. transplantation is short-lived and MNCs do not stimulate significant improvement in perfusion in this model.

INTRODUCTION

Peripheral artery disease (PAD) currently affects over 27 million people in North America and Europe and is associated with impaired leg function and decreased quality of life, leading to significant morbidity and mortality.[1, 2] Despite a variety of treatment options, including percutaneous transluminal angioplasty, stenting, and bypass surgery, a cluster of patients do not respond to therapy, leaving no other option than amputation in one third of patients within this group.[3]

Recently, stem cell therapy has emerged from bench to bedside as a treatment for end-stage PAD, potentially offering a last option for revascularization of the ischemic limb. While results from pre-clinical experiments using bone marrow-derived mononuclear cells (MNC) appear hopeful, outcomes from clinical studies are mixed[4], raising questions about transplanted stem cell behavior and mechanisms of action involved in the benefits of stem cell transplantation. As to cell behavior, two major issues are the lack of donor cell survival after introduction into ischemic target tissue and the absence of cell homing to the injured area following systemic administration.[5] Donor cell death would hamper three mechanisms believed to be of importance for the beneficial effects seen after cell transplantation: a lasting scaffolding effect, transplanted cell-derived neovascularization, and the secretion of protective paracrine factors by the transplanted cells.

To study stem cell behavior, one must be capable of monitoring cell location, migration, proliferation, and death. Recent proof-of-principle studies have demonstrated the ability to track cell fate following cardiac injections.[5, 6] In the present study, we monitor by molecular imaging the presence of MNC after transplantation in mice with induced hind limb ischemia. These experiments are designed to answer critical questions regarding cell survival and homing patterns to the affected leg, as well as functional consequences of different transplantation strategies.

METHODS

Experimental animals. Animal study protocols were approved by the Animal Research Committees from both institutions (Stanford University and Leiden University). The donor group for imaging experiments consisted of 8-week old male F6 mice (n=10), which were bred on FVB background and ubiquitously express green fluorescent protein (GFP) and firefly luciferase (Fluc) reporter genes driven by a β-actin promoter as previously described.[7] Recipient animals (n=60) for these experiments consisted of syngeneic, male FVB mice (10-12 weeks old, Jackson Laboratories). To compare the efficacy of a single versus repeated injection with cells, animals were randomized into 3 groups: (1) single intramuscular (i.m.) injection of $2x10^6$ MNCs, (2) four

repeated injections of $5x10^5$ MNCs, and (3) i.m. injection of phosphate buffered saline (PBS) injection as control. To compare the efficacy of local versus system delivery, animals were also injected with (1) single intravenous (i.v.) injection of $2x10^6$ MNCs and (2) PBS i.v. as control.

Preparation and characterization of bone marrow mononuclear cells (MNC). The long bones were explanted, washed, and flushed with PBS using a 25-gauge needle to collect bone marrow. After passing through a 70 µm strainer, the isolate was centrifuged at 1200 rpm for 5 minutes, washed, and resuspended into PBS. To acquire the MNC fraction, the bone marrow isolate was centrifuged for 40 minutes at 1600 rpm using a 14 mL tube with 3 mL Ficoll-Paque Premium (GE Healthcare, Piscataway, NJ, USA) gradient and 4 mL cell/saline suspension, as described.[5] MNCs were prepared freshly before application.

Characterization of cells by flow cytometry. Cells were incubated in 2% FBS/PBS at 4°C for 30 min with 1 µL of APC-conjugated anti-CD31 (eBioscience), anti-CD45 (BD Biosciences), and anti-Gr-1 (BD Biosciences), or PE-conjugated anti-CD34 (eBioscience), anti-CD11b (BD Biosciences), anti-Flk-1, anti-Sca-1 (both eBioscience), and anti-NK1.1 (BD Biosciences), and processed through a FACSCalibur system (BD, San Jose, CA, USA) according to the manufacturer's protocol.

***In vivo* optical bioluminescence imaging (BLI).** BLI was performed on the IVIS 200 (Xenogen, Alameda, CA, USA) system. For *in vitro* characterization of luciferase expression, cells were suspended in different quantities in 1 mL PBS. Following administration of 10 µL (43.5 µg/mL) D-Luciferin, peak signals (photons/s/cm^2/sr) from a fixed region of interest (ROI) were evaluated and plotted versus cell number. For *in vivo* experiments, recipient mice were anesthetized with isoflurane, shaved, and placed in the imaging chamber. After acquisition of a baseline image, mice were intraperitoneally injected with D-Luciferin (400 mg/kg body weight). Mice were imaged on days 1, 3, 6, 9, 13, 20, and 27 post-injection. Peak signals (photons/s/cm^2/sr) from a fixed region of interest (ROI) were evaluated as described.[7] For *ex vivo* experiments, animals were euthanized immediately following the moment when peak signals were achieved. The organs were rapidly explanted and imaged according to the protocol described above.

Surgical model for hind limb ischemia and cell injections. Mice were placed under general anesthesia with either isoflurane (2%) or ketamine/xylazine combination. Ischemia was created by left sided electro-coagulation of the femoral artery just proximally to the superficial epigastric artery. One day postoperatively, 40 µL of cell/PBS injections were given into the adductor muscle, or 100 µL of cell/PBS solution into the tail vein using a 28-gauge syringe. Subsequently, the skin was closed using 6-0 silk sutures. Additionally, to induce a more severe model

of PAD, male C57BL/6 mice (n=20, Charles River) underwent left sided electro-coagulation of both common iliac and femoral arteries. Afterwards, animals were randomized to receive intravenous injection of $5x10^6$ MNCs or injection or PBS as control (n=10/group).

Laser Doppler Perfusion Imaging (LDPI). Neovascularization was monitored by measurements of perfusion of the hind limbs at the level of the paws and was performed in the mouse hind limb before and directly after the surgical procedure with Laser Doppler Perfusion Imaging (LDPI) (Moor Instruments) at weekly interval over 4 weeks. Eventually, perfusion was expressed as a ratio of the left (ischemic) to right (non-ischemic) paw. Before LDPI, mice were anesthetized with an intraperitoneal injection of Midazolam (5 mg/kg, Roche) and Medetomidine (0.5 mg/kg, Orion).

***Ex vivo* ELISA for apoptosis on digested muscle.** The selected muscle was explanted, digested using a stator-rotator homogenizer, and lysed. ELISA was performed directly on the supernatant to quantify histone-associated DNA fragments (mono- and oligonucleosomes), marking early apoptotic cells (Cell Death Detection ELISA, Roche Applied Science, Indianapolis, IN).

***Ex vivo* assays of reporter gene expression.** To validate *in vivo* BLI findings, the bone marrow was collected as described above and assayed for GFP expression by flow cytometry as described above.

Post-mortem immunohistochemistry. Immunohistochemistry was performed to visualize smooth muscle cell layers of collateral arteries with an antibody against smooth muscle actin. Furthermore, with an antibody against GFP, GFP^+ MNCs were traced in the ischemic skeletal muscle. Five µm-thick paraffin-embedded sections of skeletal muscle fixed with 4% formaldehyde were used. These were re-hydrated and endogenous peroxidase activity was blocked for 20 minutes in methanol containing 0.3% hydrogen peroxide. Skeletal muscle slides were stained with monoclonal anti-α smooth muscle actin (mouse anti-human, DAKO, dilution 1:800) or polyclonal anti-GFP (rabbit anti-mouse, Invitrogen, dilution 1:4000). Antigen retrieval was not necessary and sections were incubated overnight with primary antibody. Rabbit anti-mouse HRP (DAKO, dilution 1:300) or goat anti-rabbit biotin (DAKO, dilution 1:300) were used as secondary antibodies respectively. Negative controls were performed by using isotype controls instead of the primary antibody. For both stainings, the signal was detected using NovaRED substrate kit (Vector laboratories) and sections were counterstained with hematoxylin. Stainings were quantified from randomly photographed sections using image analysis (ImageJ).

Statistical analysis. Statistics were calculated using SPSS 16.0 (SPSS Inc., Chicago, IL, USA). Descriptive statistics included mean and standard error. Comparison between groups was performed using a one-way between groups ANOVA, or one-way repeated measures ANOVA when compared over time, and significance was assumed according to the LSD procedure.

RESULTS

Cell characterization. Following isolation and Ficoll selection, the MNC population showed subpopulations of CD31$^+$, CD34$^+$, CD45$^+$, and Sca-1+, but Flk-1$^-$ cells, representing hematopoietic but not early endothelial progenitors cells. Moreover, strong expression of CD11b, Gr-1, and NK 1.1, representative of macrophages, granulocytes, and natural killer cells, indicated the largely inflammatory character of this donor cell population (**figure 1a**).

Reporter gene characterization. To be able to follow cells in an *in vivo* fashion by bioluminescence imaging (BLI), we first set out to characterize the expression of the reporter gene Fluc *in vitro*. As suggested in **figure 1b**, luciferase expression intensity increased with increasing cell numbers. When maximum expression per well was plotted versus the number of cells, a robust correlation was observed with an r^2 value equaling 0.97 (**figure 1c**). Thus, BLI signal intensity is closely representative of the number of living cells carrying the luciferase reporter gene. Moreover, the robust activity of GFP in the donor-specific Fluc-GFP double-fusion reporter gene construct was confirmed by *in vitro* fluorescence microscopy (**figure 1d**).

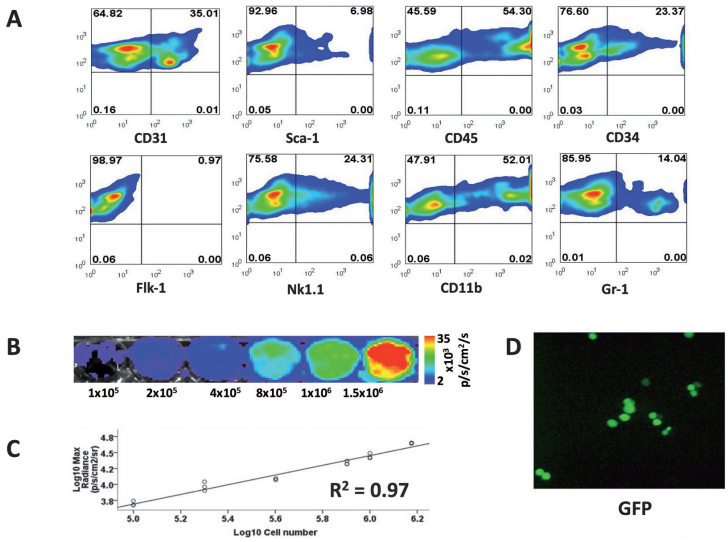

Figure 1. Bone marrow mononuclear cell (MNC) characterization. (a) Flow cytometric analysis following Ficoll-selection of MNCs indicates low numbers of stem/endothelial progenitor cells (Sca-1, flk-1) and high numbers of adult hematopoietic cells of a predominantly inflammatory phenotype (CD45, CD11-b, Gr-1, NK 1.1) (axes

present counts). (b) *In vitro* BLI signals from various numbers of Fluc$^+$ MNCs show (c) robust correlation with cell numbers (r^2=0.97). Scale bars represent BLI signal in photons/s/cm^2/sr. (d) *In vitro* fluorescence microscopy confirms the expression of GFP by the donor cells.

Monitoring kinetics of transplanted MNCs by *in vivo* bioluminescence imaging (BLI). In the current study, MNCs were injected into the left adductor muscles one day following creation of ischemia by left femoral artery occlusion. By doing so, it is possible to study the efficacy of MNCs in stimulating arteriogenesis (the process of collateral artery formation[4]), instead of studying the angiogenic effect which is less influential on restoration in blood flow.[8] To compare the efficacy of a single versus repeated injection with cells, animals were randomized into 3 groups: (1) single MNC injection, (2) repeated MNC injection, and (3) PBS injection. Following single transplantation of 2x10^6 MNCs, a short-term post-transplant increase in BLI signal from 6.6±1.5x10^4 at day 1 to 8.9±2.5x10^4 p/s/cm^2/sr at day 3 (*P*=NS), suggesting an increase in cells in the adductor muscle region during the initial days. Thereafter, however, cell death resulted in a rapid decrease in signal intensity, reaching background levels after 4 weeks (**figure 2**). In order to overcome the problem of poor long-term cell survival, a modified transplantation technique was analyzed in which a similar cumulative dose, but divided in 4 weekly doses of 5x10^5 MNCs, was transplanted. This lead to a relatively stable presence of donor cells, although there was no statistically significant difference after 4 weeks (5.1±0.8x10^3 in single vs 5.7±0.3x10^3 p/s/cm^2/sr in multiple dose group; *P*=NS).

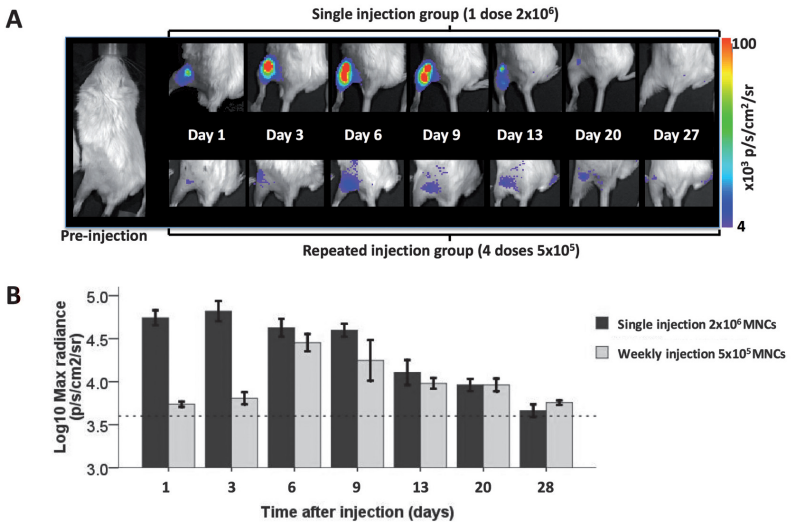

Figure 2. MNC survival following intramuscular injection into the adductor muscles of FVB mice after femoral artery ligation. (a) *In vivo* BLI pictures of mice that received either a total of 2x10^6 MNC by single injection (upper panel) or by weekly injections (lower panel) show MNC survival is short-lived as most of the signal

intensity died off at 4 weeks post-transplant. (b) Quantification of signals showed a somewhat more stable level of MNC presence following repeated injections although the difference did not reach statistical significance. Scale bars represent BLI signal in photons/s/cm^2/sr.

***Ex vivo*, postmortem localization of GFP$^+$ MNCs in the ischemic adductor muscles.** The distribution of GFP$^+$ MNCs was assessed in the post-ischemic adductor muscle of mice treated with a single injection of 2x10^6 MNCs and weekly injections of 5x10^5 MNCs. As shown in **figure 3**, skeletal muscles were harvested 28 days after the induction of ischemia. Low numbers of engrafted GFP$^+$ MNCs were observed in the adductor muscle of mice that received weekly injections of MNCs, concordant with *in vivo* BLI signals. These GFP$^+$ MNCs surrounded vessels within the muscle tissue, suggesting a potential role of these cells in inducing neovascularization. In contrast, GFP$^+$ MNCs were not observed in the adductor muscles of mice receiving a single injection of MNCs at week 4, and corresponding to BLI results.

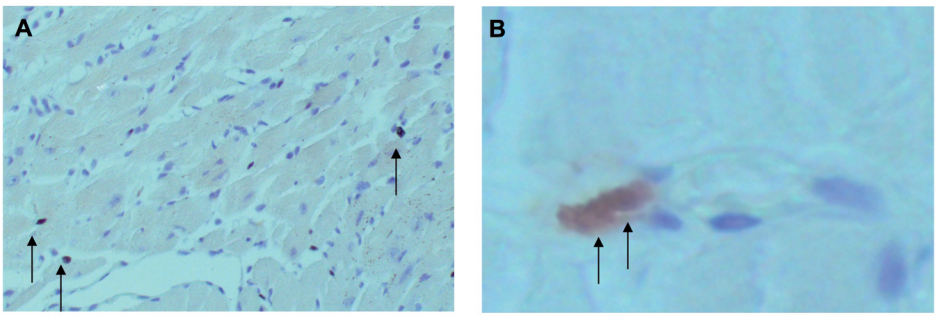

Figure 3. Immunohistochemistry of GFP$^+$ MNCs within the post-ischemic adductor muscle. Representative pictures of anti-GFP muscle staining of (a) positive control slide (magnification 20x), (b) adductor muscle of mouse receiving four weekly 5x10^5 MNC-injections, showing 2 GFP$^+$ cells near a blood vessel (magnification 80x).

Laser Doppler Perfusion Imaging (LDPI) of blood flow restoration following MNC transplantation in FVB mice. For the experiments described above, we used FVB mice to perform a syngeneic transplantation model with our transgenic FVB mice constitutively expressing Fluc$^+$/GFP$^+$ reporter genes. In these mice, femoral artery ligation resulted in a significant decrease in paw perfusion when compared to the healthy right hind limb (P<0.001 for all groups, **figure 4**). Three days following MNC transplantation, a trend was observed towards better flow recovery with increased MNC number, as the ligated/healthy paw perfusion ratios in the 2x10^6 MNC and 5x10^5 groups were 0.75±0.07 and 0.67±0.07, respectively, as compared to 0.62±0.07 in the PBS group (P=NS). However, no significant differences were observed during the prolonged follow up, with robust recovery of paw perfusion in all groups by week 4.

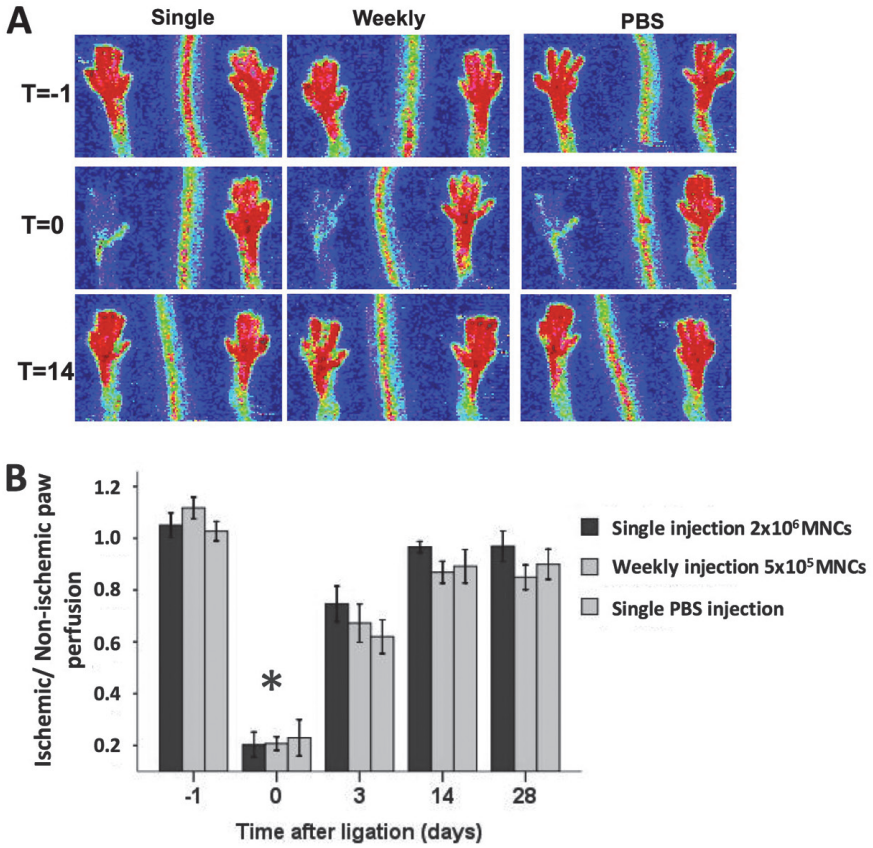

Figure 4. Laser Doppler Perfusion Imaging (LDPI) of ischemic hind limbs following intramuscular MNC therapy. (a) Graphic representation and (b) quantification of paw perfusion by LDPI show a significantly decreased perfusion in the affected left hind limbs as compared to the healthy paw. While a dose-dependent trend towards faster recovery can be observed 3 days after ligation, no significant differences were measured over a total time period of 28 days (Repeated measurements ANOVA, * indicates $P<0.05$).

Histological confirmation of short-term LDPI findings. To investigate whether *in vivo* LDPI matched the actual presence of collaterals, post-mortem histological staining for α-smooth muscle actin was performed. As shown in **figure 5,** no significant differences in collateral density and collateral size in the post-ischemic adductor muscle were found after a single MNC injection, repeated MNC injections, and saline (PBS) injection at week 4, further confirming the lack of functional improvement seen in LDPI results.

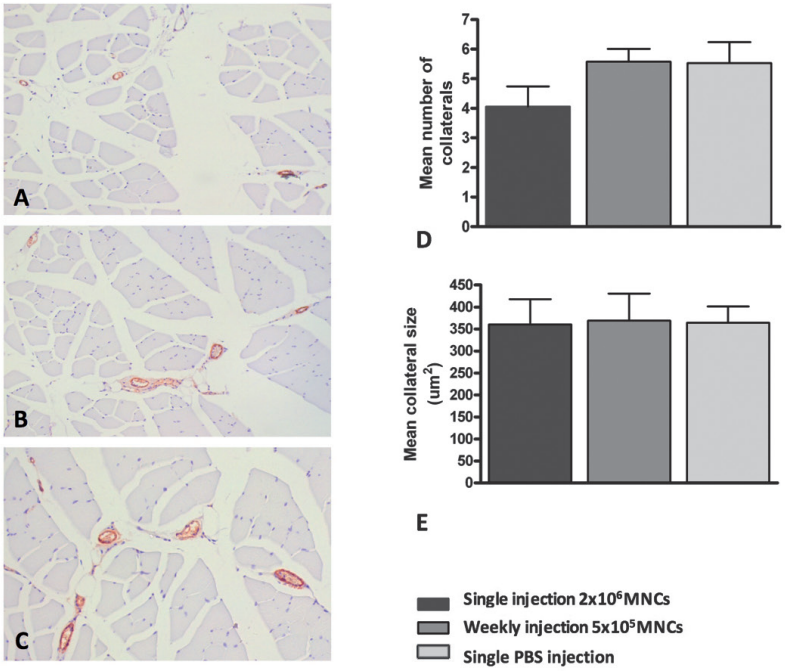

Figure 5. Immunohistochemistry analysis of arteriogenesis within the post-ischemic adductor muscle. Representative pictures of anti-α smooth muscle staining of (a) single $2x10^6$ MNC-injection, (b) weekly $5x10^5$ MNC-injection, and (c) PBS treated mice. Quantification of (d) mean number of collaterals and (e) mean collateral size showed no significant differences among different study groups four weeks after surgery(P=NS, ANOVA).

Confirmation of short-term LDPI findings. To further explore the observed short-term effect of cell therapy on paw perfusion, we performed an apoptosis specific ELISA on the affected gastrocnemius muscles. We hypothesized that increased monocytic cell numbers may have beneficial effects on ischemia-induced apoptosis in the muscular tissue. Thus, to investigate if higher perfusion ratios lead to tissue preservation, gastrocnemius muscles were assayed for DNA fragments in mono- and oligonucleosomes. As shown in **figure 6**, treatment with both single $2x10^6$ MNCs and weekly $5x10^5$ MNCs led to significantly (P=0.03 and P=0.02, respectively, ANOVA) decreased amount of fragmented DNA (mirroring apoptosis) as compared to the PBS group, which had an almost 3-fold higher expression than its healthy contralateral counterparts.

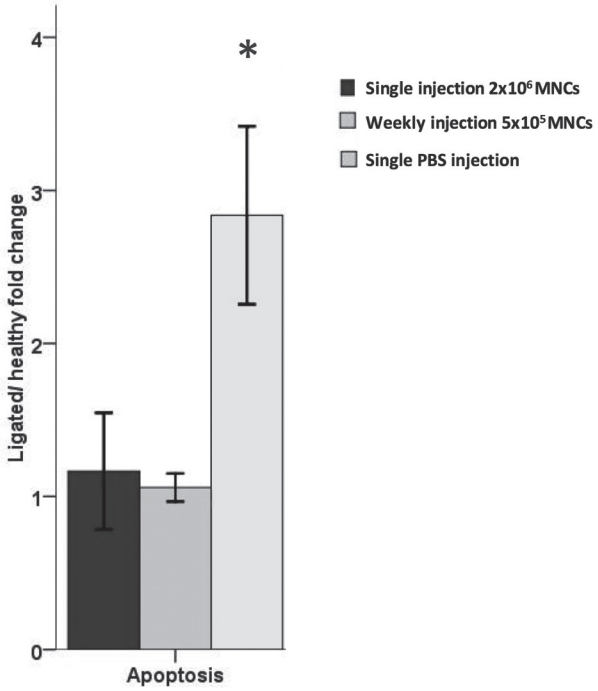

Figure 6. Quantification of short-term apoptotic rates in gastrocnemius muscles of MNC treated animals. ELISA for histone-associated DNA fragments in mono- and oligonucleosomes of digested gastrocnemius muscles revealed an almost 3-fold increase in apoptosis following left femoral artery ligation and PBS treatment as compared to the healthy contralateral muscle as well as compared to MNC treated animals (*P<0.05, ANOVA).

***In vivo* molecular imaging of MNC homing.** To date, most clinical trials have used a transplantation approach that is based on direct delivery into the affected muscle.[9] Others have chosen strategies that rely on stimulation of natural homing of progenitor cells to the affected area.[10] While the current studies with intramuscular injections of MNC suggest that low cell survival might underlie a lack of functional effect, there is no such data available for systemic injection of MNC. Therefore, FVB mice were injected i.v. with $5x10^6$ MNC 1 day following ischemia and were imaged by BLI until day 14. As shown in **figure 7**, the initial BLI signals on day 0 (1 hour after transplantation) equaled background levels, thus confirming the cells were spread out through the circulatory system, without signs of retention in the pulmonary capillaries as observed in previous studies with larger size cell types such as mesenchymal stem cells.[11] Over time, however, signal intensity to the injured area increased. In addition, signals arose from the bone marrow, spleen, and liver, which indicate homing patterns that mimic endogenous myelomonocytic pathways.[12]

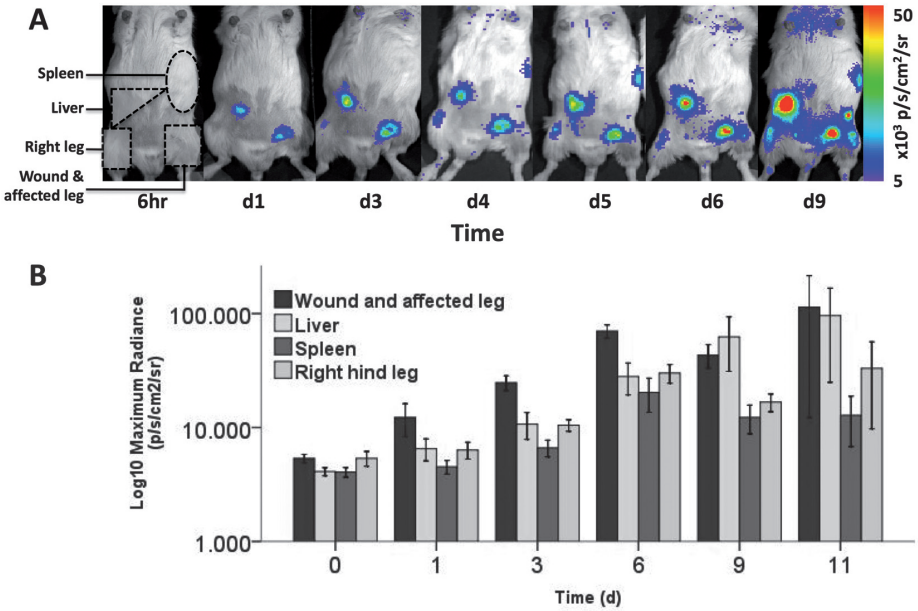

Figure 7. *In vivo* visualization of systemically injected MNC by BLI. (a,b) One day after left femoral artery ligation, $5x10^6$ MNCs were injected via tail vein injection and monitored for 10 days. *In vivo* BLI pictures and signal quantification on multiple time points show that after an initial low signal period due to scattered MNCs throughout the body, cells then travelled to the injured area but also showed preference for the liver, bone marrow, and spleen. Scale bars represent BLI signal in photons/s/cm^2/sr (P=NS, ANOVA).

***Ex vivo* confirmation of *in vivo* patterns of cellular kinetics.** To validate and further specify the observed *in vivo* findings, organs were procured immediately following euthanization. As shown in **figure 8a**, BLI following dissection of the skin showed *in situ* signals from liver, spleen, and the long bones similar to *in vivo* results. However, the signals that were previously observed from the injured area *in vivo* were now largely concentrated in the subcutaneous fat pad as well as in the femoral bone. Indeed, when the different tissues were explanted, it became clear that there was only a low signal from the adductor muscle, while equally strong signals were observed from the scarred skin, the subcutaneous fat pad, and the bone marrow in the femoral bone. Thus, this *ex vivo* imaging confirmed the *in vivo* signals from liver and spleen. Moreover, the presence of GFP^+ donor MNCs in the bone marrow was validated with flow cytometry (**figure 8b**). Taken together, these experiments showed that BLI is a reliable method to monitor MNC trafficking in an *in vivo* fashion. Homing to the injured area was not limited to the adductor muscle, but also occurred to other areas of injury as well as more natural biological niches such as marrow, liver, and spleen.

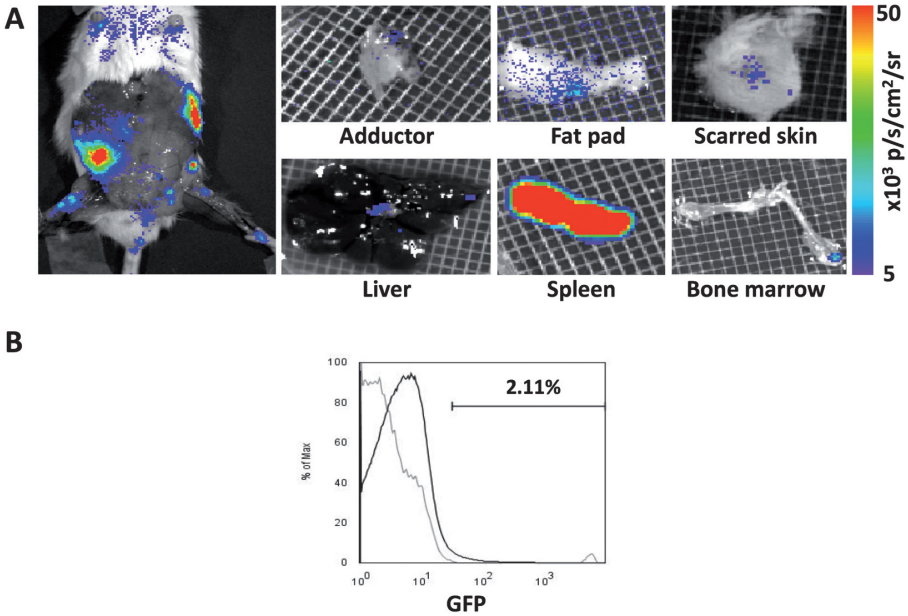

Figure 8. *Ex vivo* confirmation of *in vivo* MNC distribution patterns. (a) Graphic *in vivo* representation of MNC retention in liver, spleen, and bone marrow. Surprisingly, removal of the skin leads to a remarkable reduction of signal intensity from the scarred area. After explantation of various organs and ex vivo BLI, the signal that was previously observed from the injured area during *in vivo* experiments appeared to be a cumulative signal from MNC retention from skin, subcutaneous tissue, and muscle. Scale bars represent BLI signal in photons/s/cm^2/sr. (b) To confirm the BLI signals from the bone marrow, the marrow was flushed from the bone and processed through flow cytometry for GFP$^+$ donor cells. The flow cytometry results correlated with the BLI results, as the recipient bone marrow indeed contained Fluc$^+$/GFP$^+$ donor MNCs.

Monitoring effects of intravenously injected MNC therapy in severe PAD. The PAD model as described above has been used and validated multiple times in C57BL/6 mice.[13] The reason for using FVB mice in the previous experiments was to establish a clinically equivalent model of autologous cell transplantation as our F6 transgenic donor mice were bred on FVB background. However, we observed a robust endogenous recovery of arteriogenic response following ischemia by 4 weeks (see the PBS injection group in Figure 4B), which can be specific for FVB mice.[14] Therefore, to investigate the functional effects of intravenous injection and subsequent MNC homing to the ischemic environment, another strain of C57BL/6 mice underwent electro-coagulation of both the common iliac and femoral artery to ensure profound and more durable ischemia. One day post-operation, 5x10^6 MNCs or PBS as control were injected (n=10 per group), and paw perfusion was again measured by LDPI. As shown in **figure 9**, the ischemic/non-ischemic paw perfusion ratio decreased dramatically from an overall mean of

1.04±0.04 pre-operation to 0.04±0.01 post-operation (*P*<0.0001). Indeed, the current surgical model resulted in sustained loss of perfusion over 4 weeks. However, intravenous injection of MNCs was still incapable of restoring paw perfusion in a significant matter, with ratios of 0.60±0.07 in the cell group compared to 0.57±0.08 in the PBS group (*P*=NS) 4 weeks after operation.

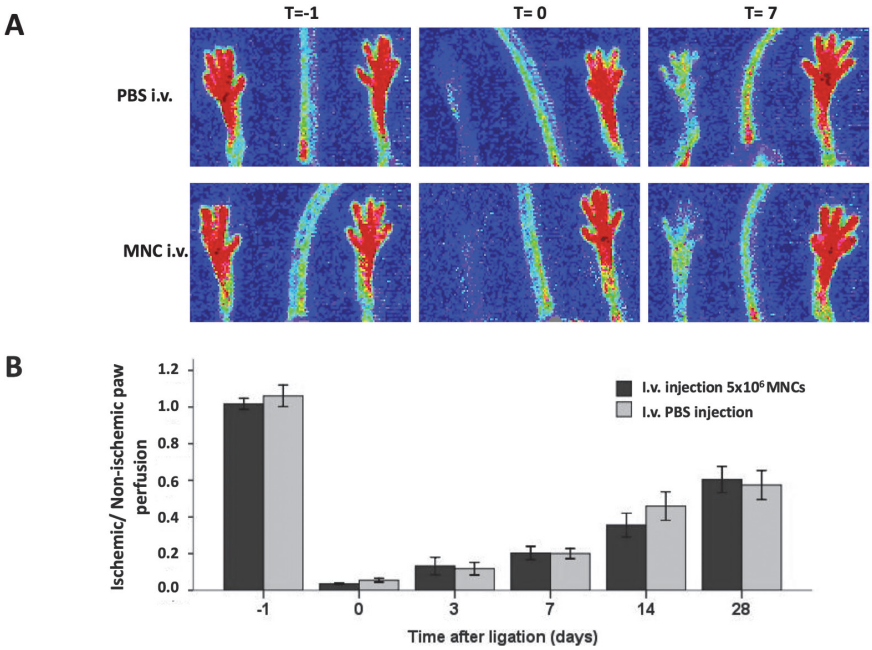

Figure 9. Functional results following systemic MNC injection after severe hind limb ischemia. (a) Following ligation of both the femoral and iliac arteries, markedly decreased paw perfusion was observed for a prolonged period. (b) Quantification of paw perfusion revealed systemic MNC injection was not capable of restoring paw perfusion significantly better than PBS treatment during. (P=NS, Repeated measurements ANOVA).

DISCUSSION

This is the first study to evaluate post-transplant MNC behavior in a murine model of PAD using *in vivo* molecular imaging techniques. The major findings can be summarized as follows: (1) BLI is a valid tool to monitor MNC survival, proliferation, and migration; (2) MNC survival following a single intramuscular injection is short-lived; (3) repeated MNC injections do not provide significantly prolonged cell survival; (4) homing of MNCs following intravenous injection is not limited to the area of injury; and (5) neither intramuscular nor intravenous injection of MNC results in an increased paw perfusion.

The clinical relevance of these findings is significant. Since the pioneering work of Tateishi-

Yuyama and colleagues[9], over 25 clinical trials have been registered on www.clinicaltrials.gov, using either intramuscular or systemic injections into the ischemic leg. Although the findings from this first study were hopeful, so far these results have not been confirmed by large randomized clinical trials. The initial thought behind the use of progenitors cells in regenerative medicine was that it could truly regenerate the damaged tissue by forming new blood vessels[15], skeletal muscle[16], or even myocardium.[17] However, since the true regenerative capacity has been questioned[18], and considering the poor survival capacity of MNC and other progenitor cells in this and other studies thus far[5], a more plausible explanation for a possible beneficial effect would be the secretion of protective cytokines as suggested before.[19] Indeed, it has recently been shown that a more profound angiogenic response can be achieved in ischemic muscle by transplanting progenitor cells overexpressing both VEGF and SDF-1.[20] Alternatively, to achieve true regeneration, one could switch to more specialized cell types rather than whole MNCs. In this respect, it has recently been shown that embryonic stem cell-derived endothelial cells can improve perfusion due to the favorable effect of engraftment and biological activity.[21] Thus, in the future, it might be a feasible approach to use a set of growth factors by gene therapy, increase survival of specialized cells (e.g., embryonic stem cell or induced pluripotent stem cell derivatives), or use a combination of these two.

Previous studies have assessed MNC function and mechanism following transplantation into the ischemic leg largely using post-mortem histological techniques.[22] However, this requires euthanizing the animal, thereby increasing inter-animal variance and preventing longitudinal studies of the same subject. Moreover, the search for scant donor cells on histological slides from all organs is extremely difficult and time consuming. As a consequence, these techniques are less suitable for studying the kinetics of cells through the body over time. In contrast, in this study we have used our molecular imaging platform based on the double-fusion reporter construct carrying $Fluc^+/GFP^+$, to yield valuable insight into longitudinal cell fate. By doing so, we were able to track the spatiotemporal kinetics of MNC homing, retention, and survival in a murine model of PAD.

Interestingly, we observed a relatively limited cell survival after intramuscular injection in the adductor muscle. After a short-term post MNC transplantation increase in BLI signal until day 3, a rapid decrease in BLI-signal intensity to background levels after four weeks was observed. The limited cell survival was confirmed by the immunohistochemical staining against GFP^+ cells. One week after the fourth transplantation of $5x10^5$ MNCs, low numbers of these cells could be found near blood vessels, suggesting a role in neovascularization, or indicating these cells prefer the adjacency of oxygenated blood. The poor survival in the adductor muscle, however, is interesting since femoral artery ligation results in less profound ischemia in the ad-

ductor muscle as compared to the gastrocnemic muscle. This suggests that even in a normoxic niche, MNCs require more biologically attractive environments to be capable of robust survival. This once again stresses the need for development of cell survival augmenting approaches such as scaffolds or transduction of cells with pro-survival factors.

Results from this study show that, following systemic injection, MNCs migrate extensively to the bone marrow, spleen, and liver. This pattern indicates MNCs travel to their natural biological niches as all of these organs play a role in intra- and extramedullary hematopoiesis. Confirming this observation, our BLI findings are concordant with previous leukocyte scans showing retention in the liver and spleen.[23] Apparently, the chemoattractant properties of these organs are stronger than the ischemic environment in the affected muscle. For future experiments, it is important to improve homing to the ischemic muscles which may increase arteriogenic response as measured by LDPI. This can be realized in two ways: 1) improving the attractiveness of the target environment with, for example, the MNC mobilizer stromal-derived factor-1 (SDF-1)[24]; or 2) manipulating the cells to become more specifically guided. In this respect, it might be a better approach to isolate a subset of the mononuclear fraction such as the $CD14^+$ expressing cells that are expected to play a more active role in the restorative process after ischemia.[25]

Taken together, this is the first study to monitor the kinetics of MNCs in PAD in an *in vivo* fashion using molecular imaging techniques. Results from this study highlight caution should be exercised when interpreting results from experimental and clinical studies. The poor survival and homing patterns warrant further research toward better retention and increased biological activity of the cells in the injured area. By doing so, cell therapy might develop as a valuable option for treating end-stage PAD.

ACKNOWLEDGEMENTS

This study was supported by BWF CAMS, NIH RC1HL099117, and R01EB009689 (JCW). Koen van der Bogt was supported by the Michaël van Vloten fund. The authors gratefully acknowledge the support of the TeRM Smart Mix Program of the Netherlands Ministry of Economic Affairs and the Netherlands Ministry of Education, Culture and Science for Alwine Hellingman.

REFERENCES

1. Rosamond W, Flegal K, Furie K, Go A, Greenlund K, Haase N, Hailpern SM, Ho M, Howard V, Kissela B, Kittner S, Lloyd-Jones D, McDermott M, Meigs J, Moy C, Nichol G, O'Donnell C, Roger V, Sorlie P, Steinberger J, Thom T, Wilson M, Hong Y. Heart disease and stroke statistics--2008 update: a report from the American Heart Association Statistics Committee and Stroke Statistics Subcommittee. *Circulation.* 2008;117(4):e25-146.
2. Belch JJ, Topol EJ, Agnelli G, Bertrand M, Califf RM, Clement DL, Creager MA, Easton JD, Gavin JR, 3rd, Greenland P, Hankey G, Hanrath P, Hirsch AT, Meyer J, Smith SC, Sullivan F, Weber MA. Critical issues in peripheral arterial disease detection and management: a call to action. *Arch Intern Med.* 2003;163(8):884-892.
3. Norgren L, Hiatt WR, Dormandy JA, Nehler MR, Harris KA, Fowkes FG, Bell K, Caporusso J, Durand-Zaleski I, Komori K, Lammer J, Liapis C, Novo S, Razavi M, Robbs J, Schaper N, Shigematsu H, Sapoval M, White C, White J, Clement D, Creager M, Jaff M, Mohler E, 3rd, Rutherford RB, Sheehan P, Sillesen H, Rosenfield K. Inter-Society Consensus for the Management of Peripheral Arterial Disease (TASC II). *Eur J Vasc Endovasc Surg.* 2007;33 Suppl 1:S1-75.
4. van Weel V, van Tongeren RB, van Hinsbergh VW, van Bockel JH, Quax PH. Vascular Growth in Ischemic Limbs: A Review of Mechanisms and Possible Therapeutic Stimulation. *Ann Vasc Surg.* 2008.
5. van der Bogt KE, Sheikh AY, Schrepfer S, Hoyt G, Cao F, Ransohoff KJ, Swijnenburg RJ, Pearl J, Lee A, Fischbein M, Contag CH, Robbins RC, Wu JC. Comparison of different adult stem cell types for treatment of myocardial ischemia. *Circulation.* 2008;118(14 Suppl):S121-129.
6. Wu JC, Chen IY, Sundaresan G, Min JJ, De A, Qiao JH, Fishbein MC, Gambhir SS. Molecular imaging of cardiac cell transplantation in living animals using optical bioluminescence and positron emission tomography. *Circulation.* 2003;108(11):1302-1305.
7. Cao YA, Wagers AJ, Beilhack A, Dusich J, Bachmann MH, Negrin RS, Weissman IL, Contag CH. Shifting foci of hematopoiesis during reconstitution from single stem cells. *Proc Natl Acad Sci U S A.* 2004;101(1):221-226.
8. Schaper W, Scholz D. Factors regulating arteriogenesis. *Arterioscler Thromb Vasc Biol.* 2003;23(7):1143-1151.
9. Tateishi-Yuyama E, Matsubara H, Murohara T, Ikeda U, Shintani S, Masaki H, Amano K, Kishimoto Y, Yoshimoto K, Akashi H, Shimada K, Iwasaka T, Imaizumi T. Therapeutic angiogenesis for patients with limb ischaemia by autologous transplantation of bone-marrow cells: a pilot study and a randomised controlled trial. *Lancet.* 2002;360(9331):427-435.
10. van Royen N, Schirmer SH, Atasever B, Behrens CY, Ubbink D, Buschmann EE, Voskuil M,

Bot P, Hoefer I, Schlingemann RO, Biemond BJ, Tijssen JG, Bode C, Schaper W, Oskam J, Legemate DA, Piek JJ, Buschmann I. START Trial: a pilot study on STimulation of ARTeriogenesis using subcutaneous application of granulocyte-macrophage colony-stimulating factor as a new treatment for peripheral vascular disease. *Circulation*. 2005;112(7):1040-1046.

11. Schrepfer S, Deuse T, Reichenspurner H, Fischbein MP, Robbins RC, Pelletier MP. Stem cell transplantation: the lung barrier. *Transplant Proc*. 2007;39(2):573-576.
12. Hallgren J, Gurish MF. Pathways of murine mast cell development and trafficking: tracking the roots and routes of the mast cell. *Immunol Rev*. 2007;217:8-18.
13. van Weel V, Toes RE, Seghers L, Deckers MM, de Vries MR, Eilers PH, Sipkens J, Schepers A, Eefting D, van Hinsbergh VW, van Bockel JH, Quax PH. Natural killer cells and CD4+ T-cells modulate collateral artery development. *Arterioscler Thromb Vasc Biol*. 2007;27(11):2310-2318.
14. Harmon KJ, Couper LL, Lindner V. Strain-dependent vascular remodeling phenotypes in inbred mice. *Am J Pathol*. 2000;156(5):1741-1748.
15. Al-Khaldi A, Al-Sabti H, Galipeau J, Lachapelle K. Therapeutic angiogenesis using autologous bone marrow stromal cells: improved blood flow in a chronic limb ischemia model. *Ann Thorac Surg*. 2003;75(1):204-209.
16. Liu Q, Chen Z, Terry T, McNatt JM, Willerson JT, Zoldhelyi P. Intra-arterial transplantation of adult bone marrow cells restores blood flow and regenerates skeletal muscle in ischemic limbs. *Vasc Endovascular Surg*. 2009;43(5):433-443.
17. Orlic D, Kajstura J, Chimenti S, Jakoniuk I, Anderson SM, Li B, Pickel J, McKay R, Nadal-Ginard B, Bodine DM, Leri A, Anversa P. Bone marrow cells regenerate infarcted myocardium. *Nature*. 2001;410(6829):701-705.
18. Balsam LB, Wagers AJ, Christensen JL, Kofidis T, Weissman IL, Robbins RC. Haematopoietic stem cells adopt mature haematopoietic fates in ischaemic myocardium. *Nature*. 2004;428(6983):668-673.
19. van Weel V, Seghers L, de Vries MR, Kuiper EJ, Schlingemann RO, Bajema IM, Lindeman JH, Delis-van Diemen PM, van Hinsbergh VW, van Bockel JH, Quax PH. Expression of vascular endothelial growth factor, stromal cell-derived factor-1, and CXCR4 in human limb muscle with acute and chronic ischemia. *Arterioscler Thromb Vasc Biol*. 2007;27(6):1426-1432.
20. Yu JX, Huang XF, Lv WM, Ye CS, Peng XZ, Zhang H, Xiao LB, Wang SM. Combination of stromal-derived factor-1alpha and vascular endothelial growth factor gene-modified endothelial progenitor cells is more effective for ischemic neovascularization. *J Vasc Surg*. 2009;50(3):608-616.
21. Huang NF, Niiyama H, Peter C, De A, Natkunam Y, Fleissner F, Li Z, Rollins MD, Wu JC,

Gambhir SS, Cooke JP. Embryonic stem cell-derived endothelial cells engraft into the ischemic hindlimb and restore perfusion. *Arterioscler Thromb Vasc Biol.*30(5):984-991.

22. Aranguren XL, McCue JD, Hendrickx B, Zhu XH, Du F, Chen E, Pelacho B, Penuelas I, Abizanda G, Uriz M, Frommer SA, Ross JJ, Schroeder BA, Seaborn MS, Adney JR, Hagenbrock J, Harris NH, Zhang Y, Zhang X, Nelson-Holte MH, Jiang Y, Billiau AD, Chen W, Prosper F, Verfaillie CM, Luttun A. Multipotent adult progenitor cells sustain function of ischemic limbs in mice. *J Clin Invest*. 2008;118(2):505-514.
23. Datz FL, Luers P, Baker WJ, Christian PE. Improved detection of upper abdominal abscesses by combination of 99mTc sulfur colloid and 111In leukocyte scanning. *AJR Am J Roentgenol*. 1985;144(2):319-323.
24. Ceradini DJ, Kulkarni AR, Callaghan MJ, Tepper OM, Bastidas N, Kleinman ME, Capla JM, Galiano RD, Levine JP, Gurtner GC. Progenitor cell trafficking is regulated by hypoxic gradients through HIF-1 induction of SDF-1. *Nat Med*. 2004;10(8):858-864.
25. Urbich C, Heeschen C, Aicher A, Dernbach E, Zeiher AM, Dimmeler S. Relevance of monocytic features for neovascularization capacity of circulating endothelial progenitor cells. *Circulation*. 2003;108(20):2511-2516.

CHAPTER 10

Summary and Discussion

INTRODUCTION

Over the past years, stem cell therapy has raised tremendous enthusiasm as a potential treatment for cardiovascular diseases. However, questions remain about the *in vivo* behavior of the cells after transplantation and the mechanism of action with which the cells could potentially alleviate disease symptoms. The objective of the research described in this thesis was to visualize the survival, proliferation, and migration of both embryonic and adult stem cells using non-invasive molecular imaging techniques in small animal models of cardiovascular diseases. The major findings can be described as follows: (1) Non-invasive bioluminescence imaging is a validated tool to monitor donor cell survival, proliferation, migration, and misbehavior; (2) Embryonic stem cells (ESC) are a potential source for a true regenerative therapy; (3) ESC form teratomas; (4) Adult stem cell survival is short-lived, but of all adult stem cells currently used in the clinic, mononuclear cells show the most prolonged survival; (5) Transplantation of mononuclear cells can preserve cardiac function in the short term after myocardial infarction in mice; (6) Compared to other measurements of cardiac function in mice, Micro-CT is a superior, three-dimensional, non-invasive method to assess cardiac geometry and function; and (7) Transplantation of mononuclear cells in peripheral artery disease is hampered by dismal cell survival and homing.

MONITORING EMBRYONIC STEM CELL THERAPY

In this thesis we have provided, largely for the first time, insight in the *in vivo* cellular behavior of adult and ESC. In **Chapter 2**, we have shown that ESC transplantation results in superior preservation of cardiac function in the short term compared to fibroblasts, as measured by small animal MRI that was confirmed by invasive hemodynamic measurements. However, novel bioluminescence imaging of the GFP+/Fluc+ ESC revealed a robust increase in BLI signal as early as two days post-transplant. After having shown that increasing BLI signal is in fact representative of an increase in cell number *in vitro* by BLI and that *in vivo* BLI signals correlated well with *ex vivo* TaqMan PCR, the increasing signal *in vivo* was clearly a consequence of cell proliferation. This early, *in vivo* suggestion of teratoma formation was supported by gross histology showing intense accumulation of donor cells.

As a follow-up study, **Chapter 3** nicely outlined the importance of using BLI to monitor cell fate after ESC transplantation. Indicative of the sensitivity of this technique, we observed increasing signals, implying teratoma formation, as early as one week after subcutaneous transplantation of as little as 1000 ESC. Correlating with the BLI results, teratoma formation was indeed confirmed by post-mortem histology showing differentiation of ESC to progeny from all three germ layers. The chapter also showed the importance of being able to perform whole-body imaging as ESC migrated through the body and formed teratomas at distant locations that

were easily identified by BLI. Finally, the stable integration of the GFP/Fluc construct in the donor ESC and the persistence of cell retention in the heart was illustrated by experiments showing follow-up of intramyocardially transplanted ESC *in vivo* as long as 10 months. These above mentioned advantages of using molecular imaging techniques to monitor ESC transplantation were summarized and related to the great potential of ESC to treat a wide variety of diseases in **Chapter 4**. **Chapter 5**, on the other hand, focused on the potential of ESC to differentiate into cardiomyocytes while indicating some of the hurdles that need to be overcome before ESC-derived-cardiomyocyte therapy will face the clinic. Next to the possibility of teratoma formation following inefficient pre-differentiation and subsequent transplantation of a heterogeneous population, this chapter also discussed the problems of immunogenicity and stable integration within the host myocardium.

MONITORING ADULT STEM CELL THERAPY

Chapter 6 was designed to answer the basic question: Which adult stem cell already clinically used in heart failure trials in humans can best preserve cardiac function after myocardial infarction in mice? To monitor cell fate after transplantation, all cells were isolated from donor mice that transgenically expressed both GFP and Fluc. After multimodality *in vitro* validation of reporter gene expression in all cell types, *in vivo* BLI results showed extensive donor cell death from skeletal myoblasts (SkMb), mesenchymal stem cells (MSC), and fibroblasts (Fibro, a cellular control) within three to four weeks after transplantation. Mononuclear cells (MN), on the other hand, were still present after 6 weeks, although in low numbers. Interestingly, these cells proliferated during the inflammatory phase (first ten days) after infarction, while some cells that had leaked into the circulation homed to the spleen, liver, and bone marrow later on. Our echocardiography studies, validated by invasive hemodynamic measurements, showed significantly improved cardiac function in mice that had received mononuclear cells as compared to negative (saline injection) and cellular (fibroblast injection) controls, while skeletal myoblasts were only significantly better than the negative controls. On the contrary, mesenchymal stem cells had no significant functional effect. Interestingly, however, deterioration of cardiac function was observed between 4 and 6 weeks in all cellular groups without such an effect in the saline control group, suggesting that the preservation lasts only for a short time. However, this can only be confirmed by future long-term studies.

In addition to the findings described in the previous chapter, **Chapter 7** provided for the first time *in vivo* information on the cellular kinetics of adipose tissue-derived stromal cells when transplanted into the infarcted mouse heart. This recently discovered cell population is believed to be similar to mesenchymal stem cells from the bone marrow. Indeed, these cell types shared similar morphology, cell surface expression patterns, and *in vitro* behavior. Unfortu-

nately, however, neither cell type was capable of surviving the ischemic environment of the infarcted heart and cell death ensued within 4 weeks of transplantation. Moreover, we did not observe any functional effect by echocardiography and pressure-volume loops.
In the studies described above, echocardiography proved to be an easy-to-use, quick modality to measure cardiac function in mice, and acquired diameters were generally correlative to ventricular volumes measured by conductance catheters. However, echocardiography is limited by means of its two-dimensionality while performing pressure-volume loops with a conductance catheter is a terminal procedure. In **Chapter 8**, we therefore introduced a novel, three-dimensional, *in vivo* modality to our inventory. The model of murine myocardial ischemia was used to show good correlations between Micro-CT and the more conventional imaging modalities. However, Micro-CT proved to gain the most detailed, precise measurements of systolic and diastolic cardiac geometry and subsequent functional parameters. Moreover, *in vivo* images acquired with Micro-CT resembled *ex vivo* post-mortem histological pictures of ventricular morphology.

Finally, **Chapter 9** provided insight into the kinetics of mononuclear cells (MN) after intramuscular and intravenous transplantation into a mouse model of peripheral artery occlusive disease. Intramuscular injection, either by single or repeated dosages, resulted in dismal cell survival without any effects on restoration of perfusion as measured by Laser-Doppler Perfusion Imaging. Following intravenous injection, regular *in vivo* BLI revealed homing to the injured area, although not exclusively. Signals were also observed from liver, spleen, and bone marrow. Moreover, *ex vivo* BLI showed that signals from the injured area were predominantly the result of homing to the scarred skin and the manipulated subcutaneous fat pad rather than the ischemic muscle. These findings translated into a lack of functional effect on paw perfusion.

NON-INVASIVE MOLECULAR IMAGING: KEEPING AN EYE ON TRANSPLANTED CELL SURVIVAL, PROLIFERATION, MIGRATION, AND MISBEHAVIOR.

The common technique used in the studies described in this thesis was non-invasive bioluminescence imaging. The double-fusion reporter construct carrying GFP and Fluc, on which this imaging technique was based, proved to be stably integrated into the donor cell's DNA as confirmed by *in vitro* BLI and luminometry. Moreover, *in vivo* BLI signals were validated by *ex vivo* quantitative PCR techniques as well as post-mortem histology and flow-cytometry with staining for GFP. Thus, BLI is a validated tool to image cell quantity as its signal is representative of cell number due to the equal transmission of the reporter genes to daughter cells. Subsequently, the adult stem cell studies have shown this technique to be suitable to image cell survival and migration. The fact that dead cells lack the transcriptional and translational process of reporter protein production underlies the capability to monitor cell death by loss of BLI signal.

Furthermore, the ESC studies have emphasized the excellent value of BLI to monitor cell location, proliferation, and misbehavior. Taken together, BLI is an indispensible tool for imaging the effects and safety of cell therapy. However, BLI uses low-energy 2-3 eV photons, which leads to photon attenuation and scattering within deep tissues.[1] Moreover, at present the imaging system containing the ultrasensitive CCD camera is unavailable for large animals or humans. These factors make this technique currently unsuitable for large animal or clinical safety studies. Instead, clinical molecular imaging techniques are currently based upon the utilization of Positron Emission Tomography (PET) with its associated reporter construct herpes simplex virus thymidine kinase (HSV-tk). Following injection of a radiolabeled thymidine analog (e.g. [18F]fluoro-3-hydroxymethylbutylguanine or [18F]-FHBG), the donor cells carrying HSV-tk will phosphorilate and subsequently trap the probe inside the cell, producing a signal consisting of high-energy photons strong enough for deep tissue imaging. This HSV-tk reporter gene construct has been used in small[2] and large animal[3] studies as well as in human trials.[4] Due to the fact that every imaging modality has its advantages and drawbacks, it is important to develop reporter gene constructs that combine different techniques. In this respect, we have shown the promise of the double fusion construct carrying Fluc and GFP for BLI and immunohistochemistry (IHC) in the studies described, respectively. Moreover, our group has developed a triple fusion construct containing Fluc, red fluorescent protein (RFP), and tk, thereby enabling BLI, IHC, and PET imaging.[5] Additionally, reporter gene imaging can be combined with magnetic labeling to enable superior imaging of acute localization of transplanted cells by MRI.[6]

CLINICAL UPDATE

To date, over 250 and almost 30 clinical trials are registered for heart disease and peripheral artery occlusive disease, respectively (http://clinicaltrials.gov/), illustrating the huge enthusiasm for cell therapy among doctors, patients, and media. As to cardiac cell therapy, studies greatly differ in patient population (acute vs. chronic ischemia), cell type and the administered quantity, method and timing of delivery, and duration of follow-up. Moreover, the majority of results comes from non-blinded trials.

So far, two meta-analyses have been published, both of which analyzed the efficacy of cell therapy for acute ischemic heart disease. Abdel-Latif and colleagues analyzed 18 controlled studies and generally, cell injection showed no increase in adverse events. Improvements in cardiac function with cell transplantation included a significant 3.66% increase in left ventricular ejection fraction and a significant 5.49% reduction in infarct size.[7] A second meta-analysis was performed by Lipinski and colleagues. After analysis of 10 studies, intracoronary cell therapy showed a significant decrease in recurrent myocardial infarction, but no difference in mortality risk and rehospitalization. Cell therapy resulted in a 2.97% increase in ejection fraction,

decreased end-systolic volume, and a 5.28% reduction in perfusion defect size.[8] Despite the statistically significant numbers from both meta-analyses, these studies do not clearly provide information whether these numbers translated into clinically relevant improvements in quality of life.

A recent Cochrane systematic review by Martin-Rendon and colleagues described 13 randomized controlled trials with a cumulative of 880 patients that received percutaneous intracoronary infusion of cells following acute ischemia. This review modestly concluded that cell therapy for acute myocardial infarction may be safe and moderately beneficial. However, the trials included were too small to demonstrate whether this therapy may have an effect on the incidence of mortality and morbidity.[9]

Regarding cell therapy for peripheral artery occlusive disease, the data are still rather preliminary, as most studies do not provide adequate patient numbers for definitive conclusions. Although small studies such as the initial TACT investigation show promising results including a 4-week increased ankle-brachial index, decreased rest pain and increased pain-free walking time,[10, 11] these observations require large, multicenter randomized trials to confirm the ability of cell therapy for relieving symptoms and improving quality of life in peripheral artery occlusive disease.

FUTURE DIRECTIONS

This thesis has shown that there are certain advantages and drawbacks of stem cell therapy for cardiovascular diseases. On adult stem cells, a functional benefit, if present, may be the result of paracrine signaling protecting host cells from dying, attracting native stem cells, attenuating remodeling, and inducing arterio-/ angiogenesis. However, this activity may be limited by poor cell survival which may explain short-term effects in our studies and some large clinical trials.[12] Therefore, one major goal should be to develop strategies that improve cell survival or increase the downstream effects as described above. In this regard, it may be of significant benefit to stimulate the cells using specific growth factors. Overexpression of certain factors might both increase survival as well as augment the biological function of adult stem cells. Supporting this hypothesis, researchers have shown that transfection of mesenchymal stem cells with the pro-survival gene *Akt* not only increased cell survival, but also augmented the functional effect on the infarcted heart.[13] More research will nevertheless be needed to discover the optimal combination of transcriptional factors needed to establish a significant, clinically relevant benefit of cell therapy. However, one must keep in mind the mechanism that might lead to this objective. If the stem cells do not have the capacity to become cells of the target tissue (cardiomyocytes in case of intramyocardial transplantation or endothelial cells when used in peripheral

artery disease) the question remains whether prolonged survival is necessary. If the effect of adult stem cells is merely a consequence of paracrine signaling, an approach whereby a slow-release cocktail of cytokines is infused might be just as effective. Alternatively, a gene therapy approach whereby the host tissue is modified to express pro-angiogenic or pro-survival genes could still be very promising. Taken together, in the case of cardiovascular disease, adult stem cell therapy seems to be more of a preservative therapy rather than a true regenerative therapy and has yet to be optimalized on the basis of more mechanistic studies.

ESC, on the other hand, have shown to be capable of really rebuilding the heart muscle, as we have observed that they form cardiomyocytes *in vivo*. Even if the frequency of this rare event can be increased or if ESC-derived cardiomyocytes can be purely grown in culture and subsequently transplanted, it remains questionable if these cells can truly integrate with native tissue and, importantly, will contract synchronously and respond effectively to the natural pacing of the heart. This problem has an extra dimension because ESC-derived cardiomyocytes appear to consist of both atrial and ventricular types that may react differently upon pacing. This illustrates the great caution warranted when using these cells for transplantation. Two other major problems we have visualized or addressed in this thesis concern tumorigenicity and immunogenicity. The development of more efficient pre-differentiation systems may make it possible to obtain 100% pure populations of a desired cell type from undifferentiated ESC cultures, thus limiting the possibility of present undifferentiated, potentially tumorigenic cells. Accordingly, it should be stressed that imaging cell therapy is indispensible as malignant events should be detected at an early stage. In this respect, one major advantage of using reporter gene imaging with the HSV-tk construct is the possibility to use this construct as a suicide gene as it is responsive to gancyclovir treatment. As such, the donor cells can be targeted when imaging reveals misbehavior, possibly preventing teratoma formation.[5]

One other ESC-related problem involves immunorejection. Great progress has recently been made by our group to characterize the immunogenic pattern of ESC. Similar to organ transplants, the rejection of embryonic stem cell grafts is CD4-mediated which can be largely overcome by treatment with immunosuppressive drugs.[14] Although these findings illustrate the increased understanding of ESC biology and development, consequently embryonic stem cell therapy will pose the patient to a life-long treatment to immunosuppressive drugs including the associated complications. Lastly, and very important, are the ethical issues that are associated to the derivation of cells from embryonic tissue. However, a great breakthrough has been established that has changed the field of stem cell research dramatically.

Recently, a Japanese group has published a report showing the possibility of using transcrip-

tion factors to reprogram adult stem cells (fibroblasts) to less differentiated states, where after these cells regain capability to differentiate into all germ layers.[15] These observations may redefine the differentiation patterns as described in the introduction of this thesis, now showing that, by *in vitro* manipulation, germ layer- or tissue lineage boundary limitations can be overcome. These so-called induced pluripotent stem cells (iPSc) seem to resemble ESC, but circumvent ethical and immunogenicity problems, offering the possibility to develop patient- and disease specific stem cells. Not only could this lead to new cell replacement therapies for tissue otherwise incapable of endogenous regeneration, but iPSc can also serve as *in vitro* surrogates for testing drug efficacy and toxicity specific to a disease or patient. While the opportunities seem innumerable, iPSc remain to be characterized more thoroughly regarding, among others, differentiation capacity and energy metabolism.

One last modality that will likely regain significant interest is gene therapy. As the effect of cell therapy may largely depend on the paracrine action of the cells rather than their structural, long lasting support, it would perhaps make more sense to 'train' the host cells to exhibit the paracrine character needed to stimulate, for example, angiogenesis. In order to provide a significant beneficial effect, it is yet to be investigated which factor is a key modulator of the process of angiogenesis, and create a vector that is non-immunogenic and grants an efficient, long lasting transfection. Ultimately, reporter gene imaging can be combined with gene therapy, allowing for *in vivo* monitoring of gene expression and dosing. Combining knowledge from imaging, cell therapy, and angiogenesis studies, we are currently moving forward in achieving these characteristics and hope to provide a novel gene therapy agent for cardiovascular diseases in the near future.

FINAL REMARKS

The field of adult stem cell therapy for cardiovascular disease has provoked an enormous amount of enthusiasm, leading to a clinical translation of experimental findings with unprecedented rapidity. Such transitions cannot solely be based on findings in experimental rodent models, as the results from the studies described in this thesis are not always concordant to findings from clinical studies. This emphasizes the current gap that exists between animal models and human disease and justifies extensive investigations in large animals or even primates before proceeding to any kind of clinical trial with cardiomyocytes. Regarding ESC or iPSc, it is of main importance to characterize these cells, explore the way they differentiate, and portray their genomic and proteomic patterns. Luckily, research in this field has been given a boost by recent developments since president Obama issued Executive Order 13505 entitled "Removing Barriers to Responsible Scientific Research Involving Human Stem Cells" (http://stemcells.nih.gov). As a result, federal funding of embryonic stem cell research from the National Insti-

tutes of Health was restored after being strongly limited for eight years under the previous administration. Hopefully, this will lead to a better understanding of developmental biology, disease, and therapeutic targets for the large range of diseases that can benefit from new treatments, not at the least for cardiovascular diseases (**figure 1**). In all these settings, molecular imaging should and will indisputably form an important tool in assessing the efficacy in both experimental and clinical settings of cell therapy.

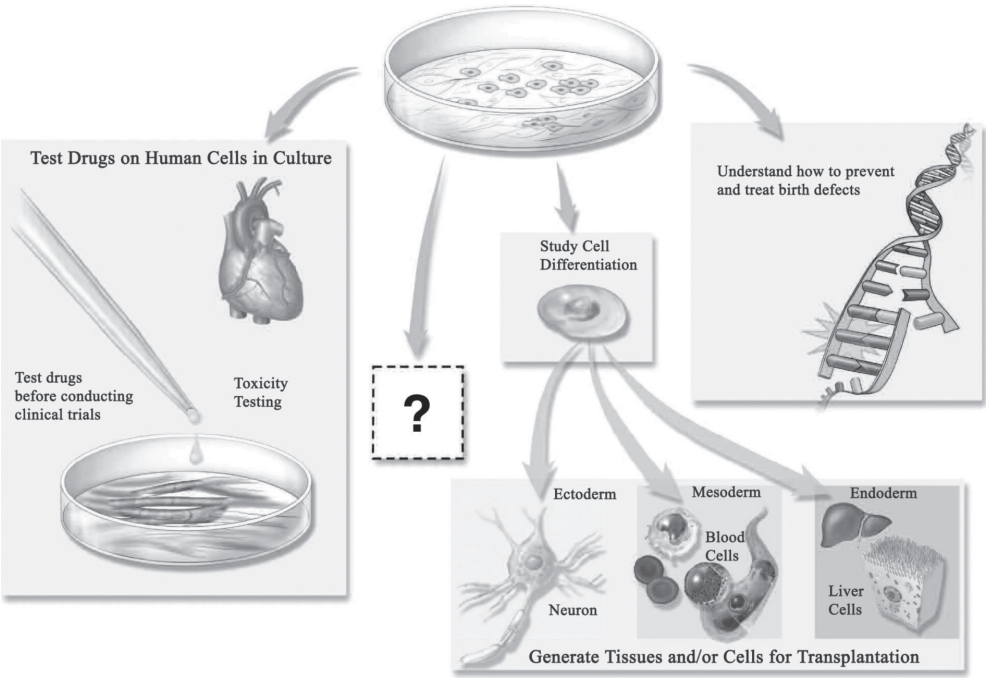

Figure 1. Promises and directions of stem cell research (www.nih.gov)

REFERENCES:

1. Sheikh AY, Wu JC. Molecular imaging of cardiac stem cell transplantation. *Curr Cardiol Rep.* 2006;8(2):147-154.
2. Wu JC, Chen IY, Wang Y, Tseng JR, Chhabra A, Salek M, Min JJ, Fishbein MC, Crystal R, Gambhir SS. Molecular imaging of the kinetics of vascular endothelial growth factor gene expression in ischemic myocardium. *Circulation.* 2004;110(6):685-691.
3. Rodriguez-Porcel M, Brinton TJ, Chen IY, Gheysens O, Lyons J, Ikeno F, Willmann JK, Wu L, Wu JC, Yeung AC, Yock P, Gambhir SS. Reporter gene imaging following percutaneous delivery in swine moving toward clinical applications. *J Am Coll Cardiol.* 2008;51(5):595-597.
4. Jacobs A, Voges J, Reszka R, Lercher M, Gossmann A, Kracht L, Kaestle C, Wagner R, Wienhard K, Heiss WD. Positron-emission tomography of vector-mediated gene expression in gene therapy for gliomas. *Lancet.* 2001;358(9283):727-729.
5. Cao F, Lin S, Xie X, Ray P, Patel M, Zhang X, Drukker M, Dylla SJ, Connolly AJ, Chen X, Weissman IL, Gambhir SS, Wu JC. *In vivo* visualization of embryonic stem cell survival, proliferation, and migration after cardiac delivery. *Circulation.* 2006;113(7):1005-1014.
6. Daadi MM, Li Z, Arac A, Grueter BA, Sofilos M, Malenka RC, Wu JC, Steinberg GK. Molecular and magnetic resonance imaging of human embryonic stem cell-derived neural stem cell grafts in ischemic rat brain. *Mol Ther.* 2009;17(7):1282-1291.
7. Abdel-Latif A, Bolli R, Tleyjeh IM, Montori VM, Perin EC, Hornung CA, Zuba-Surma EK, Al-Mallah M, Dawn B. Adult bone marrow-derived cells for cardiac repair: a systematic review and meta-analysis. *Arch Intern Med.* 2007;167(10):989-997.
8. Lipinski MJ, Biondi-Zoccai GG, Abbate A, Khianey R, Sheiban I, Bartunek J, Vanderheyden M, Kim HS, Kang HJ, Strauer BE, Vetrovec GW. Impact of intracoronary cell therapy on left ventricular function in the setting of acute myocardial infarction: a collaborative systematic review and meta-analysis of controlled clinical trials. *J Am Coll Cardiol.* 2007;50(18):1761-1767.
9. Martin-Rendon E, Brunskill S, Doree C, Hyde C, Watt S, Mathur A, Stanworth S. Stem cell treatment for acute myocardial infarction. *Cochrane Database Syst Rev.* 2008(4):CD006536.
10. Tateishi-Yuyama E, Matsubara H, Murohara T, Ikeda U, Shintani S, Masaki H, Amano K, Kishimoto Y, Yoshimoto K, Akashi H, Shimada K, Iwasaka T, Imaizumi T. Therapeutic angiogenesis for patients with limb ischaemia by autologous transplantation of bone-marrow cells: a pilot study and a randomised controlled trial. *Lancet.* 2002;360(9331):427-435.
11. Al Mheid I, Quyyumi AA. Cell therapy in peripheral arterial disease. *Angiology.* 2008;59(6):705-716.

12. Meyer GP, Wollert KC, Lotz J, Steffens J, Lippolt P, Fichtner S, Hecker H, Schaefer A, Arseniev L, Hertenstein B, Ganser A, Drexler H. Intracoronary bone marrow cell transfer after myocardial infarction: eighteen months' follow-up data from the randomized, controlled BOOST (BOne marrOw transfer to enhance ST-elevation infarct regeneration) trial. *Circulation*. 2006;113(10):1287-1294.
13. Mangi AA, Noiseux N, Kong D, He H, Rezvani M, Ingwall JS, Dzau VJ. Mesenchymal stem cells modified with Akt prevent remodeling and restore performance of infarcted hearts. *Nat Med*. 2003;9(9):1195-1201.
14. Swijnenburg RJ, Schrepfer S, Govaert JA, Cao F, Ransohoff K, Sheikh AY, Haddad M, Connolly AJ, Davis MM, Robbins RC, Wu JC. Immunosuppressive therapy mitigates immunological rejection of human embryonic stem cell xenografts. *Proc Natl Acad Sci U S A*. 2008;105(35):12991-12996.
15. Takahashi K, Tanabe K, Ohnuki M, Narita M, Ichisaka T, Tomoda K, Yamanaka S. Induction of pluripotent stem cells from adult human fibroblasts by defined factors. *Cell*. 2007;131(5):861-872.

CHAPTER 11

Summary in Dutch

STAMCELLEN VOOR HART- EN VAATZIEKTEN

Hart- en vaatziekten zijn de belangrijkste doodsoorzaak in de westerse wereld en kostten de Nederlandse samenleving in 2005 5.5 miljard euro aan ziektekosten (8% van het totaal). Met de huidige trend naar een verouderende en adipeuzere samenleving zullen deze getallen naar verwachting de komende jaren nog flink toenemen.

Ondanks een variëteit aan behandelingen is er nog een grote groep patiënten die niet goed reageert op bestaande therapie en zodoende aangewezen is op harttransplantatie in het geval van hartfalen of amputatie van een been wanneer het perifeer arterieel vaatlijden (PAV, vergevorderde aderverkalking in ledematen) betreft. Echter, harttransplantatie is, onder andere door een schrijnend tekort aan donororganen, slechts in een select aantal gevallen mogelijk en zodoende is er behoefte aan nieuwe therapeutische opties.

Stamceltherapie heeft de afgelopen jaren veel enthousiaste en hoopvolle reacties teweeg gebracht. Een stamcel is een cel die aan het begin van de ontwikkeling staat en kan uitgroeien tot verschillende soorten meer gespecialiseerde celtypen. Bovendien heeft een stamcel de capaciteit om zichzelf te vermenigvuldigen. Door deze twee eigenschappen biedt een stamcel theoretisch de mogelijkheid voor het kweken van een onuitputbare hoeveelheid weefsel-specifieke cellen om bijvoorbeeld cardiomyocyten (hartspiercellen) te vervangen of bloedvaten te vernieuwen. Omdat het lichaam dat aan hart- en vaatziekten lijdt zelf niet of zeer beperkt de mogelijk heeft tot regeneratie van deze weefsels, zou het inspuiten van stamcellen een oplossing kunnen zijn voor een groot maatschappelijk gezondheidsprobleem.

Er zijn verschillende soorten stamcellen, die grofweg verdeeld kunnen worden in drie soorten: Embryonale stamcellen (ESC), volwassen stamcellen en de recent ontdekte geïnduceerd-pluripotente stamcellen. De studies in dit proefschrift zijn gericht op de eerste twee groepen.

ESC vormen de binnenste celmassa van de blastocyst, het embryo in een zeer vroeg ontwikkelingsstadium 5 dagen na bevruchting. Na isolatie kunnen ESC onder strikt gehandhaafde condities op een onderlaag van bindweefselcellen oneindig delen. ESC zijn pluripotent en kunnen zich differentiëren naar alle kiemlagen (endo-, ecto-, en mesoderm, een soort tussenstation in celdeling) en verder naar iedere cel van het menselijk lichaam.

In tegenstelling tot ESC zijn volwassen stamcellen multipotente cellen. Dat wil zeggen dat zij al een stap in de ontwikkeling hebben ondergaan en zich reeds in een bepaalde kiemlaag bevinden. Volwassen stamcellen kunnen zich nog wel verder specialiseren naar een variëteit aan weefselspecifieke cellen, maar binnen de grenzen van de kiemlaag. Volwassen stamcellen zijn

aanwezig in het volgroeide menselijk lichaam in onder andere het beenmerg, de huid, en de darm en zijn verantwoordelijk voor de constante vernieuwing van deze weefsels.

Sinds wetenschappers aan het begin van dit millennium beschreven dat beenmergcellen na het inspuiten in de beschadigde hartspier differentiëren naar cardiomyocyten is het veld van stamceltherapie voor hart- en vaatziekten in een stroomversnelling geraakt. Ondanks het feit dat deze observatie controversieel is gebleken, werden binnen afzienbare tijd klinische trials gestart waarin de effectiviteit van beenmergcellen voor de behandeling van myocardinfarct en PAV werd onderzocht. De resultaten van deze trials zijn wisselend positief maar vertonen onderling verschillende uitkomsten. Dit onderstreept het gebrek aan kennis over wat er met de cellen gebeurt na transplantatie en op welke manier deze cellen al dan niet bijdragen aan herstel of preservatie van hart- of spierfunctie.

IN VIVO MOLECULAR IMAGING VAN GETRANSPLANTEERDE STAMCELLEN

Om het mechanisme te bestuderen waarmee getransplanteerde cellen wel of niet aan functioneel herstel bijdragen is het van groot belang om inzicht te verkrijgen in het gedrag van stamcellen na transplantatie. Dit wordt meestal gedaan door in experimentele modellen de stamcellen te markeren met conventionele reportergenen zoals Green Fluorescent Protein (GFP). GFP wordt geïsoleerd uit lichtgevende kwallen. Om GFP (en daarmee de gemarkeerde stamcellen) in beeld te brengen is het nodig om met een uitwendige lichtbron de GFP van energie te voorzien. Dit heeft tot gevolg dat er een hoog achtergrondsignaal ontstaat. Bovendien wordt een deel van het signaal geabsorbeerd door het omliggende weefsel waardoor het moeilijk is gemarkeerde stamcellen in dieper gelegen locaties te identificeren wat deze methode minder geschikt maakt voor beeldvorming in een levend dier (*in vivo*). Om deze reden wordt GFP beeldvorming meestal verricht op geëxplanteerde plakjes weefsel met behulp van histologie. Omdat dit het opofferen van het proefdier vergt ontstaat er met histologie echter slechts een beeld van een bepaald moment in plaats van een serie van gebeurtenissen over een langere periode. Echter, om het ware gedrag van getransplanteerde stamcellen in beeld te brengen is het van belang om de cellen herhaaldelijk over een langere periode, *in vivo* te kunnen volgen. Om dit te bewerkstelligen heeft onze onderzoeksgroep nieuwe, moleculaire beeldvormingtechnieken ontwikkeld.

Molecular Imaging wordt gedefinieerd als de *in vivo* karakterisatie van cellulaire en moleculaire processen. Dit staat of valt bij het ontwerpen van een geschikt reporter construct, dat bestaat uit een reporter gen gelinkt aan een promoter. Deze promoter kan altijd "aan" staan, geïnduceerd ingeschakeld worden, of weefselspecifiek zijn. In de studies die in dit proefschrift worden bechreven is bioluminescence imaging (BLI) met het reporter gen Firefly Luciferase (Fluc,

dat geisoleerd wordt uit vuurvliegjes) gebruikt achter een ß-actine promoter die in iedere cel tot expressie komt. Na het inbouwen van het reporter construct in de cel leidt transcriptie en translatie tot de productie van intracellulair Fluc eiwit. Op het moment dat de cellen in beeld gebracht dienen te worden wordt er een reporter probe (luciferin) in het proefdier gespoten, dat reageert met het reporter eiwit en een signaal afgeeft dat met een gevoelige CCD-camera opgevangen kan worden.
Bovengenoemde methode heeft een aantal voordelen: Ten eerste blijft het proefdier leven wat het mogelijk maakt een situatie op meerdere tijdstippen te bekijken; ten tweede zal het Fluc eiwit slechts geproduceerd worden door levende cellen waardoor een beeld ontstaat van de celoverleving; Ten derde is het een methode waarbij het gehele dier in beeld komt zodat de celdistributie duidelijk wordt; en ten slotte is het niet nodig extrensiek excitatielicht te gebruiken zodat er relatief weinig achtergrondsignaal ontstaat.

BEELDVORMING VAN EMBRYONALE STAMCELTHERAPIE VOOR HART- EN VAATZIEKTEN

Het doel van dit proefschrift was om duidelijkheid te verkrijgen op het gebied van stamceloverleving, -groei, en -migratie, en onbedoelde bijwerkingen van stamceltherapie.

Het eerste deel van het proefschrift is gericht op de voor- en nadelen van ESC therapie. In **hoofdstuk 2** werd onderzocht wat er gebeurt als ongedifferentieerde ESC in het geïnfarcteerde muizenhart worden ingespoten. De functionele effecten op de korte termijn werden gevolgd met MRI en getest met invasieve drukmetingen. Er leek een functioneel voordeel te bestaan van het gebruik van ESC ten opzichte van de controletherapiën. Het belang van gevoelige *in vivo* beeldvorming van ESC werd onderstreept door snel stijgende signalen in de eerste week na transplantatie. Deze stijgende signalen bleken representatief voor groei van tumoren die uit verschillende soorten cellen bestonden (teratomen) met dezelfde achtergrond (ESC). Post-mortem histologie bevestigde de aanwezigheid van tumor en liet daarnaast zien dat een klein deel van de ESC daadwerkelijk hartcellen vormde.

Om meer inzicht te verkrijgen in de kwaadaardige aspecten van ESC therapie werd de studie uit **hoofdstuk 3** uitgevoerd. De experimenten illustreren de voordelen van BLI en laten zien dat slechts 100-1000 ongedifferentieerde ESC met BLI al zichtbaar zijn en dat diezelfde hoeveelheid al genoeg is om teratomen te vormen. Bovendien werd het belang van beeldvorming van het gehele dier duidelijk omdat er niet alleen tumoren ontstonden ter plaatse van de injectie, maar ook op afstand in andere organen. Ten slotte konden ESC in het hart tot 10 maanden gevolgd worden en werd zo duidelijk dat de integratie en expressie van de reporter genen zeer stabiel is.

Hoofdstuk 4 biedt een overzicht van de voor- en nadelen van verschillende beeldvormingtechnieken voor het volgen van ESC therapie. Bovendien beschrijft dit hoofdstuk de grote variëteit aan ziekten waar ESC therapie mogelijk een nieuwe behandeling voor kan vormen. **Hoofdstuk 5** richt zich vervolgens meer specifiek op de mogelijkheid van het kweken van hartcellen uit ESC. Bovendien wordt hier bediscussieerd wat er gedaan dient te worden voordat ESC therapie veilig in klinische studies gebruikt kunnen worden. Het gevaar van teratoomvorming blijft aanwezig indien de ESC voor transplantatie niet voldoende uitgekweekt worden naar meer gespecialiseerde celtypen en ontdaan worden van ongedifferentieerde cellen. Bovendien zijn ESC nooit van de patiënt zelf en leidt ESC transplantatie, net als orgaantransplantatie, onherroepelijk tot een afstotingsreactie. Tenslotte bestaat er het probleem dat getransplanteerde ESC wellicht niet goed integreren in het hartweefsel en op een andere manier reageren op signalen waardoor de getransplanteerde cellen mogelijk een ander ritme aannemen dan het omliggende spierweefsel.

BEELDVORMING VAN VOLWASSEN STAMCELTHERAPIE VOOR HART- EN VAATZIEKTEN

Een belangrijke vraag die uit de grote hoeveelheid studies met verschillende soorten volwassen stamcellen naar voren kwam is: Welke volwassen stamcel kan de functie van het beschadigde hart het beste beschermen of verbeteren? **Hoofdstuk 6** geeft hierop voor het eerst een antwoord. Verschillende soorten stamcellen werden geïsoleerd uit het beenmerg (mononucleaire cellen –MN- en mesenchymale cellen –MSC-), de spieren (skeletmyoblasten –SkMb-), en de huid (fibroblasten –Fibro-) van muizen die in iedere cel van hun lichaam de traceerbare, lichtgevende reportergenen Fluc en GFP tot expressie brachten. Na uitvoerige *in vitro* karakterisatie van reportergenexpressie werden de cellen ingespoten in de hartspier van ongemodificeerde wild-type muizen die een hartinfarct hadden ondergaan. *In vivo* BLI liet vervolgens zien dat van alle celtypen, MN het langst overleefden waarbij er na zes weken nog een marginaal signaal aanwezig was in vergelijking tot maximaal 4 weken in de andere groepen. In overeenstemming met dit overlevingsvoordeel lieten de functionele testen (echocardiografie en invasieve hemodynamische metingen) een significant voordeel van MN transplantatie zien ten opzichte van de controlegroepen. Hierbij moet aangetekend worden dat in alle groepen die celtherapie ontvingen er een trend bestond van een verslechtering van hartfunctie tussen de vierde en zesde week na transplantatie, terwijl de hartfunctie in de controlegroep die slechts zoutoplossing ontving stabiel was. Deze bevinding suggereert dat het effect van celtransplantatie van korte duur is, hetgeen ook uit sommige klinische studies kan worden geconcludeerd.

Een nieuwe groep stamcellen binnen het palet van klinische celkandidaten is aanwezig in het

vet. Er was veel enthousiasme rondom deze adipose-derived stromale cellen (ASC) omdat ze zouden lijken op MSC uit het beenmerg maar makkelijker te isoleren zijn. Na een *in vitro* evaluatie bood **Hoofdstuk 7** voor het eerst een vergelijking van de *in vivo* kinetica en de functionele gevolgen op de beschadigde hartspier van beide celpopulaties. ASC en MSC deelden dezelfde morfolgische en groeieigenschappen en lieten een vergelijkbaar patroon van celexpressie zien. Ook *in vivo* gedroegen de cellen zich op eenzelfde manier wat helaas betekende dat zowel ASC als MSC binnen vier weken afstierven. Bovendien was er met echocardiografie en invasieve hemodynamische metingen geen functioneel voordeel te meten van celtransplantatie.
In de bovengenoemde studies werd de hartfunctie *in vivo* gemeten met echocardiografie. De metingen waren over het algemeen vergelijkbaar met de invasieve hemodynamische metingen maar het tweedimensionale karakter maakt echocardiografie toch beperkt. In **hoofdstuk 8** werd daarom onderzocht of er wellicht ruimte was voor Micro-CT beeldvorming van het hart. Het muismodel van hartfalen werd gebruikt om te laten zien dat Micro-CT een betrouwbare manier is om *in vivo* de hartdimensies en –functie te meten op een driedimensionale manier. De resultaten van de Micro-CT correleerden met meer conventionele methoden maar bleken preciezer met betrekking tot geometrie en functionele uitkomst. Bovendien bood Micro-CT *in vivo* beelden die vergelijkbaar waren met *post-mortem* histologie.

Ten slotte maakt **hoofdstuk 9** de overstap van hartziekten naar PAV. Er werd onderzocht wat er met getransplanteerde MN gebeurde na injectie in de bovenbeenspier of na systemische introductie bij muizen waarbij de bovenbeenslagader was onderbonden. Na injectie in de spier, zowel eenmalig als herhaald, waren de uitkomsten vergelijkbaar met de resultaten van de eerdere studies in het hart waarbij er marginale celoverleving was zonder effect op de doorbloeding van het ischemische been zoals gemeten met Laser-Doppler Perfusion Imaging. Na intraveneuze injectie gevolgd door regelmatige BLI werd duidelijk dat een deel van de MN naar het aangedane gebied migreert, maar dat een minstens zo groot deel naar de lever, de milt, en het beenmerg afreist. Ex vivo BLI liet vervolgens zien dat het signaal uit het aangedane gebied met name het resultaat was van retentie van de MN in de beschadigde huid en het onderhuidse vet aldaar, meer dan daadwerkelijk in de aangedane spier. Dit migratiepatroon resulteerde in een gebrek aan functioneel effect.

CONCLUSIE

Dit proefschrift beschrijft het gedrag van zowel embryonale als volwassen stamcellen in modellen van hart- en vaatziekten. Terwijl ESC therapie daadwerkelijk regeneratief kan zijn en het beschadigde weefsel zou kunnen vervangen, heeft het de nadelen dat er gevaar is voor teratogeniciteit en dat de cellen bovendien een afstotingsreactie uitlokken. Deze gevaren bestaan niet bij het gebruik van volwassen stamcellen. Echter, deze cellen overleven slecht in het

aangedane gebied en lijken in de gebruikte modellen een marginaal functioneel effect te hebben. Toekomstige studies dienen gericht te zijn op het minimaliseren van de gevaren van ESC transplantatie, de verbetering van celoverleving en functionaliteit van volwassen stamcellen, en de verdere karakterisatie van geïnduceerd-pluripotente stamcellen. Verdere ontwikkeling is nodig om stamceltherapie een waardevolle toevoeging te maken in het arsenaal van behandelingen voor hart- en vaatziekten.

CHAPTER 12

Addenda

LIST OF PUBLICATIONS

1. **van der Bogt KEA**, Sheikh AY, Schrepfer S, Hoyt EG, Cao F, Ransohoff K, Contag CH, Robbins RC, Wu JC. *Comparison of Different Adult Stem Cell Types for Treatment of Myocardial Ischemia.* Circulation. 2008 Sep 30;118(14 Suppl):S121-9.
2. **van der Bogt KEA**, Schrepfer S, Yu J, Sheikh AY, Hoyt EG, Ransohoff K, Govaert JA, Cao F, Contag CH, Robbins RC, Wu JC. *Comparison of Transplantation of Adipose Tissue- and Bone Marrow- Derived Mesenchymal Stem Cells in the Infarcted Heart.* Transplantation. 2009 Mar 15;87(5):642-52.
3. **van der Bogt KEA**, Vrancken-Peeters MPFM, van Baalen JM, Hamming JF. *Resection of carotid body tumors: results of an evolving surgical technique.* Ann Surg. 2008 May;247(5):877-84
4. **van der Bogt KEA**, Swijnenburg RJ, Cao F, Wu JC. *Molecular Imaging of Human Embryonic Stem Cells: Keeping an Eye on Differentiation, Tumorigenicity and Immunogenicity.* Cell Cycle. 2006 Dec;5(23):2748-52
5. **van der Bogt KEA**, van Baalen JM, Hamming JF. *Comment on "Carotid chemodectomas: Long-term results of subadventitial resection with deliberate external carotid resection".* Ann Vasc Surg. 2009 Mar;23(2):288-9
6. Sheikh AY*, **van der Bogt KEA*,** Doyle TC, Sheikh MK, Ransohoff KJ, Ali ZA, Palmer OP, Robbins RC, Fischbein MP, Wu JC. *Micro-CT for characterization of murine CV disease models.* JACC Cardiovasc Imaging. 2010 Jul;3(7):783-5. *Shared first authorship
7. Hendry SL*, **van der Bogt KEA***, Sheikh AY, Arai T, Dylla SJ, Drukker M, McConnell MV, Kutschka I, Hoyt EG, Cao F, Weissman IL, Connolly AJ, Pelletier MP, Wu JC, Robbins RC, Yang PC. *Multimodality evaluation of in vivo MRI of myocardial restoration by mouse embryonic stem cells.* J Thorac Cardiovasc Surg. 2008 Oct;136(4):1028-1037. *Shared first authorship
8. Cao F, **van der Bogt KEA**, Sadrzadeh A, Xie X, Sheikh AY, Wang H, Connolly AJ, Robbins RC, Wu JC.*Spatial and Temporal Kinetics of Teratoma Formation from Murine Embryonic Stem Cell Transplantation*. Stem Cells Dev. 2007 Dec;16(6):883-91
9. Swijnenburg RJ, **van der Bogt KEA**, Sheikh AY, Cao F, Wu JC.*Clinical hurdles for the transplantation of cardiomyocytes derived from human embryonic stem cells: role of molecular imaging.* Curr Opin Biotechnol. 2007 Feb;18(1):38-45
10. Sheikh AY, Lin SA, Cao F, Cao YA, **van der Bogt KEA**, Chu P, Chang CP, Contag CH, Robbins RC, Wu JC. *Molecular Imaging of Bone Marrow Mononuclear Cell Homing and Engraftment in Ischemic Myocardium*. Stem Cells. 2007 Oct;25(10):2677-84

11. Lee AS, Tang C, Cao F, Xie X, **van der Bogt K**, Hwang A, Connolly AJ, Robbins RC, Wu JC. *Effects of cell number on teratoma formation by human embryonic stem cells.*Cell Cycle. 2009 Aug 15;8(16):2608-12
12. Govaert JA, Swijnenburg RJ, Schrepfer S, Xie X, **van der Bogt KE**, Hoyt G, Stein W, Ransohoff KJ, Robbins RC, Wu JC. *Poor functional recovery after transplantation of diabetic bone marrow stem cells in ischemic myocardium.* J Heart Lung Transplant. 2009 Nov;28(11):1158-1165
13. Swijnenburg RJ, Govaert JA, **van der Bogt KE**, Pearl JI, Huang M, Stein W, Hoyt G, Vogel H, Contag CH, Robbins RC, Wu JC. *Timing of bone marrow cell delivery has minimal effects on cell viability and cardiac recovery after myocardial infarction*. Circ Cardiovasc Imaging. 2010 Jan;3(1):77-85

CURRICULUM VITAE

The author of this thesis was born on August 20th, 1981 in Nieuwveen, The Netherlands. He grew up in the village of Nieuwkoop, while attending the Ashram College (VWO) in Alphen aan den Rijn. After graduation in 2000, he applied for a decentralized selection procedure for medical school at Leiden University, and started in September of that year.

While attending medical school, he was an active participant in the Student Society Leidse Studenten Vereniging Minerva. Moreover, he worked as an allocation officer at the Eurotransplant International Foundation. In his fourth year, he got introduced to surgical research with projects concerning the surgical treatment of carotid body tumors, supervised by prof. dr. J.F. Hamming. Through this project and his work at Eurotransplant, the author got interested in transplantation and surgery and decided to spend a year abroad to gain experience in basic science.

Having received several research grants including ones from the Fulbright Foundation and the American Heart Association, he moved to Palo Alto, California, United States of America in 2005 and to San Francisco in 2006. As a visiting researcher in Stanford University's Laboratory of Cardiothoracic Transplantation, he initiated his first basic scientific studies under the supervision of prof. dr. R.C. Robbins. Soon, he was introduced to dr. J.C. Wu to collaborate on projects merging the fields of stem cell treatment and molecular imaging. After 14 months and having completed most of the work as described in this thesis, he returned to the Netherlands to finish medical school. During that time, he received the Hippocrates Foundation Research Award, the Dick Held Research Award, and a Vascular Biology Working Group Award for the publication as presented in chapter 6 of this thesis.

After finishing medical school in 2008, he received a Professor Michaël-van Vloten Foundation grant to perform more research on the topic of stem cell transplantation in order to finish this thesis. This time, he initiated a research project that was performed in part at Leiden University under the supervision of prof. dr. J.F. Hamming as well as at Stanford under the supervision of dr. J.C. Wu and prof. dr. R.C. Robbins. The work as described in this thesis was presented at the American Heart Association Scientific Sessions in 2007 and 2009. At this moment, the author lives in Amsterdam, The Netherlands, and is a surgical resident at the Leiden University Medical Center under the supervision of prof. dr. J.F. Hamming.

ACKNOWLEDGEMENTS

The road to this thesis has not been a specific one of exceptional hard work, vigorous passion or true talent. While all these factors contributed, this thesis is merely the result of multiple opportunities provided by those around me, who I'm therefore happy to acknowledge:

Bobby Robbins, who I greatly admire. You're an example of how to combine basic scientific research with a flourishing surgical practice. Your enthusiasm has been a major stimulant for carrying out the studies in this thesis and pursuing a career in academic surgery.

Dear Joe, I have watched the expansion of your lab with great admiration. In October 2005, we were having lab meetings just with four of us. When I left Stanford in 2010, we were over 20 people. Yet, you manage to return papers and answer emails within a day. Your ambition and perseverance are impressing but secondary when it comes to great mentorship. Not only have you introduced me to the world of basic science and molecular imaging, but you have also managed to provide insight in running a lab and writing grant proposals. Those aspects of your mentorship will be invaluable throughout my career. And I must admit, whenever you start a sentence with "I keep telling you guys….", in the end it turns out that you're usually right.

Dear Grant, thanks for making me feel welcome and at home from the first minute I entered the lab. Multi-tasking through micro-surgery, listening to KFOG, drinking coffee, and talking sports on the phone with your buddies all at the same time, you have done so much work for my projects. Thanks a million and we'll meet again in Oregon.

Dear Jaap, guiding me through my first research experience, then through the PhD studies, and now through the surgery program, you have been the constant factor throughout my career ever since I was introduced to you in 2004. Thank you for your mentorship, I hope we'll be able to continue the collaboration for a long time.

"The Professor", dear Ahmad. It must have been a pain having me asking you a zillion (is that more than a billion?) questions every day. However, you coped well and showed me how to handle every single machine and instrument and introduced me to all people on campus who have been incremental for the success of my studies. Finding you on the floor of our office one morning and afraid you might had died, I asked you why you had spent the night in the lab. You answered: "Good science takes time, bad science can be done overnight". Although the experiments in this thesis were performed in a fairly short period, I guess I must be happy that at least the writing of this thesis took me a long time then…

To my "paranymfen", Maarten and Willem, friends in life and science. You have been involved in this project from the very first moment. It's a great pleasure and a reassurance to have you there until the very last.

To Rutger-Jan, Johannes, Ernst Jan, Alwine, Laura, C-11-14, the girls at Peet's Coffee and all my colleagues in lab and around campus: It would have been a lot more boring without you. Thanks for your great company, humor, and hard work.

Dear Patrick and Jan, thanks for building the foundations for an extremely successful exchange program. Your tips and tricks in the preparation of my travels were invaluable.

To my family: By providing me with every kind of support I could wish for, you have contributed to every single letter in this thesis.

Lastly, I consider myself very lucky to have worked (and still work) in an environment where so many colleagues have become friends, and where so many friends have become colleagues. It has been five years since I was first introduced to stem cell research. Since that point, it has been constantly on the back of my mind. It has lead to a load of new ideas and has shaped new goals for the future. Now, it's time pursue these new goals.

Koen van der Bogt

October 2010

"Wrap it up, write it down, and you've got your paper right there!"

COLOFON

Stem Cell Therapy for Cardiovascular Disease
answering basic questions regarding cell behavior

© 2010 K.E.A. van der Bogt, Amsterdam, The Netherlands.

ISBN/EAN 978-90-70480-14-1

Cover illustration: *"Are we heading in the right direction?"* San Francisco Fleet Week 2006 from Webster@Union street.

Printed by: Ecodrukkers BV, Nieuwkoop